TITLE PAGE

Report Title:	Solid State Energy Conversion Alliance Delphi Solid Oxide Fuel Cell
Type of Report:	Technical Progress Report
Reporting Period Start Date:	01/01/03
Reporting Period End Date:	06/30/03
Principal Author(s):	Steven Shaffer Sean Kelly Subhasish Mukerjee David Schumann Gail Geiger Kevin Keegan John Noetzel Larry Chick
Date Report Issued:	December 08, 2003
Department OF Energy (DOE) Award Number:	DE-FC26-02NT41246
Submitted By:	Delphi Automotive Systems LLC 5725 Delphi Drive Troy, Michigan 48098
In Collaboration With:	Battelle/PNNL, Electricore, Inc.

DISCLAIMER

This report was prepared as an account of work sponsored by an agency of the United States Government. Neither the United States Government nor any agency thereof, nor any of their employees, makes any warranty, express or implied, or assumes any legal liability or responsibility for the accuracy, completeness, or usefulness of any information, apparatus, product, or process disclosed, or represents that its use would not infringe privately owned rights. Reference herein to any specific commercial product, process, or service by trade name, trademark, manufacturer, or otherwise does not necessarily constitute or imply its endorsement, recommendation, of favoring by the United States Government or any agency thereof. The views and opinions of authors expressed herein do not necessarily state or reflect those of the United States Government or any agency thereof.

TABLE OF CONTENTS

1.0 ABSTRACT

The objective of Phase I under this project is to develop a 5 kW Solid Oxide Fuel Cell power system for a range of fuels and applications. During Phase I, the following will be accomplished:

Develop and demonstrate technology transfer efforts on a 5 kW stationary distributed power generation system that incorporates steam reforming of natural gas with the option of piped-in water (Demonstration System A).

Initiate development of a 5 kW system for later mass-market automotive auxiliary power unit application, which will incorporate Catalytic Partial Oxidation (CPO) reforming of gasoline, with anode exhaust gas injected into an ultra-lean burn internal combustion engine.

This technical progress report covers work performed by Delphi from January 1, 2003 to June 30, 2003, under Department of Energy Cooperative Agreement DE-FC-02NT41246. This report highlights technical results of the work performed under the following tasks:

Task 1 System Design and Integration
Task 2 Solid Oxide Fuel Cell Stack Developments
Task 3 Reformer Developments
Task 4 Development of Balance of Plant (BOP) Components
Task 5 Manufacturing Development (Privately Funded)
Task 6 System Fabrication
Task 7 System Testing
Task 8 Program Management
Task 9 Stack Testing with Coal-Based Reformate

In the next reporting period, Task 6 – System Fabrication and Task 7 – System Testing will be reported within Task 1 System Design and Integration.

Task 8 – Program Management and Task 9 – Stack Testing with Coal Based Reformate will be reported on in the Executive Summary section of this report.

The next anticipated Technical Progress Report will be submitted January 30, 2004 and will include tasks contained within the cooperative agreement including development work on the Demonstration System A and the automotive 5kW System.

2.0 EXECUTIVE SUMMARY

The subject effort includes development of the Solid Oxide Fuel Cell stack and reformers. Also included are system design and integration, fabrication of development systems, testing of development systems, and reporting of results. Development of other balance-of-plant components (e.g., the air delivery system, fuel delivery system, sensors and controls, control algorithms and software, safety systems, insulation, enclosure and packaging, exhaust system, electrical signal and power conditioning) will be privately funded by Delphi and is considered outside the scope of this program. However, Delphi will report on the general status of the privately funded effort at the same time it is reporting on the Solid State Energy Conversion Alliance (SECA) program effort.

The following accomplishments were achieved under the following tasks for this reporting period.

2.1 System Design and Integration (Task 1.0)

A product development plan with intermediate achievement targets for the major subsystems has been developed over the period covered by this report. The development plan has been generated with a focus on the mobile Auxiliary Power Unit (APU) using liquid fuels. Generally, the targets defined for various design levels for mobile applications are more aggressive than those required for a Stationary Power System on natural gas fuel. Issues such as fuel handling, fuel desulfurization, and application power interfaces are application specific, and are not addressed in the defined targets at this time.

System Mechanizations have been created to support the Gen 2 and Gen 3 APU applications. In addition, a Gen 3 Mechanization has been developed to support a Natural Gas Stationary Power Unit (SPU).

Within the current generation of hardware, Gen 2, significant design updates and developments have occurred. Key shortcomings and development issues were identified at the outset of the Gen 2A design level. Many of these issues were discussed in the previous period's technical report. During the course of Gen 2B APU development, many significant control issues for the system, including process air system, reformer, and electronics control, have been resolved. Significant improvements to design integration have also been made to improve the overall function, build and serviceability of the APU. Significant gaps in power, efficiency, cost, life, and cycle durability still exist, but they have been identified and future development efforts will address these gaps as a part of technology development.

The Delphi SOFC APU control system has matured to the point where multiple completely automatic warm up cycles initiated by an external control source have been completed. Test results indicate good performance on the 9 main closed loop control points, and coordinated sequencing of the 8 major system states.

Significant advancement has also been achieved in the processes used for control development. A single software set satisfies the needs (through configuration election) of multiple target uses including desktop simulation for control and system design development, virtual runs on a development controller, real runs on system development hardware, and real runs on the production target controller through an auto-code generation process.

Models in the two primary system analysis environments (Simulink® and Hysys®) have been further matured. The Simulink® dynamic model has been employed for studies of system warm-up time sensitivity to system design. Refinements have included the addition of a representation of the current non-ideal cathode heat exchanger based on experimental data. The steady state Hysys® model now includes detailed representation of the actual heat exchangers design throughout the system.

2.2 Solid Oxide Fuel Cell Stack Development (Task 2.0)

Key progress has been made between January-June 2003 in stack development. The key achievements are:

Multiple 2x15-cell Generation 2 Integrated Stack Modules (complete stack sub-systems) have been fabricated and tested, producing greater than 1kW of power with simulated reformate composition at a stack operating temperature of 750 ^{o}C.

New cathode materials like LSCF (Sr-doped lanthanum cobalt ferrite), LSF (Sr-doped lanthanum ferrite) and LSFCu (Copper-doped LSF) have been investigated and developed to demonstrate significant improvements in power density. Development has focused on understanding key parameters in the material composition as well as changes in the processing methods for optimum performance.

Development has progressed with 7x7 cm cell stacks demonstrating high power densities of >700 mW/cm^2 at 0.7 Volts with hydrogen. Further work is ongoing to understand the processes that contribute to stable high power density performance of the cell.

Bonding using the existing glass ceramic seal G18 has been further improved by improving the application processes.

Further progress has been made in the development of alternate seals like the silver based braze. The braze has been implemented in Generation 3 cassettes. Investigation is ongoing to evaluate the durability of the braze.

Fuel utilization studies on a single cell stack (full sized), have demonstrated a power loss of 27% in going from 15% fuel utilization to 70% fuel utilization. Work is ongoing to decrease this degradation in power.

Generation 3 single cell and short stacks have been assembled and tested. Initial results indicate good sealing and stable behavior.

2.3 Reformer Developments (Task 3.0)

2.3.1 Reformer – Subsystem Level

Significant advances in the understanding of catalytic partial oxidation (CPOx) reforming and its integration into an APU system have occurred during this reporting period

Three reformer designs were involved in development.

An Initial tubular design (Gen 1.0) employing ceramic foam substrates has been produced and been tested extensively.

An improvement to this design (Gen 1.1) has been produced and has undergone significant test. It is expected, based on reformer lab experience, to be a stable and reliable platform with which to conduct necessary system level tests.

The planar reformer design (H2 planar), whose development had been suspended because of brazing difficulties, has been revived with the development of an internal to Delphi braze process. The root cause of the fundamental problems encountered when brazing this assembly in the past has been largely explained.

Carbon forming regimes and conditions have begun to be mapped using both the tubular designs as well as novel test setups to isolate this phenomena.

Thermal behavior of the reformer in relation to significant heat sinks and sources around it are becoming better understood.

The Gen 1.1 design is expected to alleviate some key system level thermal issues Lab Reactors have demonstrated initial capability of Delphi catalysts to successfully carry out steam reforming.

Initial analysis work has begun on reformer concepts with heat transfer capabilities sufficient to carry out steam reforming of natural gas.

Initial analysis work has begun on mixing geometry concepts to understand basic differences in these approaches.

Initial reformer durability has been evaluated to >100 hours with relatively low levels of degradation and the process of assigning failure modes has begun.

Reformer behavior and the control strategies that compliment it are now well enough understood to allow reasonably stable day-to-day operation and will allow for more controlled and resolute experiments.

2.3.2 Reformer Catalyst – Component Level

Most of the catalyst development work during this reporting period focused on improving washcoat formulations for increased durability, confirmation of catalyst applicability to methane reforming, and determining the effects of sulfur on reforming catalyst performance.

Several formulation methods yielded improved durability catalysts, including chemical modification of the support ingredient in washcoats to improve alumina support stability and the use of separate washcoat layers in the catalyst with different functionalities. Some of these formulations appear to have excellent durability after thermal aging; however, extensive durability testing will be required to determine the best catalyst product formulation.

Catalyst durability test stands have confirmed that the catalysts can operate for a minimum of 300 hours and have acceptable performance, defined as producing a reformate with greater than 20% H_2. The current catalyst formulations were found to be useful for methane partial oxidation, auto-thermal reforming, and for steam reforming, paving the way for future systems-level testing.

A process for converting organic sulfur to SO_2 was demonstrated. Light-to-heavy organic sulfur compounds were oxidatively desulfurized at high conversions. Significant process and catalyst development work will be required to make this process useful.

Both SO_2 and thiophene, added in ppm levels, were found to inhibit fuel reforming; the effect is reversible upon removal of the sulfur. Reforming of smaller hydrocarbons was more significantly impacted than that of heavier, gasoline range, hydrocarbons; yields from gasoline reforming were only marginally reduced. H_2 selectivity was reduced the most, while selectivity to CO was influenced only slightly by sulfur addition. These results have implications for the need to desulfurize before the reformer; and may indicate that CO and H_2 formation reactions occur on different types of active sites.

Advanced analytical techniques, including X-ray photoelectron spectroscopy, high-resolution transmission electron microscopy, and laser-Raman spectroscopy were demonstrated to be useful for catalyst characterization. These methods, together with kinetic evaluations and modeling, should permit a good understanding of structure property relations in our reforming catalysts, reveal deactivation mechanisms, and eventually permit development of realistic rapid aging tests and improved catalyst formulations.

2.4 Development of Balance of Plant Components (Task 4.0)

The Balance of Plant Components are defined as parts that support the function of the Reformer and Stack and make up the balance of the system. Task 4.4 - Develop Air Delivery and Process Air Subsystem, Task 4.5 - Develop Hot Zone Components, and Task 4.6 - Develop Fuel Delivery and Fuel Metering have been added to the normal

reporting under Balance of Plant Components and will be reported throughout this report within the corresponding Balance of Plant sections.

2.4.1 Develop Energy Recovery Unit

This subtask is part of the Reformer development activity and is reported in the Catalytic Partial Oxidation section for Reformer development.

2.4.2 Develop Hydrogen Sensors for High and Low Concentration Measurement

2.4.2.1 High Concentration Hydrogen Sensor

As reported previously, a wide range O_2 sensor developed by the Delphi sensor group (Flint) was tested as a High Concentration Hydrogen sensor targeted for use as a monitor of reformer performance and provide closed loop control feedback to the system. Since the Delphi sensor could not qualitatively distinguish CH_4 from H_2, alternative approaches have been developed.

2.4.2.2 Combustible Gas Safety Sensor

During this reporting period, the Delphi Sensor previously selected and bench tested as the combustible gas sensor, was installed in a system. This allowed for the de-bugging of the Safety Control Algorithms, for example Fail Safe/System Shut Down Procedures.

2.4.3 Develop Water Recovery Unit (WRU)

This subtask is an activity that will be addressed in Phase Two of the program and has no activity at this time.

2.4.4 Develop Air Delivery and Process Air Subsystem

Development activities on the Air Delivery and Process Air Subsystem during this reporting period focused on evolving the first basic design. This resulted in a modular design concept with component integration of air control valves and mass airflow sensors into a common manifold.

2.4.5 Develop Hot Zone Components

2.4.5.1 Gasket Development

Gasket development has focused on the design of unique high-temperature sealing devices suitable for the aggressive Solid Oxide Fuel Cell environment. Designs have been created which allow one-piece high temperature materials to seal the Stack, Reformer and Cathode Air Heat Exchangers at the Integrated Component Manifold interface.

2.4.5.2 Integrated Component Manifold

The Integrated Component Manifold (ICM) is the critical APU device on which all Hot Zone components are mounted. The manifold allows for internal ducting of all high temperature inlet and exhaust air, fuel and waste gases.

The construction of the Integrated Component Manifold is accomplished by brazing together 5 layers of high-temperature nickel alloy materials. These layers form the component mounting surface, top plate, internal gas passages, upper and lower flow plates and external inlet and exhaust connections. Integrated Component Manifold's serial numbers 6 though 8 were processed with numerous design improvements, during this reporting period.

2.4.5.2.1 Cathode Air Heat Exchangers

During this period, Delphi has continued to refine the Cathode Air Heat Exchanger design with a focus toward increased efficiency while maintaining a low backpressure. Delphi Thermal assumed brazing development and fabrication responsibility for the Cathode Air Heat Exchangers.

2.4.5.2.2 Resistance Temperature Detector Resistance Temperature Detector Development

Failures of Resistance Temperature Detector elements, continued while on bench test and at the system level. Development continues. To date, no Resistance Temperature Detector has survived the 1000-hour at 950 ^{o}C test milestone.

2.4.5.2.3 Thermocouple Development

In order to continue with APU control development and system test, reliable temperature measurement was needed. With the high incidence of failure rate of the Resistance Temperature Detector elements, a decision was made to switch to thermocouples. This allowed for system testing to continue. ANSI (American National Standards Institute) Type K thermocouples were specified, purchased and tested.

2.4.5.2.4 Igniter Developments

Ceramic igniters were previously selected due to their low current draw, rapid heat-up, and ability to withstand high temperatures. After numerous failures in both the system and reformer testing, a root cause analysis was performed. The cause of the igniter failures was determined to be due to basic material properties and the design of the igniter. Follow-up discussions with the vendor resulted in new prototype igniters with higher temperature metals and a higher temperature braze alloy. New igniters were received and are currently in use on reformer and system tests.

2.4.6 Develop Fuel Delivery and Fuel Metering

An assessment of Delphi's product portfolio has been made with respect to identifying appropriate product offerings for fuel supply and delivery. Requirements and specifications are to be developed and technology gaps will be identified.

As for fuel metering, another group of fuel injectors were fabricated, assembled and tested during this reporting period. Additionally, a source for natural gas injectors was identified, and prototype injectors have been ordered and received.

2.5 Manufacturing Development (Privately Funded) (Task 5.0)

The Manufacturing Development for Solid Oxide Fuel Cell falls into two major categories. These are time based rather than technology based. The two major categories are the short-term and long-term time frames.

The short-term time frame focuses on the processes and process improvements required for fabrication of the prototype designs using the current materials. These developments are extremely narrow and allow for the highest quality, best performance, and quickest turn around possible. While cost is of consideration, needs placed on the prototype hardware emphasizes time and performance.

The long-term time frame efforts are placed on the cost and durability needs. The success of Solid Oxide Fuel Cell will be very dependant on cost and durability. These development efforts aim to reduce the needs for exotic materials, high cost, and low through-put processes. While these developments cover all parts of the Solid Oxide Fuel Cell system, particular emphasis is placed on the areas with currently identified high-cost components and multiples of the same component.

Figure 2.5-1 shows a cost estimate based on several design improvement assumptions.

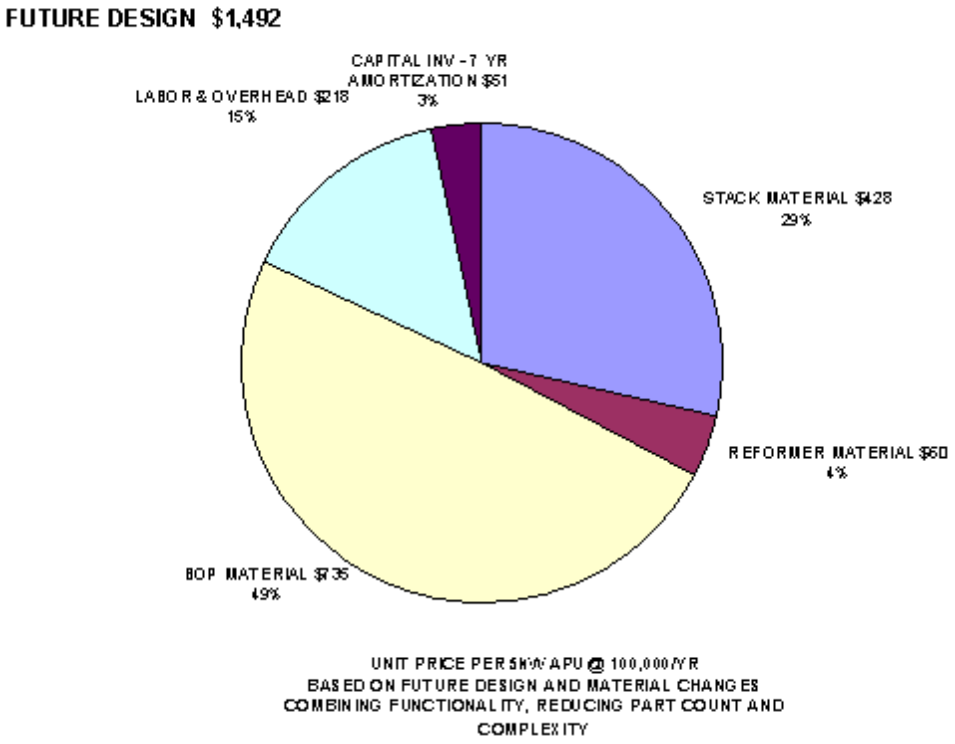

Figure 2.5-1: Cost Estimate

2.6 System Fabrication (Task 6.0)

In this reporting period, the system progressed in its use of a three-tier integration approach to fabrication and development. One change to system fabrication was that design, fabrication and development of individual components for the fuel cell product has been shifted to the Balance of Plant components team. This transfer allows the Balance of Plant team to specialize in the development of these parts while allowing the system team to focus on the fabrication and development of the larger sub-assemblies and modules that comprise the product.

Most system fabrication activity was conducted later in this reporting period due to timing of the system redesign for the Delphi Gen 2B design.

The Hot Zone Module assembly was built with new temperature sensors, a revised tubular reformer, revised stack electrodes, revised gas connection tubes (input side) and additional fasteners used to secure and seal the fuel cell stack module to the integrated component manifold, within the base of the Hot Zone Module. The insulation package for the Hot Zone Module was unchanged except for altered access points in the front to allow for Plant Support Module connections and better insulation fitment around these penetrations.

The Plant Support Module assembly (including the system space frame) underwent a layout change to utilize a new process air delivery system. The space frame redesign allows for easier assembly and development access to hardware within the product assembly. The system module now has easier air connections and clamping surfaces. The system wiring harness has been improved to higher temperature insulations and a power and ground distribution bus. This module has also had the electronics moved out to a new third module called the application interface module.

The Application Interface Module assembly brings several improvements to the preparation and adaptability of the fuel cell system. Assembly now allows the air filtration filter and sound attenuator, input/output signals, fluid connections, power conditioner and the system controller to be pre-built before inclusion to the product. This approach will also allow concurrent development of this module and allow adaptation to new markets without large disruption to the other modules.

No major changes occurred to the overall system assembly process. The main internal modules (Hot Zone Module and Plant Support Module) will be assembled and installed into an outer product enclosure that provides a structurally safe and environmentally sealed housing. The new application interface module is now fastened to form one of the outer walls of the product.

In future reporting periods System Fabrication will be covered under Section 2.1, System Design and Integration.

2.7 System Testing (Task 7.0)

Covered in Section 2.1 above. In future reporting periods System Testing will be covered under Section 2.1, System Design and Integration.

2.8 Program Management (Task 8.0)

Program management duties as outlined in the cooperative agreement have been satisfied during this reporting period.

2.9 Stack Testing with Coal Based Reformate

Two Generation 2 (2x15-cell) Integrated Stack Modules were tested with coal gas-based reformate at the Power Systems Development Facility at Wilsonville, Alabama. The test ran for over 60 hours. The test demonstrated the feasibility of using Solid Oxide Fuel Cell with coal-based reformate after cleanup of impurities that are harmful to the stack. Post-mortem analysis of the stack is ongoing to understand the effect of coal-based syngas on stack materials.

2.10 Technology Transfer from SECA CORE Group

1) The basic cell fabrication technique was developed on the CTP and transferred to the D-BP at its outset. The technique involves tape casting of the ceramic powders, tape lamination, and then cosintering of the bilayer.

2) The Lanthanum Strontium Ferrite (LSF) cathode and associated CeO_2 barrier layer and associated processing were developed by the CTP and passed on to D-BP at the outset. These layers are screen printed onto the sintered bilayer and then fired. A copper-doped-LSF cathode developed in the Core program has also be evaluated in the Delphi-Battelle test stands.

3) Three modeling tools that are used extensively on the B-DP were first developed by the CTP. These are:

   a. Spreadsheet Model of Cell Electrochemical Performance. This is the algorithm that calculates cell voltage as a function of current, temperature, fuel composition, and cell physical characteristics.

   b. Electrochemical Modeling of Stacks. This technique uses a computational fluid dynamics (CFD) code with the spreadsheet electrochemistry algorithm embedded to model the spatial distributions of electrochemical activity, temperature and fuel depletion for multi-cell stacks.

   c. Thermal Cycle Modeling. This technique uses CFD and finite element analysis (FEA) codes to model the heat transfer and resulting temperature and stress distributions in stacks during thermal cycles. These modeling tools were developed by the CTP over about a two-year period starting in mid FY

2000. Transfer to and use by the D-BP started in mid FY 2001. Refinements continue on the models under the CTP.

4) The G-18 glass being used by the Delphi- Battelle team was first developed in the Fossil Energy AR&TD (DOE) project at PNNL.

5) The silver-copper braze being used by the Delphi-Battelle team was first developed in the Fossil Energy AR&TD (DOE) project at PNNL.

3.0 EXPERIMENTAL APPROACH

The following sections describe Delphi facilities, referenced experimental methods, materials, and equipment being used for the research.

Currently Delphi APU development is focused in Rochester, New York, at the Technical Center Rochester. The facilities and floor space required for development testing began to exceed the building capabilities in 2001, and a decision was made to move into additional facilities located 5 miles north of the engineering center at 285 Metro Park Boulevard in the Town of Brighton (Metro Park). Building modification began in December of 2001, and our first test began in December of 2002.

At this time, the original engineering center houses balance of plant hardware testing labs and thirty percent of the fundamental stack development labs.

The Metro Park facility is a 2220 square meter facility, currently using 500 square meters for development labs and 450 square meters for system/subsystem build capability, with 220 square meters of office space. All labs have access to gasoline and diesel fuels as well as any mixture of H_2, CO, CO_2, N and reducing gases under Class I Div I safety standards. Currently stack, reformer, APU system, as well as catalyst extended durability labs, are operational. The building also houses an electronics development lab with emulation capabilities for system/subsystem controls and hardware development.

3.1 System Design and Integration (Task 1.0)

Test Validation Plan

The current validation plan is consistent with Phase 1 Demonstration System A deliverables:

- 1000 Hours Steady State Operation
- 10 Transient Cycles
- 500 Hours Steady State Operation

SCOPE:

To develop the facilities, tools and test plan to design and validate both the system and subsystems for the Solid Oxide Fuel Cell for the various markets using gasoline, diesel and natural gas fuels.

ASSUMPTIONS:

1) During the Technical Development Phase of the program, tests will be run with a minimal number of prototype parts to prove the fundamental operation of subsystems and then will be integrated into the complete Solid Oxide Fuel Cell Auxiliary Power Unit. System and subsystem controls will also be developed at this time. Minimal design iterations will be examined requiring only 2 to 6 test stands. These stands will require full function capability including pressure,

temperature and software/controls capabilities resulting in the most costly and complex test stands. Reformate and exhaust analysis and emissions will also be examined.

2) During the Advanced Development Phase, fundamental development will still continue, as well as more specific parallel development paths, for both system and subsystem integration. Durability testing requiring less control interaction and data acquisition will be acceptable, as a result cost and complexity of the test stands will decrease. A minimal number of 10 durability stands will be required for initial confirmation. These tests will typically run in the 100's to 1000's of hours with the intent of developing deterioration factors while other stands will require 24/7 testing with tests in the tens of thousands of hours progressing up to 40,000 hours for commercial home applications. Environmental and specialty tests will be investigated during the Advanced Development Phase and will include: vibration, thermal shock, dust intrusion, and salt spray.

3) Production Development Phase will validate the APU for the various production markets and will require minimal function test stands with multiple APU systems or sub systems running full and accelerated life cycle tests.

Number of validation test stands and actual test matrix are to be determined.

TEST CAPABILITIES:

We currently have two complete operational system test stands. These are comprised of an Aerovironment dual channel load bank, and electronics interface with a dSPACE® control system to monitor and operate all APU functions for development with LabView® data acquisition. The lab is equipped with: A Horiba emissions bench, Orbital mass spectrometer and an AVL fuel flow bench. Two additional APU durability stands will be operational by the end of 2003.

Figure 3.1-1: Systems Test Laboratory

3.2 Solid Oxide Fuel Cell Stack Development (Task 2.0)

Typical stack testing is carried out using a test stand that has a hot furnace, electrical load bank and gas mixing cabinet (Lynntech Inc). Metallic cassettes for building stacks are fabricated by standard brazing procedures and are creep flattened before use. Cells are fabricated internally or bought from suppliers. A typical experiment involves measurement of standard polarization curves and power densities at constant voltages for durability.

The TCR stack test lab is approximately 200 square meters with 2 large high-temperature ovens for process development and individual cell construction. Two smaller ovens allow the build and test of a single cell to complete integrated stack manifold assemblies, and an additional smaller oven provides continuous testing for single cell and short stack tests. Currently all stack assembly and after-test investigations are preformed in this area. Materials development furnaces are also housed here and are used to investigate: glass seal development, interconnects, cell assemblies, oxidation and creep tests. The lab includes H_2 atmosphere ovens and 7 material testing furnaces.

Currently, the Metro Park stack testing laboratory is equipped with 4 short stack test stands capable of running all gaseous blends for single to 30 cell stacks, 1 large stand capable of running a complete integrated stack module, and 3 small stands for single cell development. Two additional large stands will be brought on line for continuous integrated stack module testing in 2003. The lab is fully automated and runs 24/7 as required.

Figure 3.2-1: Stack Testing Laboratory

The Interconnect Resistance Unit is a device that is used to characterize the electronic conductivity of the interconnects at operating temperatures. A current, at a density of 0.5 A/cm^2, is run through a double cathode "sandwich" as the specimen is heated at stack operating temperature in air. Various materials combinations and configurations for separator plate, mesh, bonding paste and current collector grid can be conveniently tested in the IRU. The Area Specific Resistance (ASR, ohm-cm^2) is calculated as ½ the measured resistance multiplied by the surface area. This test set up has been described in detail in previous reports under this program.

The seal rupture strength test unit is used for quantitative comparison of seal joint strengths. A metal washer with the sample is clamped into the fixture and air pressure is increased until the seal breaks and the ceramic bilayer disk pops off. This test set up has been described in detail in previous reports under this program.

3.3 Reformer Development (Task 3.0)

Three independent development stands are fully operational for reformer sub system development. The lab is equipped with both dSPACE® development software and with LabView® data acquisition software. Each stand has individual exhaust scrubbers and access to Two Orbital mass spectrometers. A Horiba emissions bench also exists but is not yet fully installed.

Figure 3.3-1: Reformer Test Laboratory – Rochester, New York

3.3.1 Tubular Reformer Testing Setup

Reformer testing in this period largely included testing of actual product hardware. Testing done on Tubular CPOx Reformers (Gen 1.0 and Gen 1.1) in the reformer lab employed a combustor configuration that was housed within the reformer base fixture. These tubular reformers as currently configured do not have integral combustors. This fixture-based combustor is different in geometry and smaller in size and capacity than the Gas Phase Combustor incorporated into the Integrated Component Manifold. Subsequently, flow rates, ignition location, and thermal performance are somewhat different.

A thermal enclosure is made of zircar-insulated panels and packed alumina insulation is utilized to simulate the APU thermal environment. Lastly, air supplies, where needed, are provided via mass flow controllers rather than actual product blower and air control valves.

3.3.1.1 Mass Spectrometer

A gas analysis system was utilized to quantify as many as 9 compounds on a real time basis for both the reformer outlet and combustor outlet streams.

3.3.1.2 Gas Chromatograph

A Gas Chromatograph exists to provide measures that are more resolute and speciation of Hydrocarbons in particular. A Sampling Gas Dryer System was added during this

reporting period for use with the Gas Chromatograph to more effectively remove water from the sample.

3.3.1.3 Emissions Bench

Emission measurement capability has not been available during this reporting period, as a new emission bench (specific for the Fuel Cell System application) is still being installed at the new test facility.

3.3.1.4 Controls and Data Acquisition

3.3.1.4.1 dSPACE®

A flexible I/O component driver and controller (dSPACE®) were utilized for all reformer testing. The use of dSPACE® allows any control algorithm to be shared between the lab environment and vehicle or systems environment so that system control strategies can be exercised in the lab with virtual transparency.

3.3.1.4.2 Advantech Data Acquisition and Control Module

All non-system mechanized I/O devices (i.e., those not on the product intent mechanization but present for enhanced lab data or control) are handled by this controller. This allows the lab environment to have supplemental I/O and devices beyond those on the mechanization. As testing progressed we gradually have begun to rely more on the dSPACE® I/O and less so on those supported by the Advantech Data Acquisition and Control Module controller.

3.3.1.4.3 Labview

Labview now serves as the “umbrella” controller and provides 2 key functions: 1) Integration of data acquisition of all other (non-product) devices for lab / facility control, and, 2) Emulation of system components not present in the test via lab devices (i.e., makes lab environment transparent to dSPACE® controller). This system has now matured to the point were data acquisition writes to a common file, including all variables from dSPACE®, the Mass Spectrometer and the Advantech Data Acquisition and Control Module.

3.3.1.4.4 Lab Fuel / Gas Controls

A gas blending cabinet was frequently used to simulate anode tail gas representative of what might leave the stack at various fuel utilizations. This was particularly important in understanding combustor behavior. For liquid fuel metering an AVL-735 unit provided accurate fuel measurement and conditioning. This provided a measure of safety given that actual injector hardware was subject to a harsh operating environment and could be subject to flow shifts.

3.3.2 Reforming Catalyst Development

3.3.2.1 Catalyst Durability

Currently, there are 3 catalyst durability stands running 24/7. General objectives of this equipment are to evaluate: Delphi catalyst performance, fuel sensitivity, and initial

durability and deterioration as well as competitive catalyst assessment. Tests typically run from 100 to 1000 hours. Three additional stands are expected December 2003 and 5 to 10 stands will be added in 2004.

Figure 3.3.2.1-1: Catalysts Development Laboratory

3.3.2.2 Catalyst Preparation

Reforming catalysts are built using methods based on those currently employed for the commercial manufacturing of automotive exhaust catalysts. In brief, a washcoat slurry, consisting of the catalyst support dispersed in water, and adjusted for pH and particle size, is applied to the substrate. Application methods include flow through or push/pull. The washcoated substrates are then optionally dried and then heat-treated in air at about 540 °C for 2 hours.

Active metal and support modifiers can be added by several means. The most commonly employed method is to add these directly to the slurry, prior to coating of substrates. We have also employed incipient wetness of the support powder, prior to forming a slurry, or equilibrium adsorption onto washcoated substrates. Powders or parts so formed are either dried in air at 110 °C or directly heat treated at 540 °C. If required by formulation or loading, multiple washcoat passes can be applied, each pass with separate heat-treating steps.

3.3.2.3 Catalyst Testing

Catalysts were tested using fully instrumented tubular reactors equipped with external heaters, gas and mass flow controllers, optional liquid product condensers, and a gas

chromatograph for product analysis, permitting verification of set flow rates via mass balance calculations. Catalyst temperatures can be controlled by either varying reactant flow rates or by adjusting the air to fuel ratio. These adjustments are made depending on the requirements of the test. Catalysts are held in vertical tubes operated either in down- or up-flow modes. Liquid feeds are preheated so as to be fully vaporized prior to reaching the catalyst. Steps are taken to assure that good mixing between air and fuel is obtained ahead of the catalyst as well.

For durability testing, space velocity is lowered so as to produce a catalyst center temperature of about 950 °C, while maintaining an air-to-fuel oxygen-to-carbon molar ratio of about 1.05. This results in catalyst center temperatures close to the recommended use temperature of the current catalyst product. For the 'aggressive testing protocol', the same oxygen to carbon of 1.05 is used, but the space velocity is raised so as to give a catalyst center temperature of about 1050 °C. To reach higher temperatures during aggressive testing, the oxygen to carbon ratio is increased by increasing air flow rate and keeping fuel flow rate constant.

Oxidative aging, designed to thermally stress catalysts, is conducted by exposing catalysts samples to 1200 °C, in air, for six hours, followed by an extended cooling period. These aged samples are then tested as described.

The same catalyst test stands were employed for methane partial oxidation, auto-thermal reforming, and steam reforming, using the same basic methodologies. A more extensive use of external heating was required to maintain desired catalyst temperatures.

Likewise, for evaluation of selective oxide-sulfurization processes, the same test stands were employed. No gas analysis was conducted, and mass balances were obtained by condensation of products at ~ 2 °C.

Similar test stands were employed for studies involving sulfur addition to the fuel. In this case, a provision was made to rapidly switch fuel or gas feeds between different sulfur concentrations, resulting in step-changes in sulfur concentration.

3.3.2.4 Catalyst Evaluation

Catalysts were prepared for analytical testing by crushing of entire samples. The resultant powders were then loaded as appropriate for the particular analytical instrument.

3.4 Development of Balance of Plant Components (Task 4.0)

Balance of Plant development test labs are located at Technical Center Rochester. The lab is approximately 100 square meters and is used for the development of: Sensors, actuators, thermal insulation, air process system, and high-temperature gaskets and interconnects.

The following Balance of Plant Components have been tested independent of the Fuel Cell System, and special test methods have been developed by the Balance of Plant group:

- Hydrogen Sensors
- Air Delivery and Process Air Subsystem Components
- Hot Zone Components
- Gaskets
- Integrated Component Manifold
- Cathode heat exchangers
- Resistance Temperature Detector
- Thermocouples
- Igniter

3.4.1 Hydrogen Sensors

3.4.1.1 High Concentration Hydrogen Sensor

Delphi has identified at least three possible approaches to be evaluated as control strategies for the reformer. They are:

- Measure the functional inputs (air and fuel ratio) to the reformer, together with the exit temperature of the reformate. This technology is well established within Delphi.

- Measure the dysfunctional outputs of the reformer, like methane, and equate this gaseous level to the levels of the functional outputs of hydrogen and carbon monoxide. Theory supporting this mode is that other gas species like methane are easier to detect.

- Continue development of a hydrogen sensor that does not have the cross-sensitivity and contamination issues with other gas species.

3.4.1.2 Combustible Gas Sensor

A mounting arrangement for the Delphi sensor and controller in the APU was developed, and control algorithms incorporated into control software. The final test for the sensor will occur in a fully enclosed Solid Oxide Fuel Cell System where an artificial leak will be created and the full Safety Control Algorithms will be demonstrated.

3.4.2 Air Delivery and Process Air Subsystem

Development activities on the Air Delivery and Process Air Subsystem during this reporting period focused on evolving the first basic design. This resulted in a modular design concept with component integration of air control valves and mass airflow sensors into a manifold. This manifold also serves as the air intake for the Process Air Blower and provides a common mounting block for the blower motor. The new Process Air Module, otherwise known as the PAM unit, greatly reduced the complexity of the Process Air Subsystem and streamlined the design. Prototype assemblies were built

and testing to date involved characterization of the second generation Process Air Module with a comparison to the baseline, and characterization of a Delphi impeller. Additionally, tests were performed for characterizing and calibrating the process air control valves and mass air flow sensors, as well as investigative tests to study the effects of flow straightening devices on mass flow sensor noise. Figure 3.4.2-1 shows the new Process Air Module.

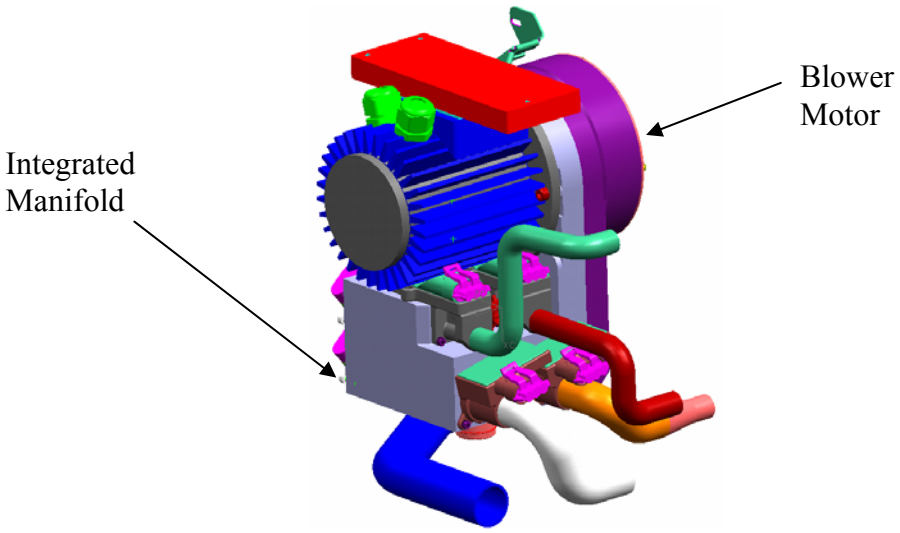

Figure 3.4.2-1: Generation 2 Process Air Module

3.4.2.1 Description of Process Air Module Components

Air Manifold – The first generation manifold supplied by Rietschle was studied and its dynamic features were incorporated into the GEN-2 integrated manifold. Within the inlet section of the manifold, inlet guide vanes were improved to better feed the air to the inlet of the impeller. The improvements to the guide vanes induced a pre-swirl to the air in the direction of rotation of the impeller. This improves the hydraulic efficiency of the machine and increases blower capacity. Flow straighteners were incorporated within the air control valve seats of the manifold to eliminate or minimize downstream mass flow measurement errors caused by flow instabilities.

Air Control Valves – Delphi's standard Idle Air Control Valve assemblies are incorporated into the Integrated Manifold shown in Figure 3.4.2-1. Specially designed pintles were fabricated to achieve better flow resolution and lower pressure drop over the design stroke.

Mass Air Flow Sensors – Delphi (Flint) continued to supply a prototype, geometry specific, hot-wire anemometer flow sensor. One version is shown in Figure 3.4.2.1-1. Currently in the GEN-2 Process Air Module there are four flow sensors with this basic geometry. The sensors have three flow ranges: 0-3, 0-6 and 0-20 g/sec. The housings for the sensors are currently manufactured using Stereo Lithography (SLA) generated parts.

Figure 3.4.2.1-1: Mass Air Flow Sensor Geometry Made From SLA Parts and Integral Honey-Cell Flow Straightener

Plant Support Module Purge Valve – This valve, currently located in the Process Air Module is a standard Delphi Canister Vent Solenoid. It is designed to be normally open, and in the Fuel Cell Application it must be energized the majority of the time to remain closed, and de-energized when a purge is desired. This presents a constant parasitic loss to the system and also creates life issues for the valve itself. During this reporting period, Delphi's supplier of the valve was contacted. The valve was re-designed to be a normally closed valve. The new valves, upon fabrication and testing by the supplier, will be incorporated into future Process Air Modules.

Rietschle Blower – The process air blower in the Process Air Module (PAM) is a two-pole, 42 VAC motor from Rietschle. It has a rated speed of 55,000 RPM, a maximum rotational speed of 60,000 and a rated current draw of 12 A DC with a maximum draw of 17 Amps. A Requirements Document was prepared which fully describes the fit and functionality of the blower motor.

Tubing/Air Hoses - In an effort to eliminate the harmful effects of silicon on Fuel Cell Stacks, all silicon hoses in the Process Air System were upgraded to Ethylene Propylene Diene Monomer Polymer Rubber (EPDM) material. During this reporting period, Delphi solicited competitive quotes, identified a supplier for prototype hoses, ordered and received prototype hoses.

There were three main tests developed for the Process Air Module. They include: airflow sensor calibration, a flow instability investigation, and Process Air Module comparison (second generation versus baseline). Below are excerpts from Delphi's

standard test documentation process. The excerpts describe the test objective and general test approach for each of the tests.

3.4.2.2 Mass Airflow Sensor Flow Calibration Test

TEST OBJECTIVE:

To calibrate mass airflow sensor voltage.

APPROACH:

Calibration of sensor to occur using a Delphi flow stand with sensors installed in the Process Air Manifold. Pressurize Manifold to 15 KPa. Connect outlet of flow stand to inlet supply of process air manifold. Adjust stand flow to desired flow-point and record sensor volts for the given flow.

3.4.2.3 Mass Airflow Sensor; Flow Induced Instability Test

TEST OBJECTIVE:

To quantify and correct flow instabilities caused by the Air Control Valves (pintles) on the Mass Air Flow Sensors.

APPROACH:

The test will involve placing and characterizing various types and positions of Flow Straighteners. Figure 3.4.2.3-1, position 'A' is with straightener located directly after the pintle. Position 'B' is with straightener farther down stream of the pintle and located in the Mass Air Flow Sensor. Test fixture set-up is depicted in Figure 3.4.2.3-1.

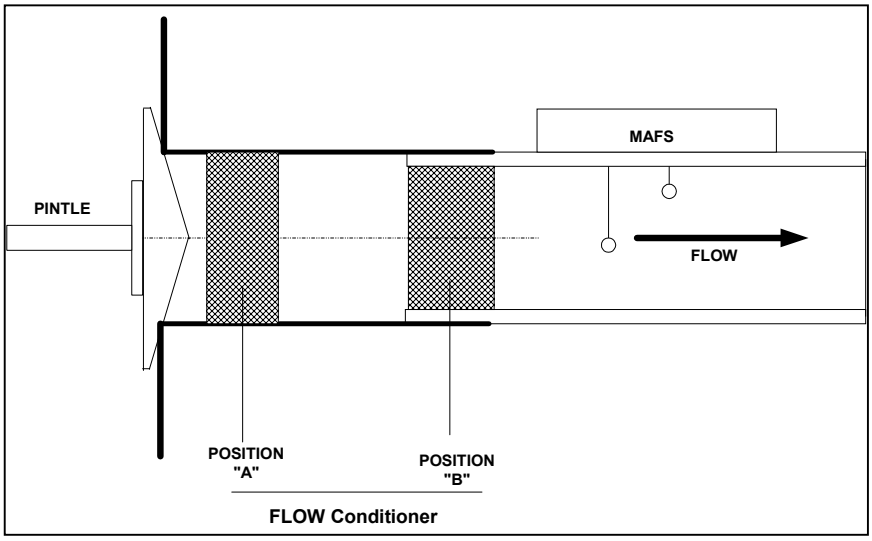

Figure 3.4.2.3-1: Flow Condition Position in Relation to Pintle

3.4.2.4 Comparison of Rietschle Impeller to Impeller Designed by Delphi Test

TEST OBJECTIVE:

To compare the performance between the compressor wheel supplied by Rietschle and one designed by Delphi to ensure that the Delphi Impeller meets and/or exceeds design requirements.

APPROACH:

Use a previously calibrated Mass Air Flow Sensor. Establish a baseline performance using the Rietschle impeller in the manifold supplied by Rietschle. The test is to be conducted at the rotor maximum speed. Start recording data with no load (discharge restriction fully open) on the compressor wheel. Record flow as indicated by the Mass Air Flow Sensor versus discharge head.

Without changing motor control settings, remove the Rietschle impeller and install the Delphi impeller. Record flow as indicated by the Mass Air Flow Sensor versus discharge head of the new impeller.

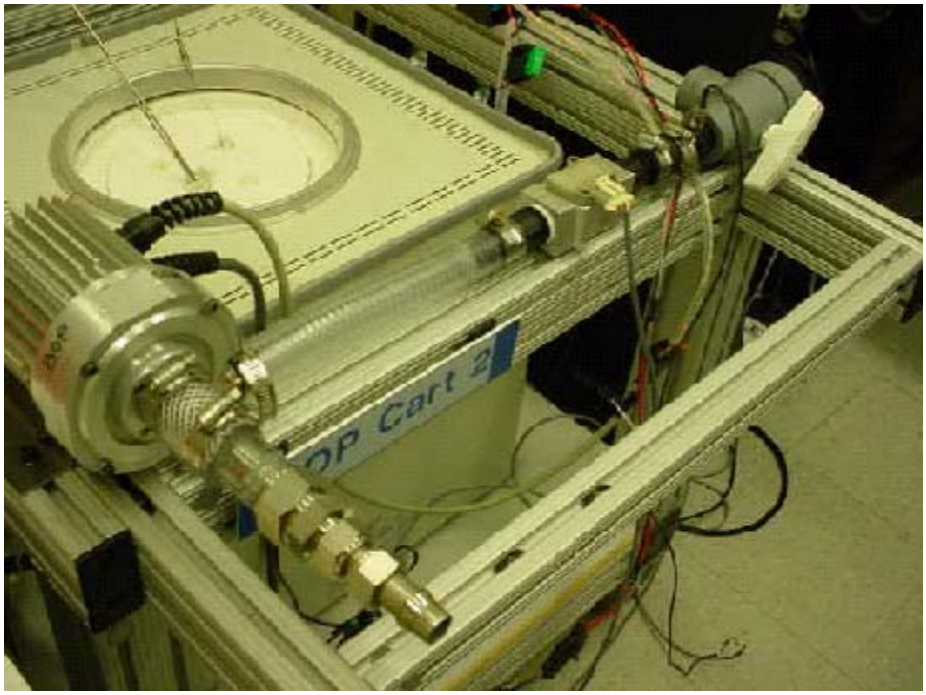

Figure 3.4.2.4-1: Impeller Test Set-Up

3.4.3 Hot Zone Components

3.4.3.1 Gaskets

Gasket development has focused on the design of unique high-temperature sealing devices suitable for the aggressive Solid Oxide Fuel Cell environment.

Gasket testing is performed on a leak detection bench capable of measuring airflow from .1 to 5000 sccm, (standard cubic centimeters per minute). Gaskets are placed between plate fixtures and bolted together such that the loading produced is similar to what they would be subject to in a full system. The plates are ½" thick inconel or stainless steel with surface finishes set to the same guidelines governing the sealing faces of the system. Between the plates, the pass-through ports of the gasket create cavities that can be pressurized to check for seal integrity. Individual taps for each cavity through one of the plates connect to a source of pressurized air in-line with the flow meters of the leak detection bench. Each cavity is tested individually.

A valve lies between the leak detection bench and the fixtured gasket. While the valve is closed, pressure in the line is regulated to a point within the range expected during system operation for the particular gasket and port. Upon opening the valve, the pressurized air is applied to the cavity and the resulting leak rate is recorded along with the amount of pressure retained by that particular port. All testing is currently conducted using room temperature air (23 ^{o}C).

3.4.3.2 Integrated Component Module

The ICM, Integrated Component Manifold, is the critical APU device on which all hot zone components are mounted. The manifold allows for internal ducting of all high temperature inlet and exhaust air, fuel and waste gases. In the system, this component is exposed to steady state operating temperature ranges of 700 ^{o}C to 1000 ^{o}C and internal pressures that range form 15 to 45 KPa gage. Overall, the internal passages of this component are exposed to temperature ranges are from –40 ^{o}C on cold start-up to 1650 ^{o}C internal flame temperatures. The construction of the ICM is accomplished by brazing together 5 layers of High Temperature Nickel Alloy materials.

Figure 3.4.3.2-1: ICM Assembly and Thermal Enclosure

After two to three thermal cycles during routine system tests, the surface of the top plate appeared to be distorted and was no longer flat. This exacerbated leaks at gasket sealing interfaces. A root cause investigation was undertaken. The investigation first involved developing a reliable measurement procedure to quantify the ICM's top plate surface profile, identifying specific locations and exact amounts of distortion.

ICM SURFACE PROFILE CHARACTERIZATION:

The SOFC / APU hot zone component mounting surface of the Integrated Component Manifold is a ground planar surface. This surface requires a flatness of 0.127 mm across the entire X & Y plane. Distortions have occurred after high temperature operation requiring extensive rework. The purpose of this procedure to record the methodology developed to measure the surface flatness before and after the thermal cycling of each APU system assembly.

MEASUREMENT EQUIPMENT:

Coordinate Measuring Machine (CMM), manufactured by Ziess, in Germany

Model number = 18070

Last calibration = February 6, 2003

Measured repeatability = 1 micron (4 x 10-8 inch) reported by operator, actual repeatability not known at this time

Floor isolation is by air pads to the concrete floor

Recorded data is to three decimal places (0.xxx), in millimeters

All measurement locations are pre-programmed and computer controlled

Time required for complete profile is approximately 20 minutes

ICM SETUP:

The procedure for establishing a reference plane on the Top Plate follows:

Three precision ground standoffs of uniform height ground within 0.0127 mm (0.0005 inch) are used as standoffs. An ICM is placed on the standoffs establishing a three-point plane. See Figure 3.4.3.2-2 and Figure 3.4.3.2-3. The CMM stylus is lowered to establish six points of reference in the Z-axis. On board computer calculates an average reference height plane. The X & Y coordinates are referenced from (2) 5/16" cap-screw clearance holes near the outer edges of the ICM. See Figure 3.4.3.2-4 and Figure 3.4.3.2-5. This allows repeatability of measurement locations one ICM to another or repeated measurements of any ICM. After the reference plane is calculated a series of points are measured in the Z-axis forming an X, Y matrix of 290 points spaced at 10 mm centers across the face of the ICM Top Plate. See Figure 3.4.3.2-6. Each point measured is recorded with a (+ or –) value relative to the calculated reference plane.

Figure 3.4.3.2-2: ICM Positioned On Three Point Plane

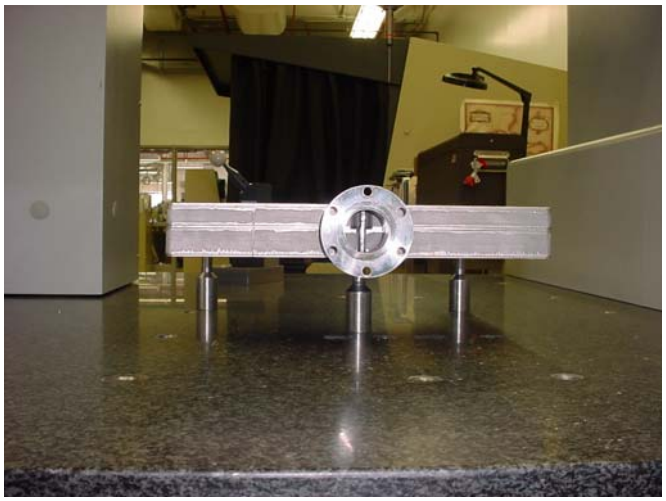

Figure 3.4.3.2-3: BOP ICM Positioned On Three Point Plane As Viewed Back

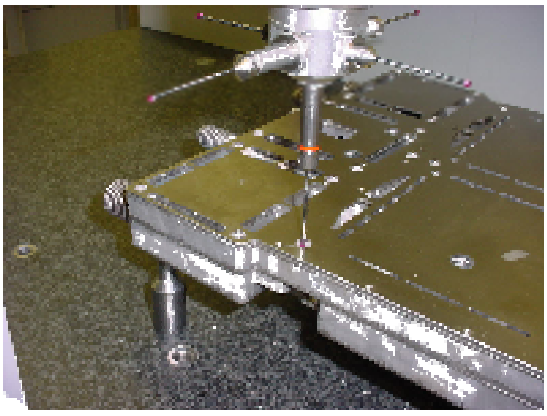

Figure 3.4.3.2-4: ICM Positional Right Side Datum Hole

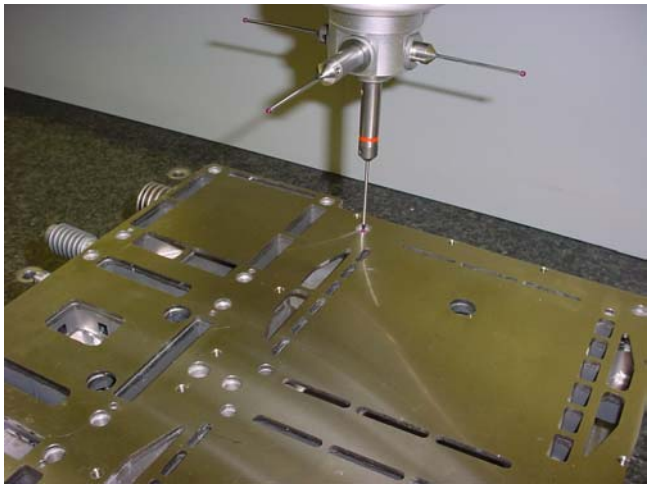

Figure 3.4.3.2-5: ICM Positional Left Side Datum Hole

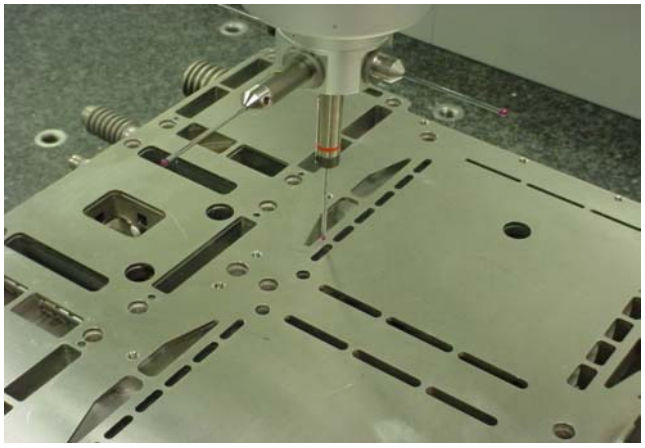

Figure 3.4.3.2-6: ICM Typical Surface Profile Scan

In addition to the surface profile characterization, a Finite Element Analysis, FEA Investigation was performed to give further insight to the problem.

ICM STRUCTURAL LOAD CONTRIBUTORS:

Operating temperature gradients

Bolt reactions to seal pressure (e.g. stack Fbolt, max~100lbs)

Seal pressure (e.g. Pstack~400N/4000mm2=15psi)

Machining stresses, effects of re-grind operations

Thermal cycling

Gravity

Braze/Haines 230 Coefficient of thermal expansion (CTE) mismatch

Loads considered in present analysis

FINITE ELEMENT ANALYSIS DESCRIPTION:

ABAQUS solver with second order tetrahedral elements

Nonlinear (large displacements & material plasticity due to yielding and creep)

Half symmetry model

Analysis is a two-part process. The FEA is a:

1. Steady state heat transfer to obtain SS thermal map
2. Structural to obtain displacements, stresses, etc., as a result of (1)

Finite Element Mesh of ICM is shown in Figure 3.4.3.2-7.

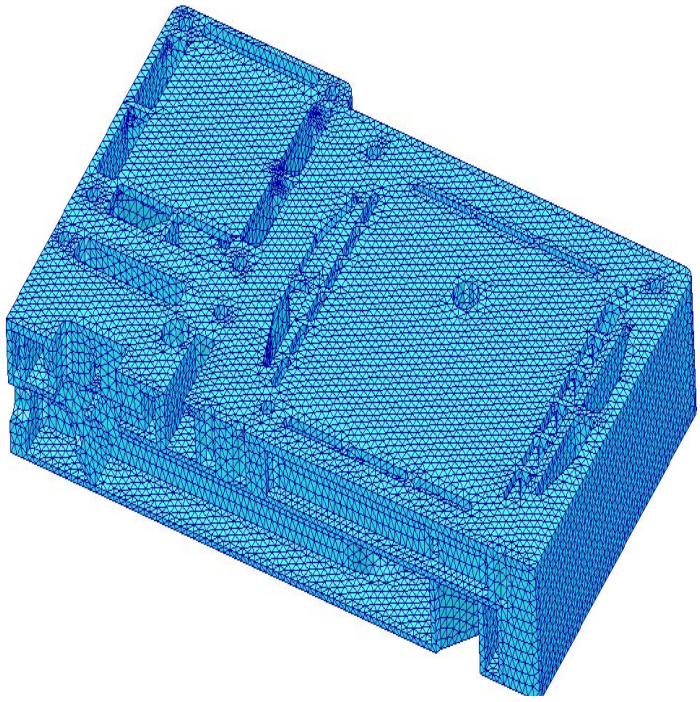

Figure 3.4.3.2-7: Finite Element Mesh of ICM

HAYNES 230 MATERIAL PROPERTIES USED IN MODELING:

Young's Modulus: E(25 ºC) = 211 GPa

E(500 ºC) = 138 GPa

E(900 ºC) = 118 GPa

Yield Strength: YS = 180 MPa

Ultimate Strength: UTS = 300 MPa

Elongation at Break: e = 65%

Thermal Conductivity: k(25 ºC) = 8.9 W/mK
k(500 ºC) = 18.4 W/mK
k(900 ºC) = 26.4 W/mK

Creep Law: (time hardening)
dcreep/dt = Aqntm
where A = 5.1777E-22
n = 9.2541
m = -0.1
q = stress potential
t = time

Figure 3.4.3.2-8 below shows the boundary conditions used in the modeling.

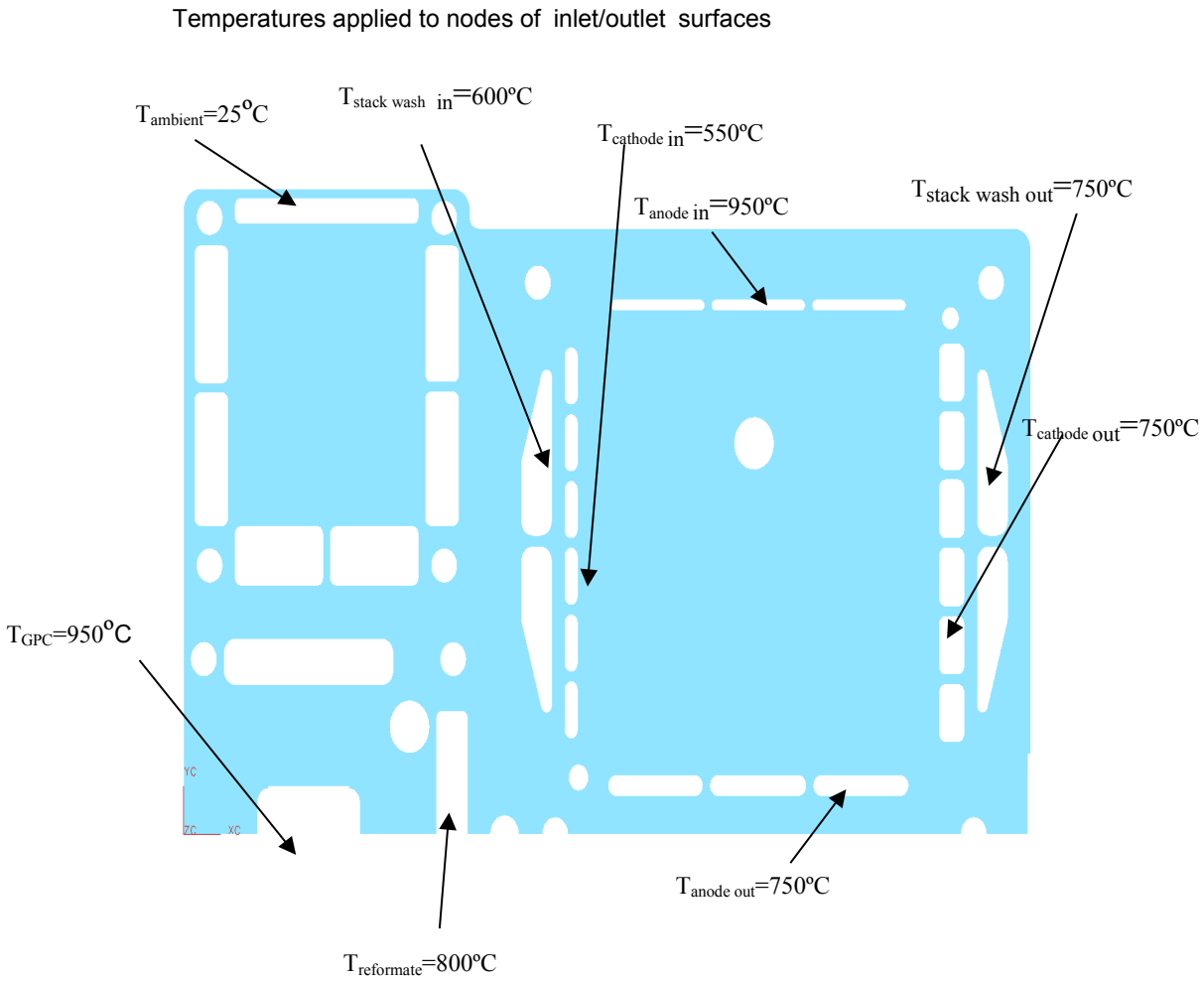

Figure 3.4.3.2-8: Finite Element Temperature Conditions

3.4.3.3 Cathode Air Heat Exchangers

During this period, Delphi has continued to refine the Cathode Air Heat Exchanger design with a focus toward increased efficiency while maintaining a low backpressure allocation. The basic flat plate design was modified by the inclusion of a fin material in the bar area to increase surface area for heat transfer. The added material mass, required further braze development and braze process optimization. Destructive analysis of the first fin parts showed gaps between the fin and plate material. These gaps reduce heat transfer and thus impact effectiveness. The gaps were eliminated by minor part specification changes and improving the quality of component parts. Figure 3.4.3.3-1 below, shows the Non-fin and Fin Heat Exchangers.

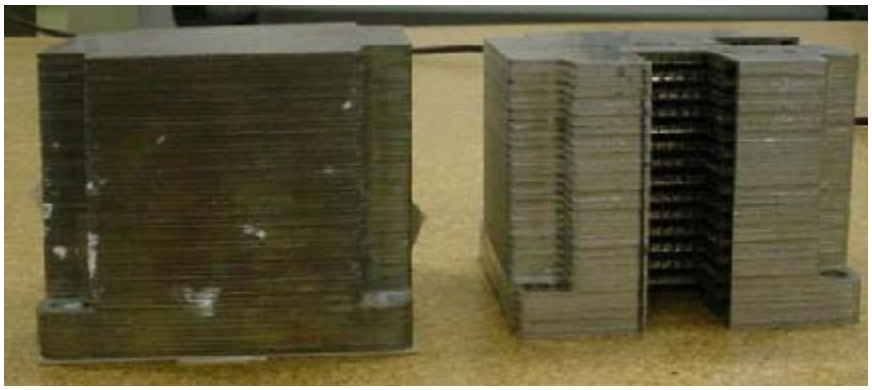

Figure 3.4.3.3-1: Non-Fin and Fin Heat Exchangers

The turn-down ratio over the operating range will be addressed by manipulating the backpressure of the heat exchanger. Two configurations have been identified and will be tested. The two approaches are varying the angle of the fin material orientation in respect to the air path and introducing restrictions on the exit side of the air paths. Initial test of fin orientation will be at a 45-degree angle to the air path. For the exit airflow restriction investigation, restrictions of 30, 40, and 63% have been selected for investigation.

Cathode Air Heat Exchangers have been tested on Reformer test stands, temporarily configured, to accommodate heat exchangers. This allowed the use of standardized test procedures and data collection analysis. The heat exchangers were mounted to a test fixture manifold in a horizontal orientation. An incoming air supply was manifolded into two streams. One stream (acting as the heated air from the Integrated Component Manifold) was passed through a mass flow controller, then an air heater, introduced into the heat exchanger and exhausted to outside vent. The second air stream (acting as the systems incoming fresh air supply) passed through a mass flow controller, then into the heat exchanger and exhausted to an outside vent. Thermocouple monitoring of the air streams (in and out) allowed efficiency calculations. Pressure sensors allowed monitoring of the pressure drop of the air streams. Both the temperatures and flows of the two air streams are independently manipulated to approximate actual conditions in the system.

A new, dedicated test stand for heat exchangers is currently being assembled utilizing a similar approach. This stand will be independent of the Reformer test stands, and will increase test throughput. Features of the new stand will include:

- Vertical mounting of heat exchangers to duplicate application and provide for easier mounting.
- Fixturing and sensors for two exchangers at a time - duplicates quantity of heat exchangers in the APU and increases throughput.
- A blower to provide cool air stream similar to actual operation of the APU.
- An increased number and sensitivity of temperature and pressure sensors to better refine characterization of exchangers.
- Smaller footprint (approximately two-thirds smaller than reformer stand); thus occupying less lab space.

A test program will be designed with the goal of automation to allow testing to automatically step from one flow level/temperature to another and ultimately shut down when the test cycle is complete.

3.4.3.4 Resistance Temperature Detector (RTD)

The development trend for an accurate and reliable Resistance Temperature Detector shown in Figure 3.4.3.4-1 has changed from a Platinum wire wound construction to a Platinum thin film type.

Figure 3.4.3.4-1: Thin Film Resistance Temperature Detectors

The thin film construction promises to be less sensitive to thermally induced stresses, and with improved encapsulation material, oxidation of the Platinum will be minimized. Currently, there are several of these Resistance Temperature Detector types on 1000-hour test. Test completion and evaluation is due later this year. Continued development and testing of Resistance Temperature Detector is planned because of the

advantageous characteristics of these devices, such as higher accuracy, good linear response and less noise susceptibility as compared to thermocouples.

TECHNIQUE TO TEST RESISTANCE TEMPERATURE DETECTOR:

TEST OBJECTIVE:

To characterize the durability, accuracy and drift of Resistance Temperature Detector's, and evaluate failure modes of the devices.

APPROACH:

Record initial resistance of each Resistance Temperature Detector at ambient room temperature using calibrated multi-meter. Group Resistance Temperature Detector elements tightly and place thermocouple in a group. Place in calibrated oven at a test temperature of 950 ^{o}C for 1000 hours. Audit at daily intervals, recording resistance.

3.4.3.5 Thermocouple Development

In order to continue with APU control development and system test, reliable temperature measurement was needed. With the high incidence of failure rate of Resistance Temperature Detector elements, a decision was made to switch to thermocouples. This allowed for system tests to continue. ANSI (American National Standards Institute) Type K thermocouples were specified and purchased from Marchi Systems, a Celerity Group company.

The Marchi thermocouple signal conditioner/amplifier system is a small footprint self-contained solution for converting the milivolt output from a thermocouple into an analog control voltage. The systems are contained on a single PC board with up to seven channels of I/O. They operate on a single ended DC supply voltage and can be configured to generate a linear voltage signal at either of the two standard control ranges of 0-to-5 Vdc or 0-to-10 Vdc. The supply voltage can be any available supply from 12 Vdc to 30 Vdc without affecting the outputs. All thermocouple channels are individually processed and ice point compensated.

Thermocouple amplifiers allow easy integration of thermocouples into a typical Programmable Logic Control (PLC)-based control system or other analog voltage input system without the need for expensive temperature indicators. For applications requiring voltage control, a Resistance Temperature Detector is the typical solution, but often, operating temperatures are too high or too low for Resistance Temperature Detector's. Thermocouples are capable of stable indication over a much wider range than Resistance Temperature Detector's and survive at much higher temperatures. Thermocouples are largely immune to damage from vibration and shock that can easily destroy a Resistance Temperature Detector. To date, Delphi has successfully completed a 1000-hour endurance test of the Marchi thermocouple system at an operational temperature of 950 °C.

TECHNIQUE TO TEST THERMOCOUPLES:

TEST OBJECTIVE:

The test objective is to characterize the durability, accuracy and drift of Thermocouples and signal conditioner.

APPROACH:

Place five thermocouple elements in calibrated oven at a test temperature of 950 ^{o}C for 1000 hours. Audit at daily intervals, temperature.

3.4.3.6 Igniter Developments

Ceramic igniters were previously selected due to their low current draw, rapid heat-up, and ability to withstand high temperatures. After numerous failures in both the System and Reformer testing a root cause analysis was performed. The cause of the igniter failures was determined to be due to basic material properties and the design of the igniter. The failures occurred at the junction of heating element and electrical wire connection interface. This junction is embedded in a ceramic sealant inside the hard ceramic shell of the igniter. Failure was evident by the degradation of electrical response of the device. Figures 3.4.3.6-1 and 3.4.3.6-2 show the common failure mode. Follow-up discussions with the vendor resulted in new prototype igniters with higher temperature metals and a higher temperature braze alloy. New igniters were received and are currently in use in reformer and system tests.

Figure 3.4.3.6-1: Failed Igniter Showing Connection Weakening, Burn Diffusion Along Interface With Tube Shell

Figure 3.4.3.6-2: X Tip/Connector/Wire Junction Failure

3.4.4 Plant Support Module Components

3.4.4.1 Fuel Delivery and Fuel Metering

Another group of fuel injectors were fabricated, assembled and tested during this reporting period. Results of this group were similar to prior builds, and thus show this injector design concept to have good manufacturing repeatability. The fuel injectors were tested using Delphi's standard Automotive Fuel Injector Tests; specifically flow curves, particle size measurement and spray patternation tests.

Testing/characterization of the natural gas injectors is to be performed by the Reformer team.

3.5 Manufacturing Development (Privately Funded) (Task 5.0)

Significant developments are reported in individual subsystem areas.

3.6 System Fabrication (Task 6.0)

Subsystem parts were fabricated and up-integrated into system sub-modules for evaluation. These system sub-modules allow for easier assembly, service access, troubleshooting, and instrumentation deployment over full Auxiliary Power Unit level system hardware. Details of this development strategy are given in Section 4.1.

In this reporting period, the system fabrication experimental approach continues to focus on preparation of modules for development. This period had the system efforts looking at many second-generation components configured into new modules. In interest of increasing the flexibility of the product to adapt to various applications and allow more modular fabrication, the application interface module has been added to the system approach. This module, much like the other two, will able to be designed, fabricated and assembled / tested independent of the final product assembly.

The three-tier approach (Independent system module development, close-coupled module system development, and Product Assembly System) focused on fabrication and development of the revised Gen 2B system modules and the operation of these 3 system modules in a close-coupled configuration. This allowed the system controls

development to progress with all required parts of the system without the added difficulty of the Product Assembly packaging.

3.6.1 Generation 2A System Fabrication Assessment

An analysis of the system to date was completed. Assessment of assembly and fabrication issues of the modules was completed along with mass and volume measurements. These established some of the design goals of the future generations of system components and modules. This data will be the basis for several significant Gen 3 design decisions in the second reporting period of 2003.

3.6.2 Hot Zone Module Fabrication and Assembly Approach

The Hot Zone Module assembly approach maintained an increased level of measurement ports for additional data collection during system tests. As the core module of the product, a majority of the testing is done with this hardware. Fabrication and assembly of the insulation systems was compromised at times for this access. Better fitting and developed insulation solutions will be accomplished in final product assembly efforts. Sample ports, repairs, and modifications were added during initial brazing and build. Additional work after was done using a manual TIG welding process.

3.6.3 Plant Support Module Fabrication and Assembly Approach

The Plant Support Module assembly approach (including the system space frame) was to assemble and complete fabrication of the bracketry and wiring not completed in the basic solid modeling / CAD used to layout the components. Changes were necessary for the application interface module and the functions that it would undertake for the product. When complete, this module receives the Hot Zone Module for close-coupled testing. An additional test cart for the system for airflow delivery and control was developed and fabricated to allow simple reconfigurations of system flows. This approach allows for more precise measurement and fast implementation of air metering concepts (both hardware and software driven).

3.6.4 Application Interface Module Fabrication and Assembly Approach

The Application Interface Module assembly approach focused on fabricating a compact interface that combined all the inputs and outputs to the system (except for system exhaust). The housing for this needs to be low in mass and volume. The air filter housing and the electronics hardware dominate the interface module fabrication. This approach will also allow concurrent development of this module and ultimately allow the adaptation to new markets without large disruption to the other modules.

3.6.5 Product Enclosure Fabrication and Assembly Approach

The housing for the system had no change in approach in this period except for the new coordination of the application interface module. The main internal modules (Hot Zone Module and plant support module) are assembled and installed in a vertically oriented manner. The product enclosure fabrication did not address additional environmental and safety issues in this period.

3.7 System Testing (Task 7.0)

See Section 3.1 on Experimental Approach.

4.0 RESULTS AND DISCUSSION

This section will summarize all relevant data, and interpret how results relate to developing the overall 5 kW Solid Oxide Fuel Cell system.

4.1 System Design and Integration (Task 1.0)

4.1.1 Define System Requirements

A product development plan with intermediate achievement targets for the major subsystems has been developed over the period covered by this report. The development plan has been generated with a focus on the mobile Auxiliary Power Unit (APU) using liquid fuels. Generally, the targets defined for various design levels for mobile applications are more aggressive than those required for a Stationary Power System on Natural Gas fuel. Issues such as fuel handling, fuel desulfurization, and application power interfaces are application specific, and are not addressed in the defined targets at this time.

The definition of product design level generally follows the Solid Oxide Fuel Cell Stack design level, with a suffix letter defining a System Auxiliary Power Unit design level. For example, the current generation of APU hardware with Generation 2 Solid Oxide Fuel Cell Stack technology is identified as Gen 2B. This represents an evolution of APU design over the Gen 2A design discussed in the previous technical report.

High-level, Solid Oxide Fuel Cell Stack and Fuel Reformer performance targets, as well as Subsystem allocations for system mass, system package volume, component efficiency, parasitic load, and subsystem costs have been created each design level in the product development plan during the period covered by this report.

4.1.2 Develop Conceptual System Design

The conceptual system design (Gen 2B) for the system has progressed during the period covered by this report. New features in the design include:

- Configurable Application Interface Module (AIM)
- Modified Open Access Space Frame
- Improved Process Air Module (PAM)
- New Gen 1.1 Tube Pox Reformer
- Improved Solid Oxide Fuel Cell Stack Terminal Interface
- Improved Reformer Insulation Pass-Through Collar

The Gen 2B conceptual system design is shown in Figure 4.1.2-1 with the Gen 2A design for reference.

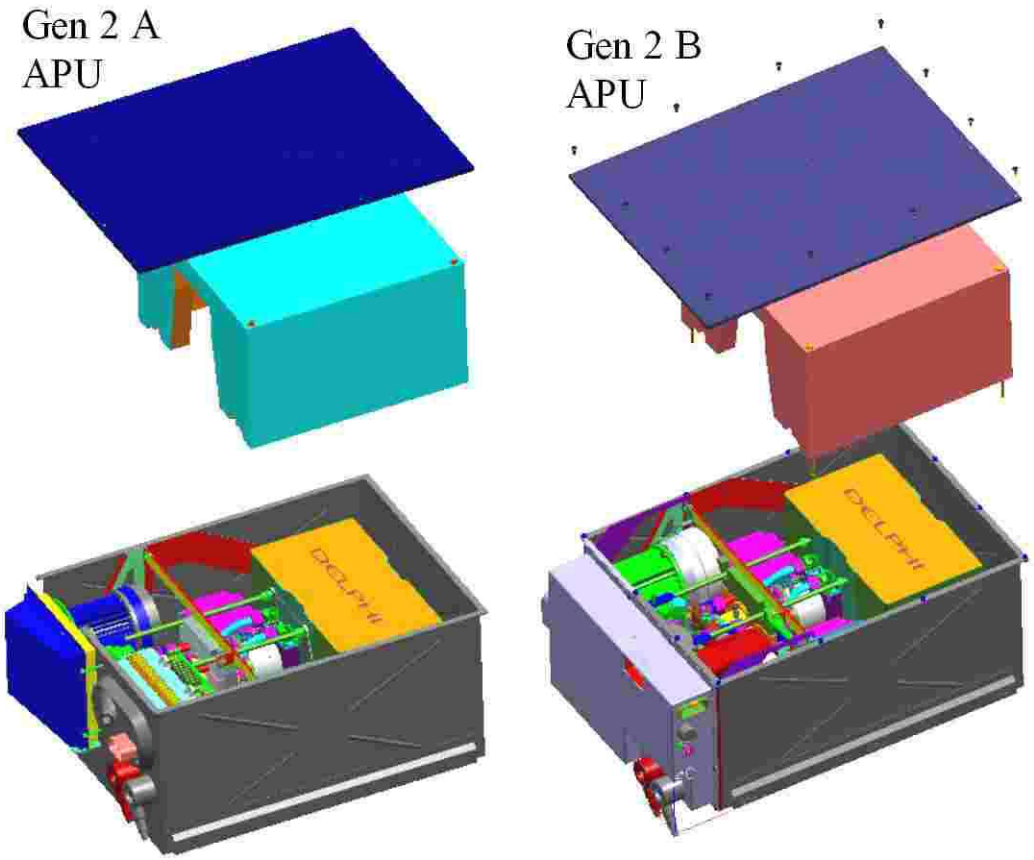

Figure 4.1.2-1: Generation 2 Auxiliary Power Units

4.1.3 Develop System Mechanization (schematic)

System Mechanizations have been created to support the Gen 2 and Gen 3 APU applications. In addition, a Gen 3 Mechanization has been developed to support a Natural Gas Stationary Power Units (SPU).

4.1.4 Establish System Thermal Insulation Requirements

No new activity during this reporting period.

4.1.5 Provide System Design Support for the Fuel and Air Delivery Systems

See Section 4.6 (Balance of Plant).

4.1.6 Systems Control Development

The Delphi Solid Oxide Fuel System Control System is now approaching a fully functional system capable of completely automatic control of the auxiliary power unit. Fully automatic control of auxiliary power unit warm-up, initiated from an external control source, has been demonstrated multiple times. The system now sequences

automatically through passive initialization, active self-test, multi-phase reformer light off, stack warm up, and normal run. During these phases, 9 temperature and flow control loops are active, and are monitored by a security system for many conditions including in-range sensors, and in control closed loop performance. In the current system, when enabled, any failure will cause an immediate shutdown. More sophisticated and graceful response to system failure is planned.

4.1.6.1 Control System Development Stage

Though all the algorithms intended for this level of development are coded, some still require further debuging, calibration and development. Reformer control, process air control, and system temperature control are basically complete. The stack control and power management and safety and diagnostics areas are approximately 75% developed. Completion of these areas is expected within the month.

4.1.6.2 Control Development Environment

The control development process has also advanced during the reporting period. Further refinement in the distributed algorithm and calibration development environment, with corresponding control, plant, and operator interface models upgrades, has resulted in highly coordinated and integrated single focus control system. By single focus it is meant that multiple developers and calibrators are able to modify the control system at the same time, within daily releases. These releases are then distributed to multiple sites for use in multiple purposes ranging from desktop simulation, to embedded auxiliary power unit emulation at a customer site, to auto-code source for a production intent controller.

4.1.6.3 Integrated Dynamic Simulink® Model for Control

Embedded in the overall control development structure is a Simulink® model of the auxiliary power unit plant. This model receives actuator commands from the control model, and sends back sensor states to the control module. This model has enabled rapid development of system control, and hybrid real-time control of a system where partial or not-fully competent system hardware is available. The plant model is used in virtual runs for example on the electric emulation bench to develop power management control algorithms. In addition, the plant model has been used to evaluate “plant support module (blower, air control valves, and air meters)” function throughout a virtual run using different simulated temperatures without having to heat up the system. In a later section, we will discuss results from this plant model, and how they compare to actual hot test runs.

4.1.7 System Analysis

4.1.7.1 Dynamic Simulink® System Model

The dynamic Simulink® model of system performance, in addition to being used in control system development, it is also used for system design analysis. The model now includes a representation of the real cathode pre-heater performance as measured experimentally. Previously this model was an “ideal” heat exchanger since the experimental data had not been completed. Pressure dynamics, which were competed

at the time of last report, have not been utilized since the model now takes substantial time to simulate a full warm up. The model runs approximately in real time on an HP workstation. The batch run environment has been utilized with an enhanced run schedule environment to try out different combinations of control set points (e.g. gas phase combustor temperature set-point) and plant component configurations (e.g. different cathode pre-heater design representations). These runs have shown us the sensitivity of the starting time to such things as the stack mass, gas phase combustor temperature set-point, cathode heating flow rate, and heat exchanger characteristics.

4.1.7.2 Steady State Hysys® Model

The Hysys® system model is a steady-state thermodynamic and chemical equilibrium model of the Solid Oxide Fuel Cell System. Significant advancement has been completed in this model since the last reporting period.

4.1.7.2.1 Updated Stack Model

The stack model has been upgraded to include a regression form of the polarization curve for any particular stack design. Previously, the stack voltage was assumed to be constant (.7v /cell) and therefore the model was accurate only at maximum power. Now, a multi-order regression for the actual stack voltage as a function of current is included. Yet, to be completed is to make the stack model responsive to utilization. We are investigating the possibility that the PNNL stack model can be made a sub-system and included directly in Hysys®.

4.1.7.2.2 Real Heat Exchangers

At the time of the last report, the Hysys® system model provided “heaters” at points of heat exchange rather than “real heat exchangers”. The implication is that the old results, while thermodynamically correct did not account for the possibility that the heat transferred by the exchanges may not have been able to happen in reality due to limited temperature difference. This limitation has been eliminated by the introduction and debuging of elements that model actual heat exchangers at all points. In particular, the heat exchange between the gas phase combustor, and the reformer during endothermic (high recycle) reforming has been included. This exchange is particularly difficult to model at a lumped parameter level since the practical system design will include an intimate physical coupling of the gas phase combustor and the reforming function. Physical geometries become very important in the accurate modeling of the performance.

4.1.7.2.3 Excel Interface

An Excel interface to Hysys® has been completed. This interface allows multi-case set-point “batch” runs with data export to Excel and subsequent convenient plotting. Additionally, specific calculations (e.g. determination of required fuel and air for a given target current, oxygen to carbon ratio in reformate, recycle level, and target utilization) are re-used directly (literally the same spreadsheet) from Excel models of the actual calculations used in the control system.

4.1.8 Perform Design Optimization

The Gen 2A APU System design fell short of initial expectations due to incomplete development of key subsystem areas:

- Solid Oxide Fuel Cell Stack
- Fuel Reformer
- System Control Software
- High-Temperature Sensors
- High-Temperature Component Interfaces
- Thermal Insulation System and Pass-Throughs

A thorough review of the issues was undertaken and critical open development items were identified. Much development progress has been made in all subsystem areas to support the Gen 2B design level of APU. The specific issues and current status are covered in Tables 4.1.8-1 and 4.1.8-2.

	Solution Implemented and Verified at System Level.
	Solution Implemented / Not Verified at System Level.
	No Solution Implemented

Subsystem:	APU System Issues 02.28.03 (Week 9)	Identified Development Activities	Current Status 06.25.03 (Week 26)
Integrated Stack Module (ISM)	Gen 2 Stacks have limited cycle capability at system level (< 3)	Limited further Gen 2 stack development; Development focus on Gen 3 SOFC stacks	Improvement demonstrated on small cell stacks. No solution demonstrated at system level for more than 1 cycle on a Gen 2 Integrated Stack Module (ISM)
	Gen 2 Stacks limited to 2 x 15 Cells	Plan for 2 x 15 cell stacks for Gen 2B system.	Low voltage power conditioner will be used to handle low stack voltage.
	Insufficient gasket seals at base of Integrated Stack Module (ISM)	Test/develop gasket solutions (Balance-Of-Plant)	Mica gaskets have best performance to date in System (Stand 1). Other gasket technologies will also be available for evaluation. New Integrated Component Manifolds will have additional screws for Integrated Stack Module mounting
Reformer	Reformer exhibits excessive carbon production	Control software development; Investigate air mass-flow sensor accuracy; Investigate reformer temperature profile; Improve sensor positioning inside reformer	Perfomance maps being generated in reformer lab. Generally, low carbon operation currently demonstrated in both reformer lab and system lab.
	Reformate quality sub-standard and unstable at system level	Improve air mass-flow sensor performance; improve control software	Stable reformate within quality standards demonstrated at system level
	Mass spectrometer (reformer outlet) input still required at system level to "steer" reformer		Automatic operation and control demonstrated. Solution demonstrated; turn-down issues to be determined.
	Start-up sequence of reformer not reliable	Control software development; Implement temperature-based start control (vs. time-based)	Solution demonstrated. Reliable reformer starts demonstrated in System.
	Injector tip temperature excessive during soak	Develop injector tip insulator / heat sink hardware	Injector tip temperature management not verified during soak at system level. Heat sink hardware implemented but not tested at System level.
	Heat transfer from reformer body causes overheating of PSM compartment	Improve thermal insulation at reformer body and insulation pass-through	Gen 1.1 Reformer and Insulation collar designed to reduce heat leakage. Has not been verified at System level.

Table 4.1.8-1: Performance/Design Optimization Summary – Stack/Reformer

	Solution Implemented and Verified at System Level.
	Solution Implemented / Not Verified at System Level.
	No Solution Implemented

Subsystem:	APU System Issues 02.28.03 (Week 9)	Identified Development Activities	Current Status 06.25.03 (Week 26)
Electronics and Controls	APU controller hardware/software not implemented in APU	Develop / test communication and software interfaces. Verify hardware & software at APU level.	Good progress to date, controller not implemented or tested in system.
	Automatic control software requires "engineer-in-the-loop"	Control software development / testing	Full automatic control demonstrated in system.
	Safety and control diagnostic software not developed or implemented		Safety and diagnostic software coded but not tested at System Level.
Balance of Plant	Significant thermal management issues within APU; APU runs only as open frame assembly with fans	Improve thermal insulation at reformer body and insulation pass-throughs; Improve wire harness routing and Plant-Support-Module packaging.	Motor controller packaging/cooling, and insulation/passthroughs have been improved. Not verified/tested in System.
	Reducing gas currently used for anode oxidation protection	Test/ develop check-valve and nickel foam protection system at system level	Solution implemented, but not tested.
	Reformer outlet gas sensor technology not fully developed for APU application	Characterize reformer performance and sensitivities. Develop reformer "steering" controls and sensor set	Gas sensor (S1) will not be used for Gen 2B, Reformer mapping will replace need for sensor.
	New bead-style gaskets available but not tested in system	Test/ develop capable gasket solutions	Mica gaskets perform adequately at system level for low-cycle operation.
	Air inlet cooling system in APU not tested	Test/develop APU air inlet cooling system	Air inlet cooling system tested. Some concerns about blower motor driver cooling. Plant-Support-Module heat input critical factor.

Table 4.1.8-2: Performance/Design Optimization Summary – Electronics/Controls/ Balance of Plant

From Gen 2A to Gen 2B design levels, the following improvements have been made:

- New Gen 1.1 Tube Reformer
  - Improved temperature control
  - Reduced mass air mix manifold
  - Simplified pass-through geometry for reduced heat leakage
  - Internal start-igniter for reduced external interfaces
  - Improved base interface geometry for better sealing and mounting
- New Insulation Collar Geometry
  - Reduced heat transfer from hot to cool zones
  - Improved assemble ability
- Updated Integrated Component Manifold (ICM)
  - Improved access to oxygen abatement materials
  - Improved air-feed manifolds
  - Reinforced gasket seal surfaces

- Improved gasket materials/technology for reduced leakage at high temperature interfaces.

- High temperature rating igniters for improved cycle durability

- Improved Space Frame for improved access and assemble ability

- Improved application interface through introduction of the Application Interface Module (AIM)
  - Modular / flexible interface
  - Improved assemble ability and serviceability of APU

- New Process Air Module (PAM)
  - More integrated unit for better APU packaging and air hose routing
  - Reduced external interfaces and fittings - reduced potential for air leaks

- Fully Automatic Controls

4.1.9 System Integration Status

System integration will be covered in Section 4.6: System Fabrication.

4.1.10 System Cost Estimate

The cost estimate was discussed in Section 2.5.

4.2 Solid Oxide Fuel Cell Stack Development (Task 2.0)

This task focuses on the development, fabrication, and demonstration of Solid Oxide Fuel Cell stacks.

4.2.1 Design Stack

Design work has focused on developing the complete Generation 3 integrated stack module (including gas header and manifolds) with load frame, base plate and retaining plate. The design has been completed and prototype parts are being fabricated for assembling a complete Generation 3 Integrated Stack Module.

4.2.2 Model Stack Under Steady-State Conditions.

Modeling of the electrical conductivity of the interconnect electrical pathway has commenced. Preliminary studies with the ANSYS finite element code indicate that it is a suitable modeling tool to develop an understanding of the electrical losses in the interconnect train and to optimize the design. Sheet resistance tests are being conducted on the cathode materials to validate the modeling method. The model will be capable of representing the resistance of the oxide scale in addition to the geometrical contact issues.

4.2.3 Model Stack Under Transient Condition.

No activity this reporting period. Modeling has been completed for Gen 3 design. Next anticipated major need for modeling will be after Gen 3 has been tested and design for Gen 4 commences.

4.2.4 Develop High-Performance Cathode.

Cathode development efforts have focused on testing of button cells to characterize and optimize the performance of several cathode materials. The cathode materials of primary interest were:

- Sr-doped lanthanum cobalt ferrite [$(La,Sr)(Co,Fe)O_3$: LSCF],
- Sr-doped lanthanum ferrite [$(La,Sr)FeO_3$: LSF] and
- Copper-doped LSF [$(La,Sr)(Fe,Cu)O_3$: LSFCu].

Button cell tests were normally conducted at 0.7 V and 750 °C using 1:1 mixture of nitrogen and hydrogen as a fuel in order to simulate the reformate gas used in full scale testing. $(La,Sr)(Co,Fe)O_3$ were found to exhibit initial power densities >700 mW/cm^2 under normal test conditions (0.7V, 750 ^oC, 1:1 H_2/N_2).

Button cell tests on the SECA Core Technical Program (CTP) cathode material, $(La_{0.8}Sr_{0.2})_{0.98}Fe_{0.98}Cu_{0.02}O_3$, achieved power densities of ~ 900 mW/cm^2 under standard test conditions (see Figure 4.2.4-1). When pure hydrogen was used as fuel, the power jumped up and approached a maximum near 1.5 W/cm^2, similar to power densities reported from the CTP. While pure hydrogen showed no diffusion limit up to 7 amps (~2.5 A/cm^2), the I-V curve of the cell under 50:50 mixture revealed a diffusion limit around 5.8 A. This result indicates that in the case of 50:50 mixture, hydrogen diffusion through the anode is a more serious problem at high power (or current).

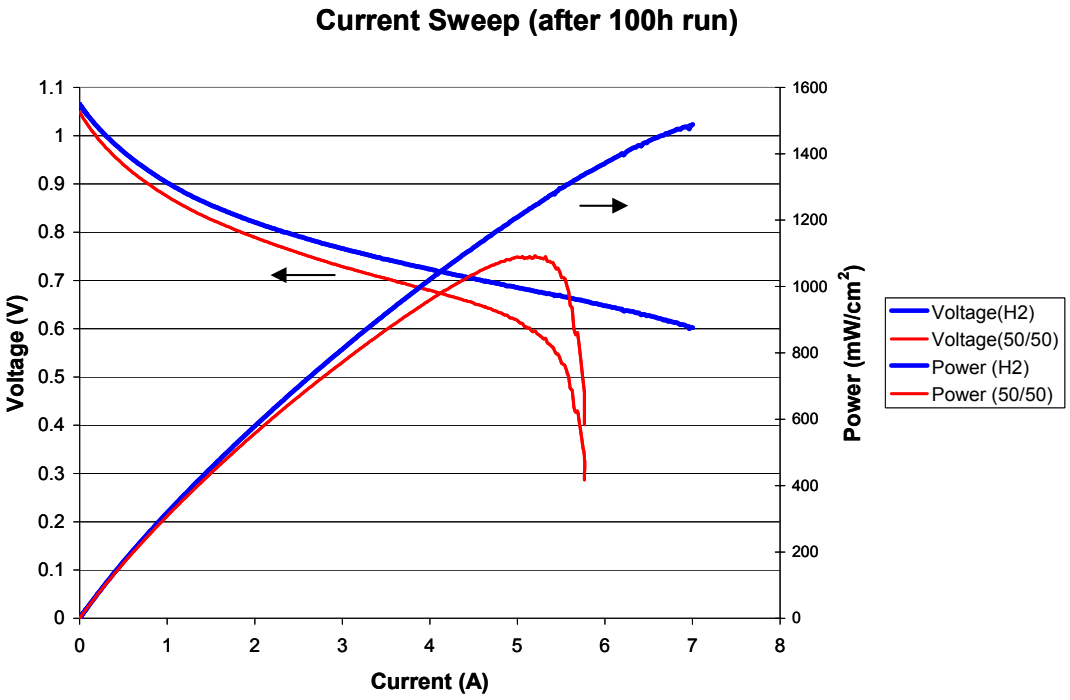

Figure 4.2.4-1: Current Sweep Behavior of LSFCu$_2$ Under Pure Hydrogen and 50:50 Mixture

4.2.5 Develop High-Performance Anode

The standard electrolyte tape cast formulation used in cell production was determined to lack the desired robustness necessary to produce consistent high quality. Slight variations in the solids loading, binder content or solvent lead to lower part yields through formation of pinholes in the YSZ electrolyte. Research efforts have been directed at developing an improved electrolyte formulation providing an improved sintered density and a reduction in the number of pinhole defects in the sintered electrolyte. Cells fabricated with the improved electrolyte composition showed minimal pinhole formation as determined by an alcohol penetration test. Research efforts focused on optimizing the anode tape cast formulation have been shown to improve part quality and aid in the reduction of cell camber.

4.2.6 Develop Cell Fabrication Techniques

Included in Section 4.2.5.

4.2.7 Develop Separator and Support Components

As discussed in previous reports, ferritic stainless steel is the material of choice for separator development. It has been well established that the largest contributor to resistance in the interconnect train electrical pathway is the oxide scale formed on the mesh and the separator. An alternative interconnect design is being developed which fundamentally changes the interconnect train and the role of the separator plate, potentially eliminating the oxide scale from the interconnect conduction pathway.

4.2.8 Develop Gas Distribution Meshes

As discussed in previous reports, the anode and cathode gas distribution meshes are two key components of the interconnect train. These components must provide a low-resistance electrical connection between the separator plate and the corresponding electrodes and allow access of air and fuel gas to the electrodes. A study of mesh welding parameters is underway to ensure that joining of the mesh to the separator is optimized for strength and also to ensure that the spot weld provides a minimum contribution to the total electrical resistance of the interconnect train.

4.2.9 Develop Mesh/Electrode Interface Materials

Advanced concepts for current collecting materials and interfaces are being developed for the cathode side of the cells.

4.2.10 Develop Glass and Glass-Ceramic Seals

As discussed in the previous report, one of the inherent problems that we have found with glass sealing is the formation of an oxide scale at the interface between the glass and the metal structural component (in our case, it is the window frame or separator plate). Initially this scale layer is well attached to the underlying metal substrate, but after long-term exposure to the high temperature operating conditions of the Solid Oxide Fuel Cell stack, the scale thickens and thereby weakens, eventually become the source of failure in the glass-to-metal sealing joints, particularly upon thermal cycling. One way to overcome this problem is to fabricate a composite glass seal that structurally integrates with the substrate-sealing surface during joining.

Shown in Figure 4.2.10-1 are rupture strength results of this new composite glass seal in comparison with previously obtained strength results on glass seals. Note that the new seal essentially does not break, even up to the limits of our test rig. In addition, it retains this level of strength after thermal cycling under the following heating/cooling conditions: heating from room temperature at a rate of 75 °C/min to 750 °C, holding at 750 °C for 10 minutes, and cooling to ~100 °C within 40 minutes.

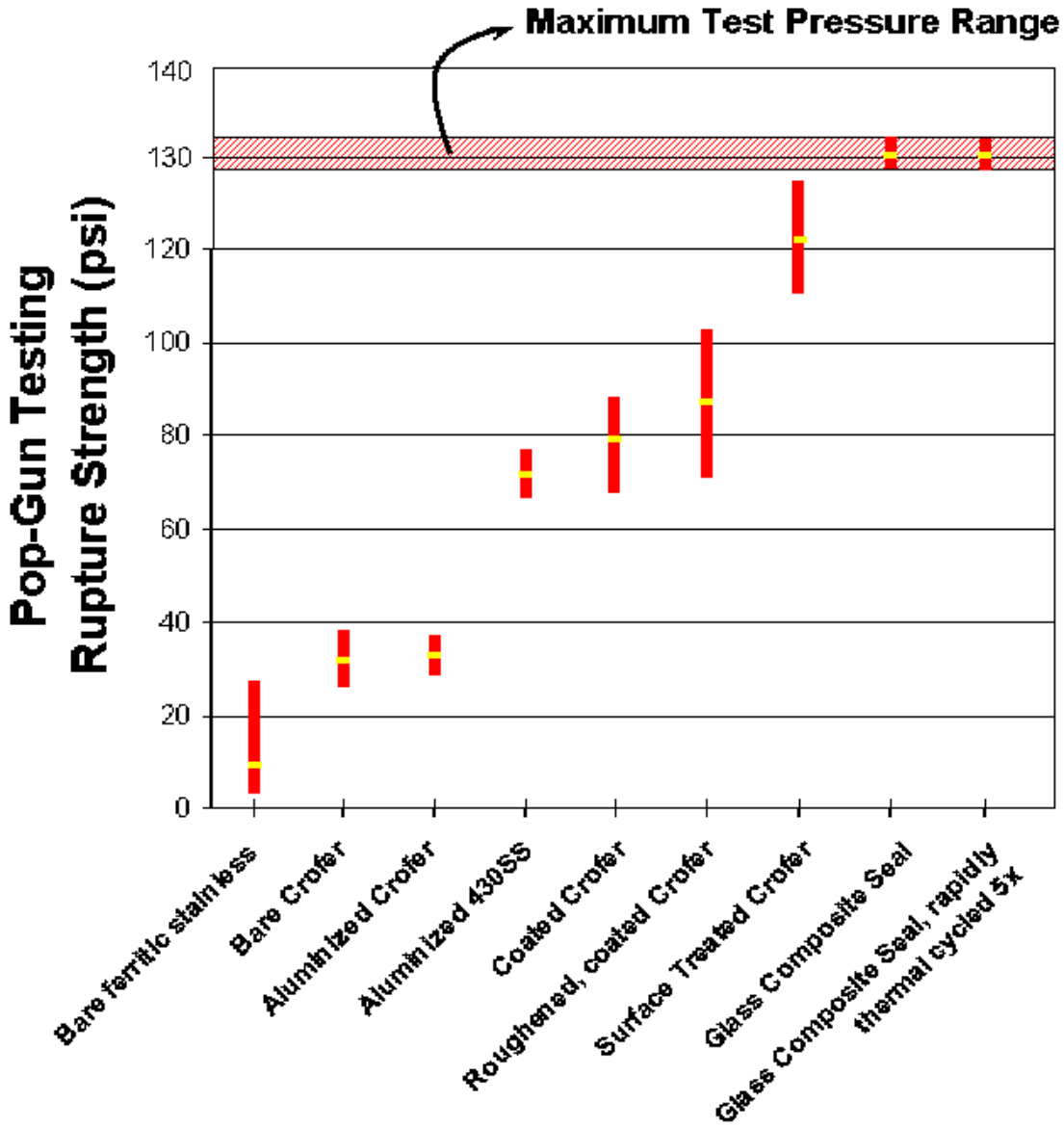

Figure 4.2.10-1: Rupture Strength Results for Glass Seals

4.2.11 Develop Alternative Seals

As discussed in the previous report, a new joining technique, referred to as reactive air brazing or RAB, has been recently used to seal the metal and ceramic components in a solid oxide fuel cell. However, a second seal is required to connect these cells into an integrated stack, which is the seal between adjacent cells or cassettes. One way to prepare this seal is again to employ brazing. However, the seal must be electrically insulating to avoid shorting the stack and since the cassette-to-cassette bond is between two metal components (i.e., separators), the joint itself must act as an electrical insulator. We are currently investigating the fabrication of such a joint using

the reactive air brazing technique by inserting a thin ceramic insulator between the two cassettes and joining each to the insulator. Presently we are optimizing this sealing concept for maximum strength under rapid thermal cycling conditions. Initial rupture strength results appear promising.

4.2.12 Develop Gas Headers and Manifolds

Discussed in Section 4.2.1.

4.2.13 Fabricate Developmental Stacks

A variety of stacks have been built and tested to understand and improve performance of the stack. The stack tests can be classified into two main categories:

- Stack tests with intermediate-sized active area cells (7 cm x 7 cm)
- Stack tests with full-sized cells (11.5 cm x 11.5 cm)

Stack test with intermediate-sized active area cells: Extensive experience has been gained in the fabrication and testing of these stacks with cell dimensions of 7 cm X 7 cm. The intermediate-sized tests are used to evaluate novel cell materials, cell processing parameters, new interconnect materials and designs, and alternate sealing techniques. Screening tests and performance evaluations can readily be performed using single-cell, intermediate-sized tests.

ANODE CONTACT RESISTANCE:

In order to evaluate the resistance of the interconnect train on the anode side of the cell; an additional voltage lead was connected to the anode surface. The voltage measured during operation between this lead and the cell negative contact was the loss associated with the anode contacts, the nickel interconnect/gas distribution meshes and their welds. The anode contact spots are formed by placing drops of nickel powder ink on the meshes. During stack assembly, these (still wet) ink drops wet the surface of the anode. During stack heat-up, the ink binder burns out and the powder sinters, forming metallic bonds. The data presented in Figure 4.2.13-1 is the anode voltage drop measured for two cells with the numbers of contacts as the only variable on the anode side. I-36 had eight contact spots while I-38 had four. As expected the voltage drop showed near ohmic behavior and nearly doubled when the contact count was halved. However, even in the worst case the ohmic loss was only 0.053 ohms/cm^2. At such a low value, it is doubtful that the anode side of the cell has a significant effect on cell performance.

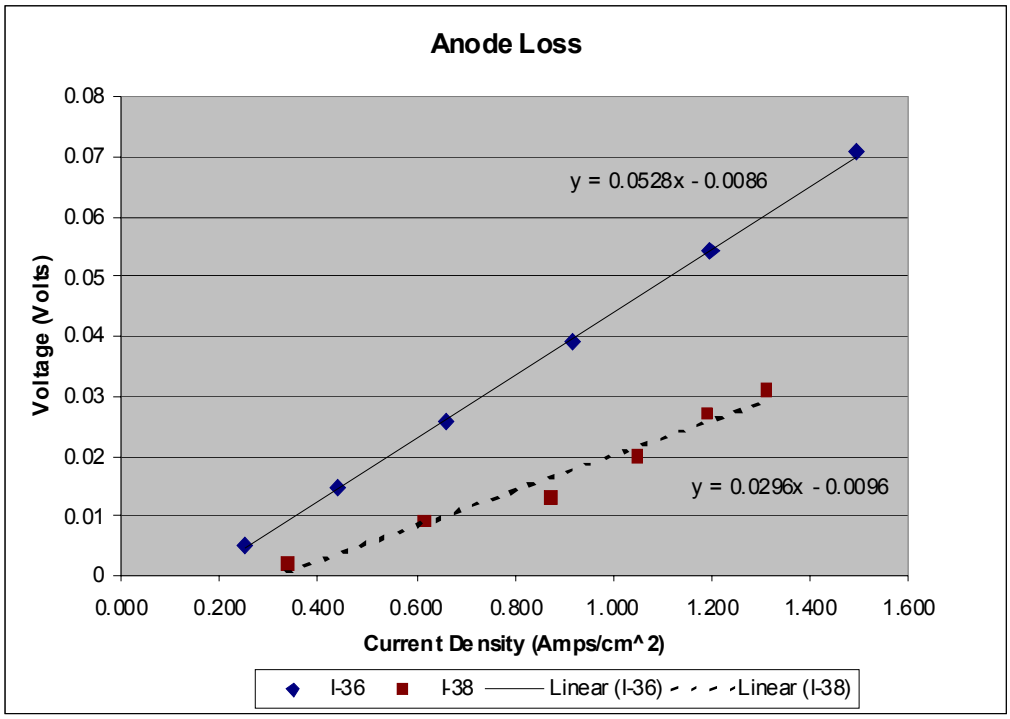

Figure 4.2.13-1: Voltage Loss in the Anode Interconnect Train as a Function of Current Density

The equations on the plots correspond to a linear fit of the data sets. The slope of the line corresponds to the resistance.

FUEL UTILIZATION:

Initial studies of the effect of fuel utilization on cell performance showed an unacceptable amount of performance loss with increasing fuel utilization. This was not observed in the larger full-sized cells, and was determined to be related to poor flow uniformity in the intermediate sized cell. By changing the anode-interconnect mesh arrangement and orientation the problem was rectified. When interconnect mesh had a high-degree of overlap or was placed perpendicular to the fuel flow, a portion of the fuel would be shunted around the area of high flow resistance. This would lower the flow rate over the active area, and cause this area to have locally high fuel utilization. This effect was minimized by placing the interconnect mesh parallel to the flow direction and arranged with no overlap. The resulting change in the fuel utilization curve is shown in Figure 4.2.13-2. The plot shows an intermediate sized single cell stack (I-57) with the improved interconnect mesh arrangement compared to intermediate sized single cell stack (I-36), which had the original orientation.

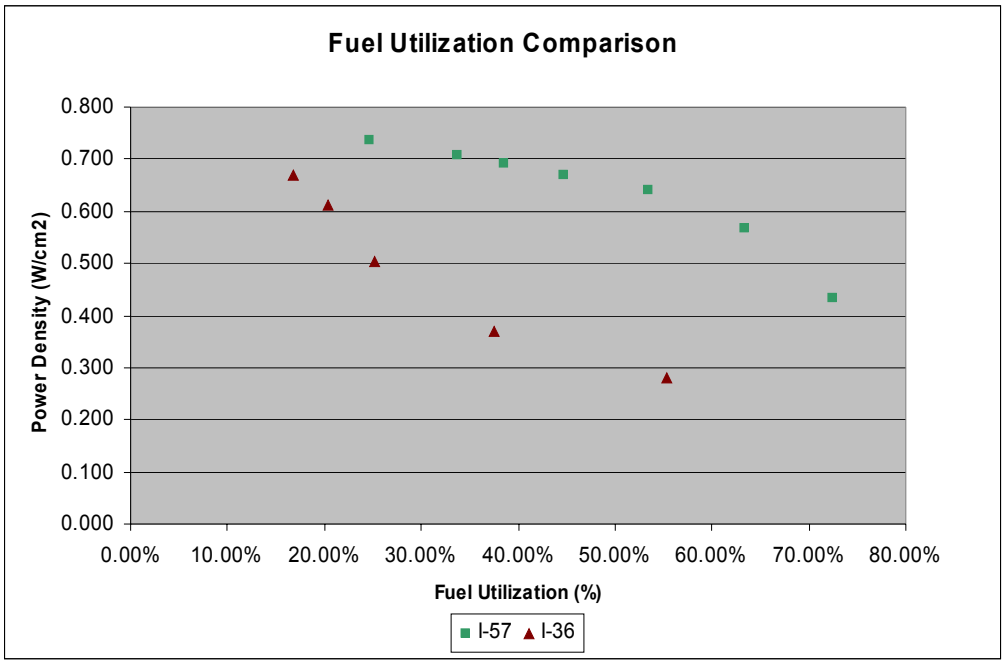

Figure 4.2.13-2: Effects of Interconnect Mesh Design on Fuel Utilization

HIGH-POWER CELL:

Power densities (at 0.7V) for stacks with LSF-20 cathodes are as high a 610 mW/cm^2. However, these values are only observed after burn-in occurs. This is difficult to achieve on a consistent basis since the burn-in mechanism is not well understood. Therefore, alternate cathode materials were investigated. The cathode material, (La,Sr)(Co,Fe)O_3, was tried and gave promising results. The initial test showed a power density of 575 mW/cm^2 at 750 °C and 0.7 volts, on 50% hydrogen fuel. This was improved to 640 mW/cm^2 though optimizing the cathode sintering temperature. Additional performance gains were shown on I-57, where the Ceria barrier layer was optimized to give a power density of 725 mW/cm^2. Figure 4.2.13-3 shows the IV plot of this cell, which was the highest performing intermediate cell to date. The power densities quoted are taken from early in the testing, since the LSCF-6428 degrades with time. The SEM analysis shows the presence of $SrCrO_4$ at the current collector cathode interface, which is the most likely cause of the degradation. This phase is formed when the cathode reacts with the Cr in the stainless steel. This reaction has been reported in the literature in the same location on the cathode (see S.P. Jiang J.P. Zhang, and X.G. Zheng; Journal of the European Ceramic Society 22 (2002) 361-373.) The degradation of a typical, (La,Sr)(Co,Fe)O_3 cell (I-57) is shown in Figure 4.2.13-4.

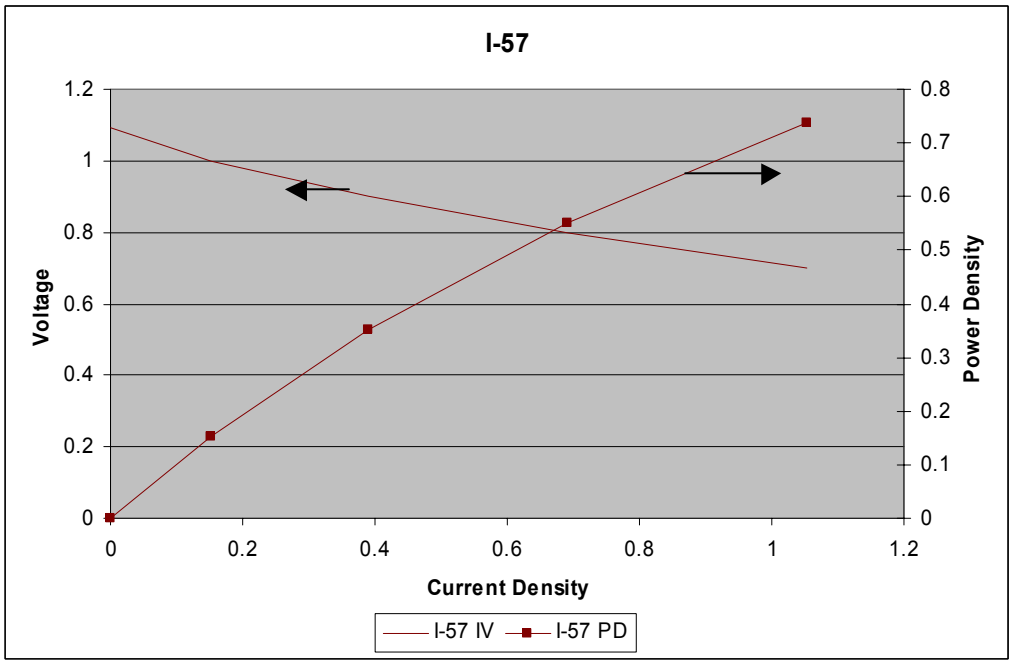

Figure 4.2.13-3: IV Plot Of The Highest Power Intermediate Cell To Date

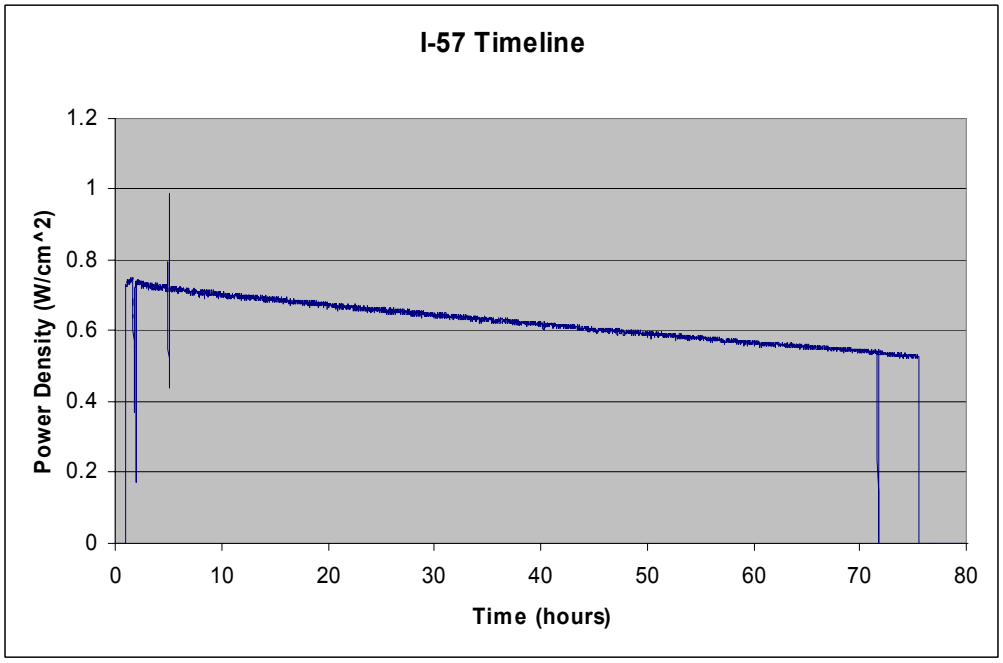

Figure 4.2.13-4: Typical Degradation with Time of the Cell with (La,Sr)(Co,Fe)O_3 Cathode

Comparison of intermediate and Full-Sized Cells in Stack Testing:

The $(La,Sr)(Co,Fe)O_3$ cathode was tested on F-10, a full-sized cell. Figure 4.2.13-5 shows the IV plot of F-10, which was the highest performing full sized cell to date. The plot shows F-10 compared to the equivalent intermediate cell I-35. Although the intermediate scale test can reproduce the results obtained on the button cells, this has not yet been achieved on the full-sized cells, which typically have 25% lower performance. The cause of this is still being investigated.

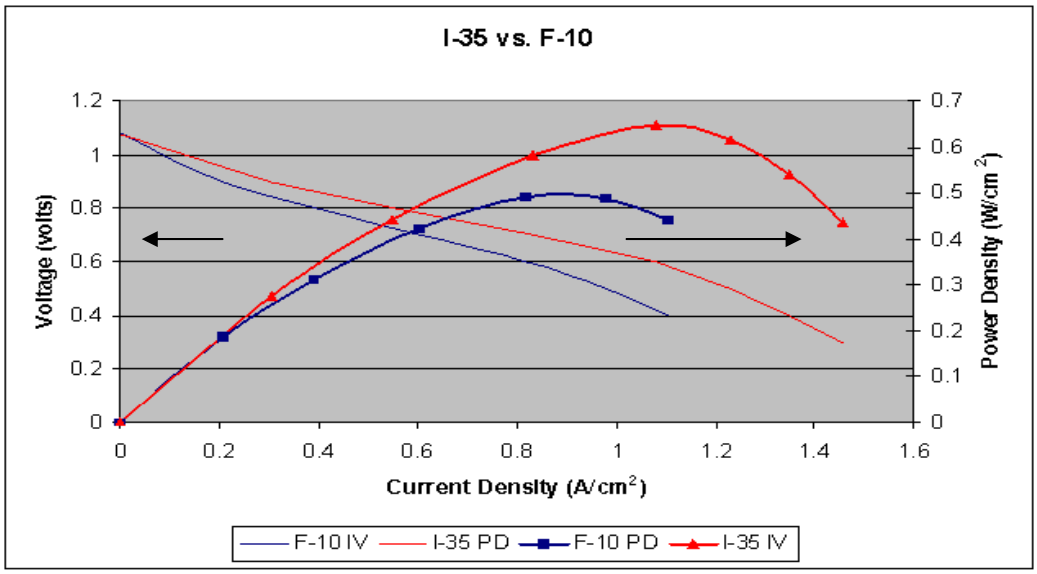

Figure 4.2.13-5: The Comparison of the Intermediate and Full-Sized Cells

4.2.14 Evaluate Stack Performance

Multiple 2x15-cell Integrated Stack Modules (ISMs) have been built and tested. An Integrated Stack Module is a "stand alone" stack sub-system that can be integrated to an APU. It consists of two stack modules in electrical series along with current collectors and the load frame. About twenty Generation 2 Integrated Stack Modules have been fabricated till now and tested and valuable lessons learnt during the build and test process. Both LSF-20 cathode containing cells as well as $(La,Sr)(Co,Fe)O_3$ cathode containing cells have been used for the fabrication of the ISMs. Figure 4.2.14-1 shows an I-V curve from a 2x15-cell Integrated Stack Module test. The cells in this ISM have LSF-20 as cathode. It produced 1025 Watts (322 mW/cm^2) at 20.5 Volts with 97% H_2, 3% H_2O, rest N_2 as the reformate. On "recycle" reformate containing 35% H_2, 40% CO, 3% H_2O, it produced 940 Watts (295 mW/cm^2) at 20.5 Volts. On "Partial Oxidation" reformate containing 20% H_2, 23% CO, 3% H_2O, rest N_2 the Integrated Stack Module produced 903 Watts (284 mW/cm^2) at 20.5 Volts. The operating temperature of the stack was 750 ^oC and the flow rates were kept constant at 100 liters per minute of reformate and air in all the tests.

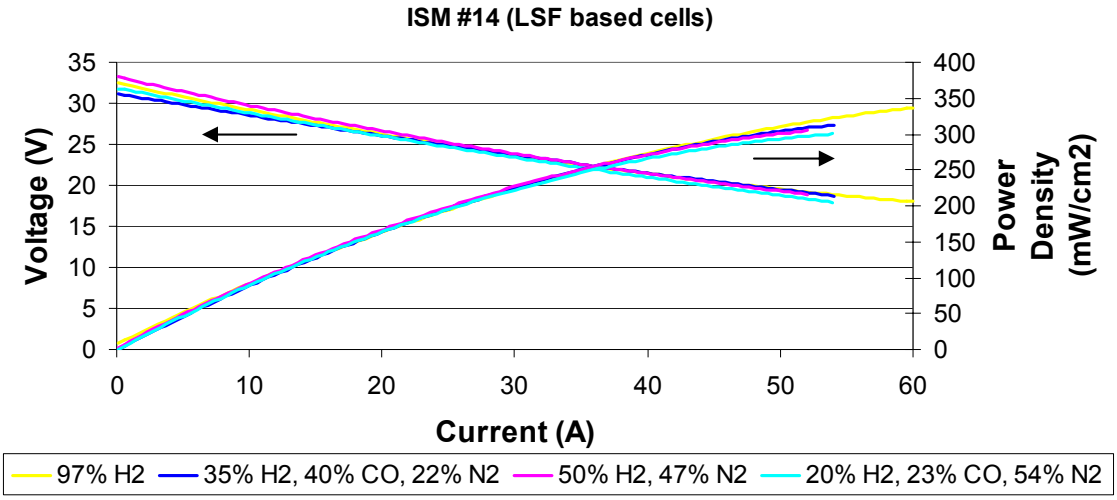

Figure 4.2.14-1: IV Curve From a Test with 2x15-Cell ISM with Cells Containing LSF-20 Cathode with Different Reformate Compositions

Similarly, Figure 4.2.14-2 shows an I-V curve from a 2x15-cell Integrated Stack Module with cells containing $(La,Sr)(Co,Fe)O_3$ cathode. Concurrent with the expected improvement in power density, the ISM produced 1340 Watts (422 mW/cm^2). At 21 Volts with 30% H_2, 40% CO, 3% H_2O, rest N_2. The operating temperature was 750 ^oC and the reformate and air flow rates were 100 liters per minute.

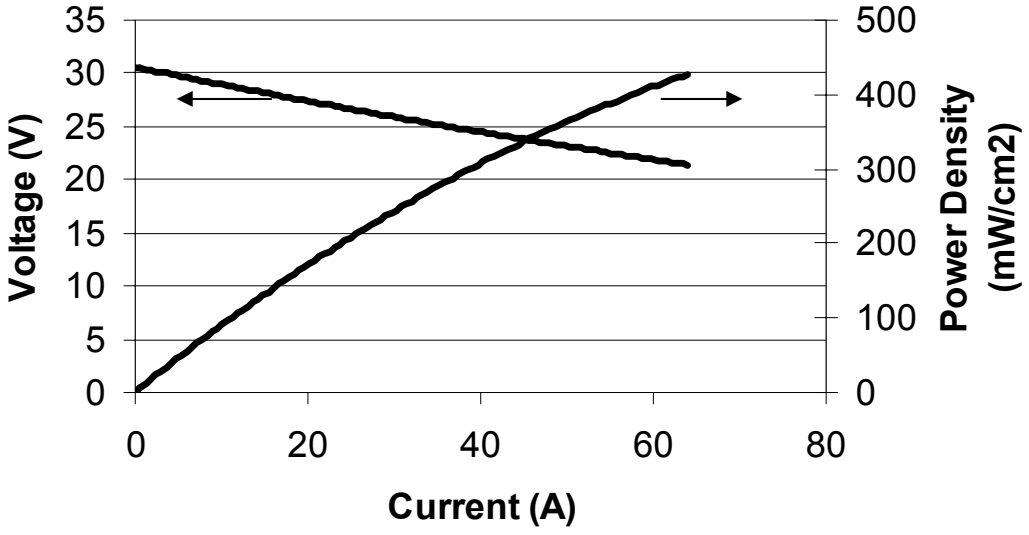

Figure 4.2.14-2: IV Curve from a Test with 2x15-Cell

The results are quite encouraging, as they seem to indicate that there exists a very good correlation between full-sized 1-cell stacks and full-sized 2x15-cell Integrated Stack Modules.

The development, currently, is focused on translating the higher power densities obtained in intermediate sized cell stacks (0.725 W/cm^2) to full sized cell stacks. Work is also targeted towards durability testing and improving power densities at high fuel utilizations.

4.3 Reformer Development (Task 3.0)

4.3.1 Develop Steam Reformer for Natural Gas

4.3.1.1 Demonstration of Methane Steam Reforming

Several catalyst products were evaluated for methane partial oxidation reforming, auto-thermal reforming, and steam reforming. This work was conducted to demonstrate that current catalysts are effective for this set of processes, that the gasoline reforming test stands are capable of methane reforming, and to provide guidance for upcoming system-level methane and natural gas reforming. These processes were evaluated in our laboratory on selected catalysts, using the same test stands employed for gasoline partial oxidation testing. The test stands were modified to permit introduction of methane and water. Major parameters investigated include steam to carbon ratio and oxygen to carbon ratio (O/C). For simplicity, methane was used as a substitute for natural gas in the experiments.

Three current catalyst products were evaluated for methane partial oxidation. Different active metals and washcoats were selected for each; each having been proven effective for gasoline partial oxidation. The results of the testing can be summarized as follows and are presented Figure 4.3.1.1-1.

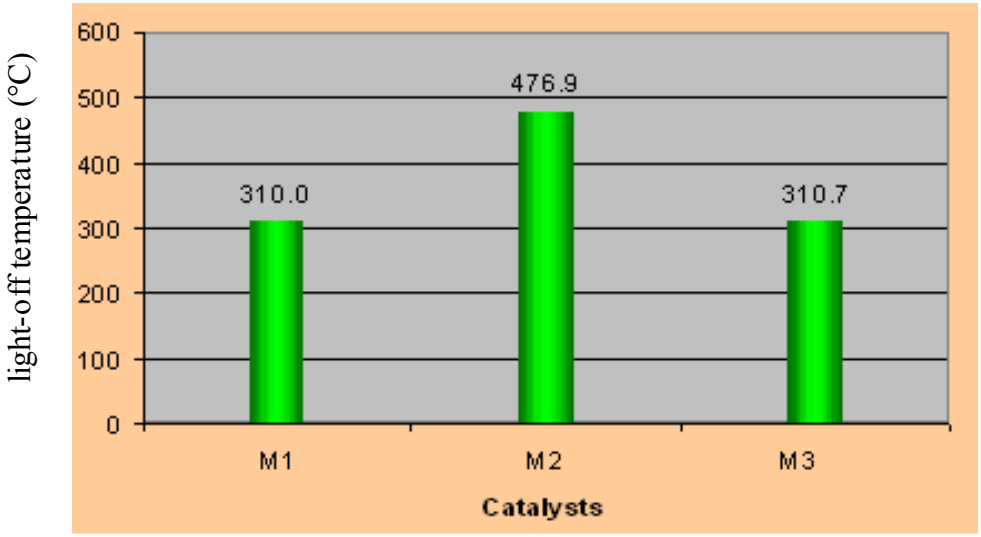

CH_4 = 2.0 slpm, O/C = 0.90, GHSV = 29765/hr

Figure 4.3.1.1-1: Methane Light-Off Activities Comparison In Partial Oxidation Mode

While the catalysts exhibited differences in light-off temperature, no distinct differences in methane conversion were found on these three catalysts. For all of the catalysts, methane conversion increased with increasing oxygen to carbon ratios. Nearly 100% conversion was achieved at oxygen to carbon ≥ 1.20 when CH_4 = 2.0 standard liters per minute (slpm, taken at 1 atm. and 0 °C), and at oxygen to carbon ≥ 1.00 when CH_4 = 3.5 and 4.5 slpm. The hydrogen selectivity was determined to be comparable among the three catalysts at low Oxygen to Carbon ratios.

Autothermal reforming was conducted on three gasoline partial oxidation catalyst products, using a statistical experimental design approach for adjusting processing parameters. Typical results for two of the catalysts are given in Figures 4.3.1.1-2, Figure 4.3.1.1-3, Figure 4.3.1.1-4, Figure 4.3.1.1-5, and Figure 4.3.1.1-6.

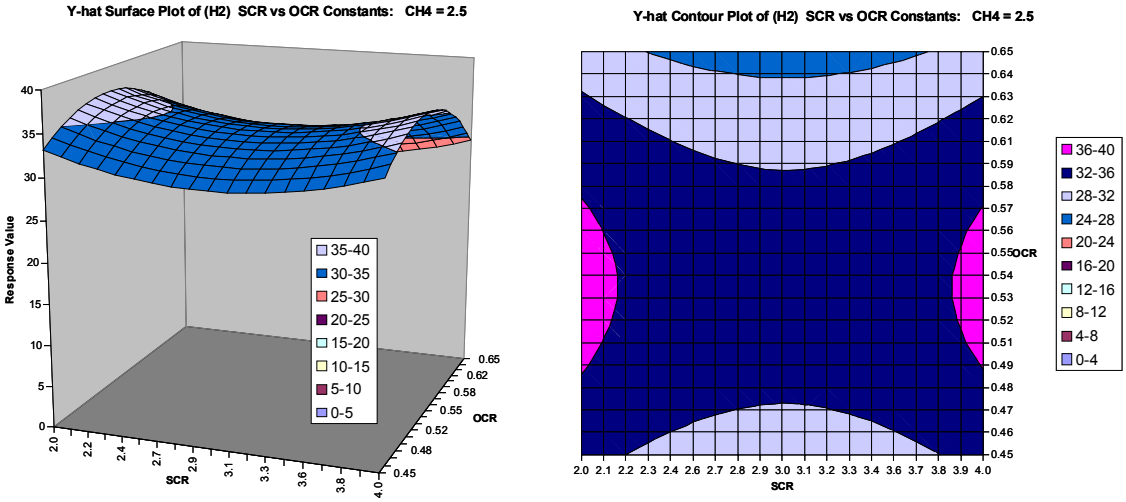

Figures 4.3.1.1-2: Methane Autothermal Reforming – H_2 Concentration Response Surface and Contour Plot (at CH_4=2.5 slpm), Using Catalyst M3

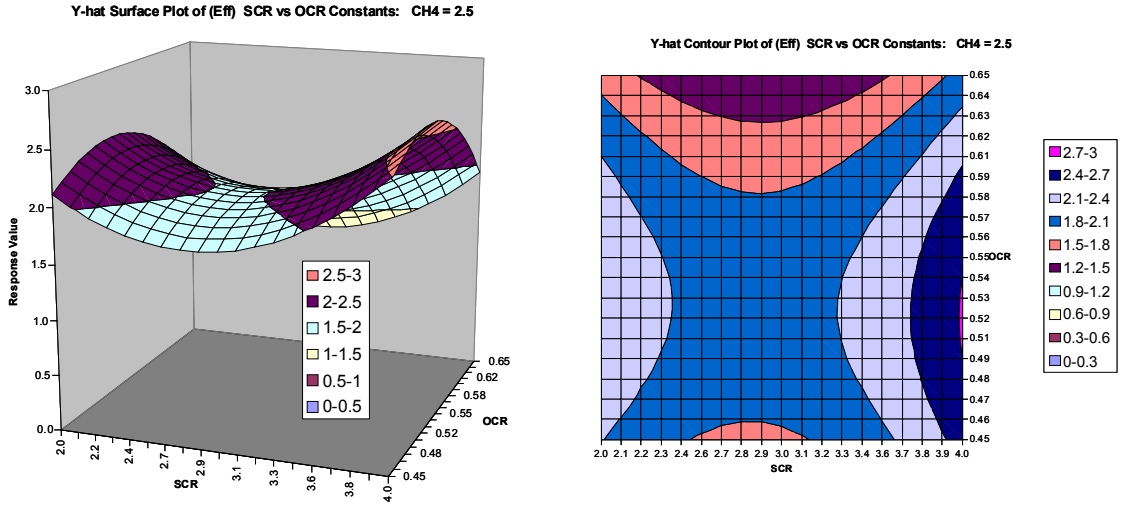

Figures 4.3.1.1-3: Methane Autothermal Reforming – Efficiency Concentration Response Surface and Contour Plot (at CH_4=2.5 slpm), Using Catalyst M3

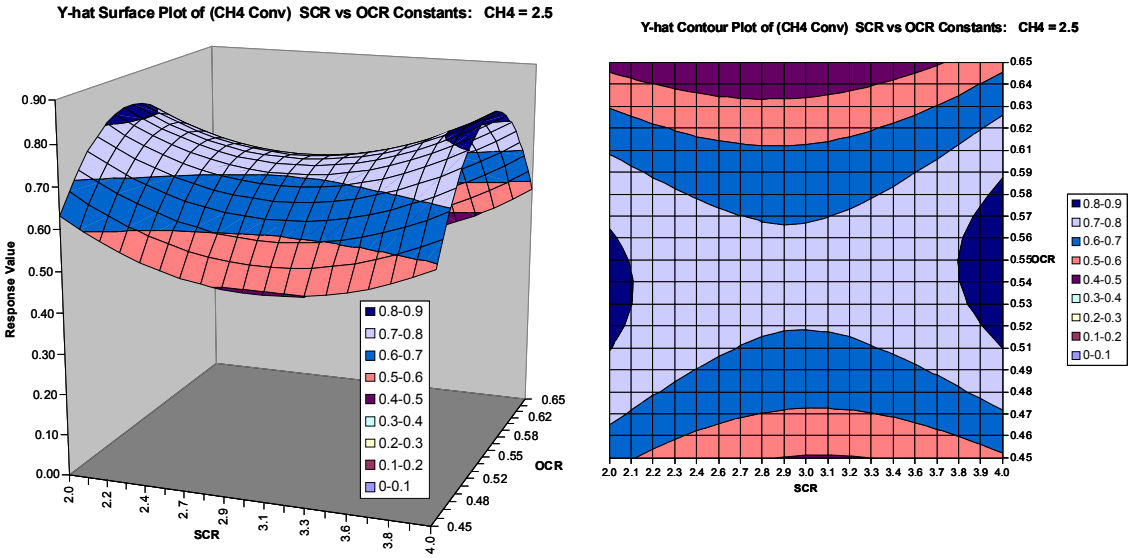

Figures 4.3.1.1-4: Methane Autothermal Reforming – Methane Conversion Concentration Response Surface and Contour Plot (at CH_4=2.5 slpm), Using Catalyst M3

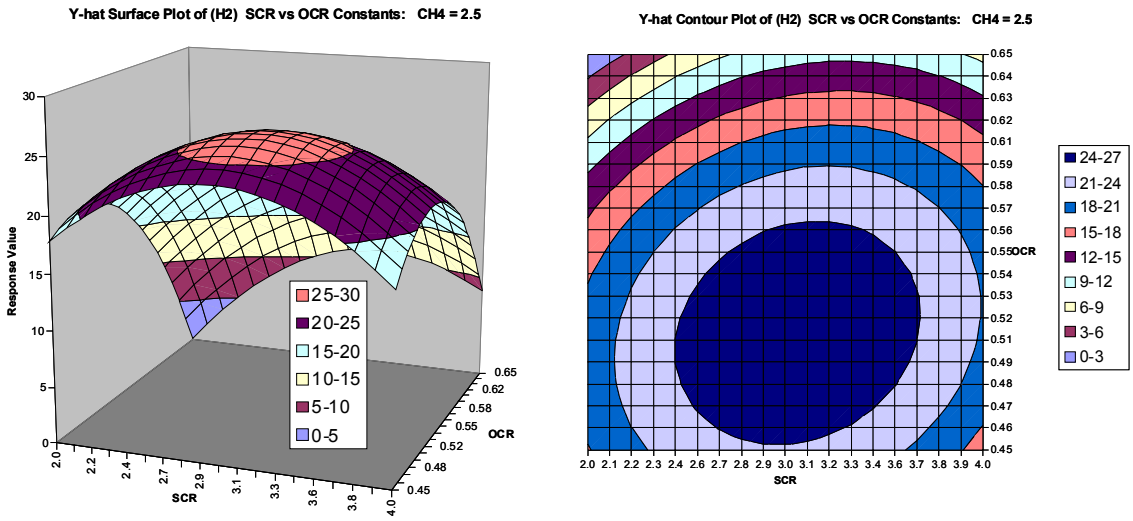

Figures 4.3.1.1-5: Methane Autothermal Reforming – Hydrogen Concentration Response Surface and Contour Plot (at CH_4=2.5 slpm), Using Catalyst M1

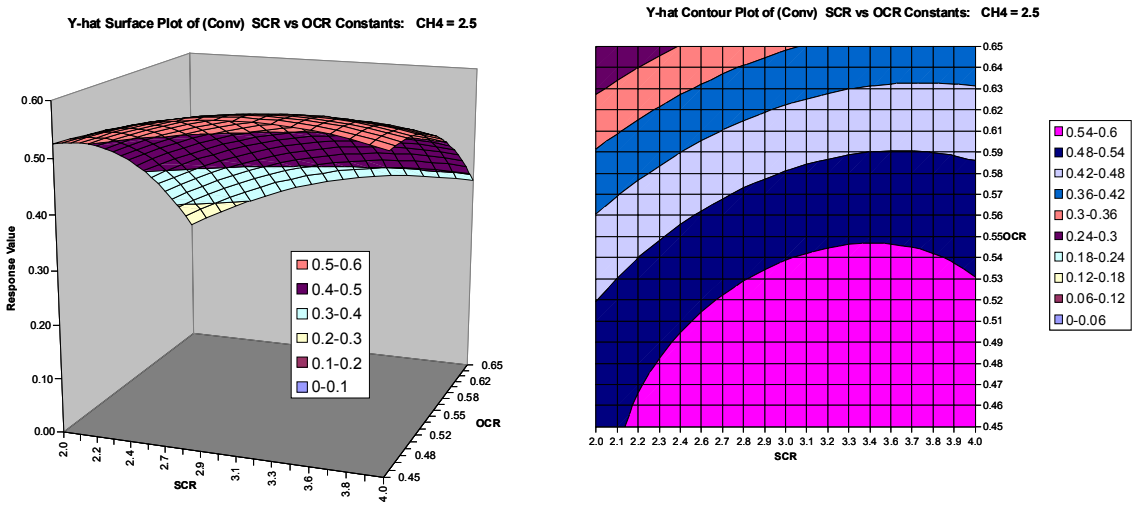

Figure 4.3.1.1-6: Methane Autothermal Reforming– Methane Conversion Response Surface and Contour Plot (at CH_4=2.5 slpm), using Catalyst M1

The maximum efficiency, defined as (H_2 + CO)/CH_4, was determined to be 2.8 which took place at CH_4 = 2.5 slpm, oxygen to carbon = 1.3, and steam to carbon = 4. While the H_2 yield and efficiency are directly proportional to the methane conversion, no direct correlation between the methane conversion and the catalyst center temperature was found. The catalyst center temperature in general increases with decreasing steam to

carbon ratio, due the cooling effect of steam. Increasing the reactant inlet temperature may alleviate this effect.

At CH_4 = 2.5 slpm, oxygen to carbon= 0.9, and steam to carbon= 2 (total oxygen to carbon= 2.9), selectivity to H_2 and CH_4 conversion varied between the catalyst samples tested, Figure 4.3.1.1-7.

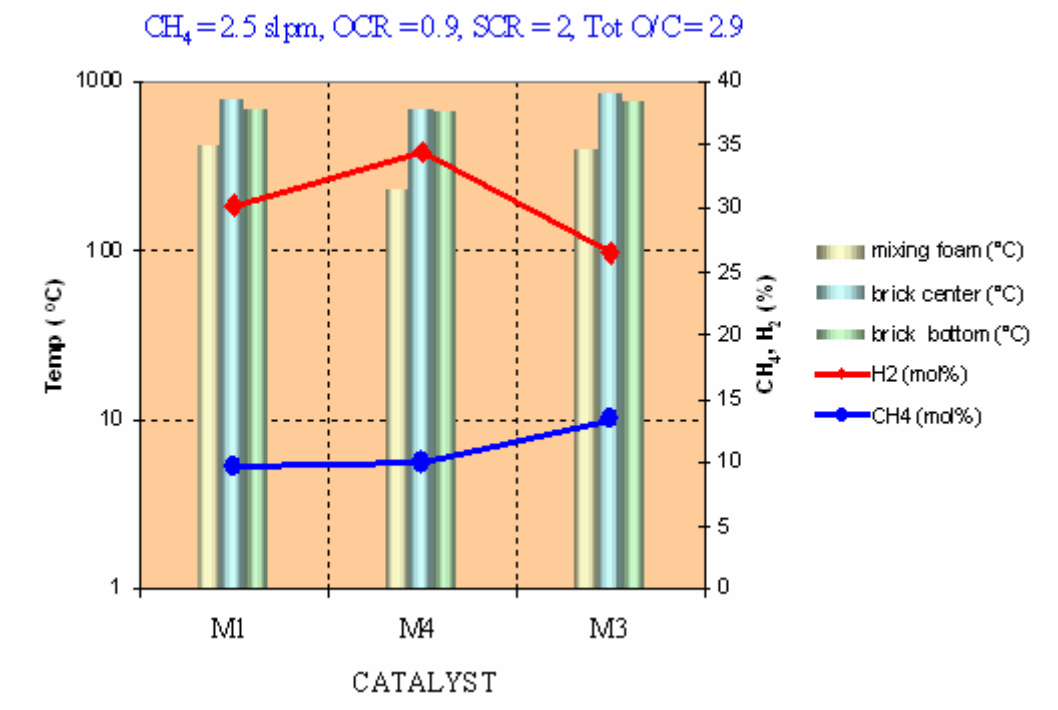

Figure 4.3.1.1-7: Methane Autothermal Reforming - Catalyst Comparison

Comparison of the reformate concentration reveals that catalyst M4 with H_2 concentration of 35%, exhibits the highest activity toward hydrogen formation. These differences can be attributed to different types and amounts of active metals on the catalysts.

Steam reforming continues to receive great attention owing to the fact that when operated at optimum processing conditions, efficiency can be greater than that for partial oxidation or auto-thermal reforming. Initial steam reforming test results reveal that our current gasoline partial oxidation catalysts, and modified versions, exhibit high steam reforming activity, with the corresponding H_2 concentration in the reformate being about 40%, as shown in Figure 4.3.1.1-8.

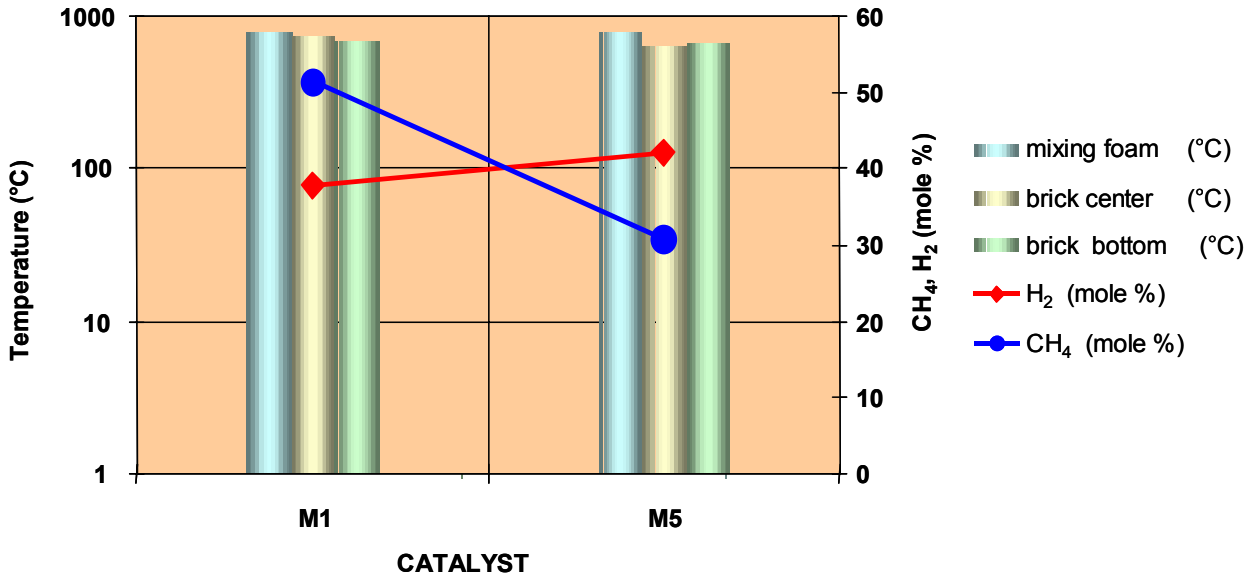

Figure 4.3.1.1-8: Methane Steam Reforming Catalyst Comparison (at CH4 = 2.5 slpm)

As evidenced in Figure 4.3.1.1-9, steam reforming is more favorable at lower steam to carbon ratio. However, further investigation is essential to determine the propensity of coke formation when operating at low steam to carbon ratio region. Future tasks will also include determination of the optimum operational window for these catalysts.

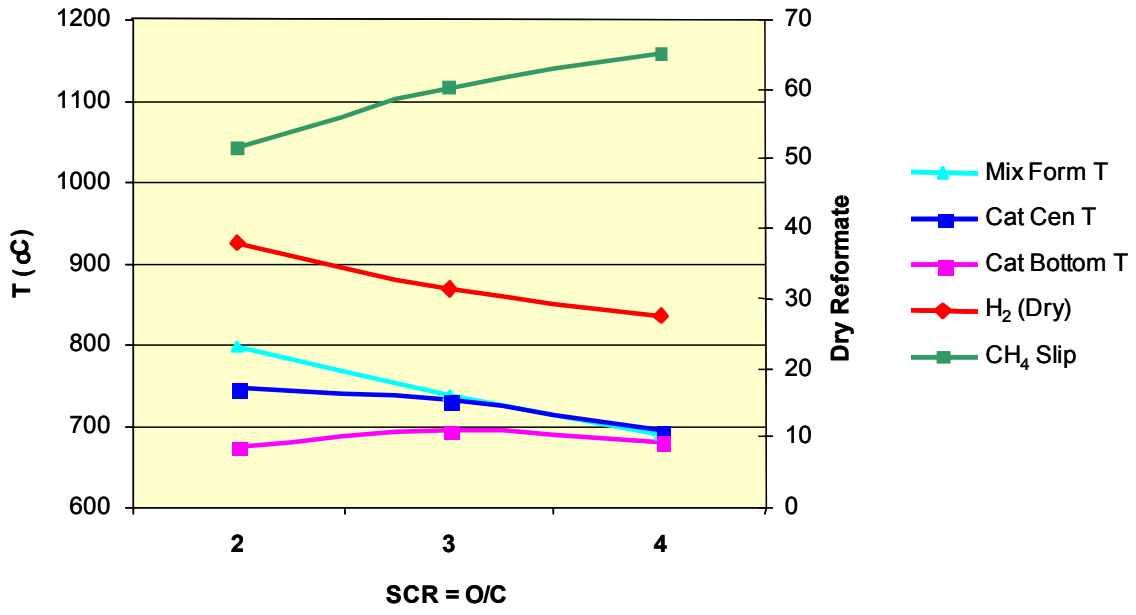

Figure 4.3.1.1-9: Methane Steam Reforming on Catalyst M1 (at CH4 = 2.5 slpm)

A comparison between methane partial oxidation, auto-thermal reforming and steam reforming for a typical gasoline partial oxidation catalyst, is given in Figure 4.3.1.1-10 Each process yields about the same H_2 concentration in the reformate, but conversion of methane decreases with increasing steam to carbon ratios, primarily due to temperature effects. We will look at increasing the temperature of steam reforming processes to demonstrate significantly improved performance for this process.

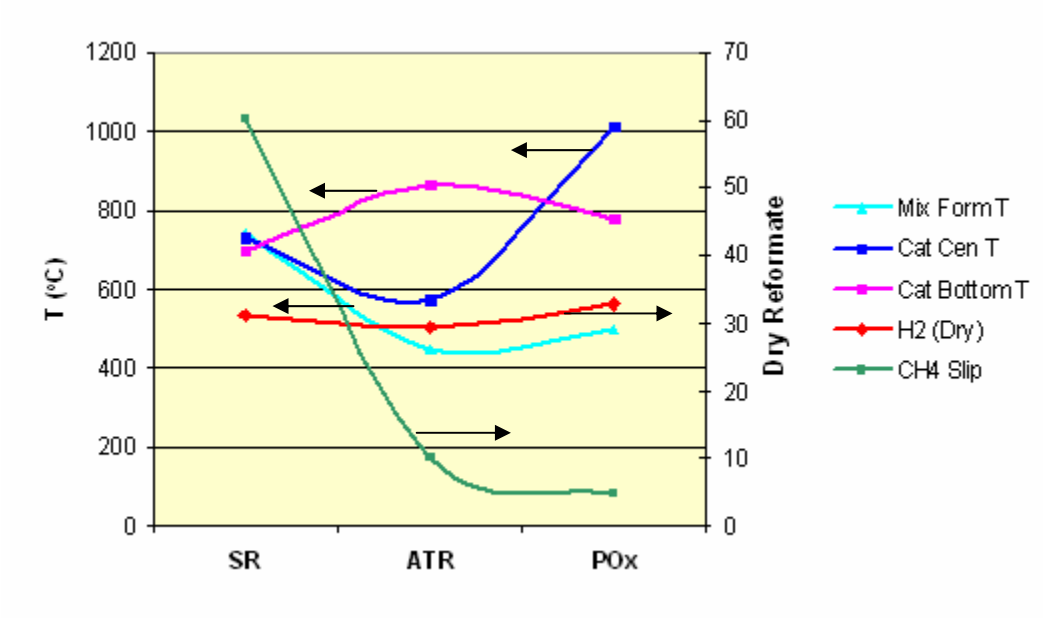

Figure 4.3.1.1-10: Comparison of Methane Partial Oxidation, Autothermal Reforming, and Steam Reforming on Catalyst M1 (at CH_4 = 2.5 slpm)

4.3.1.2 Steam reformer concept study and evaluation – Analysis

Natural gas steam reformer concepts were investigated analytically and contrasting results were compared, in order to streamline future concept selection and test. Special emphasis was given to both endothermic heat transfer function and fuel/air preparation. Computational Fluid Dynamics analysis was conducted for all design concepts and included solid/fluid conjugate heat transfer, multi species mixing, and heat sinks due to endothermic reactions in the computation of momentum, heat and mass transport phenomena. Promising endothermic reformer and fuel/air preparation concepts will be selected for further evaluation and future test. The concepts evaluated are listed below and depicted in Figures 4.3.1.2-1, 4.3.1.2-2, and 4.3.1.2-3:

- A1 – Tubular Reformer
- B1 – Tubular With Metal Ribs Or Rolled Configuration
- C1, C2, C3 – Square With Metal Ribs
- D1 – Tube Bundle Configuration
- F1, F2 - Multiple Coaxial Tubular Arrangements

- K1 – Flat Plate Design

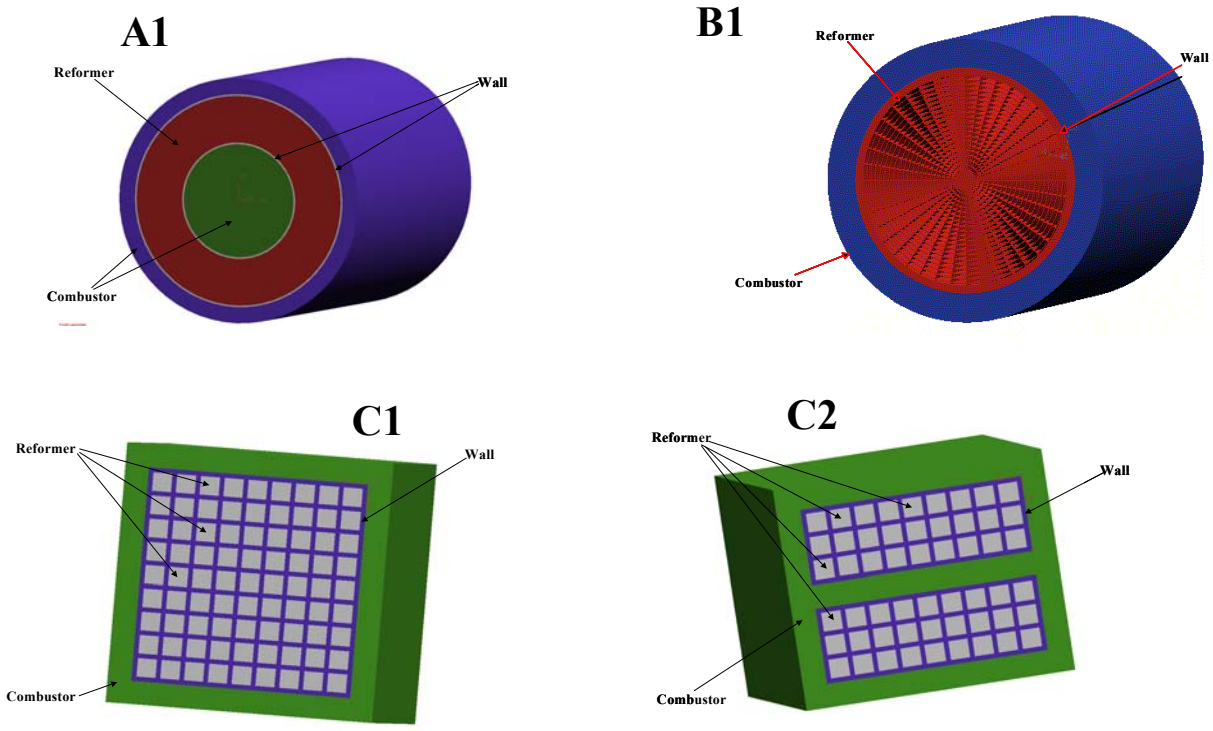

Figure 4.3.1.2-1: Steam Reformer Concepts

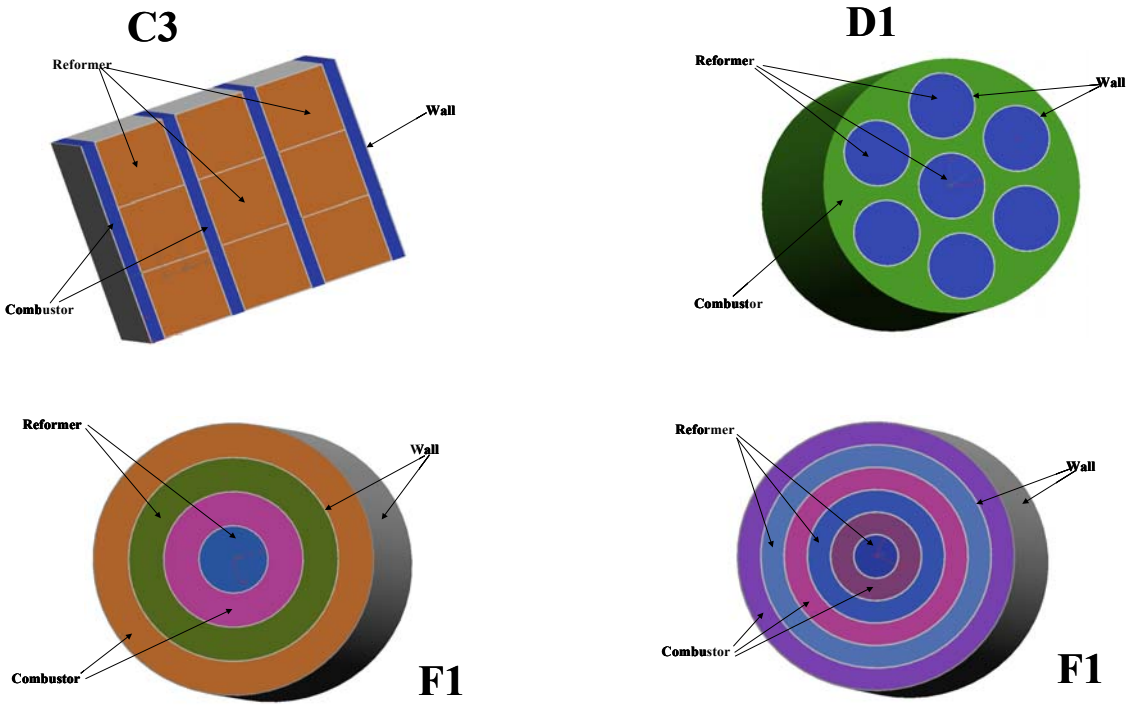

Figure 4.3.1.2-2: Steam Reformer Concepts

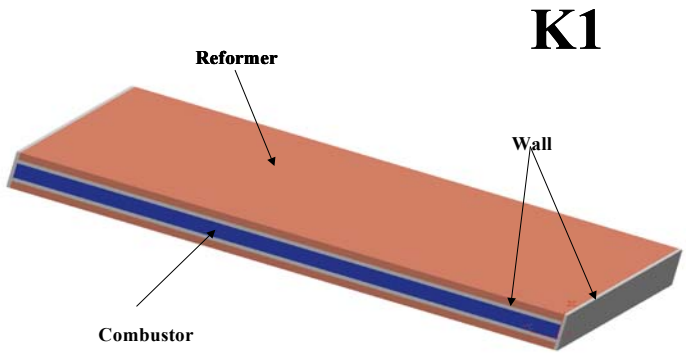

Figure 4.3.1.2-3: Steam Reformer Concepts

Each concept was analyzed under three conditions: Empty flow channels, metal foam in reformer flow channels, and metal foam in all flow channels.

Contrasting results are presented in Figure 4.3.1.2-4.

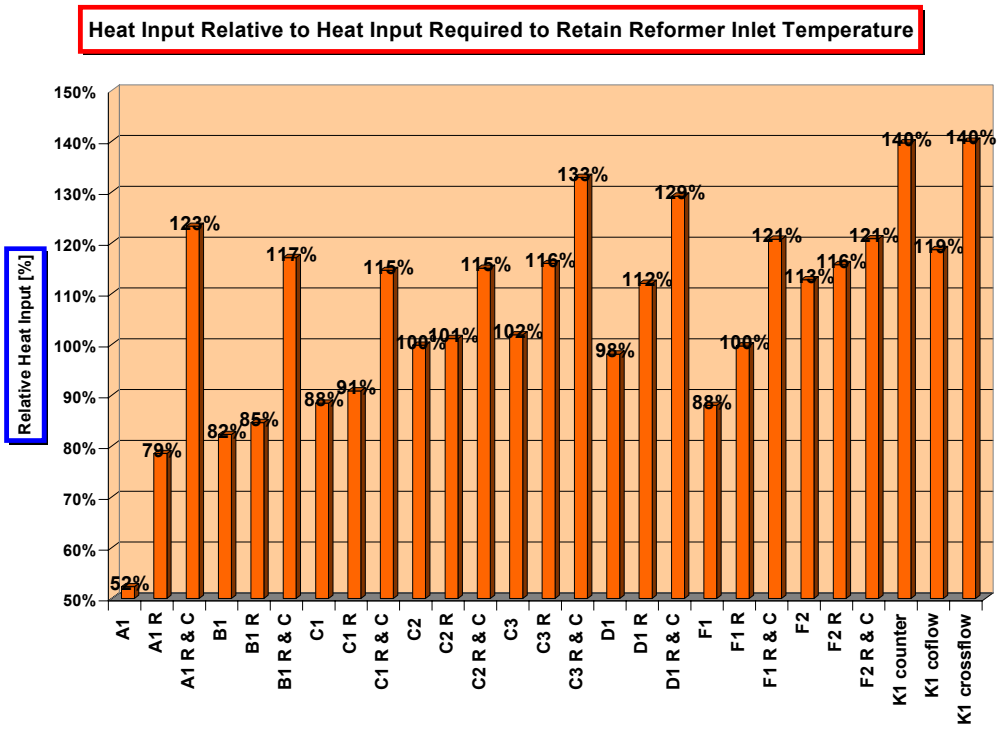

Figure 4.3.1.2-4: Heat Input Required

Note: In the figure above, no suffix implies empty flow channels; R suffix implies foam in reforming channels; R&C suffix implies metal foam in both reforming and combustion channels.

Results reveal potential natural gas reformer concepts for further concept development.

4.3.1.3 Natural Gas Mixer Concepts Study

Analysis of fluid flow and mass transfer relative to the mixing patterns and behavior of a variety of natural gas mixer concepts was conducted. The concepts evaluated are listed below and are depicted in Figures 4.3.1.3-1, 4.3.1.3-2, 4.3.1.3-3, and 4.3.1.4-4.

- A2 – Fuel Spokes
- D1 – Expansion Diffuser
- E1, E2 – Flat Mixer Concepts
- F1 – Multiple Micro Channel Mixer
- G1, G2 – Cyclone Mixer Designs
- H1 – Single Fuel Injection Point Baseline
- I1, I2 – Shifted Cone Concepts
- J1, J2, J3 – Swirler Mixer Designs
- K1 – Perforated Plate Concept
- L1 – Bluff Body Design

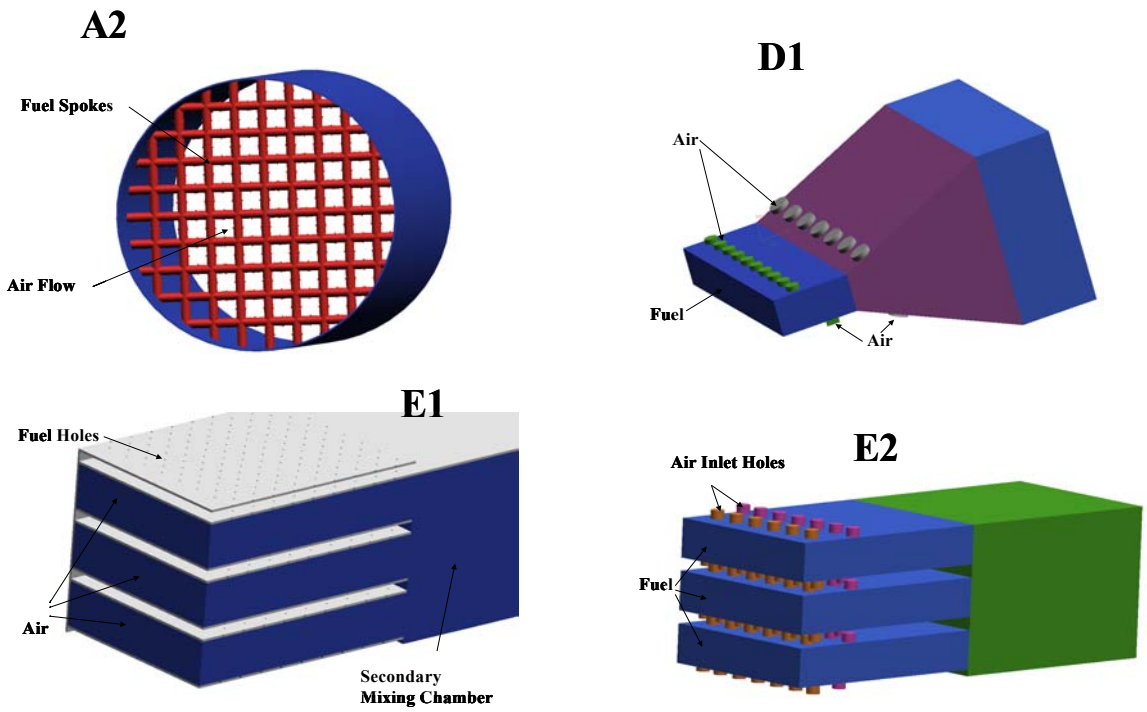

Figures 4.3.1.3-1: Steam Reformer Concepts Study

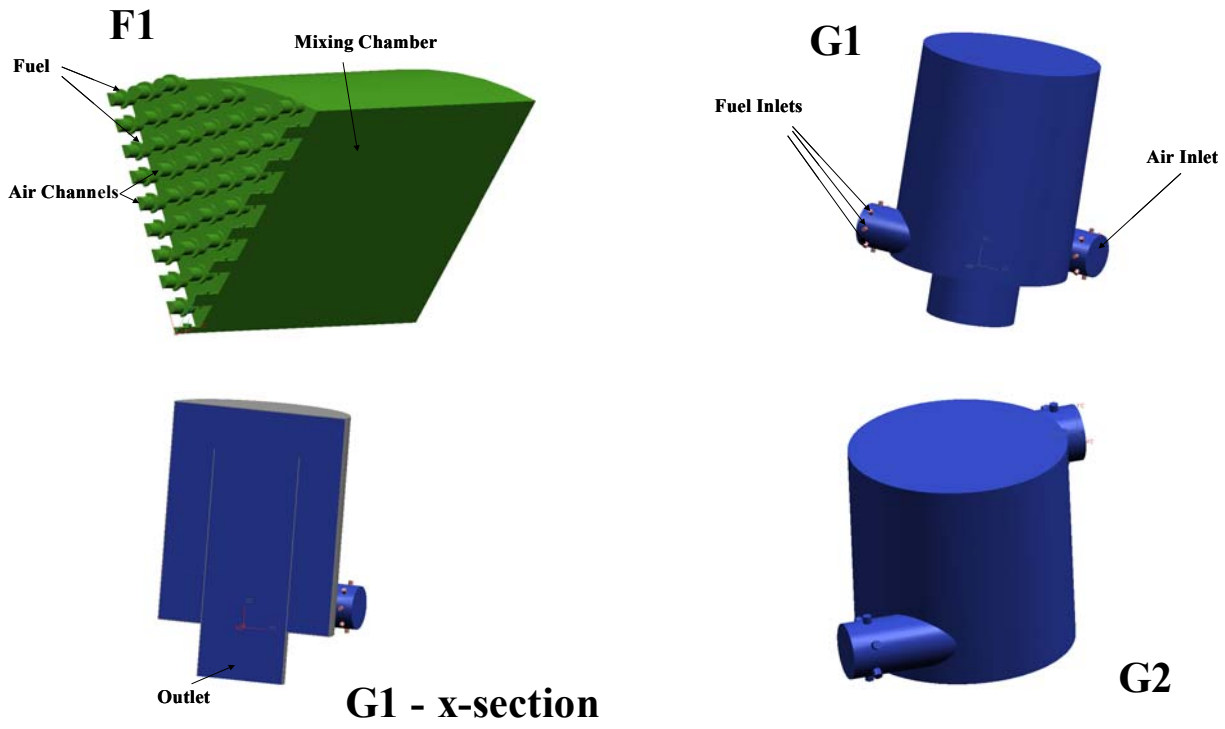

Figures 4.3.1.3-2: Steam Reformer Concepts Study

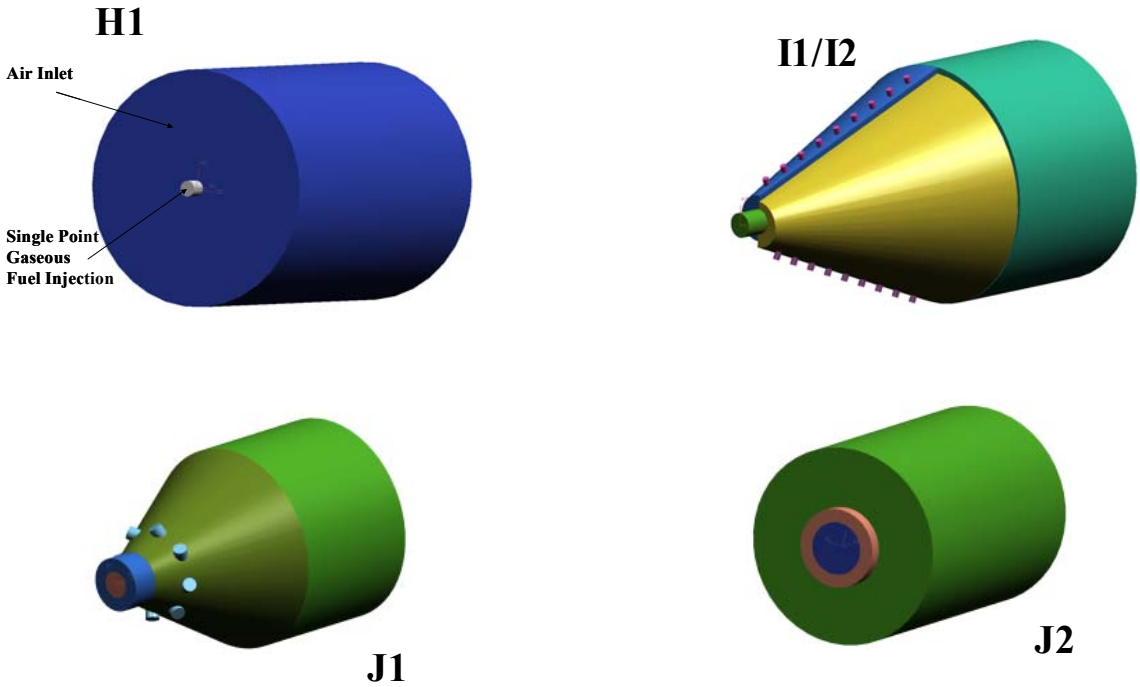

Figures 4.3.1.3-3: Steam Reformer Concepts Study

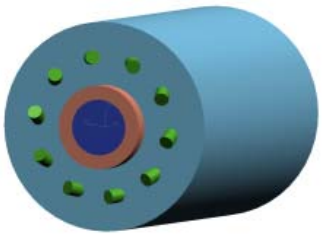

J3

K1

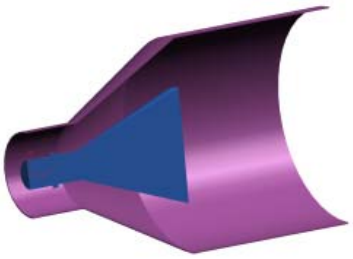

L1

Figures 4.3.1.3-4: Steam Reformer Concepts Study

Standard deviations of fuel fraction have been calculated 75mm downstream of fuel injection to evaluate mixture homogeneity. See Figure 4.3.1.3-5.

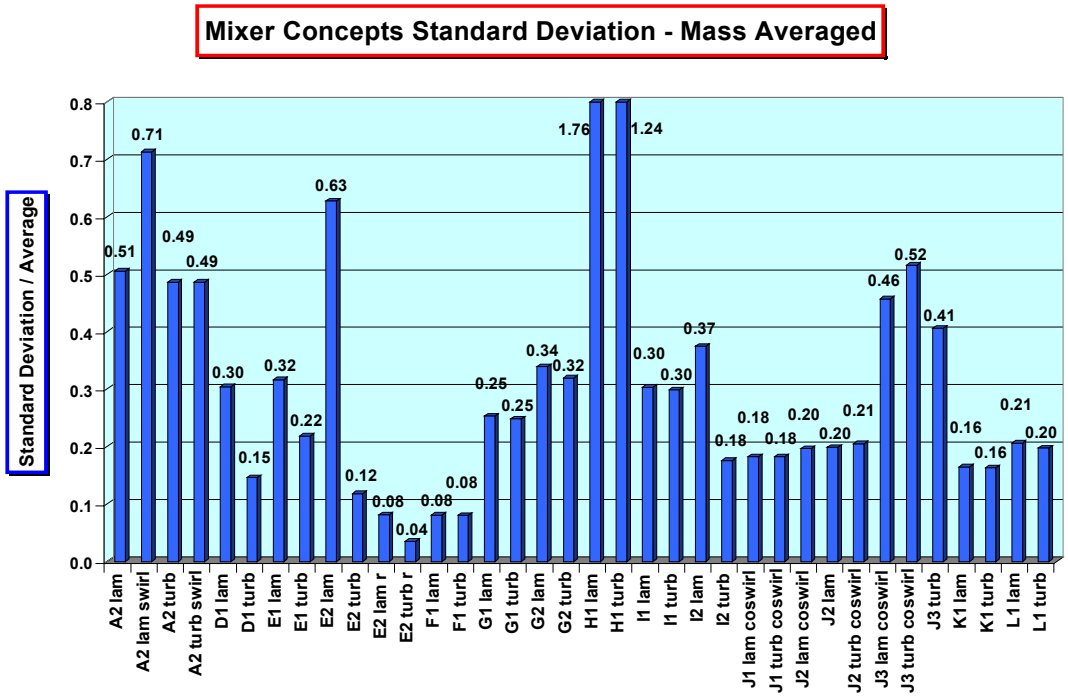

Figure 4.3.1.3-5: Steam Reformer Concepts Study

Contrasting results on all mixer concepts revealed valuable concepts for further concept development.

4.3.2 Develop Catalytic Partial Oxidation (CPOx) Reformer

4.3.2.1 Gen 1.0 / Gen 1.1 discussion

Two tubular design generations were under investigation during this reporting period. Gen 1.0 (see Figure 4.3.2.1-1) was introduced in the previous reporting period and continued on as the primary development hardware during this reporting period. Gen 1.1 (see Figure 4.3.2.1-2) was initiated to address issues uncovered during Gen 1.0 reformer and APU system level testing,

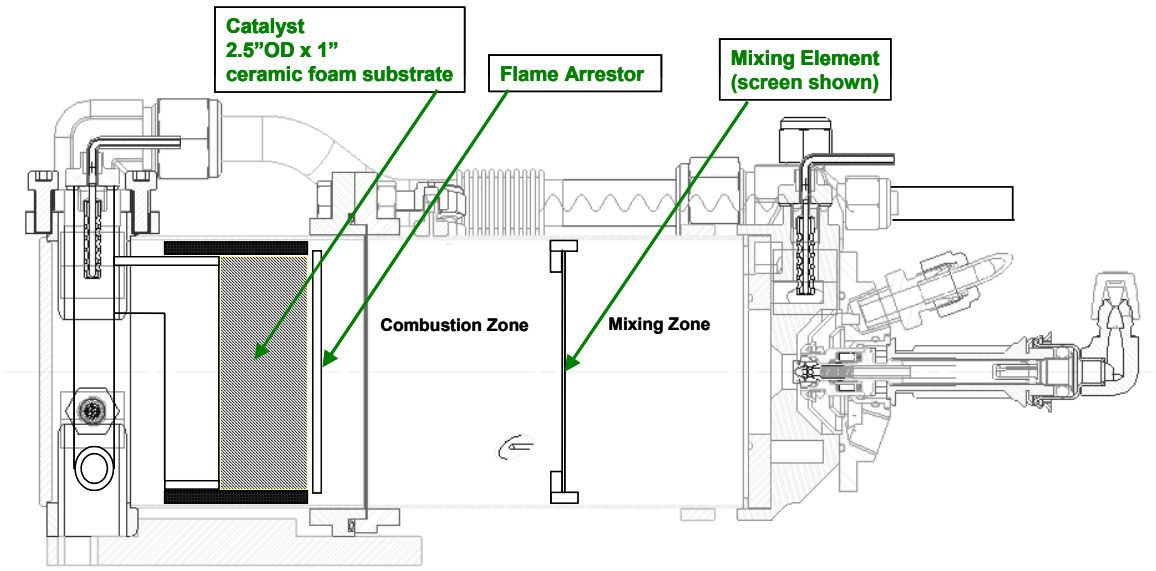

Figure 4.3.2.1-1: Gen 1.0 Reformer – Cross Section

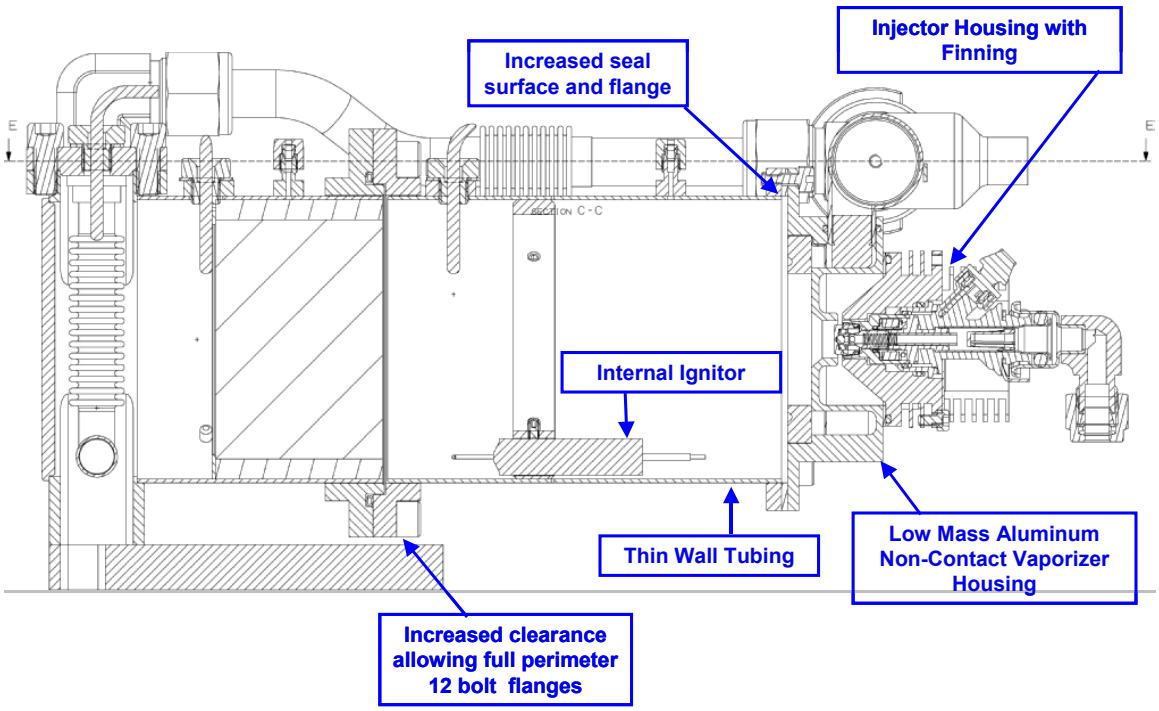

Figure 4.3.2.1-2: Gen 1.1 Reformer – Cross Section

While controls and start up profile differences between the reformer lab and the system lab existed and potentially clouded comparisons it became clear that more work was needed to develop a map of carbon forming regimes. See discussion of this work later in this report.

The key issues uncovered and therefore targeted for improvement were:

CARBON FORMATION DURING APU TESTING:

Several instances of carbon accumulation at various points within the system occurred during APU testing.

EXCESSIVE HEAT REJECTION TO PSM (PLANT SUPPORT MODULE):

APU testing revealed PSM temperatures that locally caused melting of wire insulation. These local hot spots were a result of seams / gaps within the HZM (Hot zone module) insulation. The reformer is particularly important in this heat transfer issue in that it spans both these areas with the Vaporizer / Front End of the reformer located in the PSM while the reactor / catalyst section is located in the HZM. Additionally, the complex shape at the pass thru between HZM and PSM surrounding the reformer made reducing insulation gaps difficult.

HOT RESTART / HOT STEADY STATE FLOW SHIFTS:

Several instances of suspected hot flow shifts were reported during systems testing. Differences in the thermal environment of the reformer lab test setup as compared to the system lab setup which uses product type APU enclosures can be sited a cause for not having experienced this problem to the same degree during reformer lab testing.

THE LOSS OF SEAL INTEGRITY:

Several instances of reformer leaks were reported. Base gasket interface, Reformer Main flange interface and Vaporizer to Tube interface each had a least one instance of deficient sealing.

The resolution of these issues became the goal of both Gen 1.1 hardware development and the reformer controls development.

Gen 1.1 included specific feature changes to address the hardware related issues above and are depicted above and include:

- Simplified geometry at HZM insulation interface to reduce gaps and related heat losses. This required moving the start igniter internal to body tube and repositioning several thermocouples. See Figures 4.3.2.1-4 & 5.

- Lower Thermal Mass Vaporizer design to limit heat storage during hot soak

- Injector housing design with finning to improve heat transfer around injector. This is intended to reduce the heat input to the injector during steady state and hot soak modes.

- Use of thin wall (1.0mm nom) tubing for reformer body to reduce heat transfer by conduction from the hot zone to the vaporizer

- Incorporation of full perimeter 12 bolt flange in place of 10 bolt abbreviated flange to reduce likelihood of leaks at this location

- Improved seal design at NCV housing to reformer body tube for better sealing and higher heat transfer resistance.

- Improved air temperature control and range through use of proportional air valve design in place of previous bypass valve design. Previous (Gen 1.0) bypass valve design had limited ability to control to lower air inlet temperatures. This is a result of the bypass valve situated on the cool flow path such that as it opened it reduced the restriction of cool air into the reformer. At full open it could not prevent flow from traveling through the heat exchanger path. Flow at this full open condition was a function of the relative flow restrictiveness of the 2 outlet paths and typically required adding restrictors in the heat exchange loop so that bypass flow was limited in this path. See Figure 4.3.2.1-3 for a depiction of the proportional valve geometry.

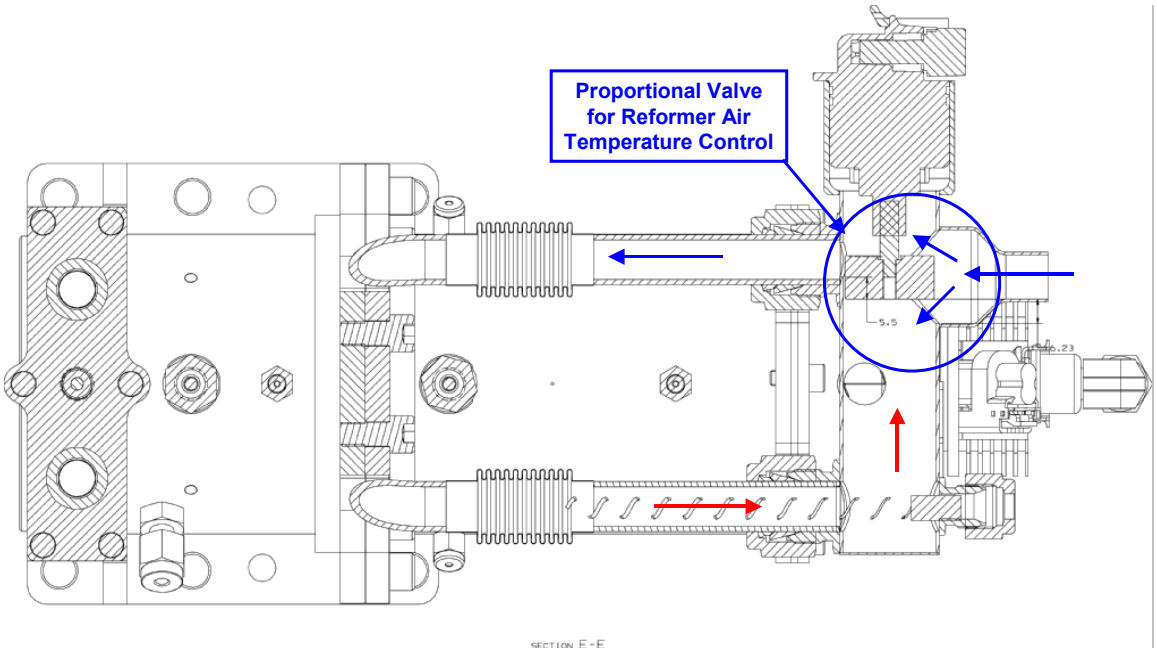

Figure 4.3.2.1-3: Gen 1.1 Tubular Reformer – Cross Section Through Proportional Valve

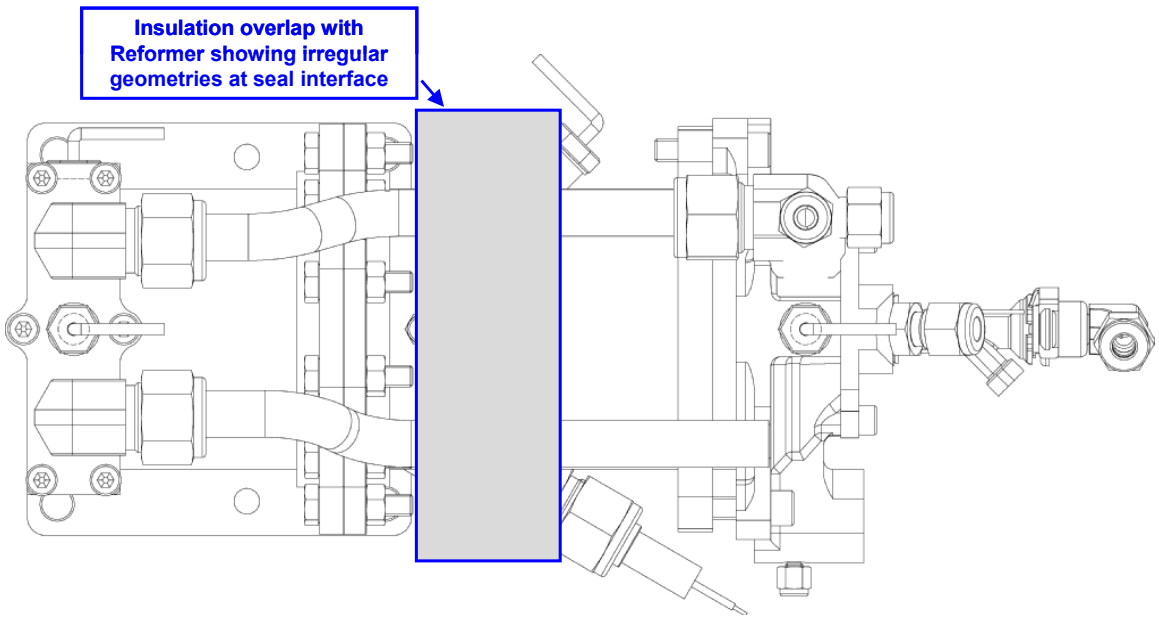

Figure 4.3.2.1-4: Gen 1.0 Tubular Reformer – Top View

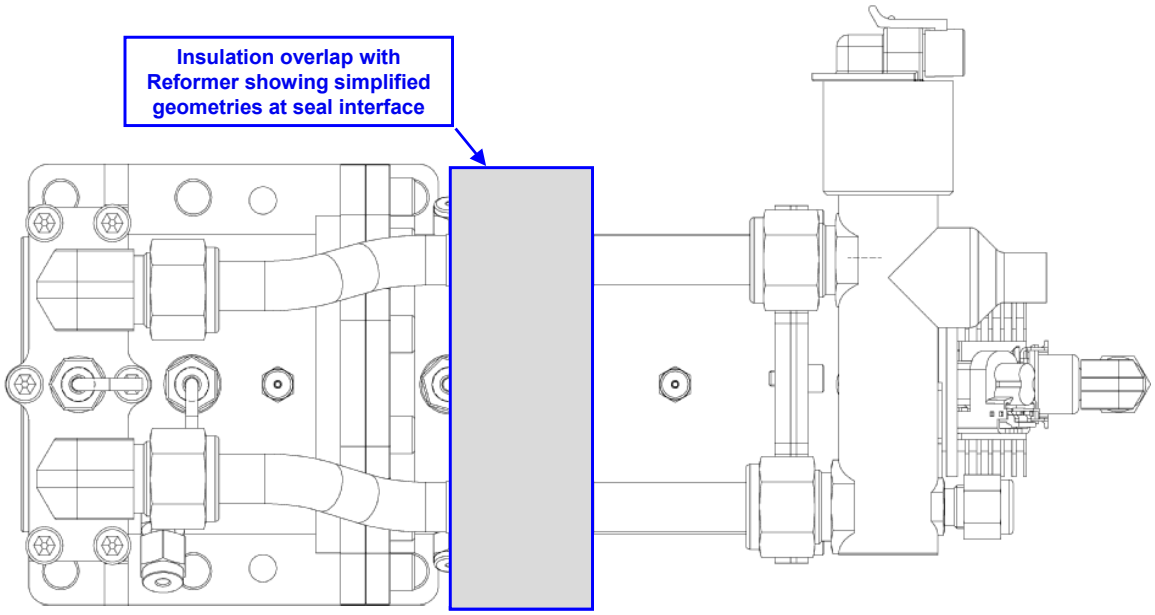

Figure 4.3.2.1-5: Gen 1.1 Tubular Reformer – Top View

4.3.2.2 Tubular CPOx - Gen 1.0

4.3.2.2.1 Carbon Formation Experience/Studies

BACKGROUND:

Previous carbon avoidance testing was focused on elimination of carbon in the reformer and reformate exit ports. Carbon formation in the reformer was evaluated by examining the Saffil material following a run (see Figure 4.3.2.2.1-1).

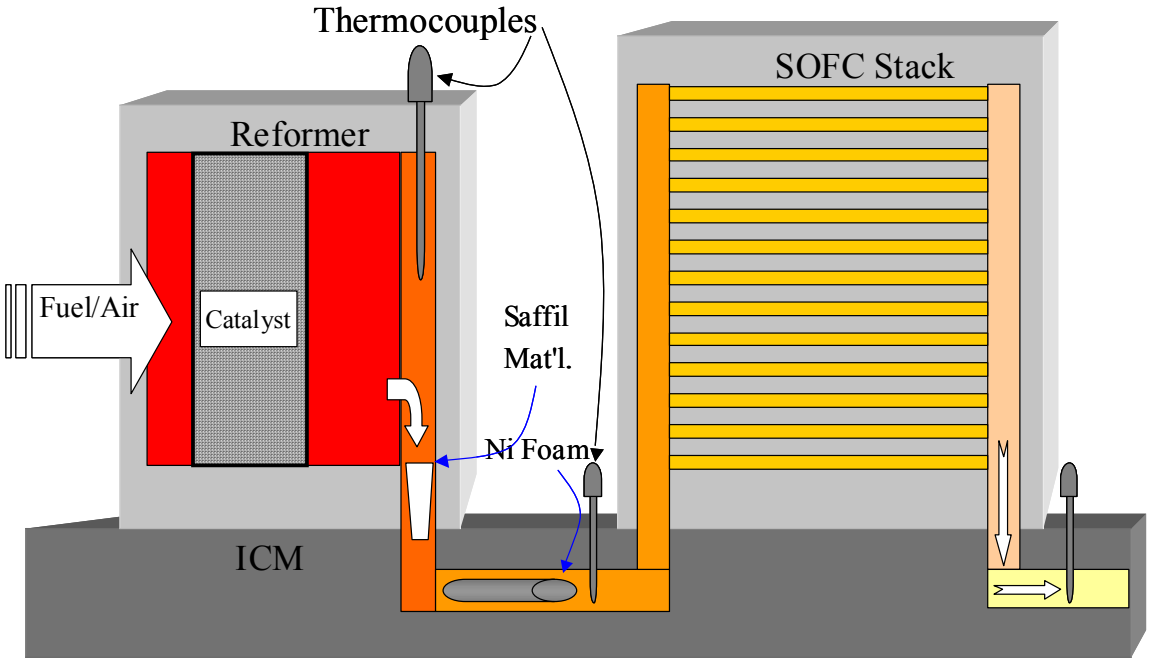

Figure 4.3.2.2.1-1: Schematic Cross-Section of Reformer, ICM and Stack Showing Reformate Flow Paths

While carbon formation in the reformer is undesirable, the more important objective for the APU is to define conditions that eliminate carbon deposition in the reformate channels of the electrochemical stack. Literature sources indicate that carbon formation is very dependent on surface composition/condition. Coupon testing in the reformer itself would have been limited space-wise and temperature-wise, hence Delphi designed and built an air-cooled extension (Cold Finger) to a Gen 1.0 reformer for the prime reason of investigating carbon formation.

Objectives of the design are as follows:

- Imposed temperature gradient of from 800 °C to 550 °C
- Allow isolation of cold finger from reformate produced during start-up from steady state running, and from shut-down conditions
- Distinguish carbon formed in the reformer from deposition downstream
- Enable coupon testing of a wide variety of materials
- Facilitate easy disassembly to shorten testing cycle times

COLD FINGER APPARATUS:

A cross section of the cold finger is shown in Figure 4.3.2.2.1-2, showing what is basically a counter flow, reformate-to-air heat exchanger.

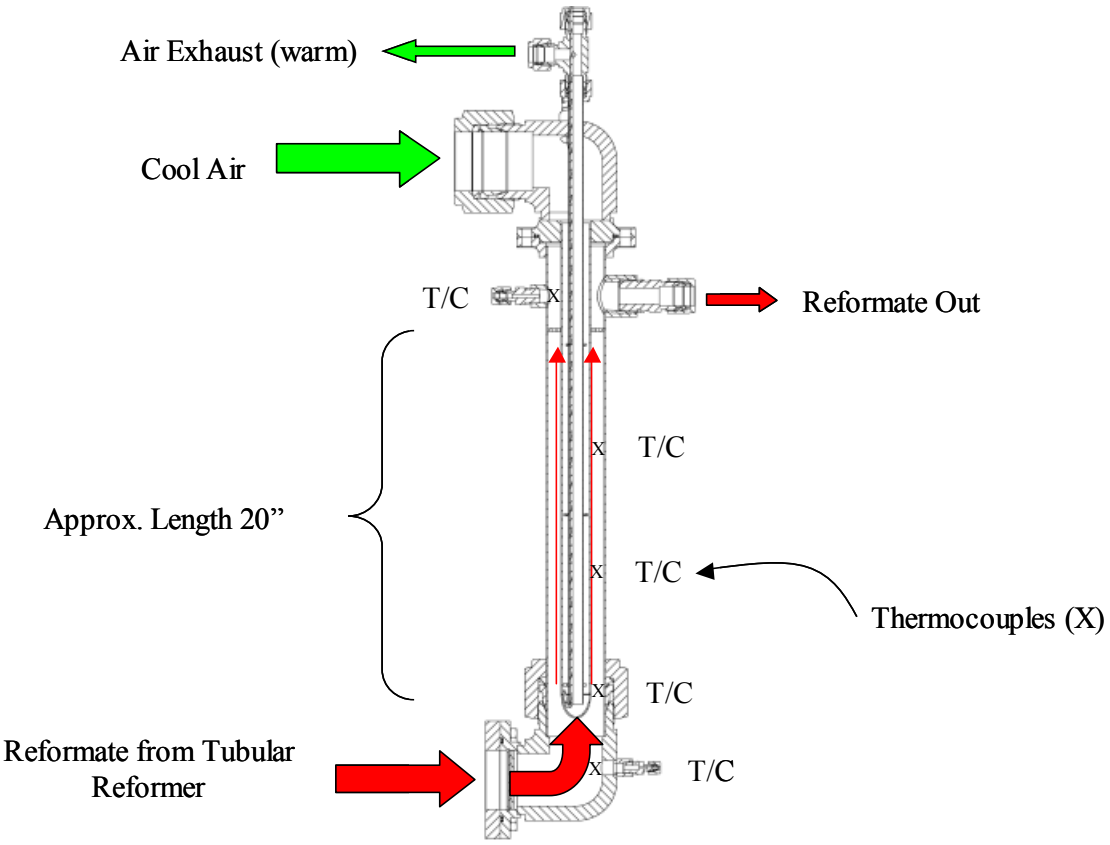

Figure 4.3.2.2.1-2: Cold Finger Cross Section

Compressed air enters at the top elbow and runs down the center small tube to the tip of the cold finger, and exhausts out the annulus created between the inner tube and the cold finger. Hot reformate enters at the bottom elbow and flows vertically around the outside of the cold finger. The cold finger apparatus is close coupled to the outlet of a Gen 1.0 tubular reformer. A high temperature filter is placed between the reformer exit and cold finger entrance to prevent particulate formed in the reformer from confounding interpretation of the cold finger results. Thermocouples are placed along the length of the cold finger to record the temperature profile. All internal surfaces that come into contact with reformate are made from Inconel 625, including the thermocouple sheaths. This alloy was used since it is the predominant material used in the reformate passages between the reformer and the SOFC stack (i.e., the ICM).

MODE OF OPERATION:

The conditions at the exit of the reformer during a cold startup are suspected as being particularly prone to carbon formation. It was therefore desired to be able to isolate the reformate formed during startup from exposure to the cold finger. This is accomplished via a remotely actuated valve, on the exhaust side of the tubular reformer reformate-out port and by back flowing a purge gas through the cold finger and into the reformer exit during the startup. The backflow was found to be necessary to prevent diffusion of reformate into the cold finger chamber rather than just a valve at the reformate discharge port of the cold finger. Once the startup period is complete, the valve is closed and the backflow is discontinued, allowing reformate to flow through the cold finger. Early tests were not conducted with the backflow procedure in place.

Generally, reforming conditions are held constant during steady state operation (i.e. while the cold finger is exposed to reformate). Air flow through cold finger is adjusted to maintain the desired cold finger temperature profile. To avoid reformate hitting a "cold" cold finger, the apparatus is brought up to temperature using a high reforming O:C (one known to not form carbon). The air/fuel rates are then changed to the O:C of interest.
A procedure similar to the startup is used, but in reverse, to shut down the system. This avoids exposing the cold finger to reformate produced during a transition.

RESULTS TO DATE:

The results of the first series of runs with the cold finger are shown in Table 4.3.2.2.1-1.

	Reforming O:C Ratio		
Surface	1.05	1.1	1.16
Inconel (fresh)	None	None	None
Inconel (seasoned)	Carbon	Trace	None
Oxidized Inconel			Carbon

Table 4.3.2.2.1-1: Summary of Cold Finger Carbon Formation Testing

The first row shows that carbon did not form, even at conditions (low O:C) that were shown to produce carbon in tests with the reformer alone. The surface of the Inconel cold finger had never been exposed to carbon forming conditions however. It was then decided to force some carbon to form, by running startup reformate through the cold finger, and then to repeat the conditions of the first test after having removed the carbon from the surface. Once the cold finger had been "seasoned" with carbon, we then observed a dividing line between carbon formation at an O:C of about 1.10 (row 2) for steady state operation. This trend more closely fits with previous observations running the reformer without the cold finger.

Figure 4.3.2.2.1-3, Figure 4.3.2.2.1-4, and Figure 4.3.2.2.1-5 illustrate the regimes for carbon formation as a function of downstream temperature for the three O:C ranges studied (row 2 of Table 4.3.2.2.1-1). A range of reformate temperatures was achieved by varying the reformer O:C ratio while holding the fueling rate constant (0.3 g/s gasoline). Reforming temperature is a direct function of O:C ratio. The vertical axis was chosen as the calculated chemical activity of carbon in the reformate as it cools downstream of the reformer in an attempt to begin to be able to predict the conditions favoring carbon precipitation. The actual reformate composition analyzed, as well as that predicted by chemical thermodynamics, is shown on each graph.

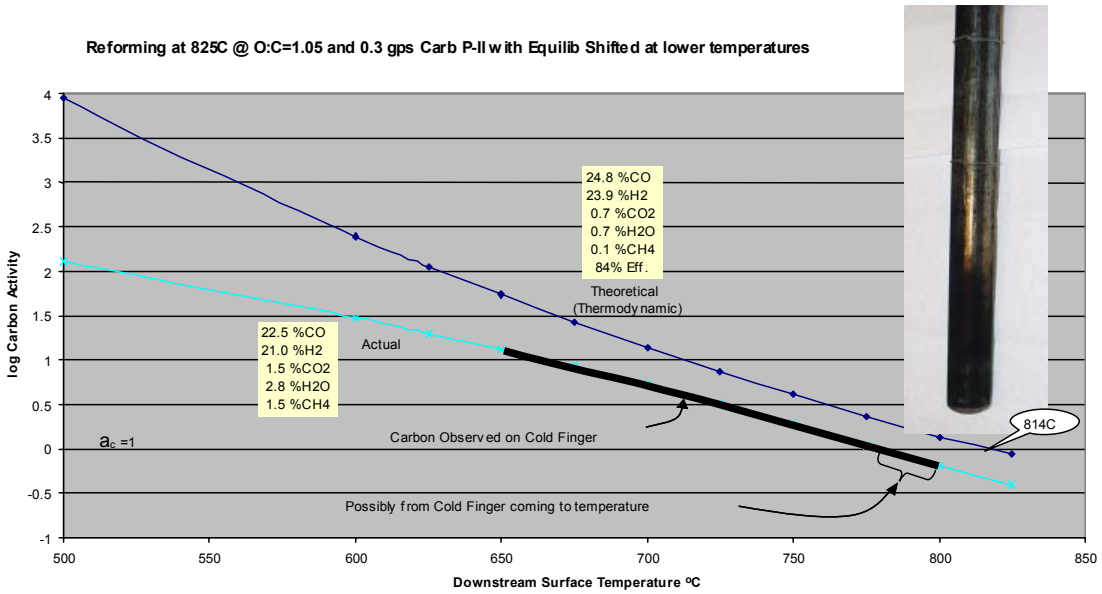

Figure 4.3.2.2.1-3: Activity of Carbon in Reformate O:C 1.05

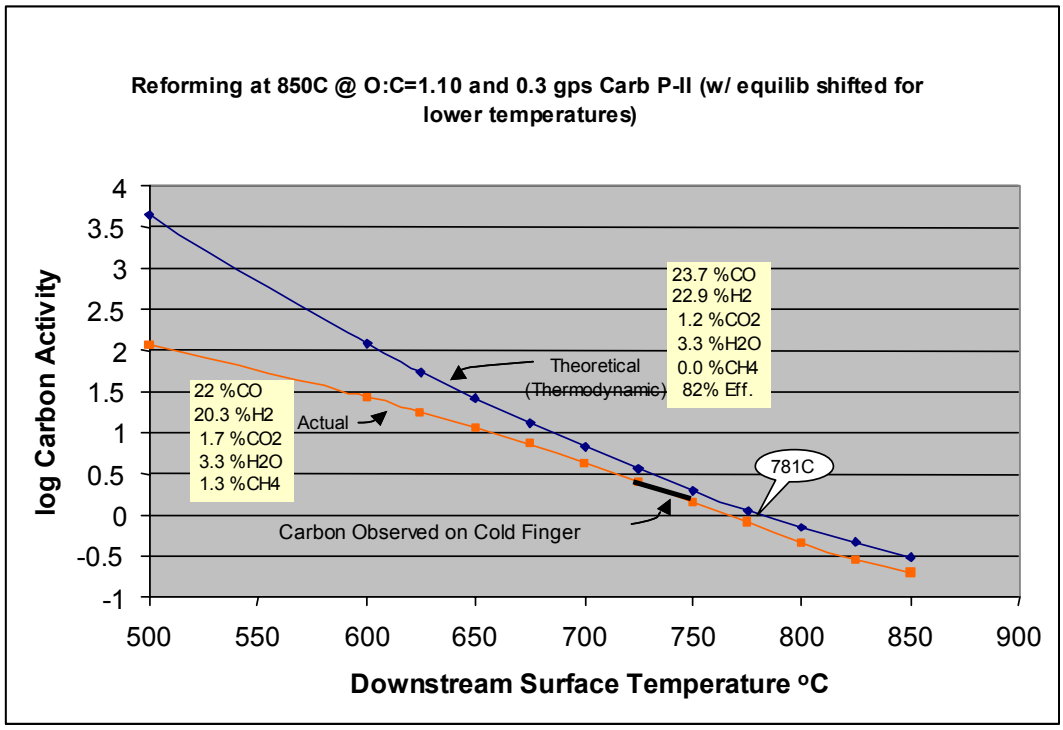

Figure 4.3.2.2.1-4: Activity of Carbon in Reformate O:C 1.10

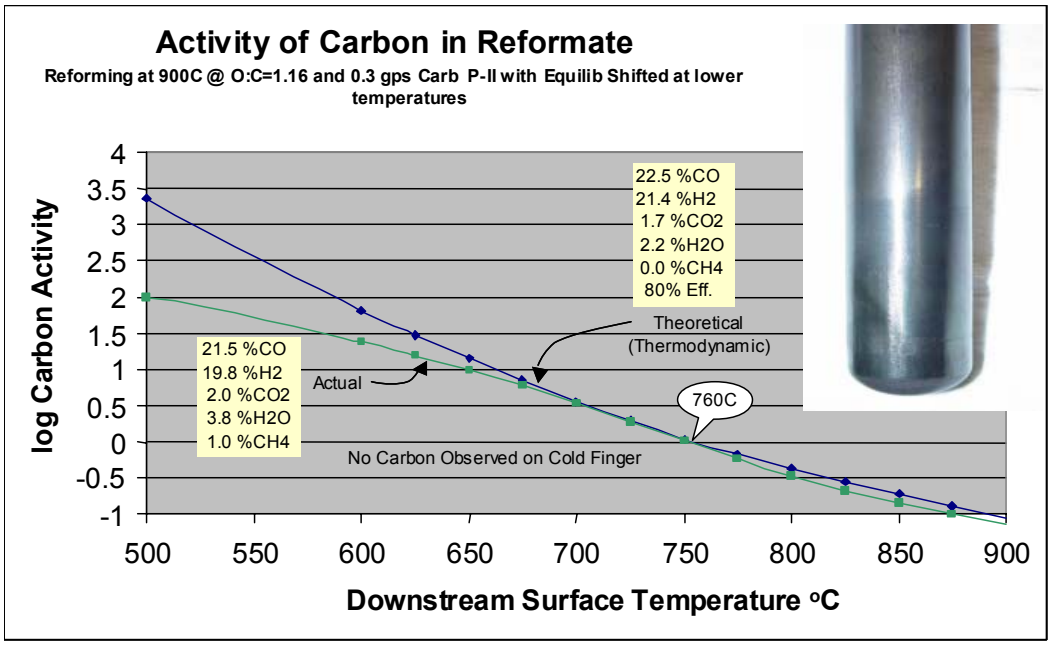

Figure 4.3.2.2.1-5: Activity of Carbon in Reformate O:C 1.16

In all figures, the lower lines of the plots represent the carbon activity for the actual reformate produced at the reforming temperature, and for a series of temperatures representing points downstream of the reformer. The points are adjusted for shifts in

the chemical equilibrium as the gas is cooled (theoretically). The thick, black lines show where carbon was observed over the temperature profile of the cold finger. For reference, the upper lines on each figure show the theoretical composition from a thermodynamically perfect reformer, again shifted for changes in temperature. The theoretical and actual lines come together at the higher reforming temperatures, possibly indicating that air/fuel charge stratification diminishes at higher gas flows/catalyst temperatures.

The carbon forming regime is broadest on Figure 4.3.2.2.1-3 at the lowest O:C, and seems to start at a temperature corresponding to a predicted carbon activity of 1.0 (Boudouard and CO reduction reactions both at Carbon Activity = 1.0). The range of temperature over which carbon deposited at the intermediate O:C of 1.10 is narrower, but again, it seems to start at a carbon activity of about 1.0 (CO reduction reaction dominates). No carbon was observed with the reformate at an O:C of 1.16, possibly because the activity of carbon crosses the 1.0 line at too low a temperature for carbon to precipitate from a kinetic perspective. Inaccuracies in the prediction may be due to diffusion of rich reformate gases into the cold finger during startup and this should be eliminated by backflowing inert gas during startup. These tests will be repeated with the backflow procedure in the near future.

During reattachment of a thermocouple, it was discovered that exposure of the cold finger surface to a high temperature in a somewhat oxidizing environment led to carbon formation in regimes that did not previously produce carbon. Carbon was observed locally only over the heat affected zone from the brazing operation. To test this phenomenon more conclusively, the cold finger was heated to about 800 °C in air to form a thin patina of oxide on the surface. It was then exposed to reformate at an O:C of 1.16. Again, carbon formed over the entire oxidized region (row 3 of table 4.3.2.2.1-1). In addition, it was very difficult to remove the affect of oxidation, even with light sanding of the surface. Only through complete re-polishing of the cold finger could the “seasoned-like” behavior be restored.

The carbon formed on the Inconel surface appears in the form of filaments, as shown in Figure 4.3.2.2.1-6. Reports from the literature indicate that this form of carbon “growing” on nickel supports is not uncommon in our temperature range when the surface area for growth is limited. Figures 4.3.2.1-6 a & b are examples of the nature of carbon deposits on the cold finger tube at 30 X. Figure 4.3.2.1-6 c is a macro photograph of carbon deposited on the cold finger tube.

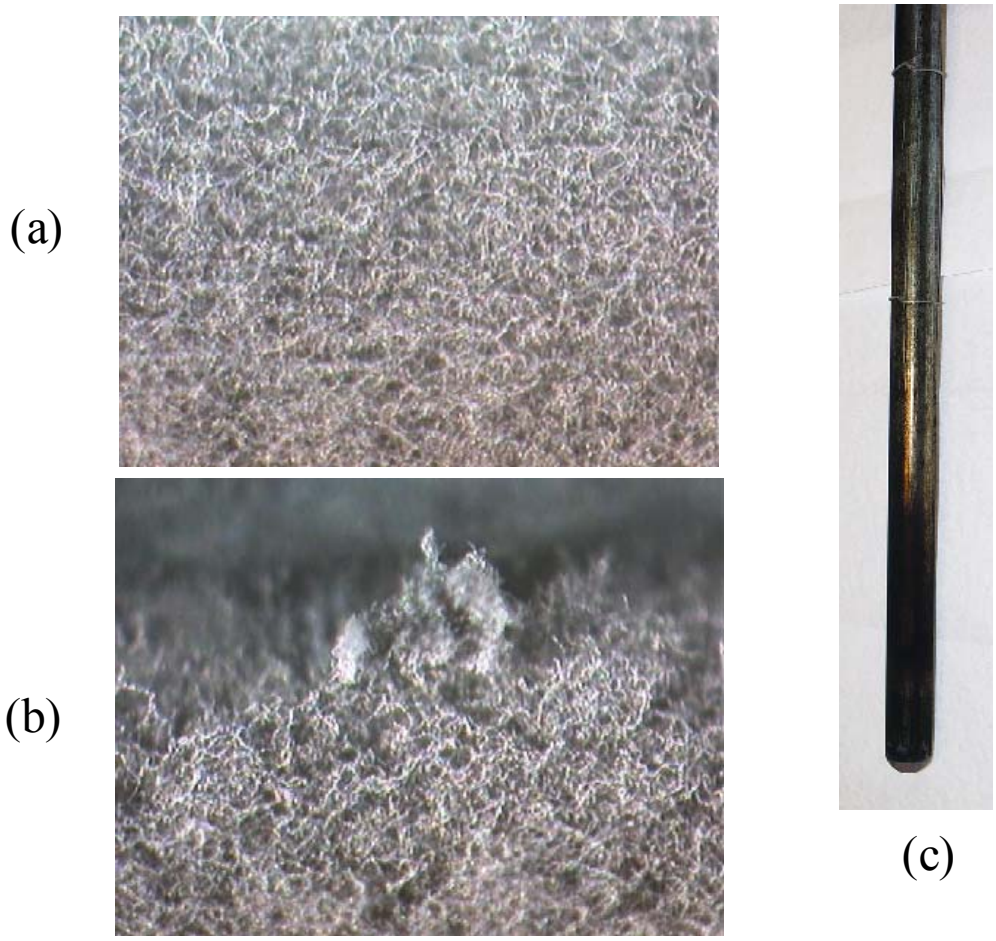

Figure 4.3.2.2.1-6: Nature of Carbon Deposited on Cold Finger

OBSERVATIONS FROM COLD FINGER TESTING:

Carbon deposition is suppressed on “fresh” Inconel surfaces (i.e., surfaces that have not been previously welded, brazed or been exposed to carbon forming conditions).

Carbon deposits are heavier toward the tip, or hottest part, of the cold finger, and carbon does not deposit at the lower temperature zones. This would appear to be in line with literature references, which suggest that the kinetics of carbon deposition are slow below about 700 °C.

Carbon deposition can be “forced” by passing startup reformate at an O:C of 1.16 through the cold finger. Once this carbon is formed, and the surface is altered, it is then difficult to inhibit carbon formation without mechanical abrasion of the surface.

Running the reformer at a steady state O:C of 1.16 avoids carbon formation, even on seasoned Inconel surfaces, but not surfaces that have been oxidized.

Carbon deposition appears well before, in terms of O:C ratio, gas phase carbon precipitation and is of primary concern for SOFC operation.

Chemical thermodynamic calculations are close to predicting carbon forming regimes, however verification that is more empirical is necessary.

FUTURE TESTING:

Tests to date were limited to Inconel 625, and modified surfaces thereof. Materials more representative of the SOFC stack construction will be evaluated in future tests. In addition, a revised procedure for operating the cold finger with inert gas backflow will be used to better define steady state carbon forming regimes. Tests aimed at understanding startup and shutdown conditions will also be conducted.

4.3.2.2.2 Thermal Performance / Injector Flow Shift

A series of tests were conducted on Gen1.0 to evaluate steady-state operating temperatures, the degree of injector flow shift, and its impact of hot restarts. These tests were conducted at two different inlet temperatures to evaluate current reformer thermal characteristics at an 180 ^{o}C inlet temperature, and to evaluate the impact on the reformer at 150 ^{o}C. It was found that an inlet temperature of 150 ^{o}C had no apparent detriment to reformer performance, and had improved chances of hot-startability and reduced the Vaporizer’s heat rejection to surrounding air space in the PSM. Therefore, the 150 ^{o}C inlet temperature was chosen as the new standard operating point for reformer testing.

Comparisons of operating temperatures, and injector flow shift between Gen 1.0 and 1.1 are discussed further in section 4.2.2.2.

4.3.2.2.3 Turndown

Testing the limitations of the catalyst relative to its turndown capacity was done to determine its max and min power output so that current and future system sizing could be evaluated. The turndown testing schedule started with nominal fuel rate (0.2gps) and an O/C at 1.16. The 1.16 O/C set point had been established as "carbon free" from previous testing experience. During the turndown test, the control system keeps O/C constant while stepping the air and fuel rate up or down.

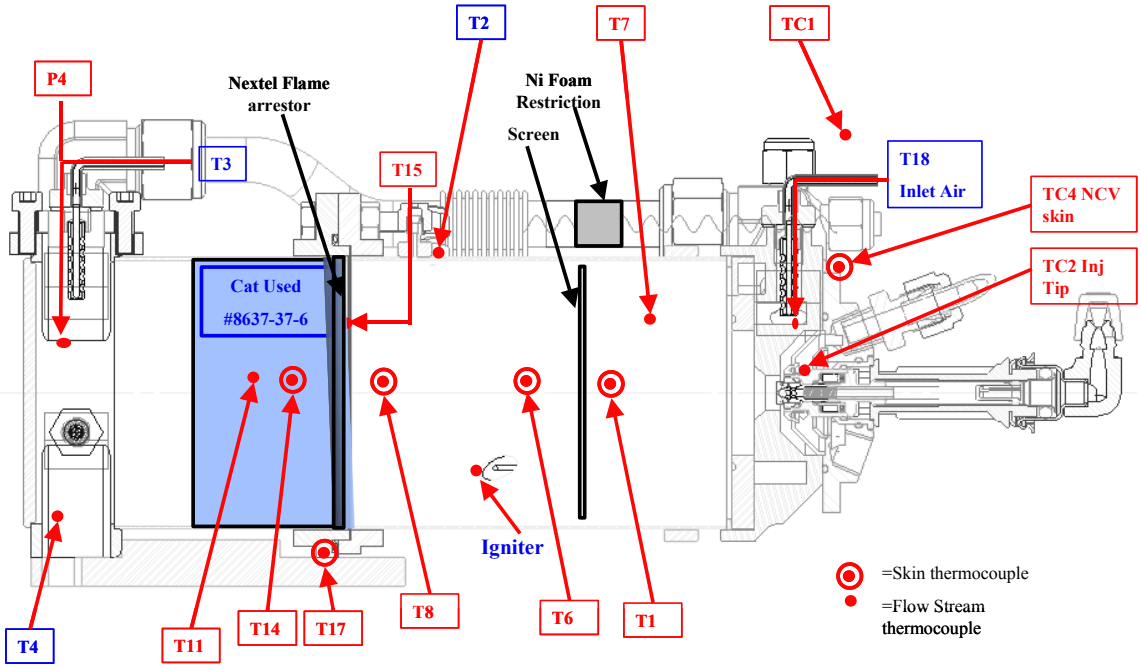

Figure 4.3.2.2.3-1: Thermocouple / Pressure Probe Locations – Turndown Testing

Figure 4.3.2.2.3-1: Illustrates the Reformer Set-Up and Thermocouple Placement.

Figure 4.3.2.2.3-2: Shows the Temperature Profile as Air and Fuel Rates are increased.

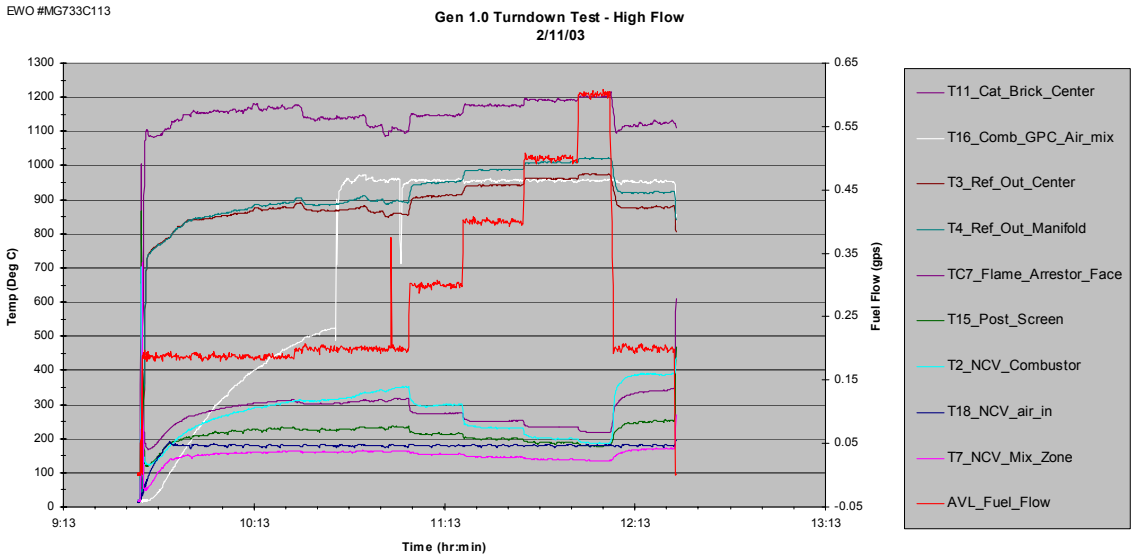

Figure 4.3.2.2.3-2: Temperature Profile During Turndown Test – Increasing Flow Rates

Notice that catalyst temperatures increase with increased flow, while upstream temperatures decrease due to increased convective cooling.

Figure 4.3.2.2.3-3 shows the conversion profile, with methane slip increasing with flow rate.

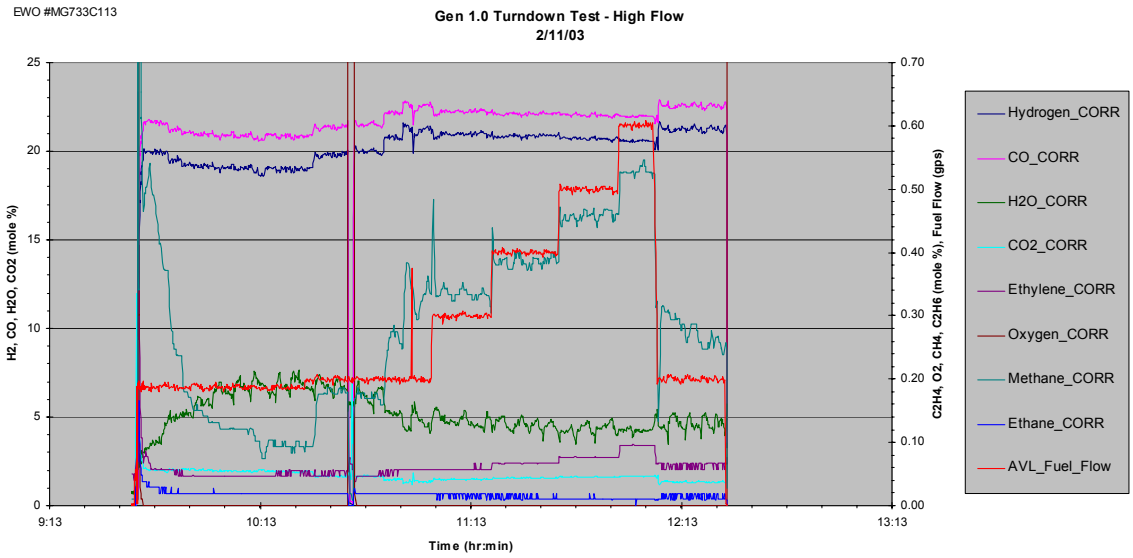

Figure 4.3.2.2.3-3: Conversion Profile During Turndown Test – Increasing Flow Rates

Figure 4.3.2.2.3-4 and Figure 4.3.2.2.3-5 show these profiles as air and fuel rates are decreased. Methane rises sharply at very low flow rates, and upstream temperatures rise. This is believed to be due to localized gas-phase combustion caused by upstream elevated temperatures from increased radiation effects from the catalyst.

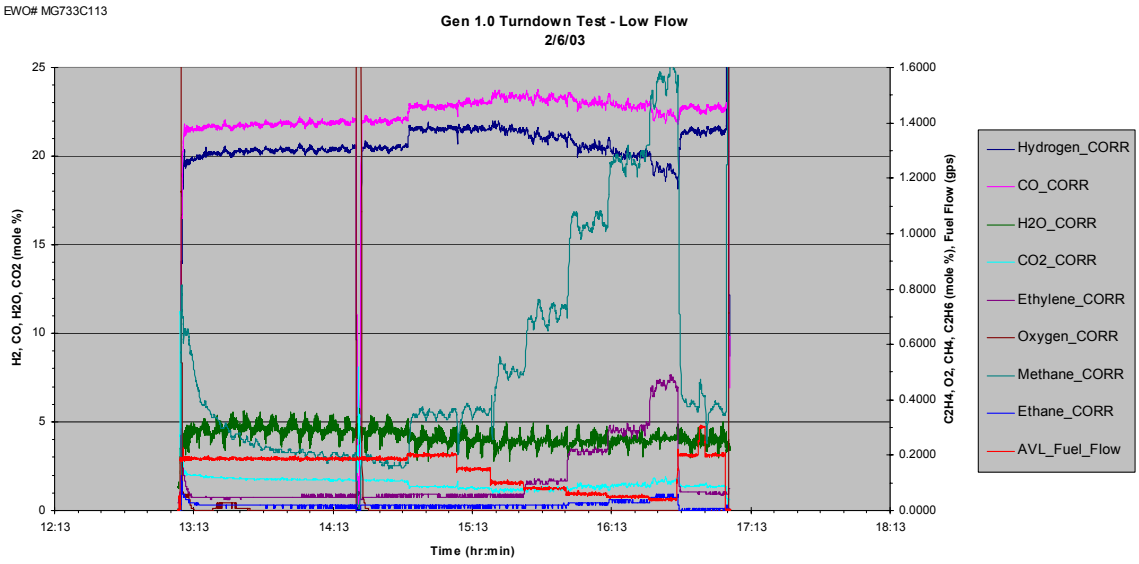

Figure 4.3.2.2.3-4: Conversion Profile Vs. Flow Rate – Decreasing Flow Rates

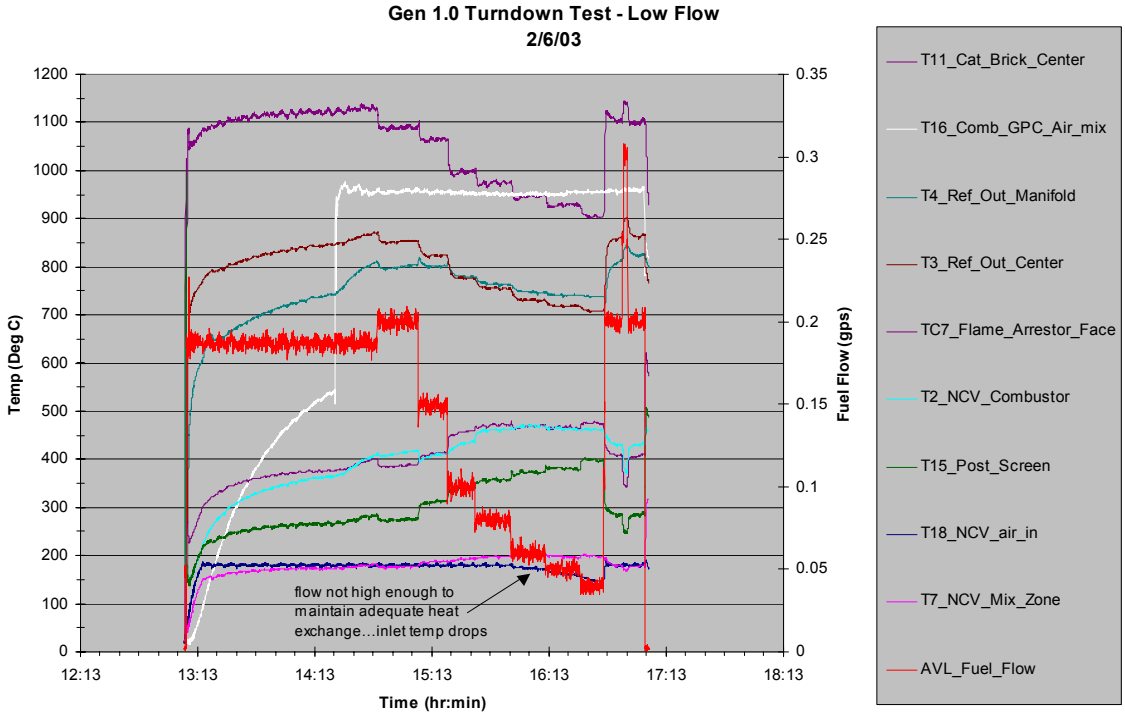

Figure 4.3.2.2.3-5: Temperature Profile During Turndown Test – Decreasing Flow Rates

In establishing the turndown ratio from this data, restrictions on hydrocarbons and H_2O/CH_4 ratio were imposed based on the expected stack tolerance to coking. Figure 4.3.2.2.3-6 shows the performance boundaries that were imposed and their application to a collection of turndown data that results in a turndown ratio of 6, with fuel flow ranging of 0.09 – 0.59 g/s of fuel.

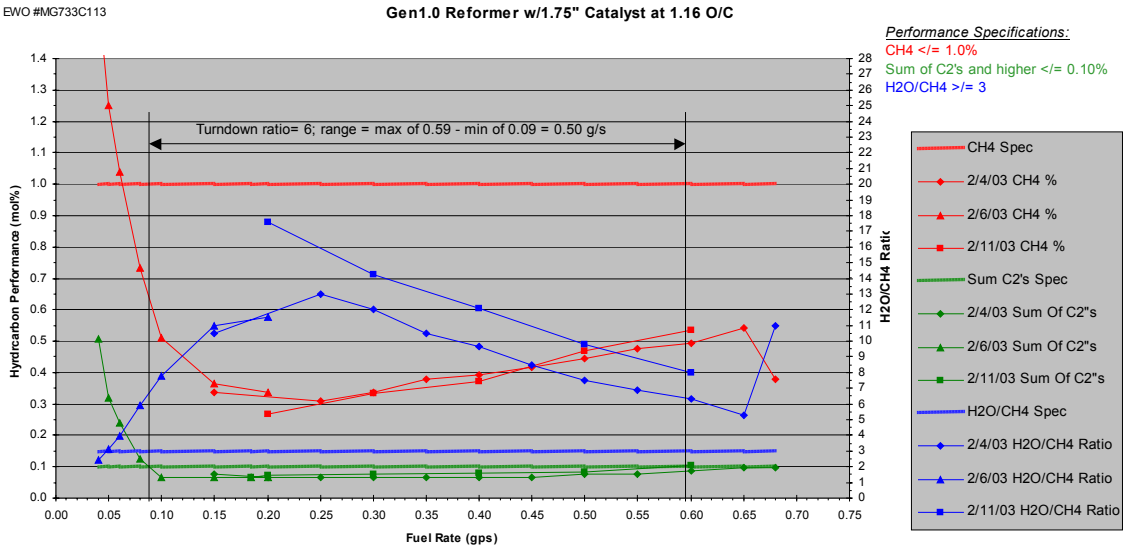

Figure 4.3.2.2.3-6: Conversion Performance vs. Fuel Flow – 1.75" Catalyst

The same specifications were used to evaluate turndown on a 1" thick catalyst (shown on Figure 4.3.2.2.3-7).

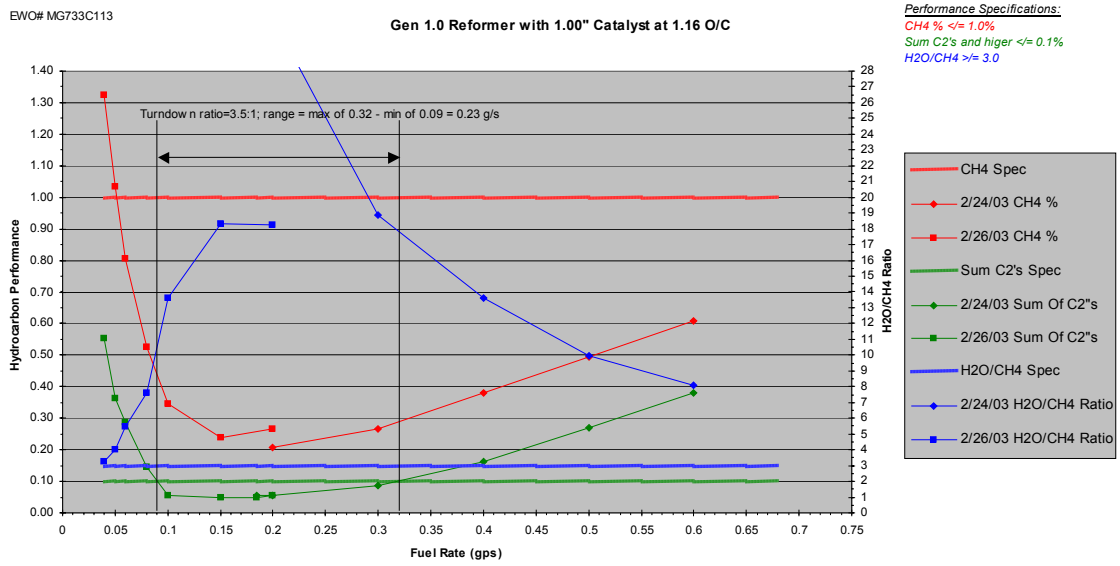

Figure 4.3.2.2.3-7: Conversion Performance vs. Fuel Flow – 1" Catalyst

Turndown on this size catalyst was reduced to 3.5:1, almost half that of the 1.75" catalyst. This begins to demonstrates the relationship between catalyst volume and reforming capacity as measured using turndown ratio

4.3.2.2.4 Durability

A 100-hour durability test was targeted on the Gen 1.0 design to demonstrate and evaluate preliminary durability results and trends. 106 hours of durability were completed under the following test parameters:

O/C set point = 1.16

180 deg C inlet temp with injector cool air flow ~ 5min. after shutdown.

Fuel close-loop around flow feedback

500 kPa fuel pressure

1.75" length catalyst 8637-37-6 (TG series) with Nextel Radiation Shield

Gas Phase Combustor (GPC) running at ~1-1.5 g/s total flow (max. capacity of test fixture)

One rebuild around ~33 hours into test.

During the course of the 106 hours accumulated run time, the reformer experienced:

- Number of cold starts = 17 + 1 restart
- Number of HOT starts = 5
- Number of un-planned shutdowns = 3

The catalyst performance summary is as follows:

After 106 hours of accumulated run time, hydrogen levels were still quite good at 21.2%. Per section 4.3.2.2.3, hydrocarbons levels remained within specification (see Figure 4.3.2.2.4-1). Gas Chromatograph results revealed very few hydrocarbons larger than C_2. Propylene was the only component consistently detected, with an average level of 0.01% and measured H_2O/CH_4 ratio was within specification. Figure 4.3.2.2.4-1 shows the specific reformate quality measures tracked over time.

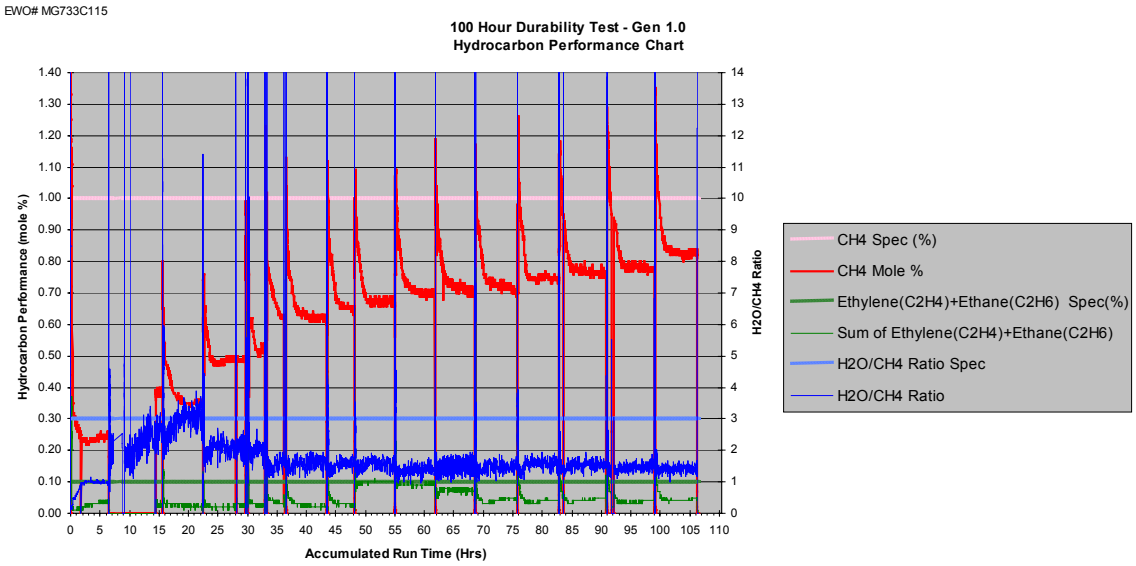

Figure 4.3.2.2.4-1: Reformate Quality vs. Run Time

Efficiency loss (calculated without CH_4) was approximately 3% after 106 hours. Figure 4.3.2.2.4-2 shows specific reformate components over the run time and thermal cycles that comprised the test.

A step change down in performance was seen after each thermal cycle, while steady-state operation within a given thermal cycle showed either sustained or improved performance.

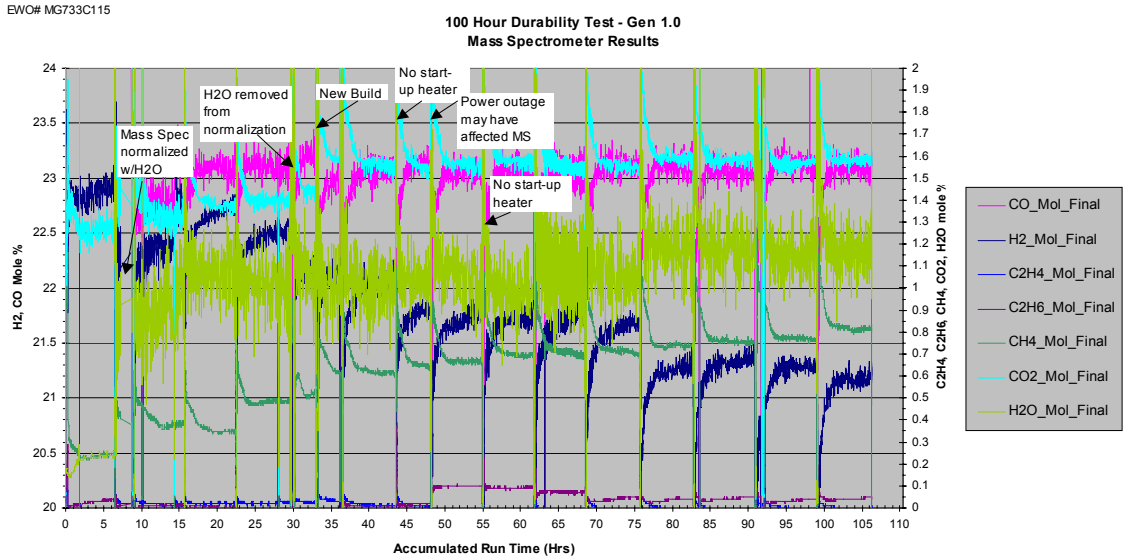

Figure 4.3.2.2.4-2: Reformate Composition vs Run Time

Gradual catalyst degradation is believed to have occurred based on the gradual increase in temperature observed at the center of the catalyst (see the T11 curve on Figure 4.3.2.2.4-3 and T11 location within reformer on 4.3.2.2.3-1). It is hypothesized that as the front face of the catalyst becomes deactivated, the exotherm moves down the length of the catalyst, causing an increase in the temperature registered at the T11 location. The fact that temperature had not yet begun to decrease during the 106 hours indicates that the majority of the exothermic reaction was still occurring upstream of the 1" deep T11 thermocouple.

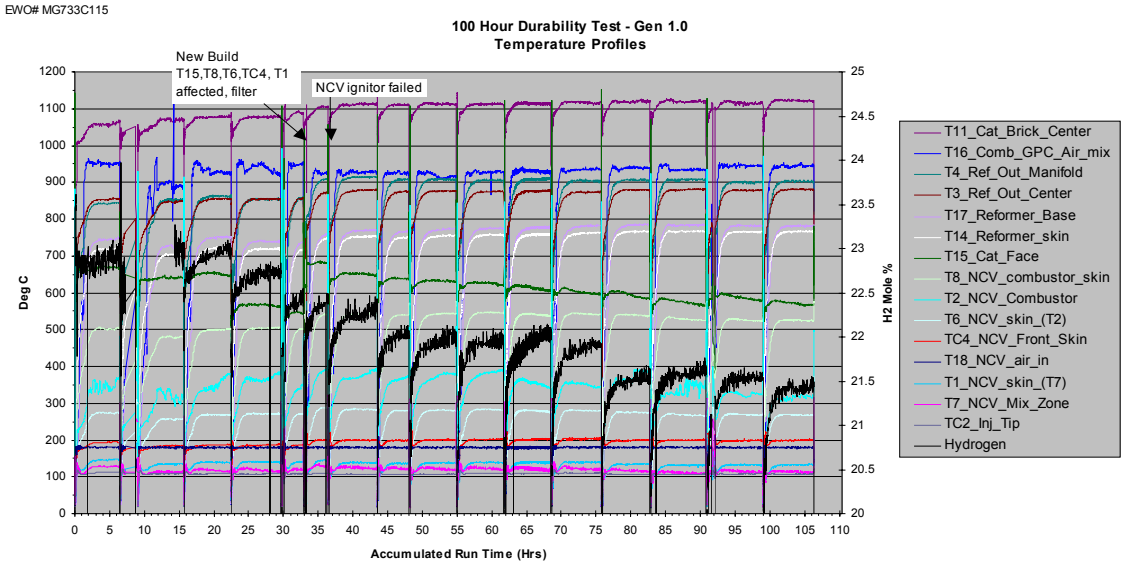

Figure 4.3.2.2.4-3: Reformer Temperatures vs Run Time

Photos from the post-test teardown inspection are shown in Figure 4.3.2.2.4-4 and revealed the following.

- The outlet filter showed concentrated carbon in the middle while the edges of the flow stream were clean Carbon formation at this O/C during each start-up had been anticipated, but a single O/C was chosen for both start and run periods to simplify the test and help reduce variables that could affect durability.

Figure 4.3.2.2.4-4: Catalyst, Outlet Filter, Base Gasket Condition – Post Test

- The Catalyst showed a darkened front face, and evidence of a strong thermal gradient at the back face, with carbon around the bottom edge.

- NCV director plate holes showed evidence of mal-distribution (See Figure 4.3.2.2.4-5). Investigation showed flow is very biased to upper holes. This could contribute to catalyst thermal gradients. Investigation showed flow is very biased toward upper holes. Prior to this test modifications were made to the manifold housing located behind the director plate as shown in Figure 4.3.2.2.4-5 in order to help alleviate a temperature control problem. There were separate hot air and cold air feeds to the manifold chamber that feeds this director. In addition these two feeds were not symmetrically located with respect to the T12 thermocouple that is used as a measure of reformer inlet air temperature. The modification involved re-routing the hot air feed to join the cold air feed before it entered the manifold feeding in the director. While this seemingly helped the temperature control problem it may have also effected radial mass distribution between director holes. This subject is discussed further in Section 4.3.

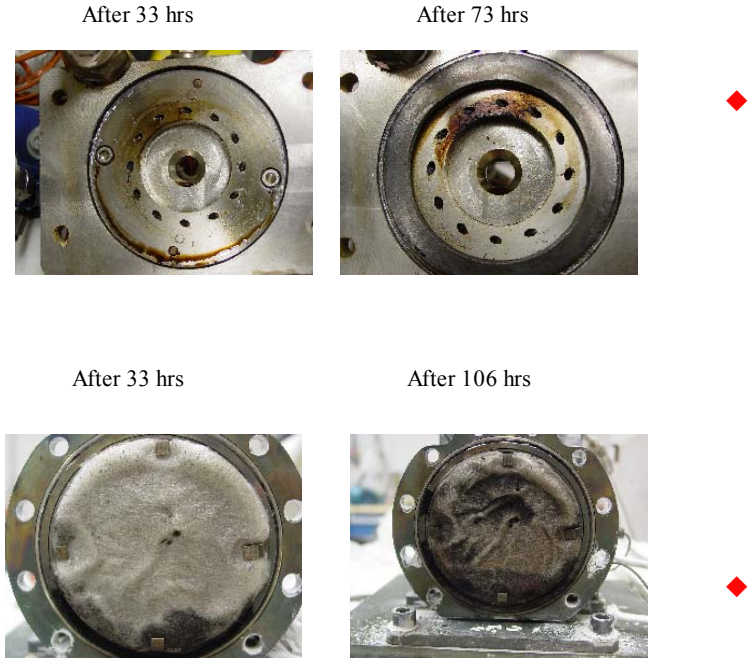

Figure 4.3.2.2.4-5: Vaporizer Director Plate And Flame Arrestor – Mid/Post Test

- Bad distribution from director plate may be due to NCV air manifold modification.
- Flame arrestor degradation with evidence of bad flow distribution.
- The Flame arrestor showed degradation and some carbon accumulation. It was very fragile and brittle (Figure 4.3.2.2.4-5). There was Igniter failure after 32 hours (igniter showed very high resistance at 600 ohms – cause of failure unknown).
- The Mica reformer base gasket showed damage/failure at both the 32-hour rebuild and 106-hour End of Test teardowns (Figure 4.3.2.2.4-4). The bottom of the reformer plate showed warpage .0025" at 32 hours.

4.3.2.2.5 Start Algorithm Enhancements

The Solid Oxide Fuel Cell Reformer will be required to start the APU unit at various temperature conditions. The catalyst can immediately reform liquid gasoline at temperatures above 450 ^{o}C. At temperatures below this threshold, a combustor is operated upstream of the catalyst face to heat it to sufficient temperature for reforming. Feedback on the correct temperature of the catalyst is difficult to obtain, and would mean an additional production temperature sensor in the system, therefore a

temperature prediction calculation was developed and is now used to predict the temperature of the catalyst face and subsequently trigger the reforming mode.
The calculation uses the following:

- LHV of fuel (kFuelPowerJperG)= 42000 J/g
- Desired fuel rate (FuelRateGps) (EcmdFuelGps in APU08)
- Heat capacity of catalyst substrate (kCpCatalyst)
- Initial downstream temperature reading (T3)
- Combustor temperature (T2) temperature rise
- Reformer mode of operation (ReforWER_Mode)

The Output of the Calculation is:

T_cat_predicted = Predicted temperature of the "Important Mass"

$$= T3_{Initial} + \int \frac{FuelLHV * ECmdFuelGps}{kCpCatalyst * k\,\mathrm{Im}\,por\,\tan tMass} dt$$

The predictor calculation initiates when it sees a rise in temperature (T2) greater than 10 ºC/sec.

The predictor then uses the initial temperature reading on T3, and integrates over time what the estimated temperature of the "Important Mass" is based on the fueling rate and its Cp, and the Cp of the "Important Mass". When T_cat_predicted exceeds a librated threshold (normally set to 1000 ºC thus far), the timed quench period is enabled.

By using the predictor algorithm, the "burn time" is adjusted based on the "thermal soak state" of the reformer. In cases where the reformer is still quite warm, the burn time is less then when the reformer is cold. This reduces the risk of precombustion during rich fueling, or failure to quench.

The temperature rise due to combustion is an added diagnostic so that the predictor will not calculate a temperature rise in the "Important Mass" without a combustion event upstream. For added diagnostics, a timeout should be used to cut fueling if T2 rise is not detected.

4.3.2.3 Tubular CPOx - Gen 1.1

4.3.2.3.1 Thermal Performance / Injector Flowshift

Following the design effort to minimize heat at the front end of the reformer, testing was conducted to evaluate the Gen 1.1 impact on injector flow shift and front-end temperatures as compared to Gen1.0.

A test was conducted on 6/12/03 with Gen1.1 to duplicate a previous test on 3/5/03 with Gen1.0. The purpose of the tests was to get a baseline for current injector flow shift with the two designs. During the test, an enclosure (referred to as the "can") was added to the front end of the reformer with insulation, and injector flow shift and temperatures were measured. The purpose of adding the "can" was to simulate an environment like that of the Process Air Module in the system.

Figure 4.3.2.3.1-1 shows the run sequence for Gen1.1, which was similar to that of Gen1.0.

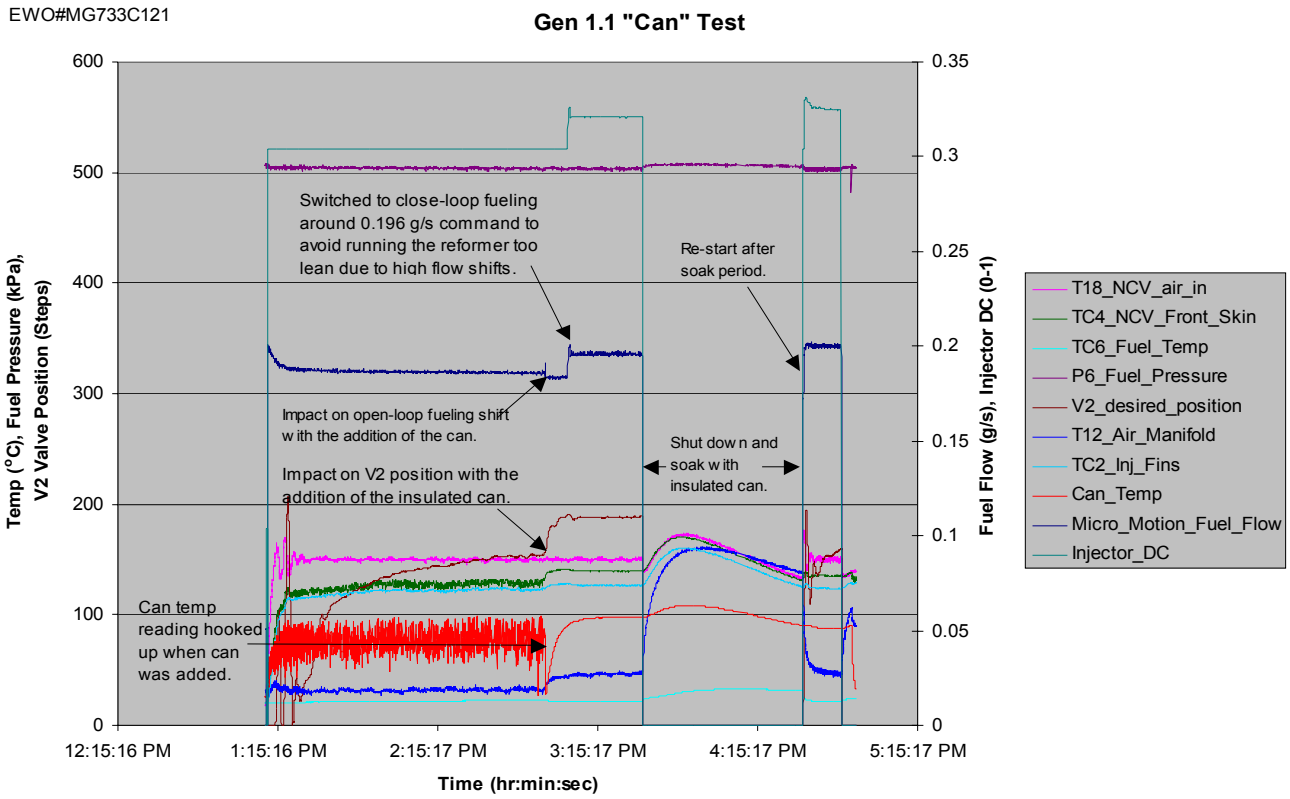

Figure 4.3.2.3.1-1: Gen 1.1 "Can" Test of 6/12/03

Figure 4.3.2.3.1-2 shows a comparison of steady-state injector flow shift between Gen1.0 and 1.1 at an inlet temperature of 150 ^{0}C. Steady state flow shift is shown to be greater for Gen1.1 (pink distribution) than the Gen1.0 (dark blue distribution). Also, the impact of insulated can on the amount of flow shift seemed to be greater for Gen1.1 than 1.0, but more investigation is needed.

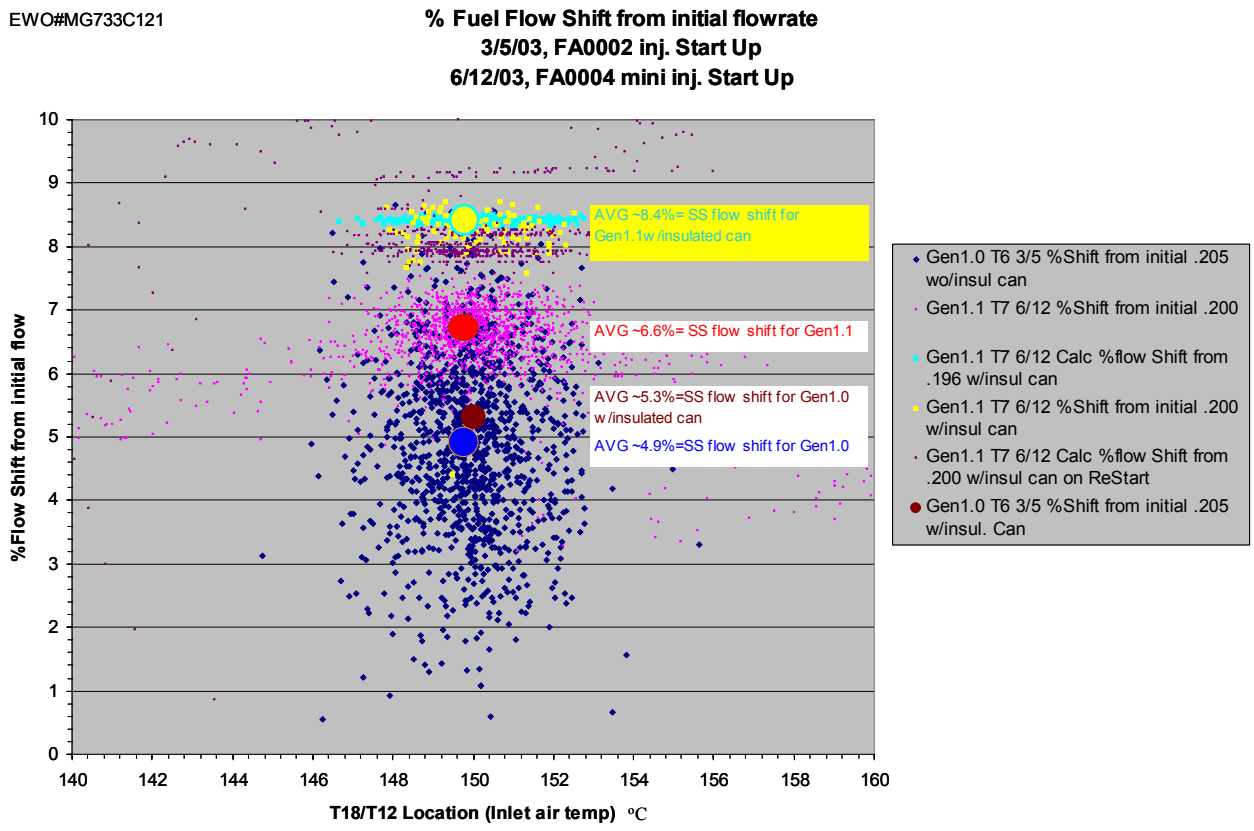

Figure 4.3.2.3.1-2: Fuel Flow Shift – Gen 1.0 & 1.1

Figure 4.3.2.3.1-3 shows the flow shift vs temperature during the initial start-up. These curves are being studied to determine if a control strategy can be used (such as a look-up table based on temperature) to anticipate and compensate for the flow shift. This Figure incorporates data from two different injectors and trends are very similar, supporting the possibility that the trend can be established and predictable.

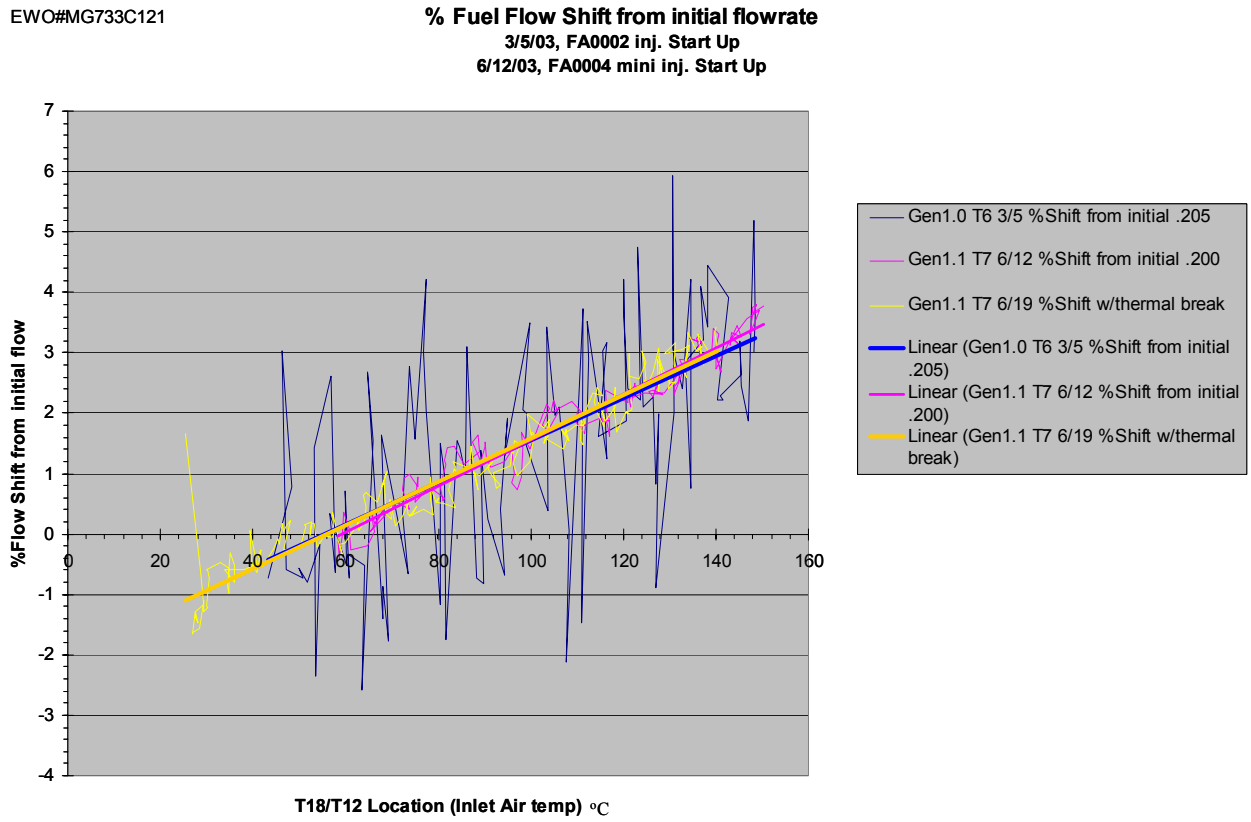

Figure 4.3.2.3.1-3: Fuel Flow shift vs Inlet Air Temperature

Figure 4.3.2.3.1-4 incorporates a comparison between Gen1.0, Gen1.1, and Gen1.1 with an alumina felt "thermal break" between the injector housing and the NCV body. The calculated flow shift shows Gen1.1 with the thermal break to be about equivalent in percent flow shift to Gen1.0 at an inlet temperature of 180 ^{0}C.

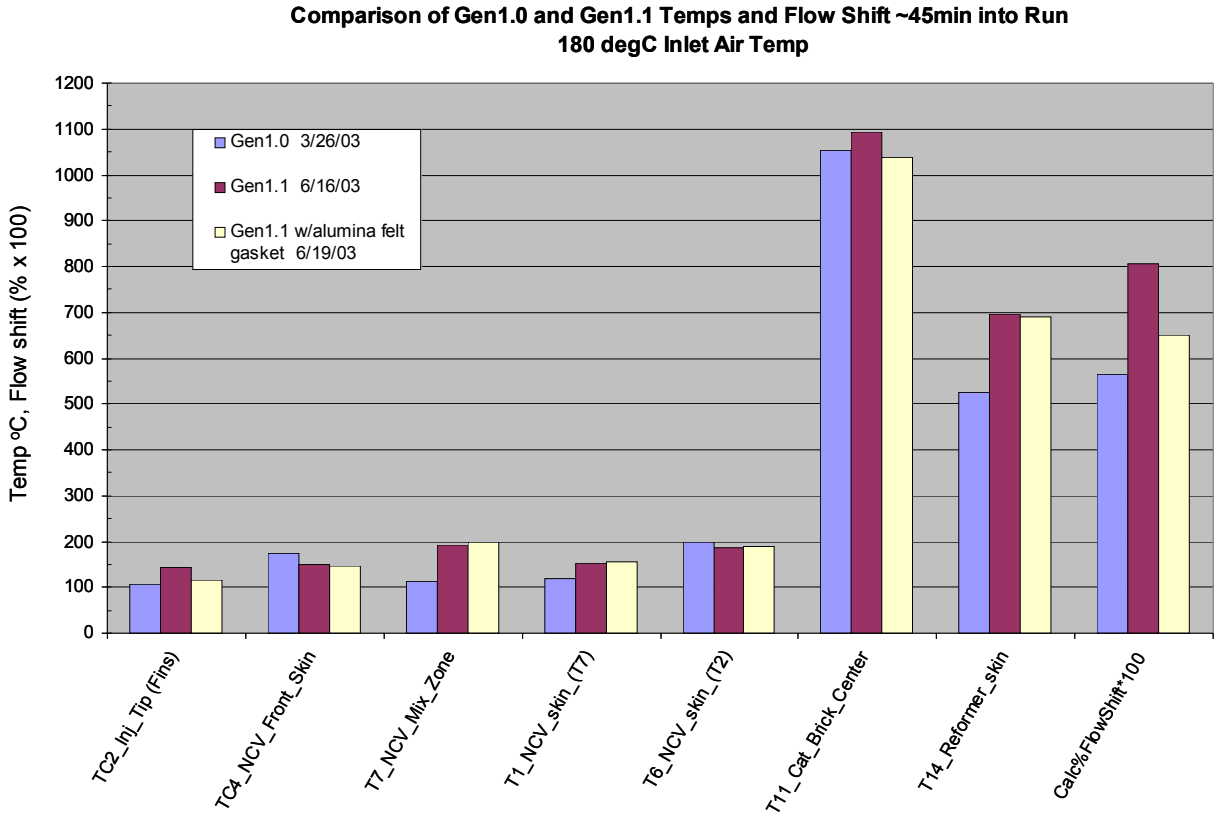

Figure 4.3.2.3.1-4: Temperature & Flowshift Comparison – Gen 1.0 & 1.1

4.3.2.3.2 Turndown with doubled washcoat content data

A turndown test on a catalyst with a doubled amount of washcoat was conducted using Gen1.1 hardware. Figure 4.3.2.3.2-1 shows the conversion results as fuel is varied.

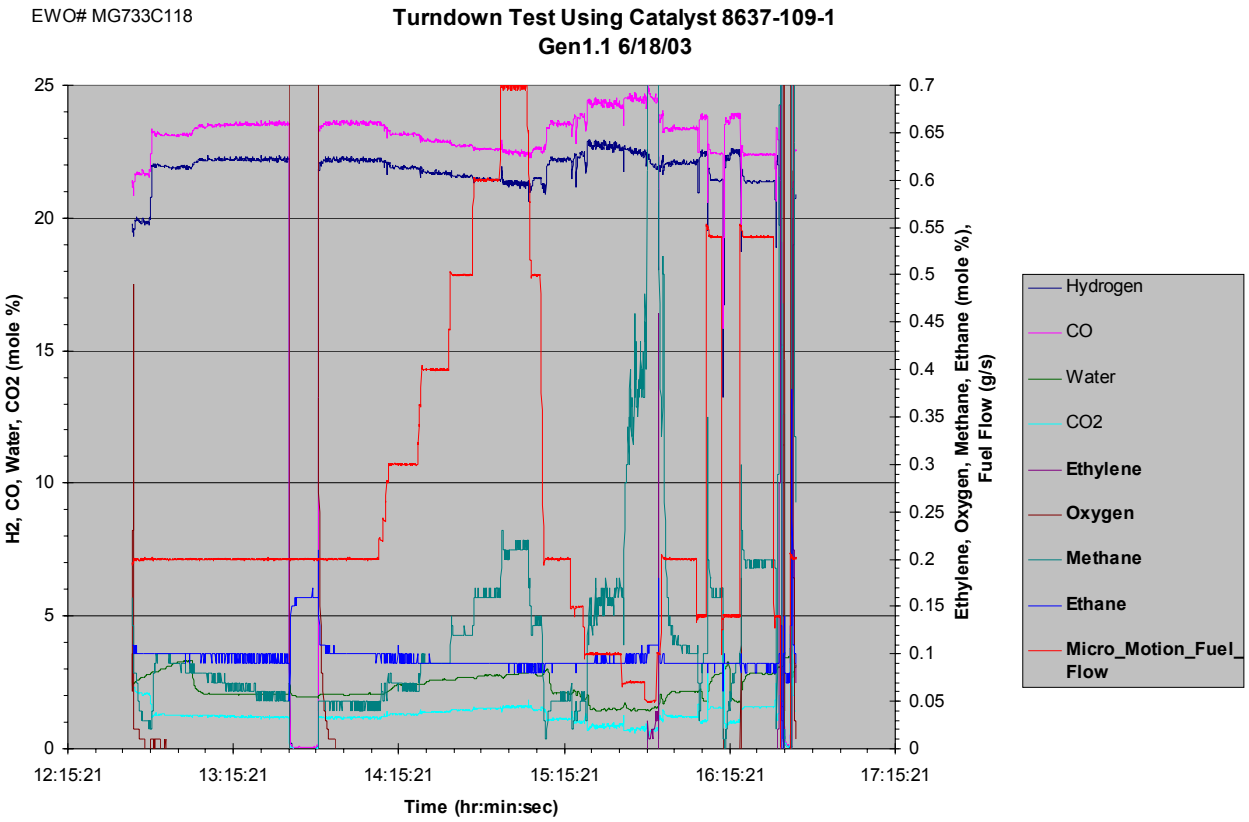

Figure 4.3.2.3.2-1: Composition Profile - Turndown Test With 2x Washcoat Loading

Figure 4.3.2.3.2-2 graphs the catalyst's performance against the specifications discussed in section 4.2.1.3. Notice that turndown capacity is shown as greater than 10:1. An upper limit was not obtained because the fuel injector's flow capacity is exceeded beyond 0.7gps.

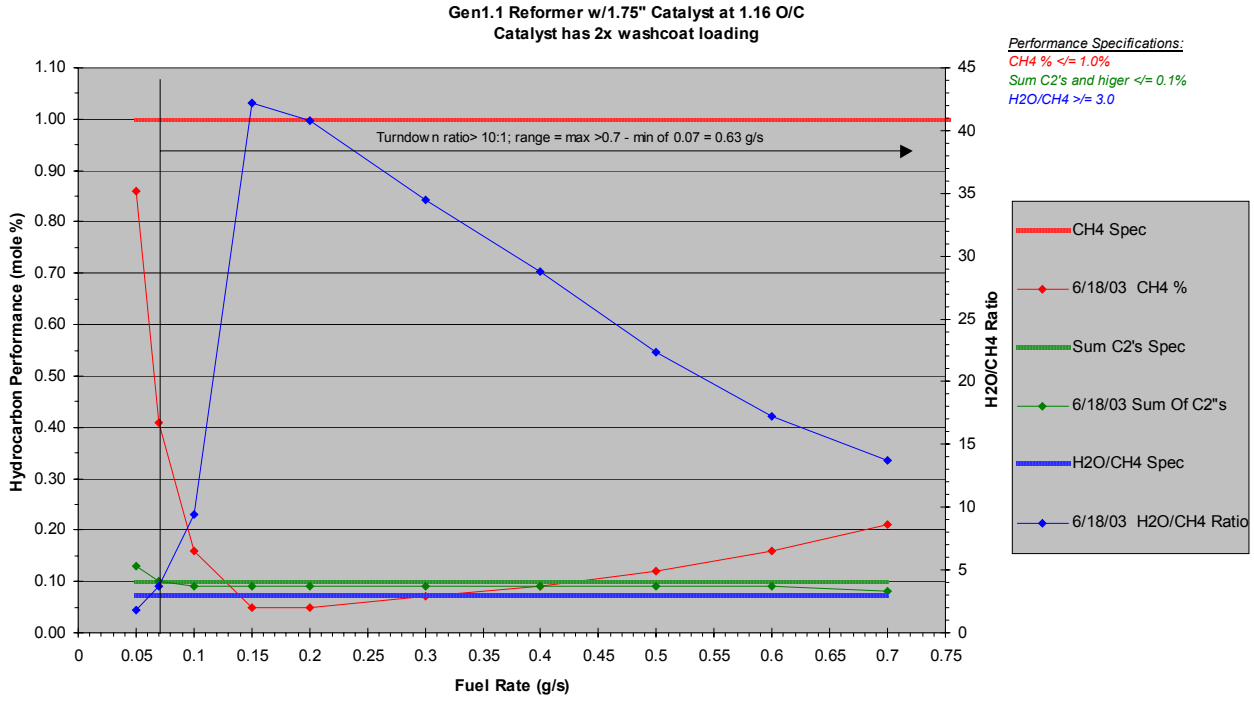

Figure 4.3.2.3.2-2: Turndown Performance – 2x Washcoat Loading

Still, enhanced performance and operating range is shown with more washcoat content on the catalyst. The catalyst with normal amount of washcoat yielded only 6:1 turndown (shown Figure 4.3.2.3.2-2)

4.3.2.3.3 Step Response

A transient response test was conducted on Gen1.1 hardware with a catalyst containing double the amount of washcoat. The test was conducted to evaluate the reformer's response to large transients in fueling. With this catalyst, a definitive maximum fueling level was not obtained due to limits on the injector's flow capacity; therefore, the turndown capacity of the base catalyst was referenced. Figure 4.3.2.3.3-1 shows this turndown test with the traditional response step calculations applied. The low and high fueling rates from which to conduct a step-change were determined as 0.15 gps and 0.54 gps respectively.

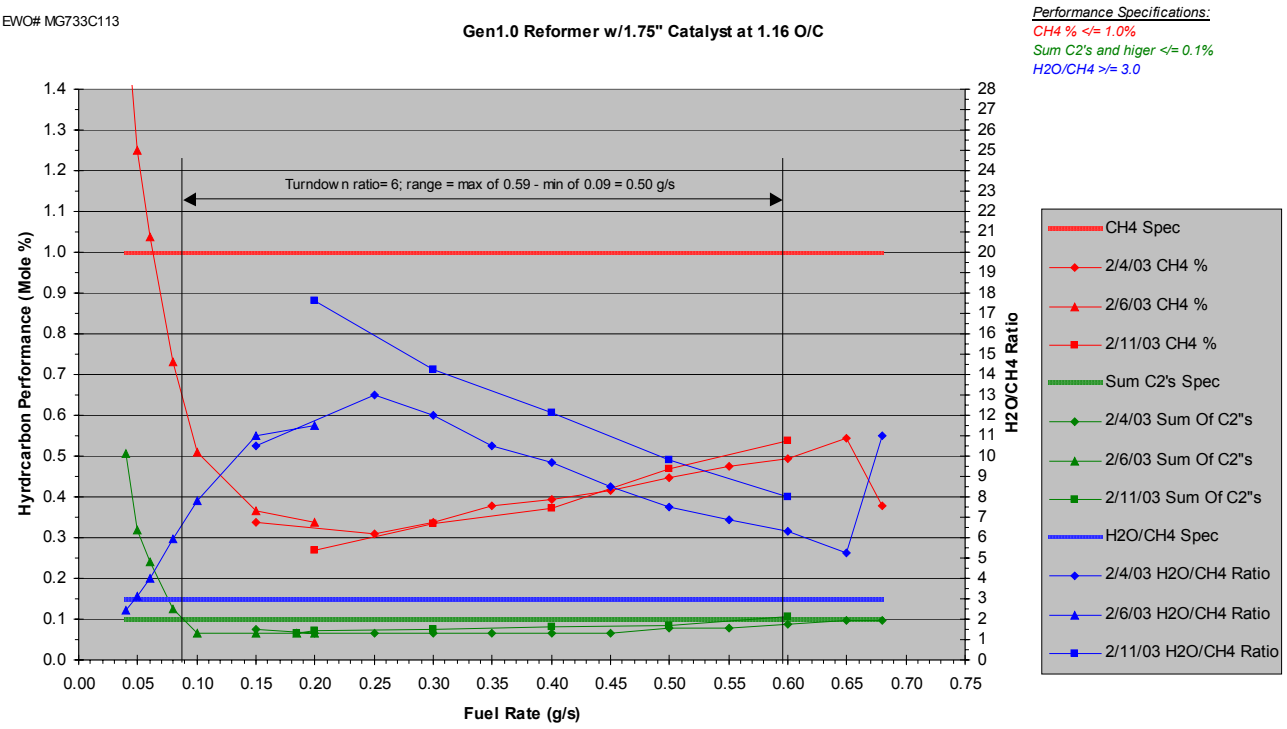

Figure 4.3.2.3.3-1: Turndown Evaluation for Step Response Testing

Figure 4.3.2.3.3-2 shows the mass spectrometer profiles during two upward transients, and one downward transient. The second downward transient resulted in precombustion for unknown reasons. The profiles show hydrocarbons spiking briefly on the upward transient before settling out, and dipping briefly during the downward transient before settling.

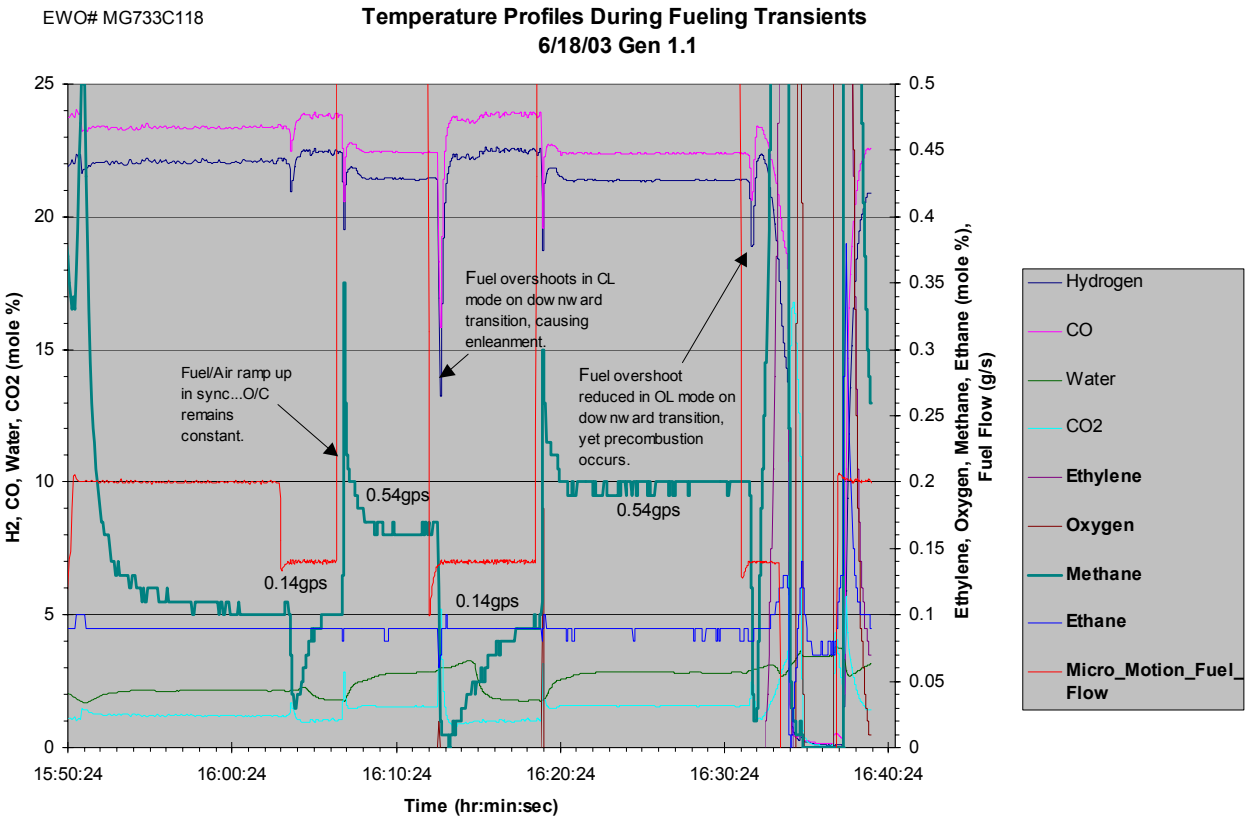

Figure 4.3.2.3.3-2: Reformate Composition During Fueling Transients

Figure 4.3.2.3.3-3 shows the temperature profiles during these transients. The spikes in the catalyst center temperature are most likely due to brief delays in air mass flow controller response. Air and fuel changes are found to be more in sync on upward transients than the downward transients, where the air change is delayed and fuel under-shoots the set point causing a temporary enleanment.

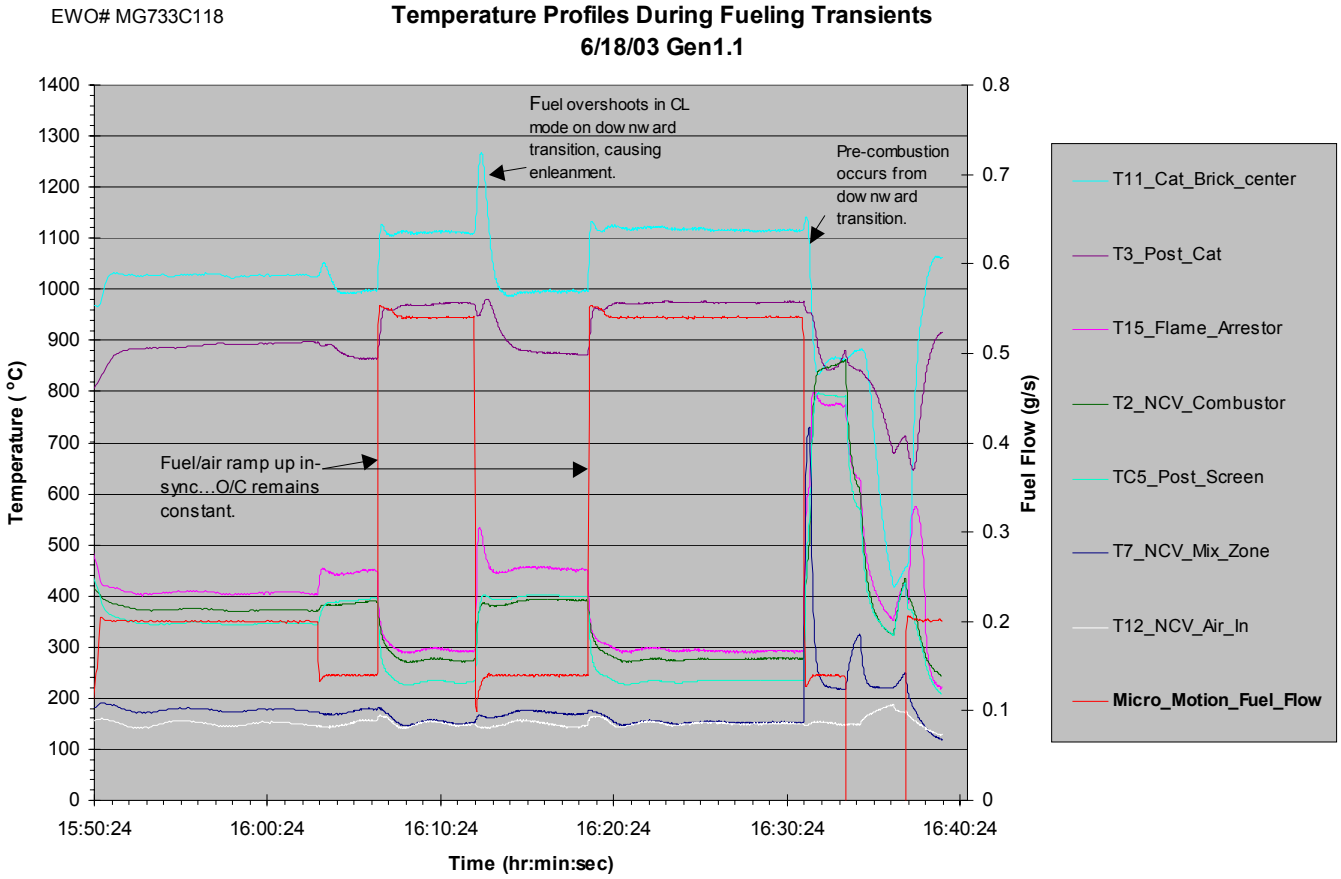

Figure 4.3.2.3.3-3: Temperature Profile During Fueling Transients

Despite caveats caused by control system delays, the behavior of the catalyst is consistent with how the rate of reaction during the transients is affected. When operating a low fueling rate, the reaction temperature is lower. When this low reaction temperature sees a higher fueling rate, the reaction rate at that temperature is not high enough to achieve the same conversion that was achieved previously. This causes the spike in methane when the higher fueling rate is commanded. As the reaction temperature rises to accommodate the new “load”, reactions proceed faster and the conversion equilibrates, causing the methane to drop and steady out.

Likewise, the reaction temperature is high at high flow, and as flow drops, the temperatures briefly remain higher, causing a higher rate of reaction than necessary for

the new lower “load”. Consequently, a brief dip in methane is seen until temperature and conversion equilibrate.

The downward transient and its responses are confounded by delays in the control system, causing enleanment of O/C ratio. Future work must be done to eliminate these variables in the controls, so that the catalyst behavior seen during this test can be verified under constant O/C conditions.

4.3.2.3.4 Vaporizer Airflow / Temperature Distribution Modeling

4.3.2.3.4.1 Gen 1 Performance Evaluation and Validation

The Gen 1.0 Reformer Vaporizer suffered from air temperature control instability related to the manner in which hot and cold air feeds entered the air director manifold and the placement of the thermocouple intended to measure this temperature.

After recurring problems with air temperature instability a modification was made to prevent hot air flow from unduly influencing mix air temperature readings.

The Gen 1.0 modified design is shown on the Figure 4.3.2.3.4.1-1 showing a semi-circular flow path that was machined into the manifold housing in order to route the hot air flow to join the cold air before entering the director manifold.

Note: The director manifold implies the donut shaped flow path that feeds air to the plurality of director holes. While this modification did improve stability of air mixture temperature readings there were still concerns regarding the accuracy of this setup.
An analytical investigation was conducted to explain both experimental findings and to improve future designs.

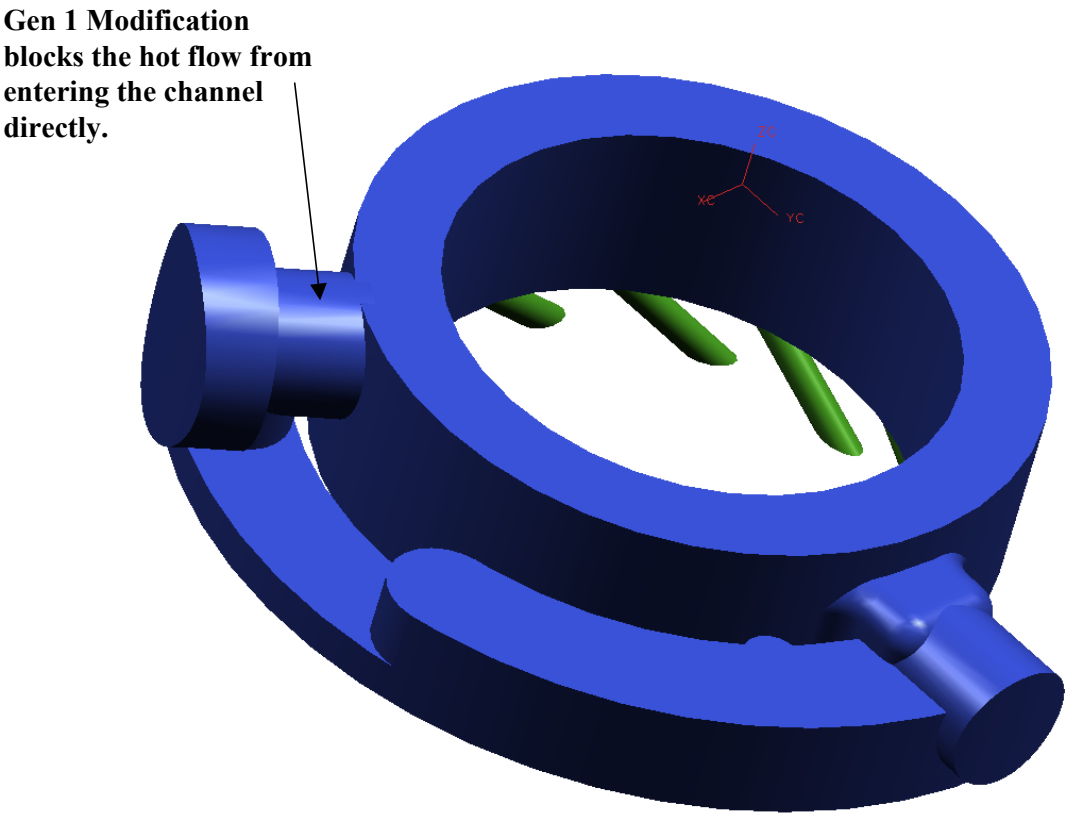

Figure 4.3.2.3.4.1-1: Gen 1.0 Vaporizer Flow Path as Solid Geometry – With Modification Shown

Director hole temperature distribution is poor for the original Gen 1.0 vaporizer design and shows significant improvement with the modified design as shown in Figure 4.3.2.3.4.1-2. Note: Swirler hole is synonymous with director hole.

Figure 4.3.2.3.4.1-3 shows how flow features within the director manifold concentrate the hot gases in a limited section of the manifold, feeding only a few holes with hot gases while most other director hole temperatures remain cold. Additionally this configuration sets up an unstable thermal front near the thermocouple location that hinders accurate average temperature measurements. It is this high thermal gradient that is believed to have been responsible for the instability problems experienced with this design.

Figure 4.3.2.3.4.1-4 shows how the Gen 1.0 modification significantly improves upon this behavior

The initiation of Gen 1.1 Reformer design afforded the opportunity to make improvements in both temperature and mass flow distribution of air as follows.

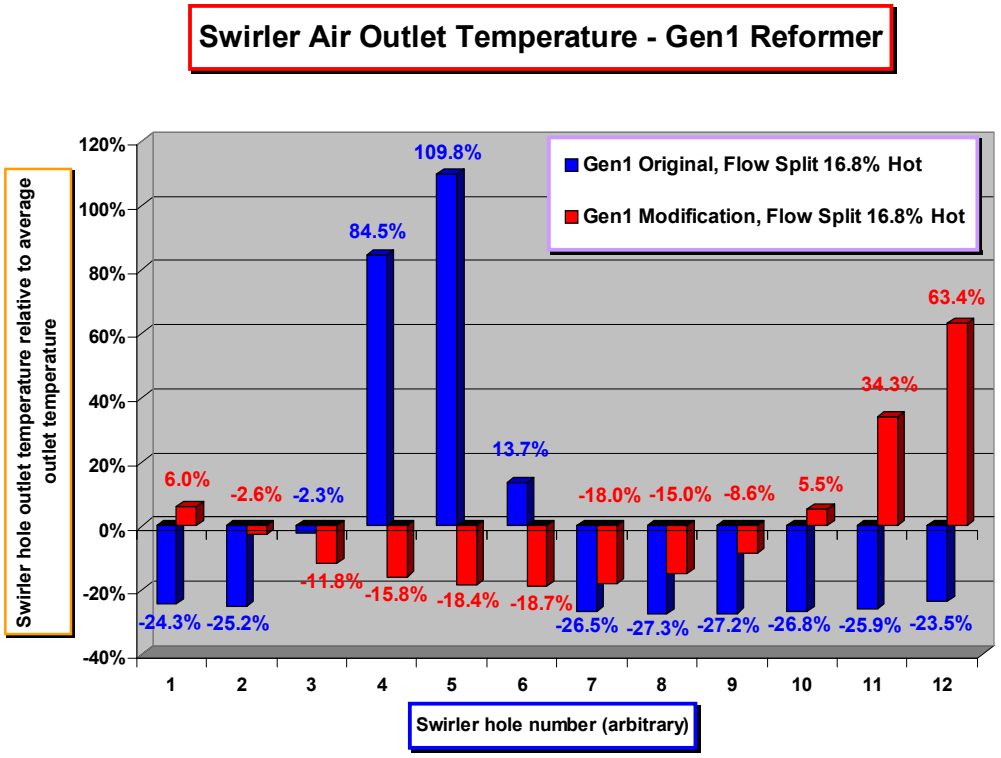

Figure 4.3.2.3.4.1-2: Gen 1.0 Reformer Vaporizer – Temperature Distribution: Original vs. Modification

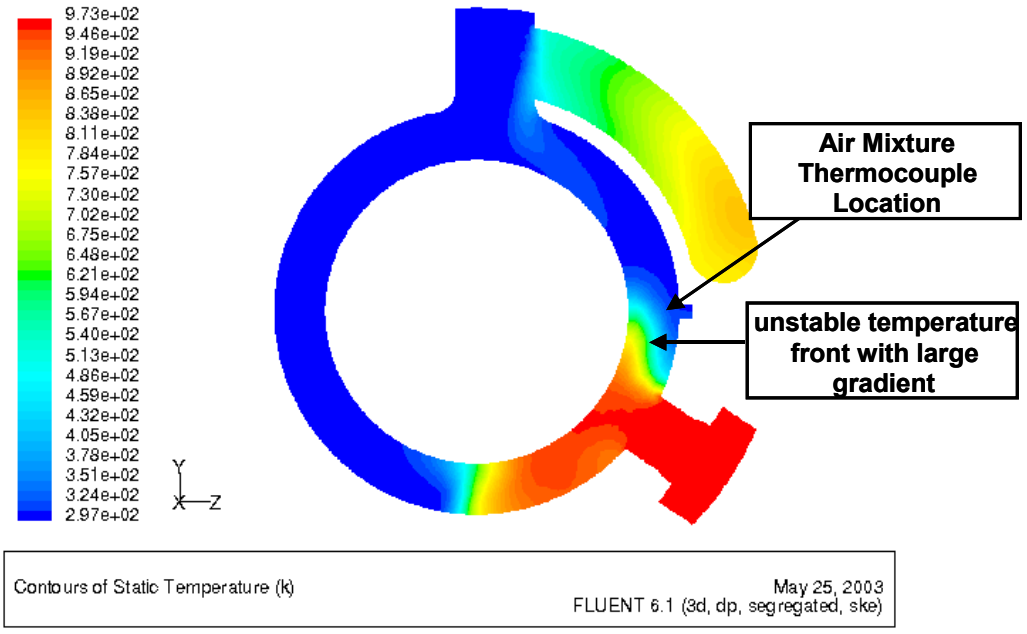

Figure 4.3.2.3.4.1-3: Gen 1.0 Reformer Vaporizer Temperature Contour – Original Design

Delphi Restricted

- Gen 1 Performance Evaluation and Validation

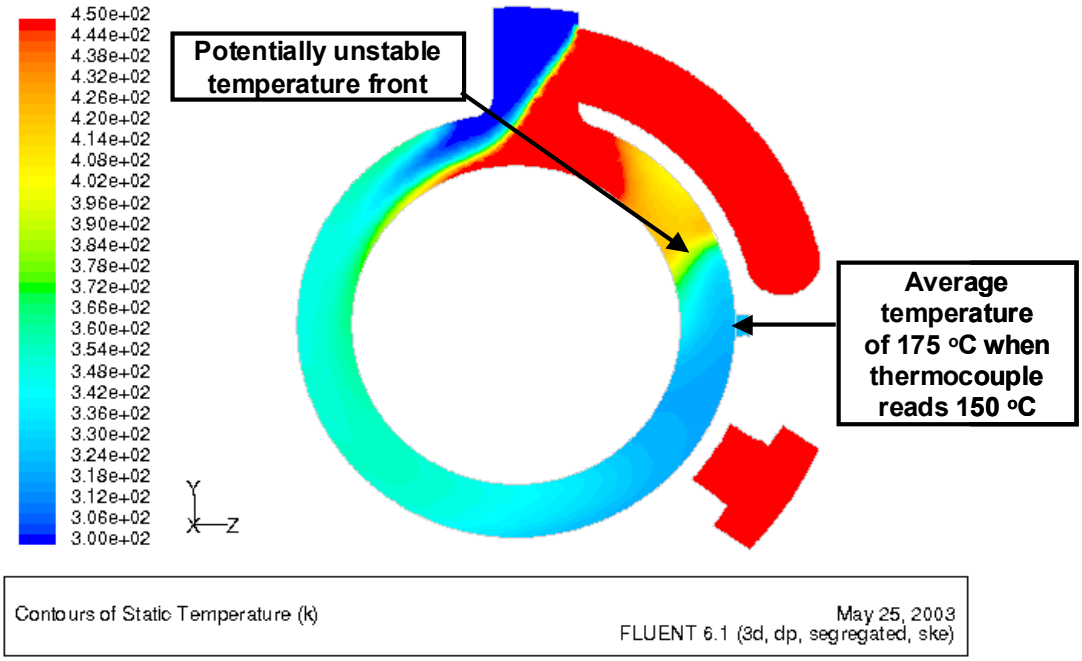

Figure 4.3.2.3.4.1-4: Gen 1.0 Reformer Vaporizer Temperature Contour – Modified Design

GEN 1.1 DESIGN IMPROVEMENT – FLOW DISTRIBUTION:

Flow distribution within the manifold and director geometry was investigated. The original design shows a director hole mass flow distribution ranging from +9.7% to –13%

Director hole mass flow distribution is strongly effected by the flow within the manifold chamber.

A design modification was proposed and analyzed and is depicted in Figure 4.3.2.3.4.1-5.

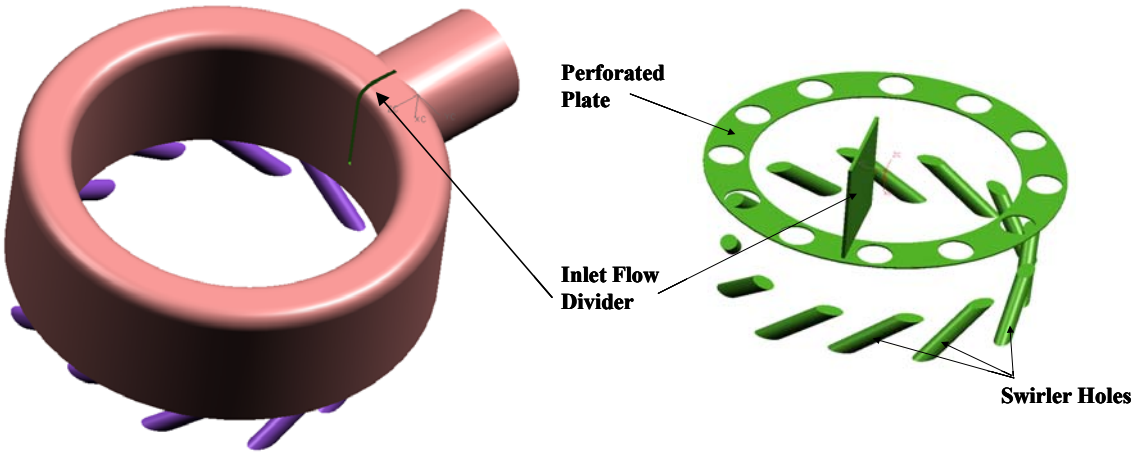

Figure 4.3.2.3.4.1-5 Gen 1.1: Reformer Vaporizer Flowpath – Modified Flow Path as Solid Geometry- (Left) Perforated Plate Baffle Geometry (Right) (Note: Swirler Hole is Synonymous with Director Hole)

The new design comprises a flow divider at the chamber inlet and a perforated plate upstream of the director holes entrance. The new design improves the hole-to-hole mass flow distribution to +1.9% to –4.8% as shown in Figure 4.3.2.3.4.1-6. Note: Swirler hole is synonymous with director hole).

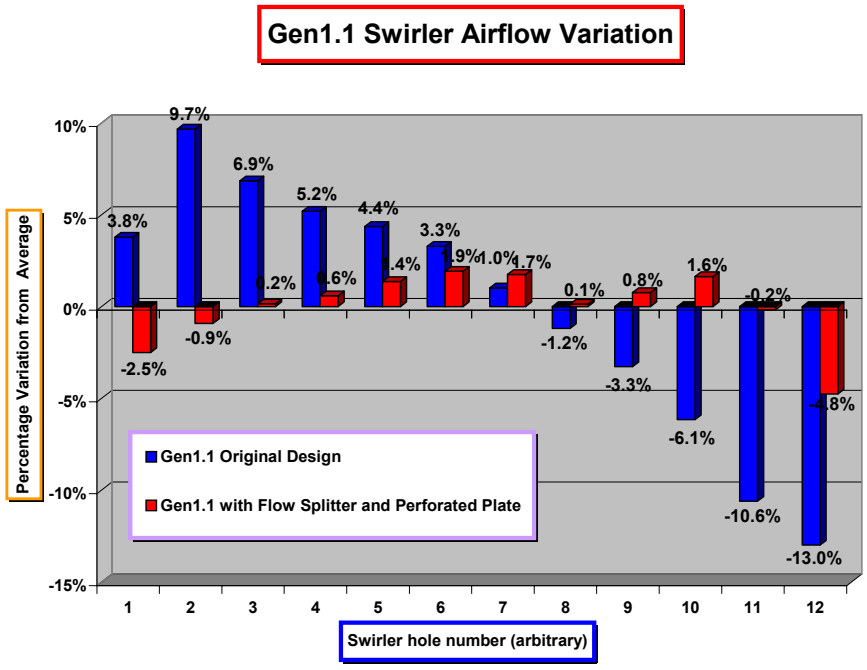

Figure 4.3.2.3.4.1-6 Gen 1.1: Reformer Vaporizer Airflow Distribution – Original vs. Modified

No additional pressure drop compared to the original Gen 1.0 design is expected.

Gen 1.1 Design Improvement – Temperature Distribution
Two alternate geometries for the valve housing that conducts hot and cold airflows into the manifold were proposed, analyzed and compared to the Gen 1.1 base design. The two alternate geometries are illustrated in Figure 4.3.2.3.4.1-7.

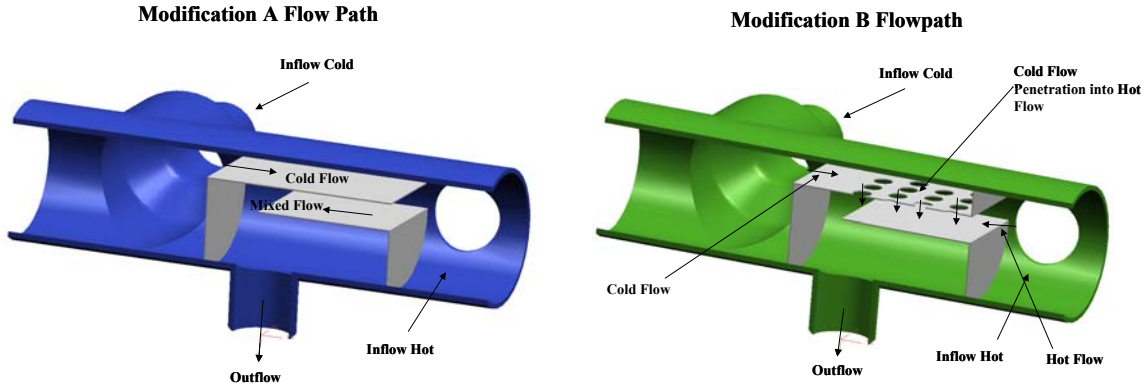

Figure 4.3.2.3.4.1-7: Gen1.1 Reformer Vaporizer – Valve Housing with Alternate Baffle Geometries

The original Gen 1.1 design did not employ baffles for hot/cold mixing. Analysis of the original Gen 1.1 design shows that the temperature variation at the hot/cold mixer exit (i.e., entrance to the director manifold) is 16% of the average temperature

Both alternate designs (A and B) improve temperature variation to 3% of the average temperature. As further mixing will take effect within the downstream director manifold chamber prior to the director holes, a temperature variation of less than 2% of the average temperature across all director holes is expected.

The pressure loss will increase from 250Pa to 500Pa with either of these modifications.

4.3.2.4 Planar H2 Reactor

Development of the planar H2 reformer was restarted again in January of 2003. Two different braze methods were under study.

4.3.2.4.1 Braze Development using Dispense Application Method

A braze development contract was entered into with Hi Tecmetal Group which utilizes a dispense process to apply braze alloy as opposed to spraying the alloy onto the parts. The development was performed in two stages. The first stage was to verify the process and establish the oven profile (Figure 4.3.2.4.1-1). These tests were performed using mini stacks. Mini stacks are made of the same materials (nickel plated Haynes 214 brazed with BNi-3 and BNi-9) as a full stack but with fewer layers. This was done to reduce the amount of scrap and conserve as many parts as possible for the second stage of development due to the lead-time and cost associated with obtaining plated Haynes 214 parts.

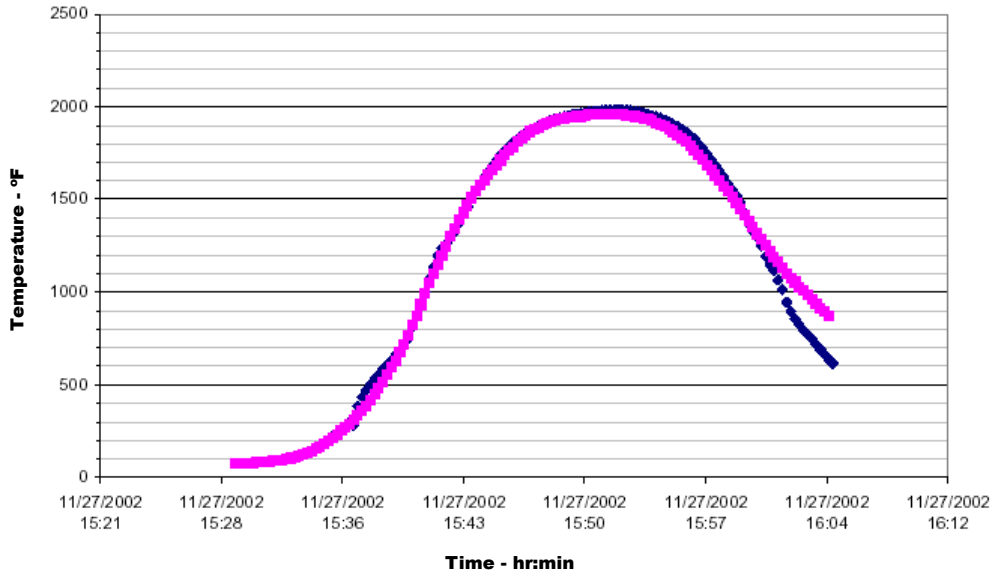

Figure 4.3.2.4.1-1: Oven Profile During Braze

The second stage involves brazing full planar reformers, with associated fittings, using the process developed in stage one.

Temperature profiles within the assembly during braze were then evaluated to insure proper braze conditions throughout the assembly. See Figure 4.3.2.4.1-2 and Figure 4.3.2.4.1-3. The braze joints were evaluated visually as well as with micrographs. See Figure 4.3.2.4.1-4.

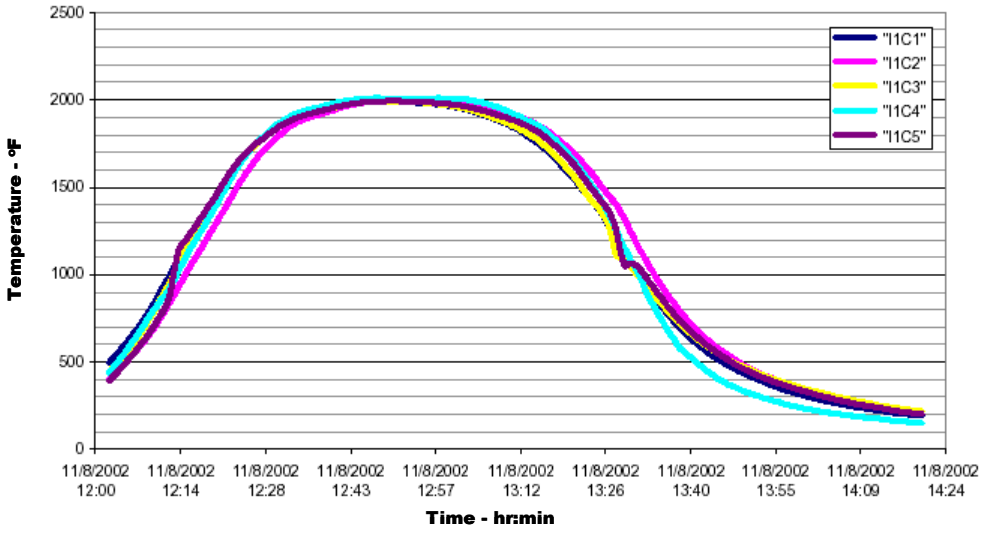

Figure 4.3.2.4.1-2: Thermal Profile within Assembly During Braze

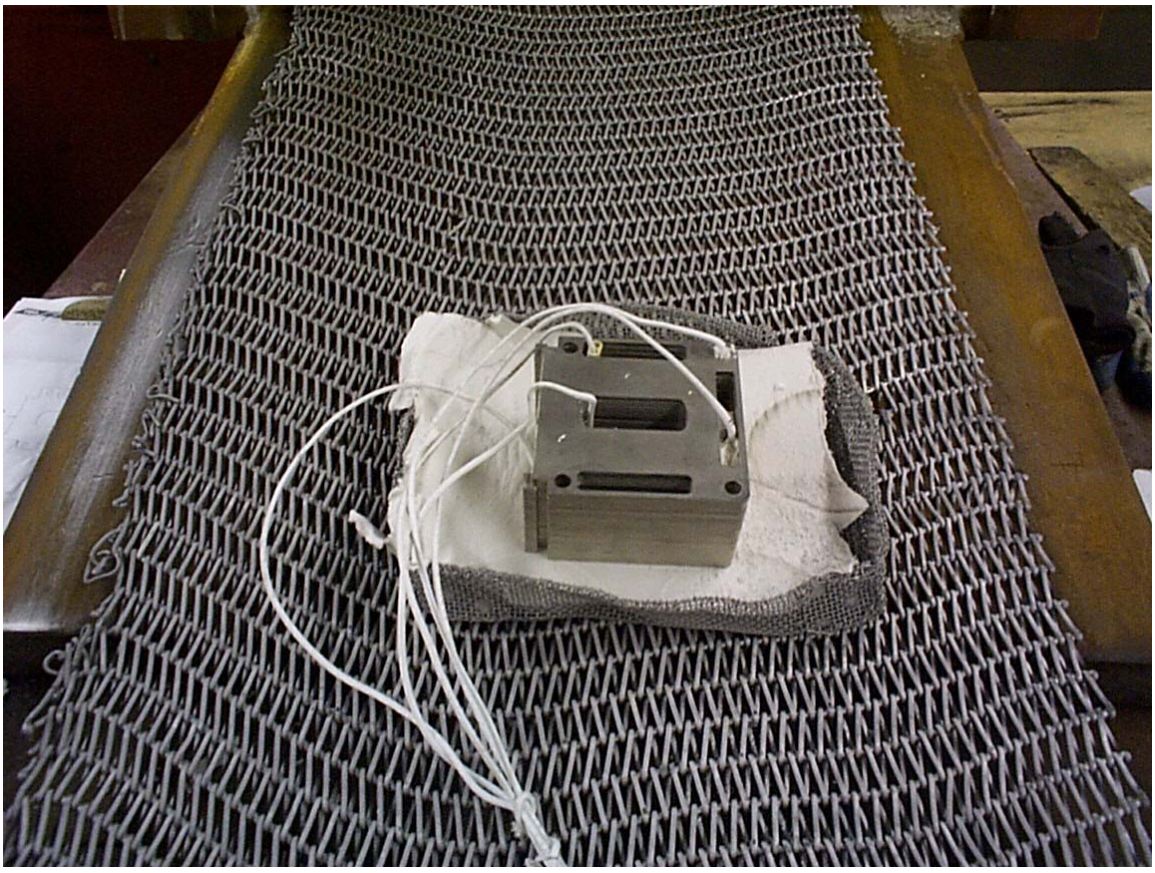

Figure 4.3.2.4.1-3: Thermocouple Location Within Assembly During Braze

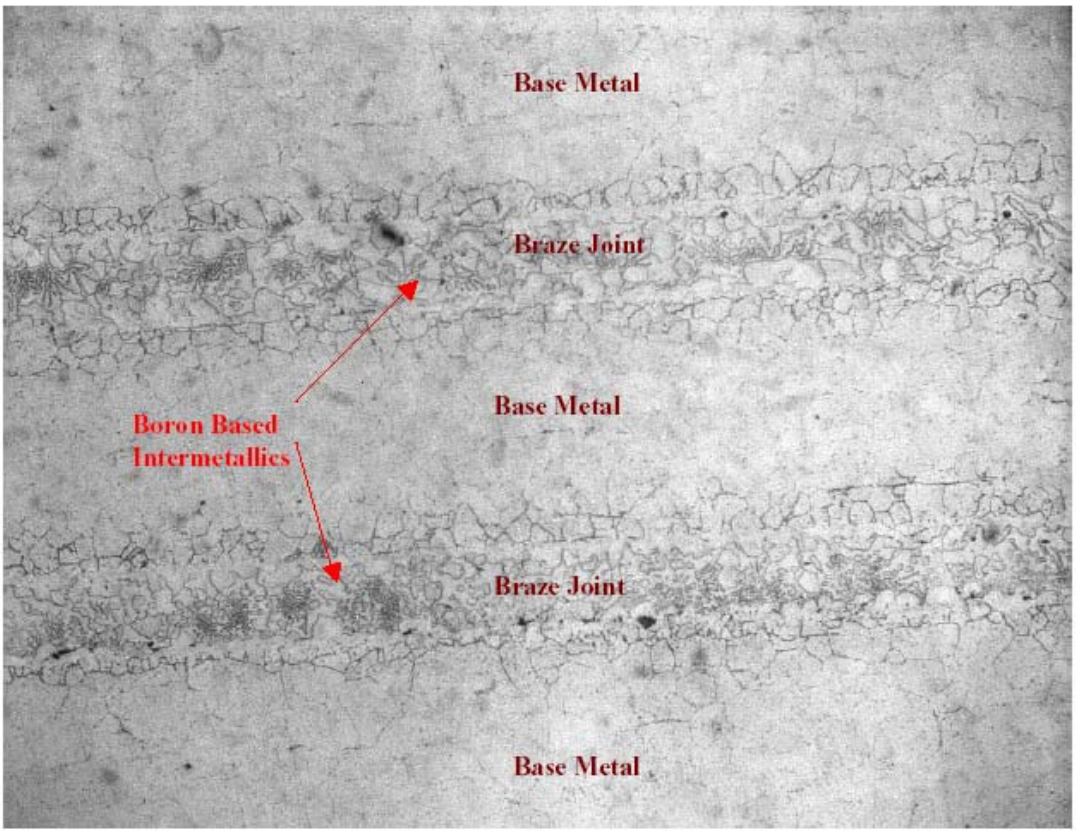

Figure 4.3.2.4.1-4: Micrograph of Braze Joint

Hi Tecmetal Group has sent two of the finished full planar assemblies to Delphi for inspection.

The second stage braze process involves brazing up repeating units using BNi-9 braze alloy.

Each repeating unit consists of one reforming plate, one combustion plate, one reforming shim, and one combustion shim. These repeating units are then stacked on top of each other and brazed along with the top and bottom plates including all fittings using BNi-3 braze alloy. The alloy is slathered on the outside of two sides of the assembly during the second braze cycle.

Upon inspection, the brazed assemblies have a couple small gaps in the stack that resulted in a failure at leak test. Hi Tecmetal Group is working on improving the process to eliminate the gaps in further assemblies.

Another brazed assembly is to be delivered to Delphi the week of July 28 for Delphi evaluation.

Some modifications to the part design were requested as part of the braze development to improve the process and the modifications have been incorporated into the design. Any further part orders will include the new design features.

4.3.2.4.2 Delphi H_2 Planar Reformer - Braze Development Summary

In February 2003, Delphi Harrison Thermal Systems began a braze development program to braze the H2 Planar Reformer. The first step was to comprehend all previous braze developments made by the Delphi Fuel Cell group and determine a course of action for this product.

The product design and material set was provided by the Delphi Fuel Cell group. The primary material set included Haynes 214 (a high temperature nickel-based alloy) and BNi-9 (a nickel-based braze-filler-metal with no silicon content.)

The original manufacturing process for brazing an H2 Planar reformer included:

- Component part fabrication
- Nickel-plating of the braze surfaces on the component parts
- Application of braze filler metal to the braze surfaces
- Assembly of planar reformer stack (no fittings)
- Braze the planar reformer stack
- Application of braze filler metal to all block fittings and pipes
- Assembly of all block fittings and pipes onto reformer stack
- Braze block fittings and pipes to the previously brazed reformer stack

Through the course of development, Delphi Harrison Thermal Systems was able to successfully braze the H2 Planar Reformer. In addition, several processing improvements were made including the elimination of Step 2 (nickel plating component parts) and the combining of steps 6 through 8 into the primary braze operation – making this a “one shot” braze process instead of the original two step braze process. Both of these improvements offer the potential for significant cost savings.

Delphi Harrison Thermal Systems undertook a thorough and methodical approach in order to develop a manufacturing process to successfully braze this product. A brief summary of some of our results is shared below. Figure 4.3.2.4.2-1 shows the H2 Planar Reformer.

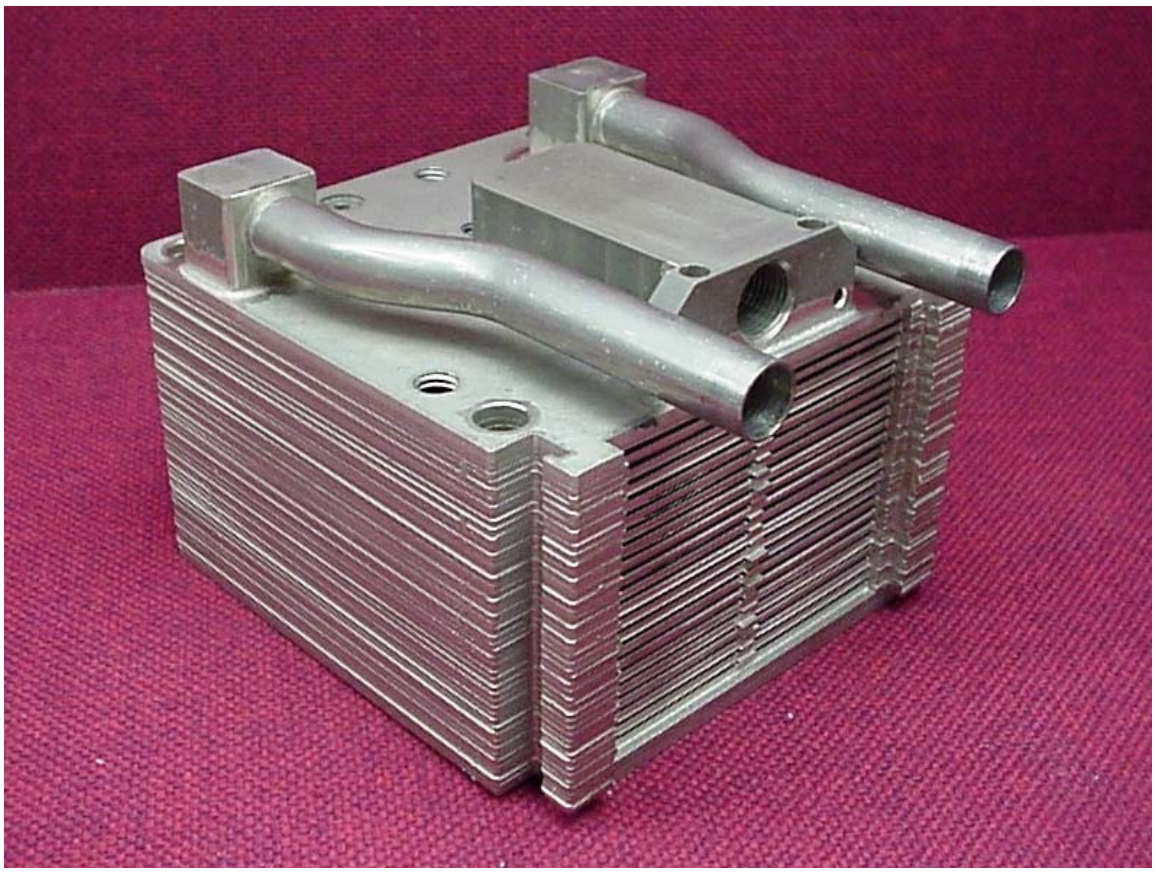

Figure 4.3.2.4.2-1: H2 Planar Reformer

Based on literature and recommendations made by the braze filler metal supplier, the recommended brazing range for BNi-9 is from 1950-2200 °F with a recommended brazing temperature of 2150 °F. This was the starting point for the braze development program.

The first braze runs were made with BNi-9 on a number of test coupons made of various base metals and in a vacuum furnace. BNi-9, which has Boron as a constituent, reacted very aggressively with many of the base metals and resulted in significant dissolution of the braze material into the base metal. This base metal dissolution was believed to be the root cause of previous part failures and was targeted as the main area for process improvement on the H2 Planar Reformer.

Several braze runs were made with BNi-9 on H2 Planar Reformer “short stacks.” These short stacks use the same component parts as the full H2 Planar Reformer but have a reduced number of plates. This was done to conserve the number of component parts consumed during the early stages of braze development. Photomicrographs and joint analysis were done at several stages throughout the development process. This was essential to our understanding of the results and helped direct our braze development process. Some of these photos are shared in this report.

Original reformer short stacks (with nickel plating) and reformer short stacks with No nickel plating were brazed. These parts showed high levels of base metal dissolution as well as braze filler metal collecting on part surfaces outside of the braze joints, blocking reformer flow passages. These flow blockages and the wicking together of the passage walls can be seen in Figure 4.3.2.4.2-2.

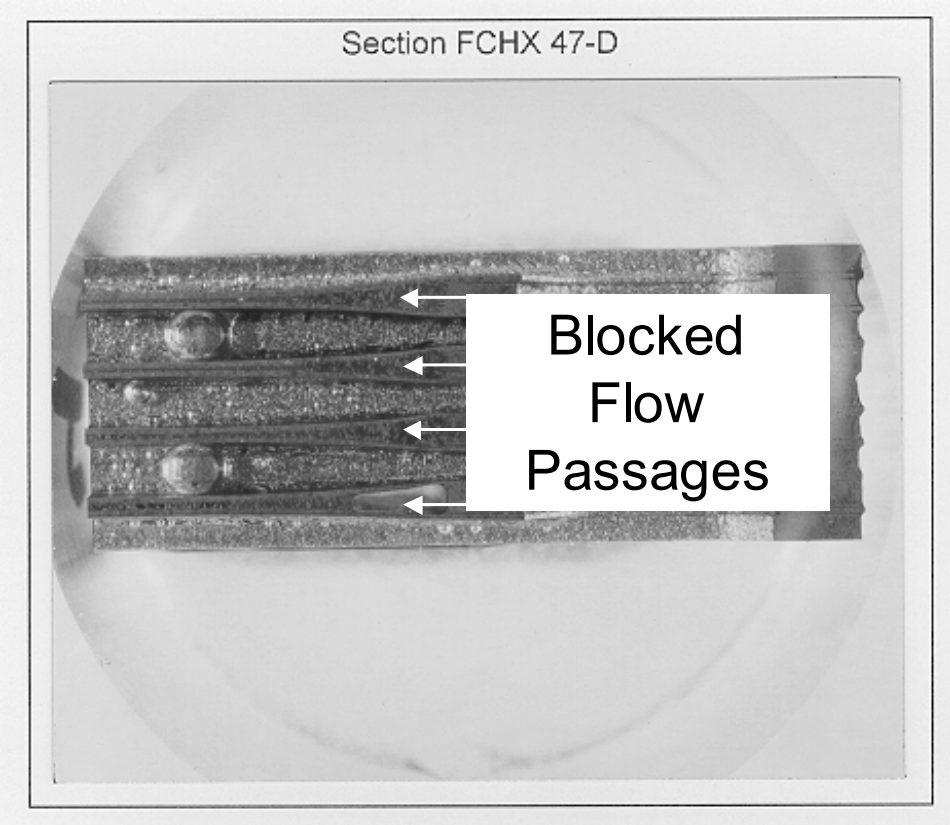

Figure 4.3.2.4.2-2 : Short Stack Section Showing Blocked Flow Passages

Base metal dissolution of the separator plates is shown as “thinning down” of the base metal in the area of the braze joint. An example of this is shown in Figure 4.3.2.4.2-3. It is thought that the flow blockages are due, at least in part, to base metal dissolution and the structural weakening of the separator plates.

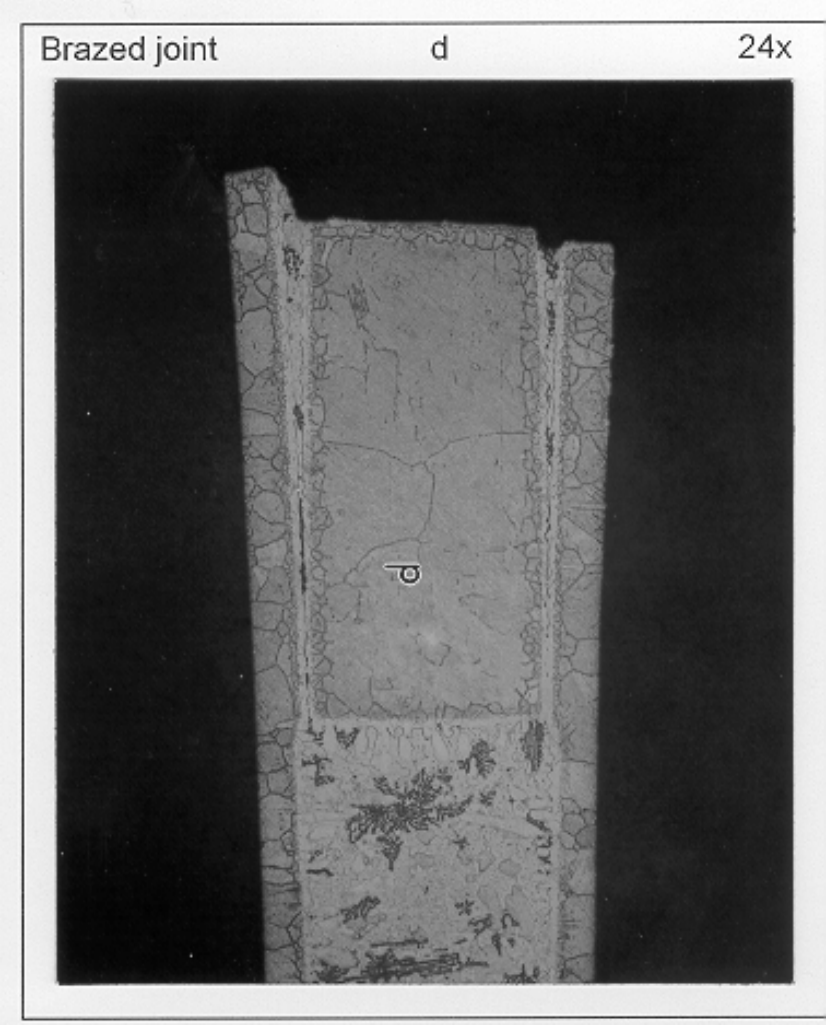

Figure 4.3.2.4.2-3: Braze Joints showing Base Metal Dissolution

Subsequent braze runs of reformer short stacks with no nickel plating were brazed under different braze cycles. Part analysis showed steady improvements in braze joint formation with reduced part deformation and base metal dissolution as evidenced by the photomicrograph picture shown in Figure 4.3.2.4.2-4.

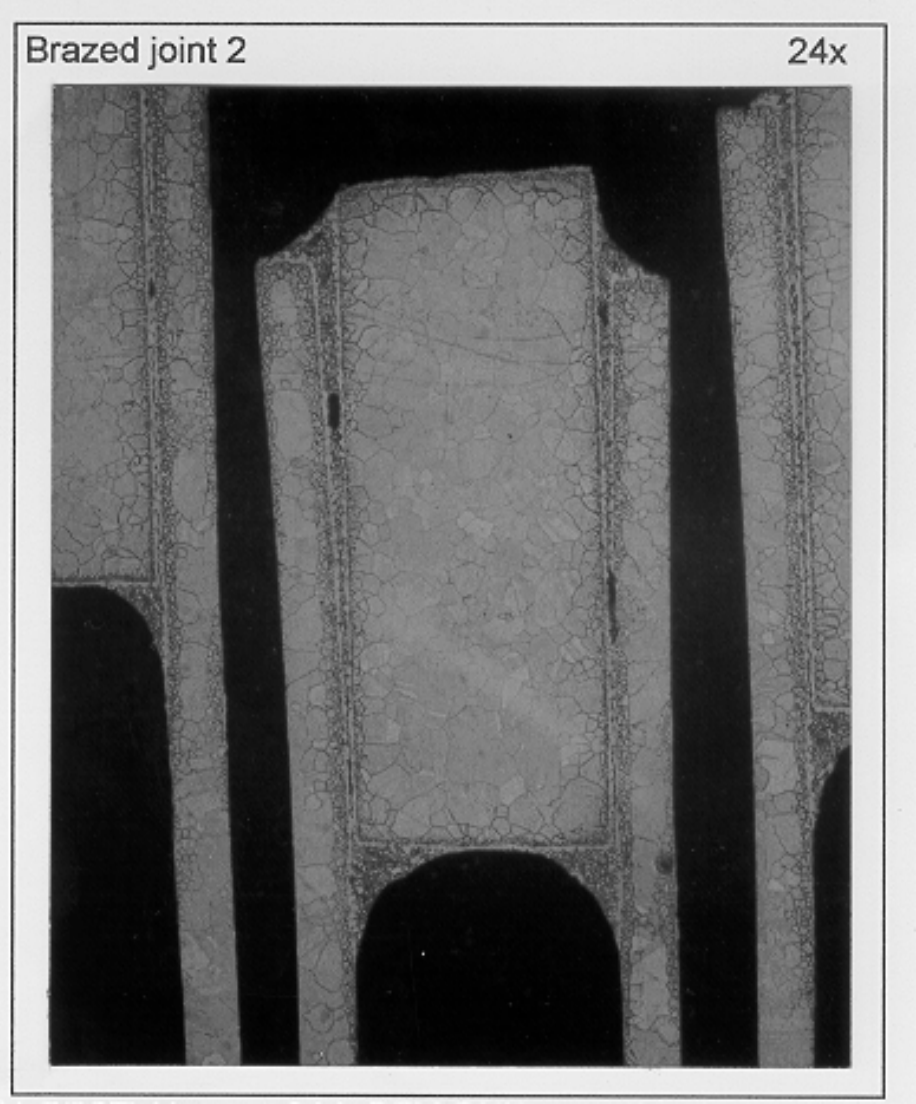

Figure 4.3.2.4.2-4: Good Braze Joint Formation & Reduced Dissolution

After the successful brazing of the reformer short stacks, a development run was planned with a full reformer stack. This full reformer stack was brazed with no nickel plating and BNi-9. This part showed deformation at the front face. Six front edge joint locations of separator-to-combustion/reformer plates showed some separation. Figure 4.3.2.4.2-5 shows one of the separated joint areas.

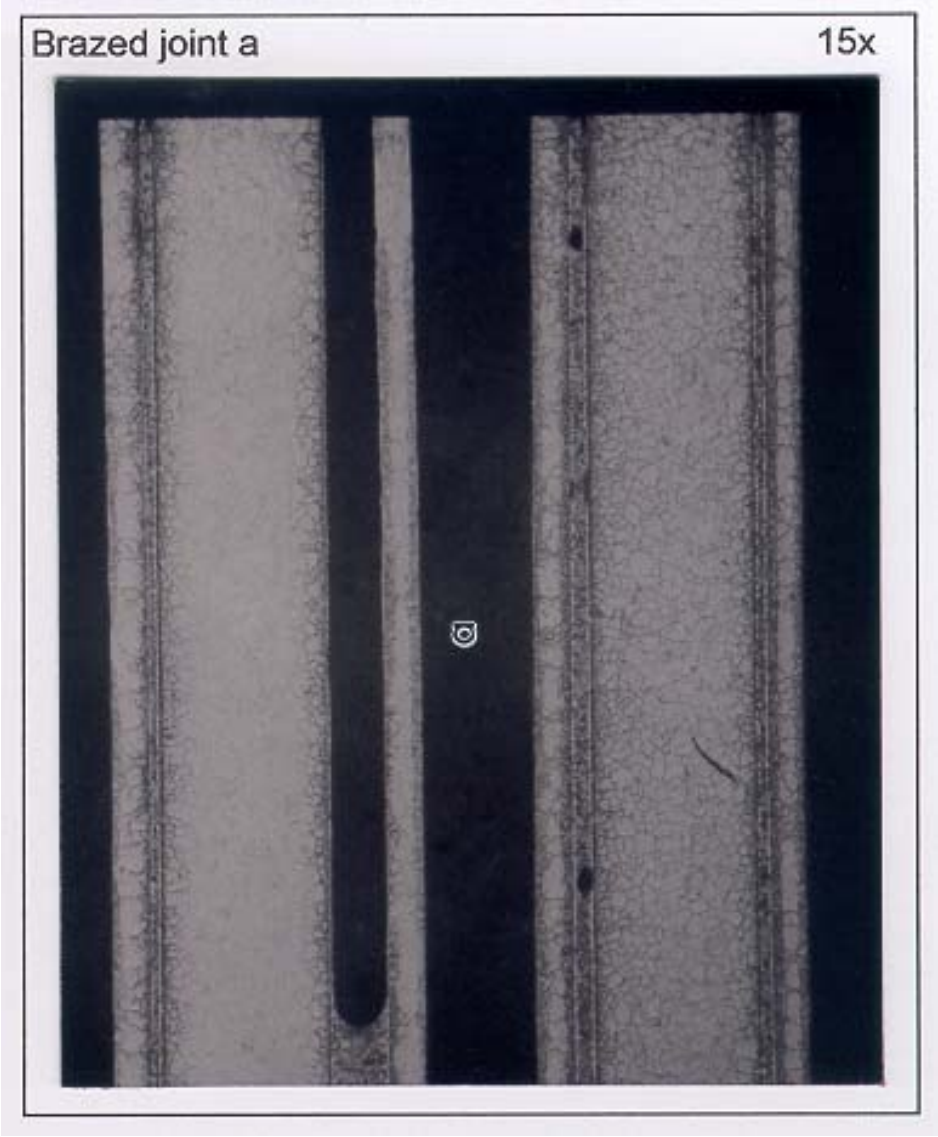

Figure 4.3.2.4.2-5: Separator Plate Separation at Front Face

The front face of the H2 Planar Reformer was changed to add strengthening features to the combustor and reforming plates. These features added structural support and made the front face thermally more similar to the rest of the reformer stack. This was done to aid in temperature uniformity of the work-piece during brazing. Furthermore, this change does not affect the functionality of the part as these features are removed during final machining and prior to the addition of wash coat.

The next logical step in braze development was the elimination of the secondary brazing operation by including all of the components (including block fittings and pipes) into the primary braze operation. This full stack reformer with fittings was brazed with no nickel plating, BNi-9 and included block fittings & pipes made of Inconel 600 in a “one shot” braze. Leaks were detected at front face and side face due to unbonded

areas at four separator-to-combustion/reformer plate locations. All other joints, including pipes and block fittings, brazed acceptably.

Photo-micrographic analysis of the un-bonded areas revealed that this was likely due to the thermal distortion of the separator plates during the braze process. Further analysis also concludes that the distortion is due to a general lack of support at the separator plates and not base metal dissolution. Figure 4.3.2.4.2-6 shows the separation on the face of the reformer stack and Figure 4.3.2.4.2-7 shows a photomicrograph of one of the joint separations with no visible evidence of base metal dissolution.

Figure 4.3.2.4.2-6: Front Face of H2 Planar Reformer Showing Separation

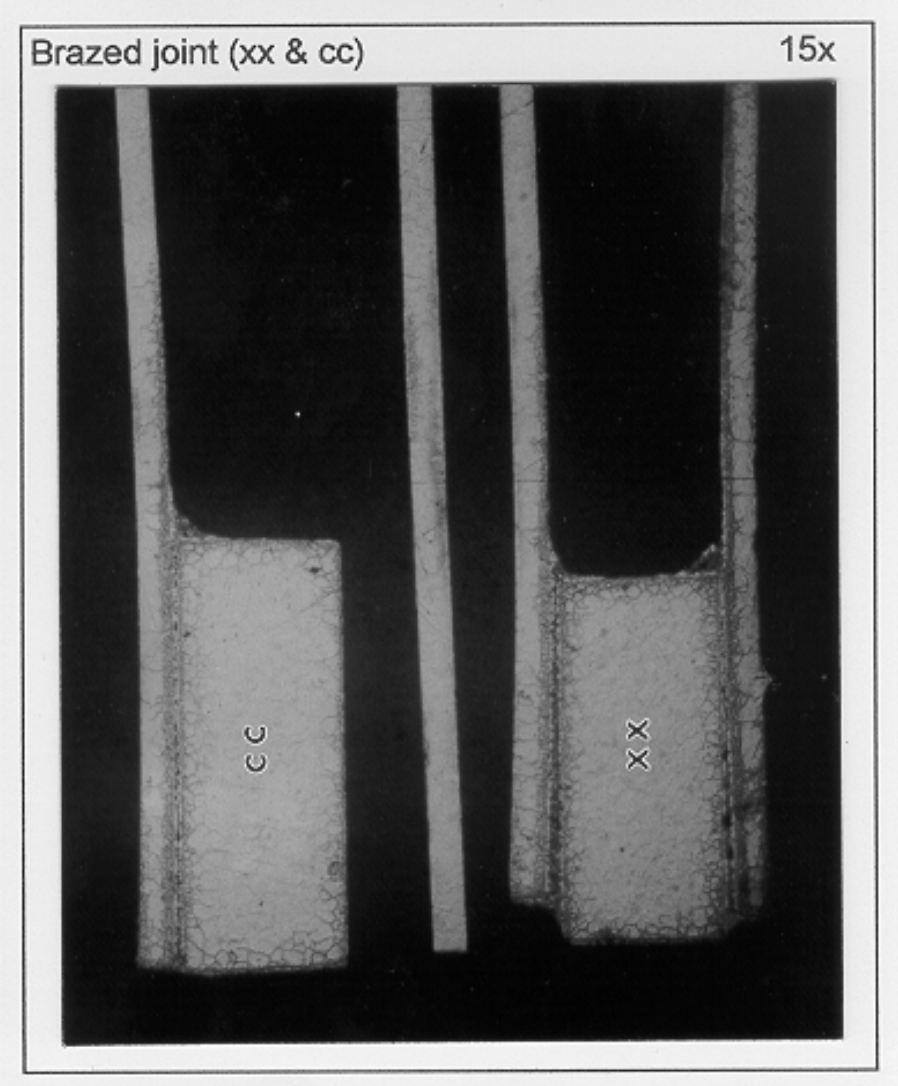

Figure 4.3.2.4.2-7: Separator Plate Separation at Front Face

Adding additional support webs when using the current .010” thick separator plates, or increasing the separator plate thickness to approximately .020” are two possible solutions. As thicker separator plates were not readily available, manually inserting additional support webs was our next step in braze development.

A braze run of a full stack reformer with no nickel plating, BNi-9, block fittings and pipes made of Inconel 600 in a “one shot” braze was made with one additional set of support webs (located between the separator plates on both reformer and combustion sides.) This unit was leak free with visually acceptable joint formation. There were, however, minor separations of separator-to-combustion/reformer plates at the front face only. Figure 4.3.2.4.2-8 shows the front face of a reformer with the added support webs and also shows the minor separations. This unit was delivered to the Delphi Fuel Cell group for testing.

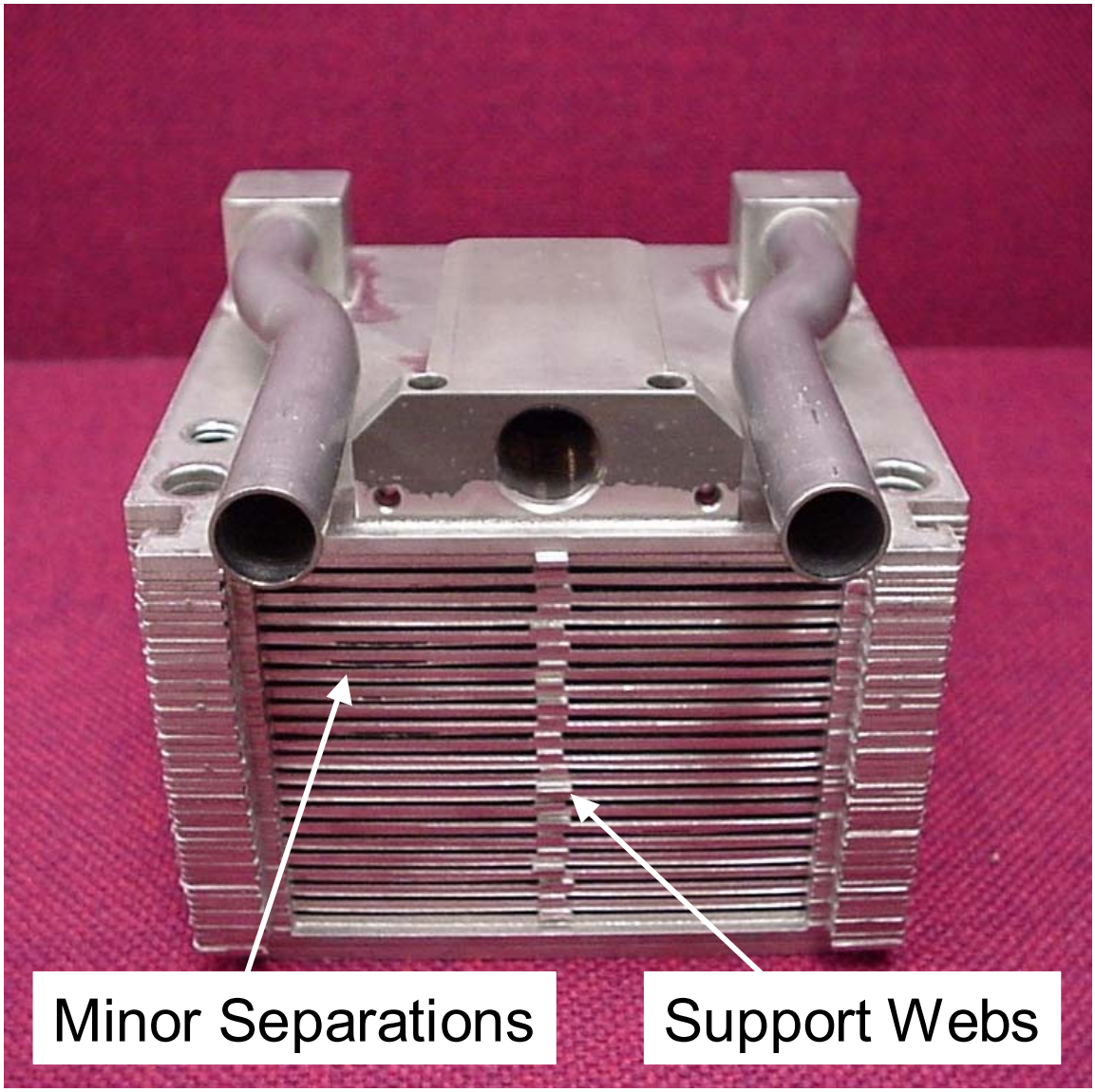

Figure 4.3.2.4.2-8: Front Face of H2 Planar Reformer with Added Support Webs

A subsequent braze run of a full stack reformer with no nickel plating, BNi-9, block fittings and pipes made of Inconel 600 in a “One Shot” Braze was made with three sets of additional web supports between the separator plates on the reformer side and one set on the combustion side. This unit was leak free with visually acceptable joint formation. In addition, the additional support webs located on the front face helped to reduce the minor plate separations found previously on the front face. This unit was also delivered to the Delphi Fuel Cell group for testing.

With preliminary success at both brazing suppliers, we are continuing on parallel development paths and evaluating the results of the two processes. Once wash coat is applied to the assemblies, the assemblies will be run on test and further evaluated for quality and durability.

4.3.3 Develop Catalysts

Catalyst development is broadly partitioned into several activity areas: formulation – which considers material selection and synthesis; product development –the chemistry of building catalysts and determination of appropriate loading and concentrations; process development – mechanical requirements and chemistry for manufacturing of catalysts; testing – performance and durability evaluation; applications – uses of the catalyst; mechanisms – understanding of underlying properties responsible for performance; and management – planning of these catalyst development activities. While interrelated, each of these areas is discussed in turn.

4.3.3.1 Catalyst Formulation

Various components of reforming catalysts: substrate, washcoat, and active metal, as well as the rationale of the performance testing are listed below. During this reporting period, extensive development work was completed on washcoat formulations, focusing on improving catalyst stability, as measured by our 'aggressive testing protocol' or our oxidative aging method.

Major components of reforming catalyst:

- Substrate - typically 20-65 pores per inch (ppi) reticulated foam
- Washcoat - a slurry of support material and active metal applied to substrate, followed by calcining step
- Usually applied in one step to substrate via production-intent hardware
- If multiple passes, each pass can be the same or differing compositions
- Support - typically a high surface area aluminum oxide with or without stability or performance modifiers
- Active metal - for partial oxidation, a platinum group metal (PGM) is preferred with or without modifier
- Performance rankings independent of testing hardware
- Catalysts tested and ranked for initial activity performance
- Use of accelerated aging methods can reduce this to 2-6 hours
- Testing conditions selected to 'stress' catalysts, excessive catalyst center temperature, usually 1000-1125 °C, achieved through high space velocity

A demonstration of our ability to improve catalyst durability is given in Figure 4.3.3.1-1, comparing the performance of modified and unmodified alumina-based washcoats. The unmodified catalyst exhibits rapid loss of performance, most likely due to sintering and phase transformation of the high surface area alumina-based support component of the washcoat to the more stable low surface-area alpha phase, with concomitant loss in

active-metal active sites. Surface modification of the alumina results in much improved maintenance of reforming performance, due to stabilization of the alumina washcoat.

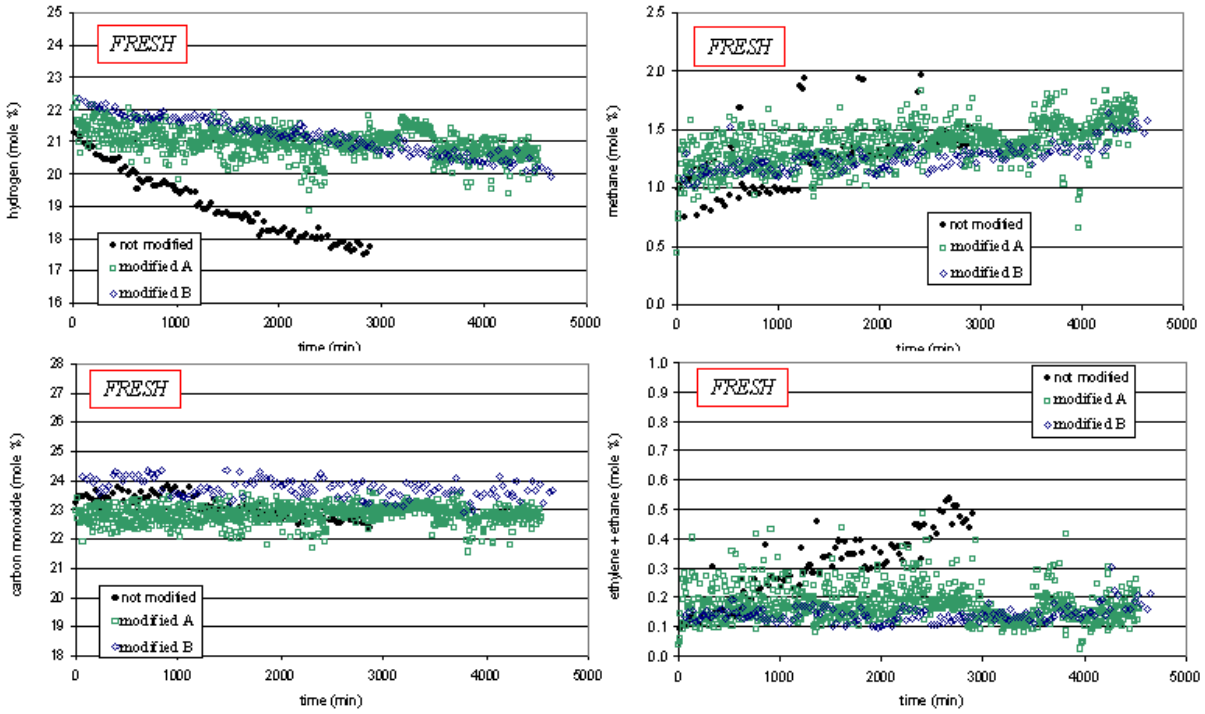

Testing with CARB Phase II gasoline, ~45,000/hr GHSV, O/C ~ 1.05 (mol/mol), analysis by gas chromatography.

Figure 4.3.3.1-1: Modified Catalyst Formulation Performance

Another approach to maintaining catalyst durability is to apply different washcoat formulations to the catalyst. A series of catalysts were prepared by first coating and heat-treating with a base washcoat, and then applying a second washcoat on top, followed by an additional heat-treating sequence. The results of testing of one of these samples are given in Figure 4.3.3.1-2**,** formulated so that each layer provides enhanced functionality to the catalyst. In this case, the base layer enhances cracking of hydrocarbons, while the top layer enhances CO_2 and H_2O conversion to H_2 and CO reactions. To demonstrate that this formulation is resistant to process upsets; the catalyst was exposed to periods of high temperatures, by increasing Oxygen to Carbon ratios. Exposing the dual layer catalyst to several periods of 1300 °C operation results in minimum change in H_2 selectivity, even after repeated exposures to temperatures in excess of 1400 – 1500 °C resulted in only a small loss in performance.

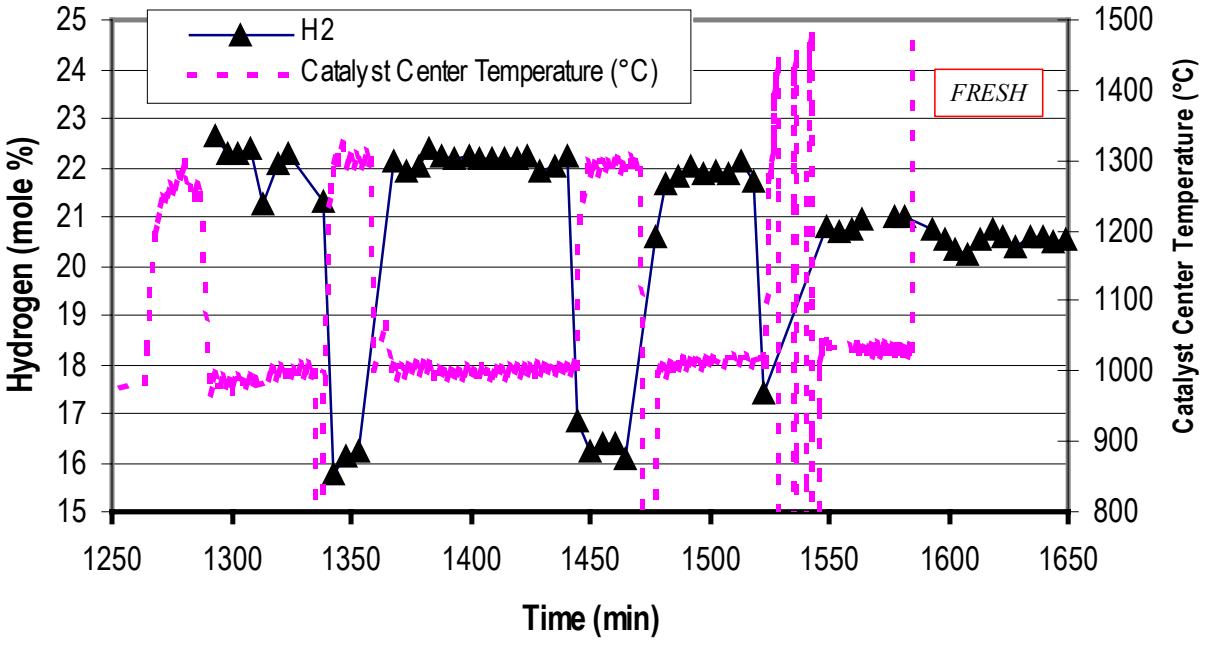

Figure 4.3.3.1-2: Dual-Layer Reforming Catalyst Formulation Performance

Results of stress test for double layer catalyst, tested as prepared, with CARB Phase II gasoline, total space velocity ~ 44,500/hr., O/C (mol/mol) ~ 1.05. O/C adjusted for about 30 minutes to bring catalyst temperature to ~ 1300 ^{0}C for another 3 cycles. Finally the catalyst was subjected to complete combustion and back to reforming conditions again.

These results indicate that catalysts can be formulated to meet performance goals of reformers that may experience temperature excursions or extended periods of elevated temperature operations.

4.3.3.2 Catalyst Product Development

The evolution of reforming catalyst products is presented in Figure 4.3.3.2-1. Testing with CARB Phase II gasoline ~ 45,000/hr GHSV, O/C ~ 1.05 (mol/mol), analysis by gas chromatography. The H_2 selectivity of catalysts tested after oxidative aging is compared to the performance of one of our reference catalysts, referred to as 'RDRCA0-300'. Product development is focused on selecting those formulation that can best meet the goal of extended catalyst durability, here determined by how close the performance of an aged catalyst can meet that of a fresh, high activity, catalyst. The figure shows our steady improvement in catalyst formulations to meet this goal, primarily through use of chemically modified washcoats. This work will necessarily be extended by evaluation through extensive durability testing, to confirm the performance of the leading catalyst products to give high selectivity over a wide range of processing conditions.

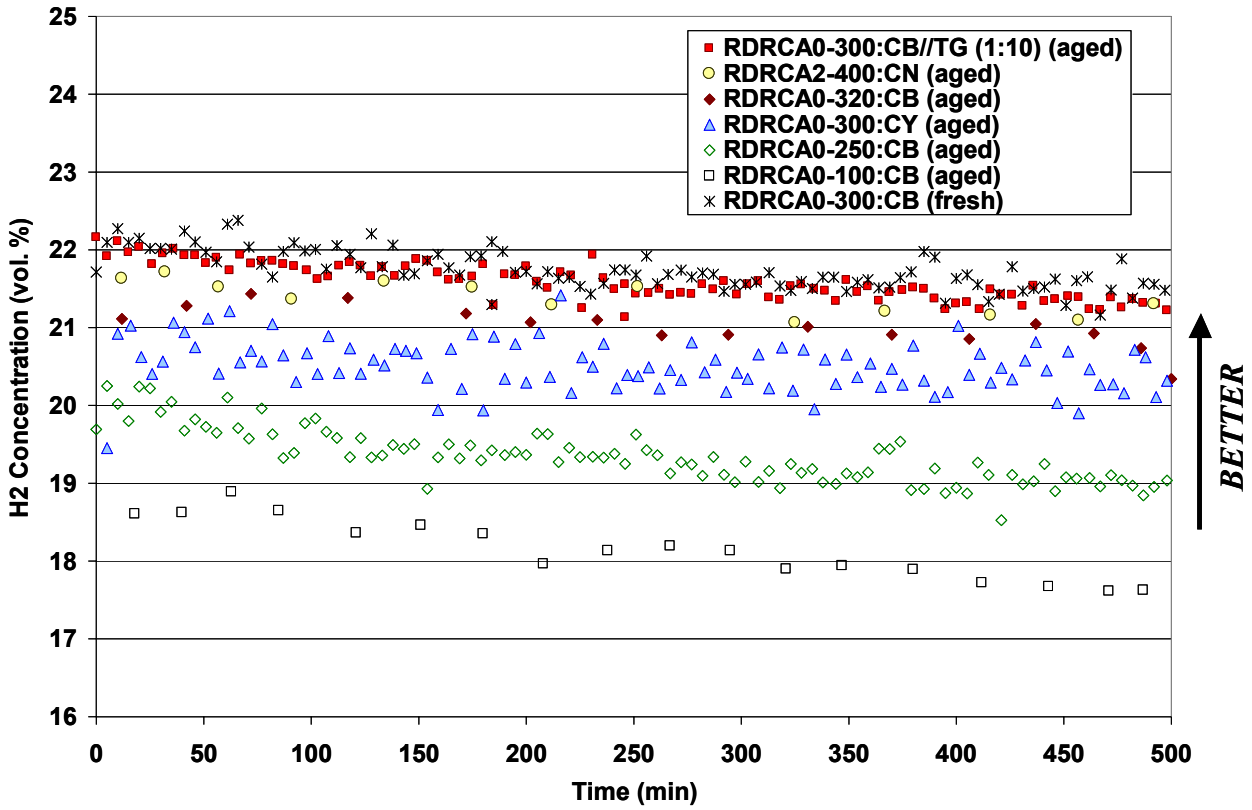

Figure 4.3.3.2-1: Performance Comparison Of Partial Oxidation Catalysts

4.3.3.3 Catalyst Process Development

No work in the area of catalyst manufacturing was performed during this reporting period.

4.3.3.4 Catalyst Testing

Using the methods described in the experimental section, catalysts are tested in either up- or down-flow tubular reactors, using CARB Phase II gasoline, containing MTBE but no other additives. Catalysts formulations and products are screened for periods from 1-70 hours using the aggressive testing protocol, or tested for durability at more mild processing conditions, to time to failure, defined as the time required to be producing less than 20% H_2 in the product gas.

Figure 4.3.3.4-1 Testing with CARB Phase II gasoline ~ 45,000/hr GHSV, O/C ~ 1.05 (mol/mol), analysis by gas chromatography, and Figure 4.3.3.4-2 Testing with CARB Phase II gasoline ~ 45,000/hr GHSV, O/C ~ 1.05 (mol/mol), analysis by gas chromatography, give typical screening test stand results for the aggressive testing protocol. Catalysts are evaluated at constant air-fuel ratios, and process equipment maintained so that space velocity is also constant. This combination of processing parameters results in acceptable mass balance closure. Provided that the catalyst retains moderate activity during the test period, no change to pressure drop is normally

noted. Typically, a period of 6-10 hours of testing is required until a noticeable change in performance is observed, Figure 4.3.3.4-2.

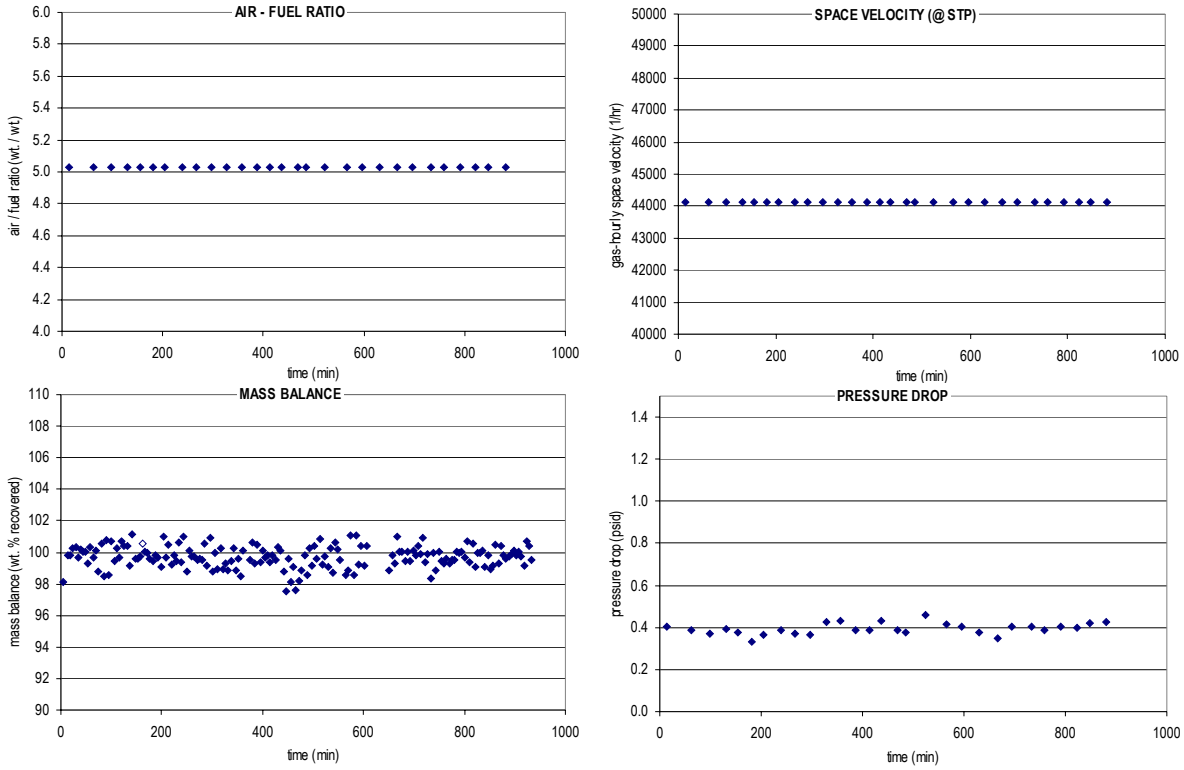

Figure 4.3.3.4-1: Typical Results for Partial Oxidation Catalyst Testing

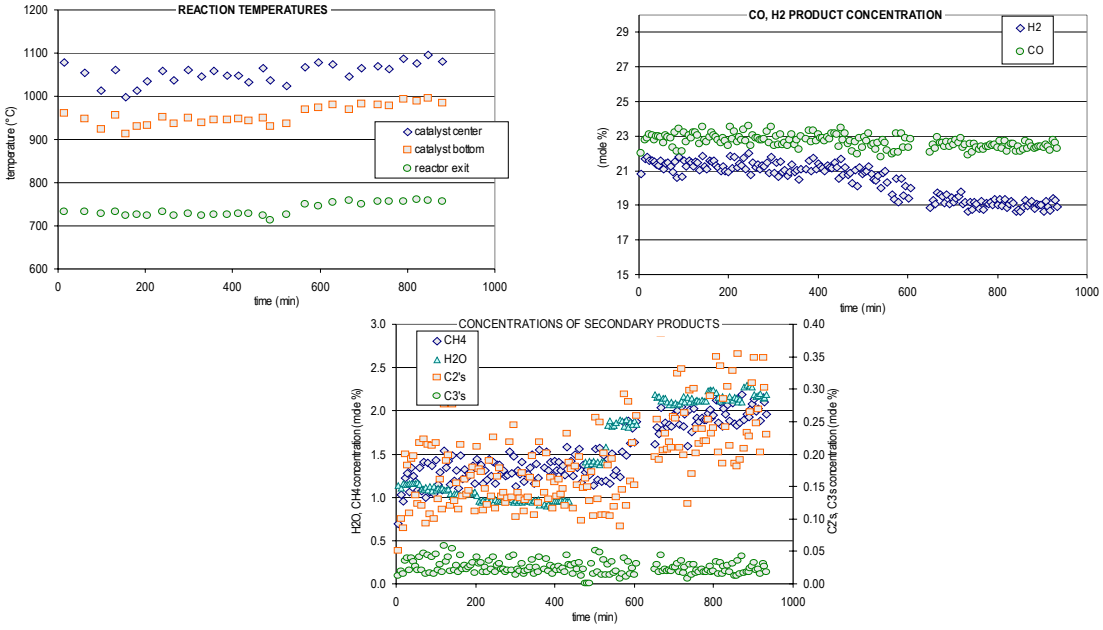

Figure 4.3.3.4-2: Typical Results for Partial Oxidation Catalyst Testing

Figure 4.3.3.4-3 compares durability results from our durability test stand and that of one of our cooperating partners, Total-Fina-Elf's Feluy, Belgium research facility. Both stands were operated at about ~25,000/hour space velocity, resulting in a catalyst center temperature of about 950 °C (as compared to a catalyst center temperature of ~1050 °C for the aggressive testing protocol). Good agreement is obtained between the two test stands, even though different catalyst formulations were tested. The slow decrease in performance may be a result of gradual changes to the dispersion of the active metal. We will be evaluating the catalysts from this and similar durability tests with the goal of determining deactivation mechanisms. However, catalysts maintained acceptable performance for over 300 hours of operation, with indications that 1000+ hours of acceptable operations will be readily obtainable.

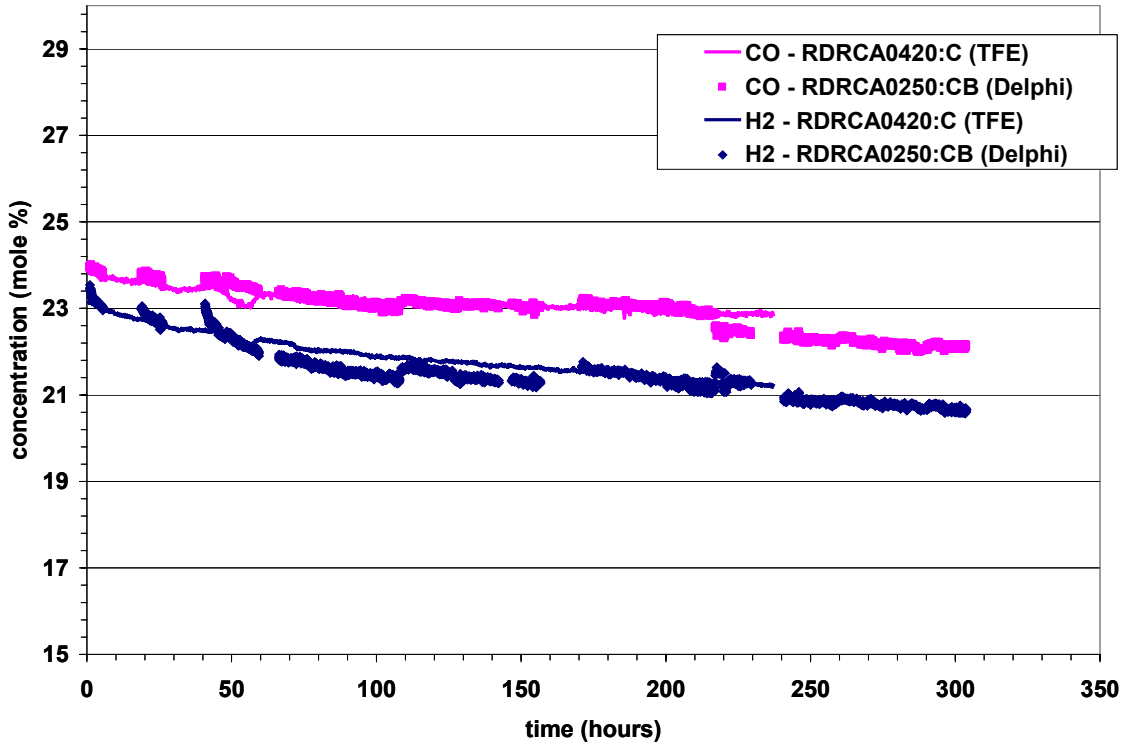

Figure 4.3.3.4-3: Results Of Durability Testing Across Different Test Sites.

Testing with CARB Phase II gasoline ~ 25,000/hr GHSV, O/C ~ 1.05 (mol/mol), analysis by gas chromatography.

4.3.3.5 Catalyst Application Development

Planning for a method to detect incipient carbon detection, results of a potential means of reducing sulfur, and extensive evaluation of methane reforming were completed during this reporting period.

4.3.3.5.1 Carbon Detection Method Development

We have been aware that Los Alamos National Laboratory (LANL) has been employing a method to detect carbon-rich particulates in product reformate gas streams. This method uses either extinction or scattering of an Argon laser beam, passed through the reformate via quartz windows strategically placed in the reactor hardware. This method can be enhanced to detect poly-nuclear aromatic compounds in the gas stream, via measurement of fluorescence. A diagram of the proposed apparatus in given in Figure 4.3.3.5.1-1.

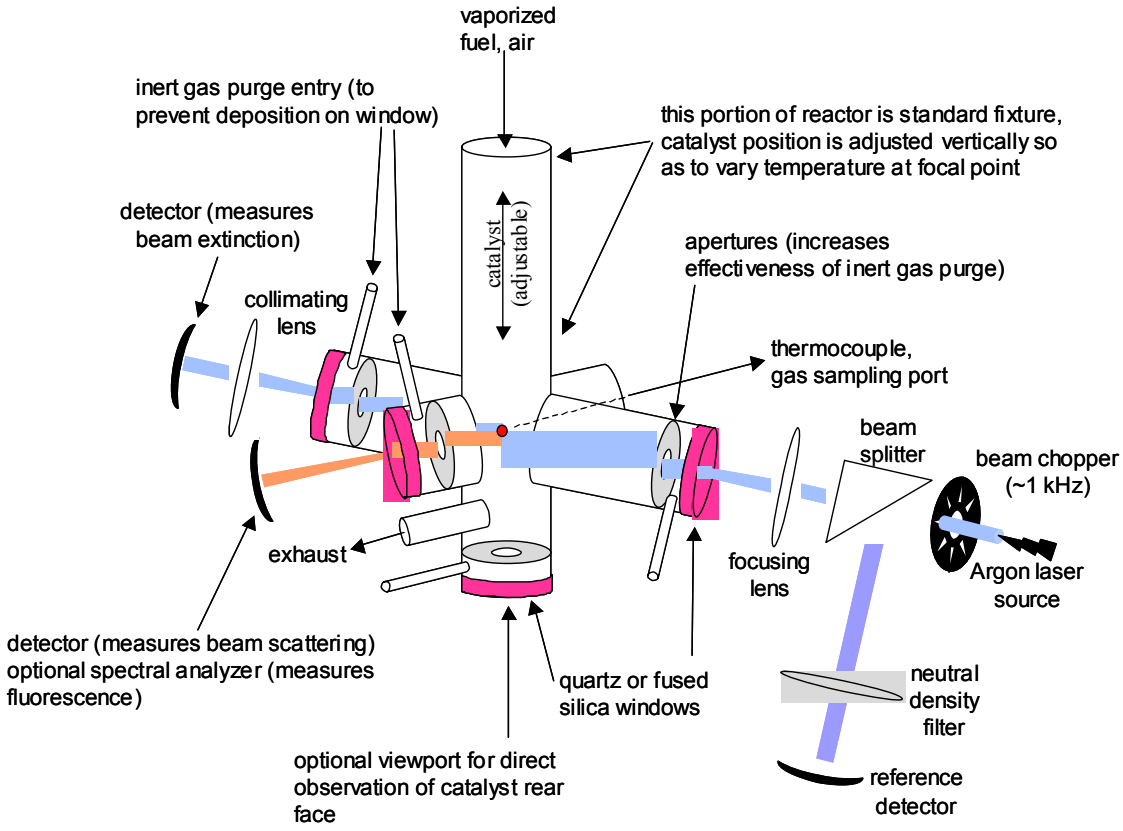

Figure 4.3.3.5.1-1: Schematic Of Proposed Argon Laser-Based Particulate Analyzer

Based on the success of this technique at LANL, we plan to build a similar apparatus during the next reporting period. This will permit us to operate reforming process at a variety of space velocities, air/fuel ratios, temperatures, and feed mixing conditions, with the goal of determining the sensitivity of these factors, as well as that of catalyst formulations, to carbon formation or carbon avoidance. While small amounts of carbon most likely do not affect reformer performance, they can have a profound effect on downstream components; avoidance of even trace amounts of carbon may be critical to extended operation of Solid Oxide Fuel Cell stacks.

4.3.3.5.2 Sulfur Removal Studies

We have been developing a process to oxidatively convert organically bound sulfur to SO_2. This can be useful as one part of a desulfurization process, as some potential sulfur removal schemes are significantly more efficient for SO_2 removal over organic sulfur removal.

Testing results are presented in Table 4.3.3.5.2-1. A mixture of fuel and air is passed over the sulfur conversion catalyst; the fuel is then condensed and analyzed for remaining sulfur content. Several sulfur bearing compounds were blended with CARB Phase II gasoline, including thiophene, benzothiophene, and dibenzothiophene, representing the range of sulfur compounds found in gasoline and diesel fuels.

410 wppm sulfur, added as thiophene, blended with CARB phase II gasoline.

		sulfur conversion vs. temperature (°C)	
LHSV	fuel (g/min)	200	300
3.18	0.50	46%	76%
6.42	1.01	26%	
12.91	2.03	15%	

Results of testing using different sulfur containing species added to CARB phase II gasoline, tested at ~ 250 °C.

	feed (wppm)	sulfur conversion vs. GHSV (1/hr) ~9000	~20,000	~42,000
octanethiol	243	81%	76%	81%
benzothiophene	610	80%	41%	61%
dibenzothiophene	344	80%	29%	45%

Table 4.3.3.5.2-1: Results of Desulfurization Testing

Depending on flow rate and temperature, significant amounts of sulfur were converted to SO_2. Errors may have been introduced into the measurements in that some of the feed gasoline was lost to evaporation, resulting in low mass balance. This loss was accounted for in determination of sulfur conversion. Undoubtedly improvements to the sulfur conversion catalyst and the process can increase the selectivity to SO_2 even higher.

4.3.3.6 Mechanistic Characterization of Reforming Catalysts

Mechanistic characterization involves catalyst analysis and carefully designed reaction studies. Work in this area was focused on demonstrating that commonly used and advanced methods for catalyst research are applicable to fuel reforming catalysts. Additional extensive work was completed on the effects of different sulfur bearing compounds on the partial oxidation of a range of hydrocarbon species. This work will serve as the foundation for characterization aimed at understanding structure – property relationships in reforming catalysts, ultimately leading to an understanding of and the mitigation of catalyst degradation mechanisms.

4.3.3.6.1 X-ray Photoelectron Spectroscopy

The same or similar formulated catalysts were evaluated by X-ray photoelectron spectroscopy (XPS). This technique can give information about the surface and near-surface environment of the catalyst, within several nanometers of the surface, with a focus on the state of the active metal. Results of this screening are given in Table 4.3.3.6.1-1.

No.	Sample Name	Relative concentration of PGM	PGM states	catalyst performance
1	RDRCA0-250:CB, fresh, not tested	3.36	M_2O_3	n/a
2	RDRCA0-250:CB, aged, not tested	0	M, M_2O_3	n/a
3	RDRCA0-250:CB, tested	2.48	M, M_2O_3 or MO_2	low H_2
4	RDRCA0-300:CY, tested	1.22	M	good H_2

catalyst tested in ‘fresh’ state

Table 4.3.3.6.1-1: Results of XPS Survey of Reforming Catalysts

XPS can clearly detect active metal species on the catalyst, and distinguish between metallic and oxide states. Relative concentrations, as a ratio to the alumina response, set to 100 (a value of 3.36 indicated 3.36 atoms observed for every 100 Al atoms), are an indication of the surface concentration of active metal on the sample. While only limited conclusions can be had from this small set of tests, decreasing amounts of active metal are observed on aged and tested catalysts, as compared to the fresh, untested, catalyst.

The observation of no observable active metal on the aged catalyst may imply that the active metal is either lost from the surface or migrated to the bulk of the catalyst during aging; however, similar samples evaluated after aging still exhibit significant reforming performance, see ‘RDRCA0-250’. In addition, the observation of less observable active

metal in the more active of the two tested catalysts is also interesting. For the next reporting period, we are planning a systematic investigation of tested catalysts, using XPS to determine if this technique can yield relevant information.

4.3.3.6.2 High-Resolution Transmission Electron Microscopy

A series of samples were studied by high-resolution transmission electron microscopy (HRTEM). As for the XPS work, the purpose of this HRTEM study was to determine the applicability of this technique to the analysis of fuel reforming catalysts. Representative micrographs are given in Figure 4.3.3.6.2-1, Figure 4.3.3.6.2-2, Figure 4.3.3.6.2-3, and Figure 4.3.3.6.2-4.

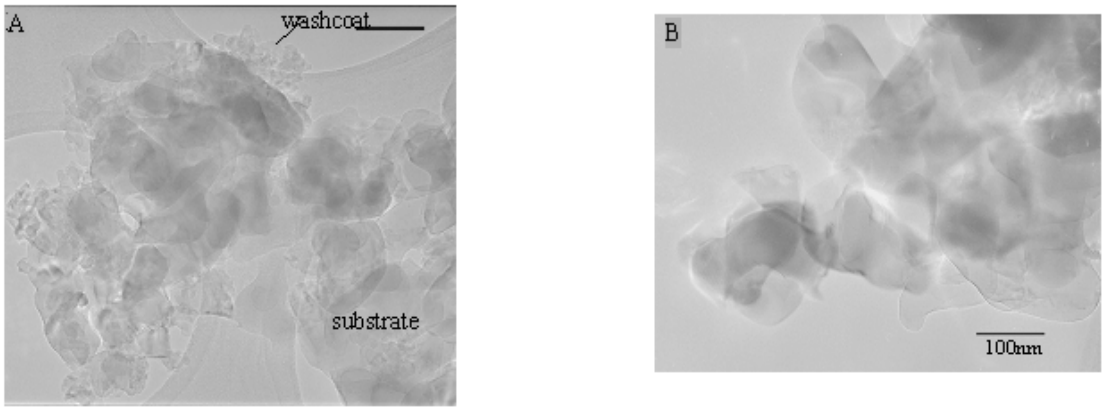

Figure 4.3.3.6.2-1: Results of HRTEM Survey of Reforming Catalysts

- In Figure 4.3.3.6.2-1, Figure A shows that substrate appears as big part8icles (with diameters greater than 50 nm), alumina washcoat appears as small crystalline particles (with diameters smaller than 10 nm). No PGM particles appeared in the TEM images.

- As shown in Figure B, washcoat particles appear to be bigger in this sample than in Figure A, suggesting washcoat sintered during the aging process. No PGM particles appeared in either the TEM images or the STEM Z-contrast images, although in some areas, weak PGM signals show up in the EDX spectra. These results suggest that most of the PGM was lost during the aging process.

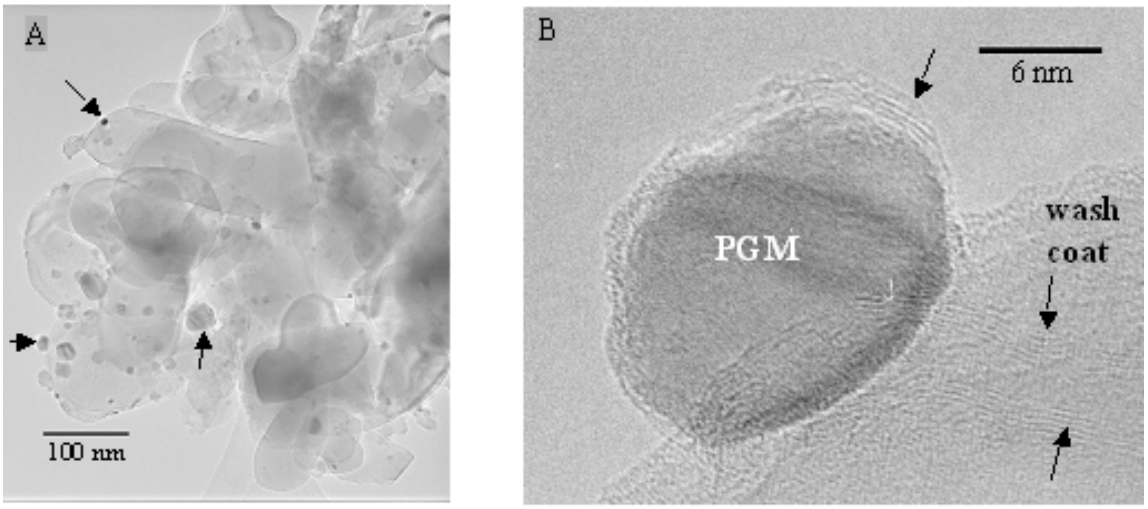

RDRCA0-250:CB, tested for reforming reaction, low H2 (18-19%)

Figure 4.3.3.6.2-2: Results of HRTEM Survey of Reforming Catalysts

In Figure 4.3.3.6.2-1, Figure A is a low-magnification image in which PGM particles are shown as small black particles (some of them are indicated by arrows) on the washcoat. PGM particles appear crystalline and faceted. Particle size ranges from a few nanometers to about 40 nanometers.

High-resolution images revealed that the surfaces of the PGM particles are coated. Some of the coatings show graphite (0002) fringes (with a spacing of 0.34 nm). This surface coating is probably the reason that no PGM was detected using a chemisorption method. A typi8cal image is shown in Figure B where the graphite (0002) fringes are indicated by arrows. It can be seen that graphite also formed on the washcoat.

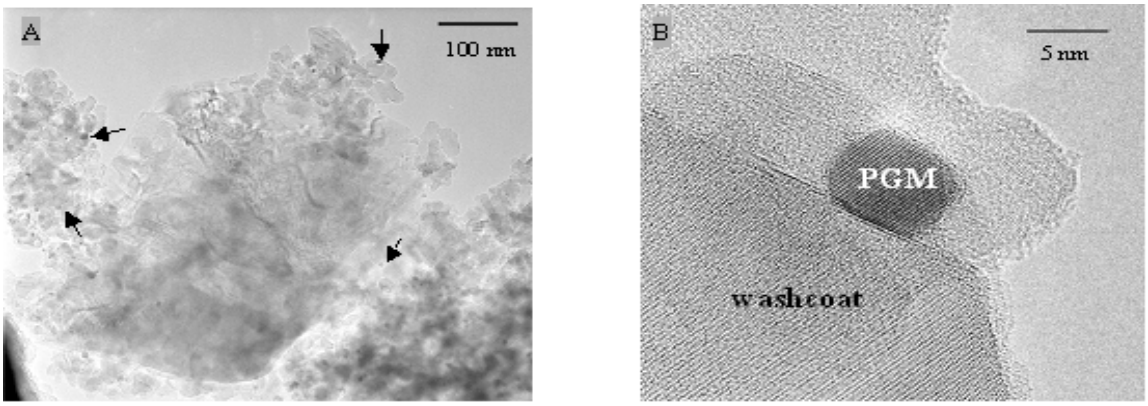

RDRCA0-300:CL, 20-21% H2

Figure 4.3.3.6.2-3: Results of HRTEM Survey of Reforming Catalysts

In Figure 4.3.3.6.2-3, Figures A and B are low- and high-magnification images, respectively, from this sample. Compared with the previous sample, which was deactivated to produce only 18-19% H_2, washcoat particles in this sample are smaller, more crystalline and more faceted.

PGM particles have sizes less than 10 nm in diameter. However, PGM particle density is lower than in the previous sample. Some of the PGM particles are indicated by arrows in Figure A. These results suggest that washcoat modification hinders the PGM and washcoat sintering process.

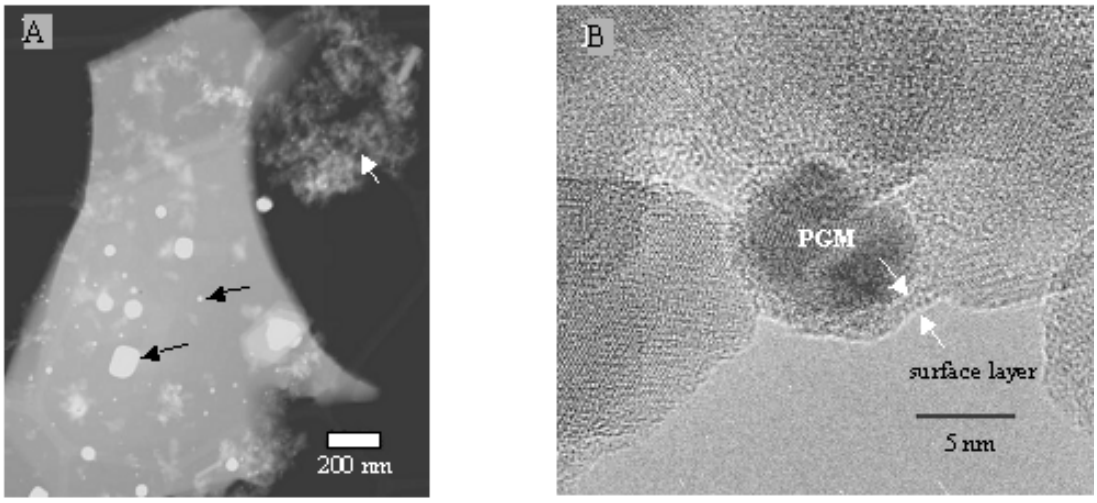

RDRCA0-320:CB, standard prep tested fresh

Figure 4.3.3.6.2-4: Results of HRTEM Survey of Reforming Catalysts

In Figure 4.3.3.1.2-4, Figure A is a low-magnification STEM Z-contrast image where PGM appears as white particles. Some of them are indicated with arrows. It shows that PGM particles have a bimodal size distribution depending on their location. In most of the areas, the PGM particles are less than 10 nm in diameter, but in some areas, their size can range from 20 to 100 nm. A particle with 260 nm in diameter was observed.

High-resolution images (Figure B) show that there is an amorphous layer formed on the PGM particles.

Depending on sample pretreatment and testing history, a range of active metal particles morphologies were observed. This includes well-faceted crystallites ranging in size from 5 to 100+ nm. In addition, the crystalline state of the washcoat, and the presence of graphitic carbon were also observed. The results qualitatively confirm the XPS observations; similarly, we are planning to conduct a more systematic survey of reforming catalyst to determine the usefulness of high-resolution electron microscopy and related nano-analysis and Z-contrast imaging techniques. The ability to directly observe active metal will most likely be invaluable in understanding these catalysts.

4.3.3.6.3 Laser-Raman Spectroscopy

Laser-Raman spectroscopy (LRS) is a technique that permits detection of chemical species containing certain classes of atom-atom bonding. For example, most platinum group elements metal to oxygen bounds can be observed, as can surface species such as adsorbed CO, CO_2, H_2, and H_2O. Consequently, this technique can be applicable to characterizing reforming catalysts under ex-situ, in-situ, and operando conditions.

We are currently installing a high-temperature stage, to permit operando analysis with simultaneous reforming chemistry and product analysis, using both UV and visible LRS. The expected results include identification of surface and gas phase species and reaction products with both spatial and temporal distributions.

Example of results obtained under ex-situ conditions are given in Figure 4.3.3.6.3-1, Figure 4.3.3.6.3-2, and Figure 4.3.3.6.3-3. No interference, other than that arising from sample fluorescence, indicating by the rising background in Figure 4.3.3.6.3-1, was observed from LRS of the alumina support, as aluminum oxides are not Raman active. A signal arising from PGM-oxygen bonding is clearly observable on two different catalyst products. While preliminary, these results suggest that LRS is an appropriate method for reforming catalyst characterization,

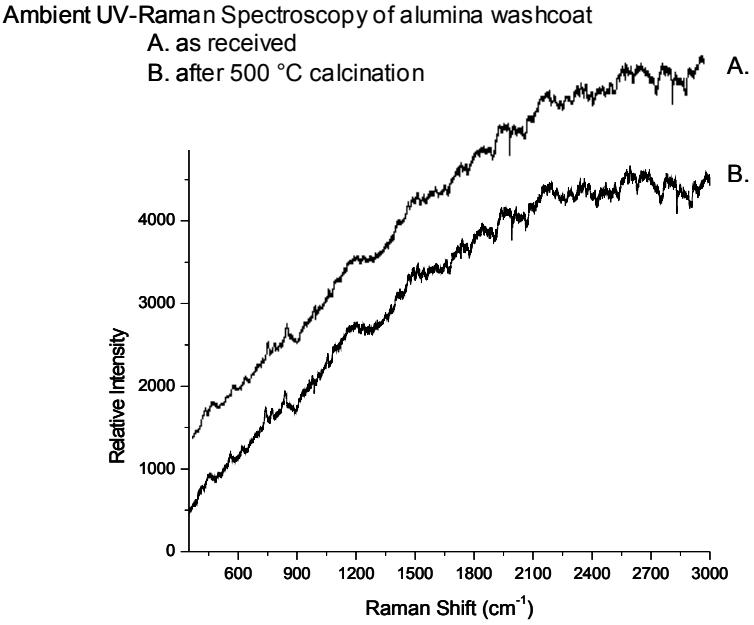

The UV-Raman spectra of the alumina washcoat only gave rise to noise due to sample fluorescence.

Figure 4.3.3.6.3-1: Results of Laser Raman Spectroscopy Survey of Catalysts

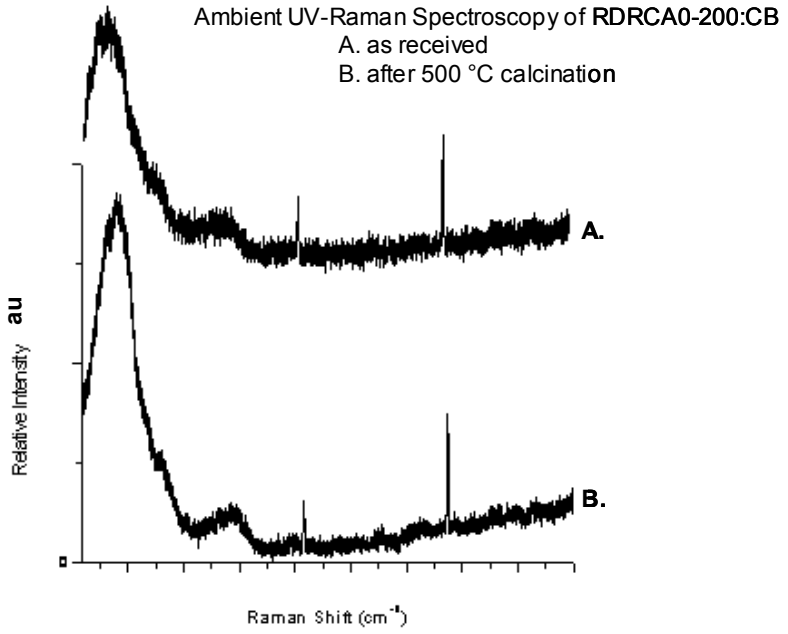

Figure 4.3.3.6.3-2: Results of Laser Raman Spectroscopy Survey of Catalysts

In Figure 4.3.3.6.3-2, catalyzed washcoat gave rise to a strong UV-Raman band, which shifted upon the calcinations at 500 ^{0}C. These strong Raman bands are due to PGM-oxide on alumina. At the present time, these small shifts are not understood and will require in-situ Raman studies to better understand their origins.

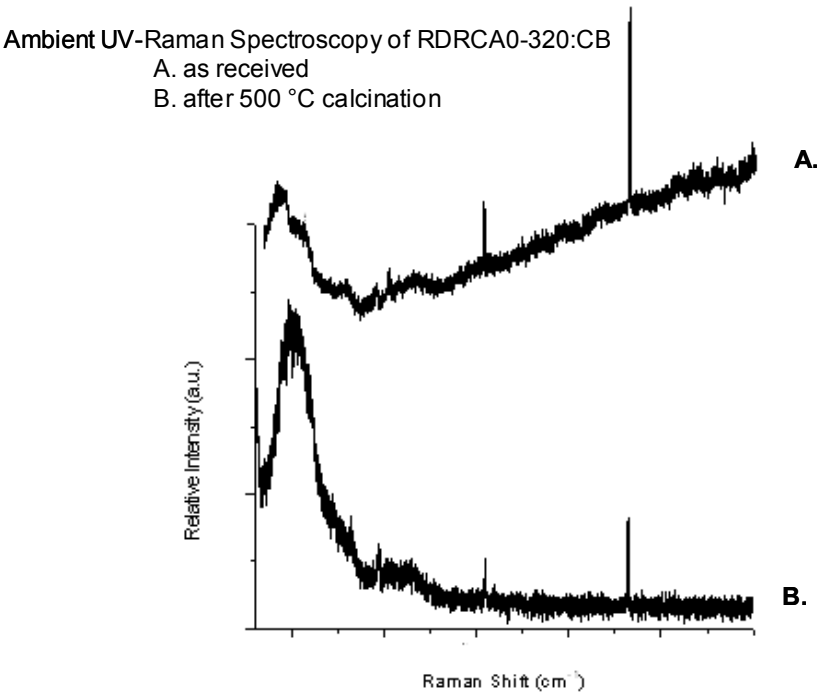

Figure 4.3.3.6.3-3: Results of Laser Raman Spectroscopy Survey of Catalysts

In Figure 4.3.3.6.3-3, the catalyzed washcoat UV-Raman spectrum gave rise to many vibrations, which indicates that the alumina fluorescence is not present when PGM is deposited. After calcinations at 500 ^{0}C, the PGM-O main vibration became much stronger.

4.3.3.6.4 Impact of Sulfur on Reforming Catalyst Performance

Of significant concern is the effects of fuel-borne sulfur on reforming catalyst performance, particularly for processing of heavy diesel fuel, which is perceived to contain highly refractory and consequently difficult to process sulfur containing molecular species. We completed a series of experiments in which hydrocarbon feedstocks were blended with up to 100 ppm of either SO_2 or thiophene, and then processed for partial oxidation reforming.

Figure 4.3.3.6.4-1 illustrates the effects of thiophene on the reforming of iso-octane, using a standard highly active gasoline partial oxidation catalyst. Selectivity decreases with increasing levels of thiophene, with hydrogen bearing species, H_2, H_2O, and CH_4, exhibiting the largest impacts. In contrast, the selectivity to CO and CO_2 is not impacted nearly as much.

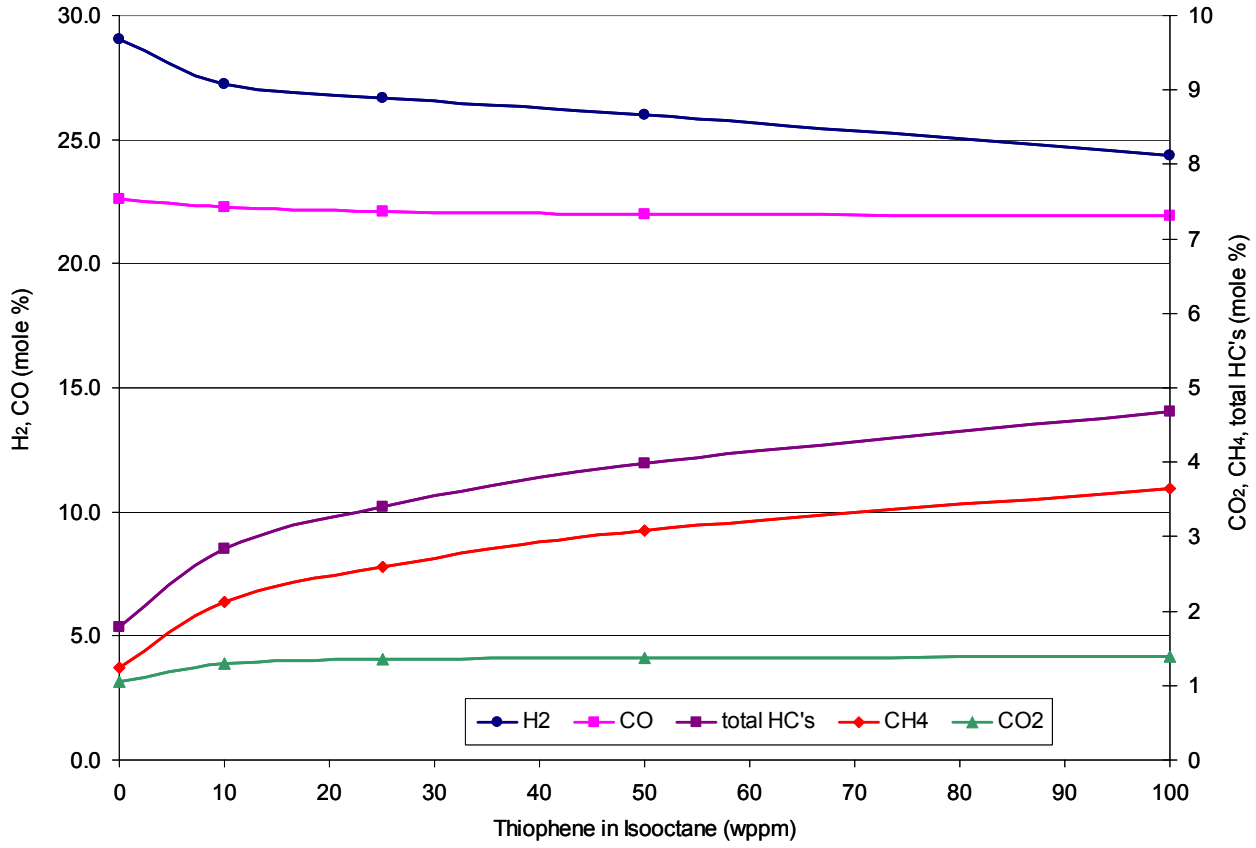

Testing with iso-octane, ~50,000/hr GHSV, O/C ~ 1.01 (mol/mol), analysis by mass spectroscopy.

Figure 4.3.3.6.4-1: Influence of Thiophene on Iso-Octane Reforming Performance

Figure 4.3.3.6.4-2, and Figure 4.3.3.6.4-3 illustrate similar behaviors for thiophene and SO_2 blended with gasoline. In these two tests, an unblended feed was tested at the conclusion of the sulfur-bearing tests, and shows that some selectivity recovery occurs, perhaps indicating that sulfur inhibits catalytically active sites, rather than poisoning them. Again, sulfur effects on H_2 selectivity are much greater than that on CO selectivity.

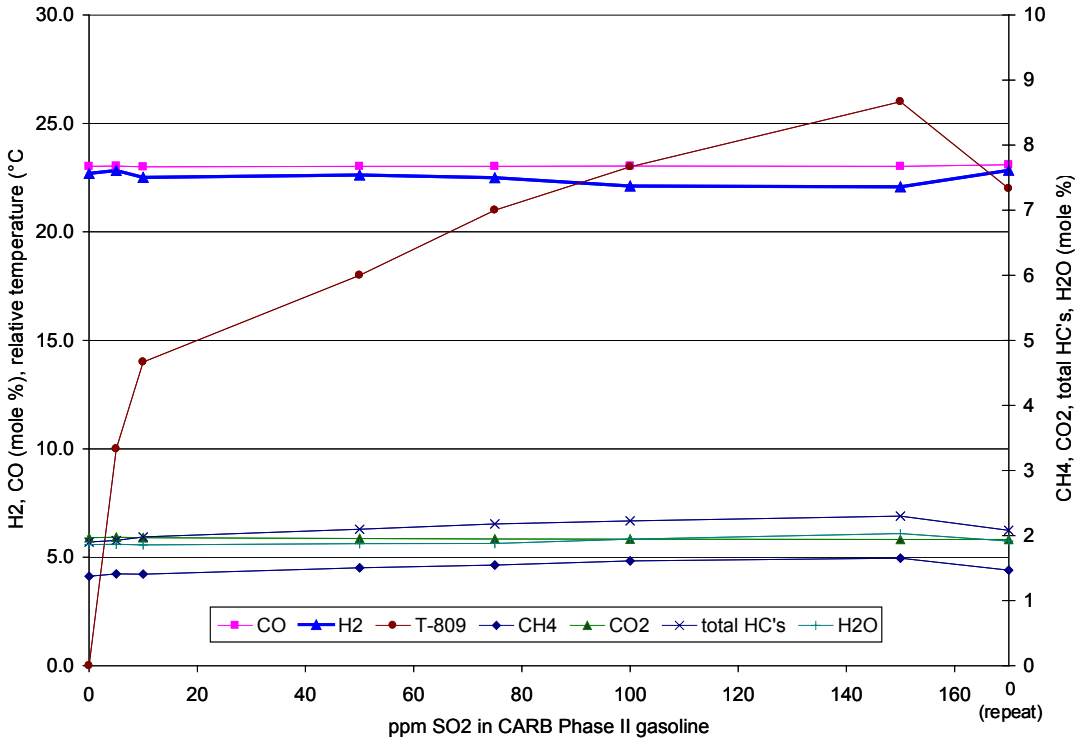

Testing with CARB Phase II gasoline, ~50,000/hr GHSV, O/C ~ 1.01 (mol/mol), analysis by mass spectroscopy.

Figure 4.3.3.6.4-2: Influence of SO_2 on Gasoline Reforming Performance

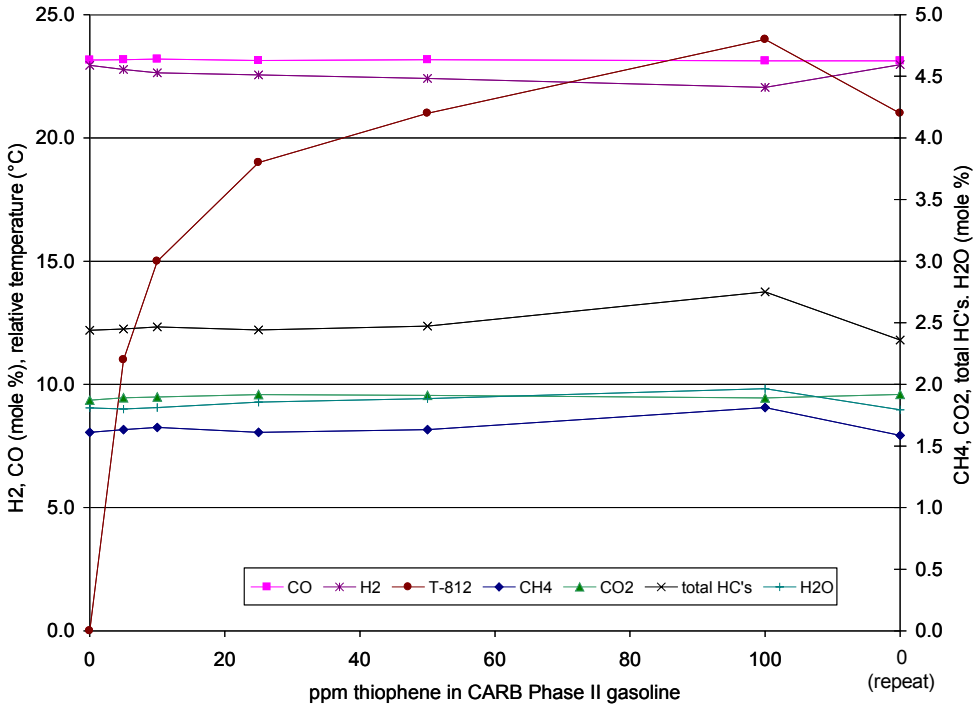

Testing with CARB Phase II gasoline, ~50,000/hr GHSV, O/C ~ 1.01 (mol/mol), analysis by mass spectroscopy.

Figure 4.3.3.6.4-3: Influence of Thiophene on Gasoline Reforming Performance

Figure 4.3.3.6.4-4 the effects of SO_2 on partial oxidation reforming for feeds ranging from methane to gasoline. Most of the tested samples' performance recovers to original selectivity after removal of sulfur. Heavier hydrocarbon reactants have much less of an H_2 selectivity impact than the lighter hydrocarbons tested, CH_4 and C_3H_8. A comparison of i-C8H18 and gasoline further shows that a more complex hydrocarbon is less impacted by SO_2. A blend of iso-octane and aromatics is intermediate in performance between that of iso-octane and gasoline.

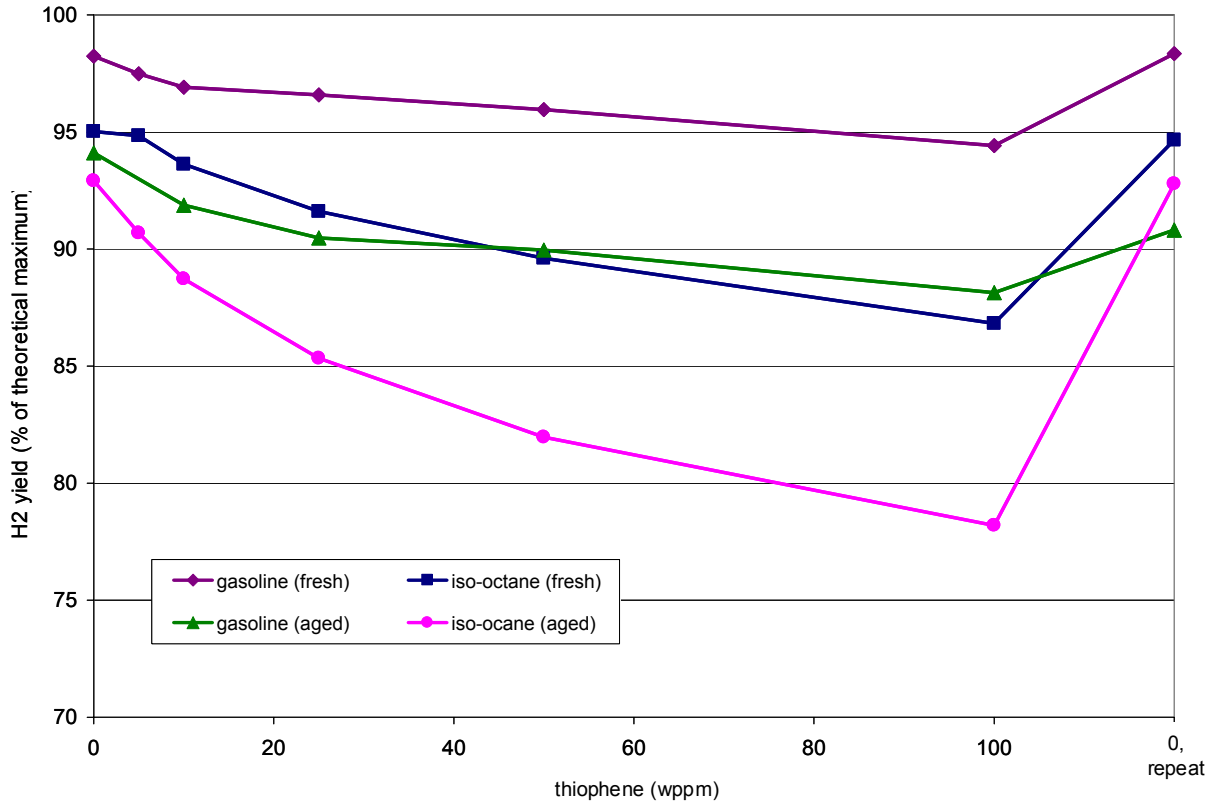

catalyst tested as received or after aging.
Testing at ~50,000/hr GHSV, O/C ~ 1.01 (mol/mol), analysis by mass spectroscopy.

Figure 4.3.3.6.4-4: Comparison of Thiophene on Reforming Performance with Fresh and Aged Catalysts

These results have implications in both the types of feeds that may need desulfurization and on potential reaction mechanisms. H_2 and CO appear to have different pathways for formation. As CO selectivity is much less affected by changes to the catalyst, seen here and in previous results from other studies, an assumption is that CO formation is either a gas-phase reaction or is not a surface-sensitive reaction. However, formation of H_2, and C-H bond cleavage, as required for CH_4 reforming, is highly surface dependant. Also assumed is that heavier hydrocarbons will crack into C_2 species and methylene radicals. The manifestation of this proposed mechanism is that methane is difficult to process when the catalyst is inhibited by sulfur, while gasoline is much less so.

4.3.3.7 Catalyst Development Planning

Activity in this area consists of determining program goals and milestones, identification of resource gaps, and alignment of existing resources with the identified needs. Outside resources and services are also identified and developed as needed.

The overall goal of this catalyst development program is to formulate catalysts that can meet the performance and durability requirements of fuel reforming, including gasoline, diesel fuel, and natural gas applications. To date, an industrial development approach has been taken, in that the primary concern is to insure the viability and usefulness of reformer and system-level devices, in that the catalysts provided to these devices will function as required. Current catalyst formulations meet the needs of the reformer and systems teams to test their devices; however, the catalyst still needs to be proven to meet durability requirements.

To date, maximum selectivities towards the desired products, H_2 and CO, are nearly identical for all of the best catalyst formulations, coming close to 100% conversion of gasoline. This evaluation is based on limited, less than 300 hour, testing. Extensive durability and stress testing will be required to identify which of these formulations best meets the needs of system level devices from both a selectivity and a durability stand-point.

The majority of current and planned work is focused on understanding catalyst durability, including formulation for improved durability, identification of deactivation and aging mechanisms, and development of a rapid aging test. Additional work related to developing processing information in support of modeling and reformer design work is also being undertaken.

A parallel-path approach to catalyst development is now underway. Improved formulations will continue to be developed, to meet the increasingly stringent and demanding requirements of the reformer and systems teams. Catalyst formulations will also be improved as more sophisticated rapid-aging tests and increasing extents of durability testing become available. Application specific formulation development, for natural gas, gasoline, and diesel fuel applications, with or without water or anode tail-gas recycle, will also take place as additional development test stands become available.

While the formulation work to meet the performance requirements will always be most important, catalyst characterization work aimed at understanding the underlying mechanisms of catalyst behavior will also be on going. An attempt will be made to develop a complete understanding of the interrelationship between catalyst structure, formulation, reaction conditions, process variability, and catalyst performance, with a focus on understanding and minimizing deactivation mechanisms. As chemical catalysis is the result of the surface expression of bulk structure, both bulk and surface analysis techniques have been selected to be used in this effort. Advanced characterization tools include high-resolution transmission electron microscopy, in-situ Laser Raman and UV spectroscopies, and X-ray photoelectron spectroscopy. These will be supplemented by more traditional analysis tools such as XRD (ex- and in-situ capabilities), BET, chemisorption, and elemental analysis. Method development will be a key component of this work, pertaining particularly to the in-situ and operando

characterization work, development of rapid aging procedures and relevant probe reactions and chemisorption methods.

4.3.3.8 Reformer Washcoat - Substrate Adhesion

4.3.3.8.1 Introduction

Successful reformer operation is dependent on the amount of catalyst used in the reformer. Hence, loss of catalyst due to spallation should be avoided or eliminated as a failure mechanism. The precious metal used as a catalyst is dispersed in a washcoat. The washcoat adheres to the catalyst support that may be a metal or ceramic material. Therefore, the bond between the substrate and the washcoat is of particular importance.

Delphi currently has two reformer designs approaches. One is tubular using a ceramic foam substrate and other planar using metallic plates as the catalyst substrate. Two parallel sets of experiments were designed to study washcoat adhesion to the substrates.. One experiment investigates the bond between a metallic substrate and various washcoat compositions and preparations. The second experiment investigates the bond between a ceramic substrate and various washcoat compositions and preparations. Both experiments will stress the washcoat/substrate interface by rapid, multiple, thermal cycles.

4.3.3.8.2 Experimental

An engineering study has been initiated employing fractional factorial experiments (L54 and L18 Taguchi constructs) designed to investigate the bond between the washcoat and the catalyst support. The L54 experiment investigates the bond between Aluminum Oxide, Cerium Oxide and Zirconium Oxide based washcoats and a variety of metal substrates. The L18 experiment investigates the bond between Aluminum Oxide, Cerium Oxide, and Zirconium Oxide based washcoats and a variety of ceramic substrates. In both these experiments the response of interest is washcoat adhesion to the substrate. Variables under study include washcoat composition, substrate surface preparations, preparation time, washcoat acidity, reforming temperature, the addition of thermal barrier bond coats and washcoat loading. The samples will be tested under thermal cycling conditions and spallation of the washcoat will be determined by weight loss. The L54 experimental plan for the ceramic substrate/washcoat couple is shown in Table 4.3.3.8.2-1. The L18 experiment for the ceramic substrate/washcoat couple is shown Table 4.3.3.8.2-2.

	Substrate / Thermal Barrier Coat	Washcoat	Geometry	Substrate pretreat	Binder %dryweight	Particle size (μ)	Washcoat pH	Slurry aging time	Substrate detergent rinse
L54	1*	3	4	5	6	7	8	15	16
1	MA956	Al2O3	thin	None	0	3	2.5	< 2hrs	DI or distilled water
2	H230	Al2O3	thin	None	0	3	2.5	7 days	Alconex
3	H214	Al2O3	thin	None	0	3	2.5	14 days	none
4	MA956	ZrO2	thin	Etched	5	3.5	3.5	7 days	none
5	H230	ZrO2	thin	Etched	5	3.5	3.5	14 days	DI or distilled water
6	H214	ZrO2	thin	Etched	5	3.5	3.5	< 2hrs	Alconex
7	MA956	CeO2	thin	Pre-oxidized	10	4.5	4.5	14 days	Alconex
8	H230	CeO2	thin	Pre-oxidized	10	4.5	4.5	< 2hrs	none
9	H214	CeO2	thin	Pre-oxidized	10	4.5	4.5	7 days	DI or distilled water
10	FeCralloy	Al2O3	thin	Etched	5	4.5	4.5	< 2hrs	DI or distilled water
11	Incoloy DS	Al2O3	thin	Etched	5	4.5	4.5	7 days	Alconex
12	I600	Al2O3	thin	Etched	5	4.5	4.5	14 days	none
13	FeCralloy	ZrO2	thin	Pre-oxidized	10	3	2.5	7 days	none
14	Incoloy DS	ZrO2	thin	Pre-oxidized	10	3	2.5	14 days	DI or distilled water
15	I600	ZrO2	thin	Pre-oxidized	10	3	2.5	< 2hrs	Alconex
16	FeCralloy	CeO2	thin	None	0	3.5	3.5	14 days	Alconex
17	Incoloy DS	CeO2	thin	None	0	3.5	3.5	< 2hrs	none
18	I600	CeO2	thin	None	0	3.5	3.5	7 days	DI or distilled water
19	29-4C	Al2O3	thin	None	10	3.5	4.5	< 2hrs	DI or distilled water
20	H230/NiCrAlY	Al2O3	thin	None	10	3.5	4.5	7 days	Alconex
21	H214/NiCrAlY	Al2O3	thin	None	10	3.5	4.5	14 days	none
22	29-4C	ZrO2	thin	Etched	0	4.5	2.5	7 days	none
23	H230/NiCrAlY	ZrO2	thin	Etched	0	4.5	2.5	14 days	DI or distilled water
24	H214/NiCrAlY	ZrO2	thin	Etched	0	4.5	2.5	< 2hrs	Alconex
25	29-4C	CeO2	thin	Pre-oxidized	5	3	3.5	14 days	Alconex
26	H230/NiCrAlY	CeO2	thin	Pre-oxidized	5	3	3.5	< 2hrs	none
27	H214/NiCrAlY	CeO2	thin	Pre-oxidized	5	3	3.5	7 days	DI or distilled water
28	I600/NiCrAlY	Al2O3	thin	Pre-oxidized	5	3.5	2.5	< 2hrs	DI or distilled water
29	FeCralloy/FeCrAlY	Al2O3	thin	Pre-oxidized	5	3.5	2.5	7 days	Alconex
30	302SS	Al2O3	thin	Pre-oxidized	5	3.5	2.5	14 days	none
31	I600/NiCrAlY	ZrO2	thin	None	10	4.5	3.5	7 days	none
32	FeCralloy/FeCrAlY	ZrO2	thin	None	10	4.5	3.5	14 days	DI or distilled water
33	302SS	ZrO2	thin	None	10	4.5	3.5	< 2hrs	Alconex
34	I600/NiCrAlY	CeO2	thin	Etched	0	3	4.5	14 days	Alconex
35	302SS	CeO2	thin	Etched	0	3	4.5	< 2hrs	none
36	302SS	CeO2	thin	Etched	0	3	4.5	7 days	DI or distilled water
37	29-4C/FeCrAlY	Al2O3	thin	Pre-oxidized	0	4.5	3.5	< 2hrs	DI or distilled water
38	H230/CoCrAlY	Al2O3	thin	Pre-oxidized	0	4.5	3.5	7 days	Alconex
39	H214/CoCrAlY	Al2O3	thin	Pre-oxidized	0	4.5	3.5	14 days	none
40	29-4C/FeCrAlY	ZrO2	thin	None	5	3	4.5	7 days	none
41	H230/CoCrAlY	ZrO2	thin	None	5	3	4.5	14 days	DI or distilled water
42	H214/CoCrAlY	ZrO2	thin	None	5	3	4.5	< 2hrs	Alconex
43	29-4C/FeCrAlY	CeO2	thin	Etched	10	3.5	2.5	14 days	Alconex
44	H230/CoCrAlY	CeO2	thin	Etched	10	3.5	2.5	< 2hrs	none
45	H214/CoCrAlY	CeO2	thin	Etched	10	3.5	2.5	7 days	DI or distilled water
46	I600/CoCrAlY	Al2O3	thin	Etched	10	3	3.5	< 2hrs	DI or distilled water
47	Mike Metal	Al2O3	thin	Etched	10	3	3.5	7 days	Alconex
48	430Ti	Al2O3	thin	Etched	10	3	3.5	14 days	none
49	I600/CoCrAlY	ZrO2	thin	Pre-oxidized	0	3.5	4.5	7 days	none
50	Mike Metal	ZrO2	thin	Pre-oxidized	0	3.5	4.5	14 days	DI or distilled water
51	430Ti	ZrO2	thin	Pre-oxidized	0	3.5	4.5	< 2hrs	Alconex
52	I600/CoCrAlY	CeO2	thin	None	5	4.5	2.5	14 days	Alconex
53	Mike Metal	CeO2	thin	None	5	4.5	2.5	< 2hrs	none
54	430Ti	CeO2	thin	None	5	4.5	2.5	7 days	DI or distilled water

Table 4.3.3.8.2-1: L54 Test Matrix for Washcoat Adhesion with Metallic Substrates

L_{18} (6^1 x 3^6)	Substrate	Washcoat	(Aluminum Hydroxide) %dryweight	Particle size (microns)	Washcoat pH	Slurry aging time
No.	1*	3	4	5	6	7
1	SiC	Al_2O_3	0	3	2.5	< 2hrs
2	SiC	ZrO_2	5	3.5	3.5	7 days
3	SiC	CeO_2	10	4.5	4.5	14 days
4	FSZM	Al_2O_3	0	3.5	3.5	14 days
5	FSZM	ZrO_2	5	4.5	4.5	< 2hrs
6	FSZM	CeO_2	10	3	2.5	7 days
7	YSZ (8% Ytrium)	Al_2O_3	5	3	4.5	7 days
8	YSZ (8% Ytrium)	ZrO_2	10	3.5	2.5	14 days
9	YSZ (8% Ytrium)	CeO_2	0	4.5	3.5	< 2hrs
10	ZTA	Al_2O_3	10	4.5	3.5	7 days
11	ZTA	ZrO_2	0	3	4.5	14 days
12	ZTA	CeO_2	5	3.5	2.5	< 2hrs
13	O2BSiC	Al_2O_3	5	4.5	2.5	14 days
14	O2BSiC	ZrO_2	10	3	3.5	< 2hrs
15	O2BSiC	CeO_2	0	3.5	4.5	7 days
16	ZTA	Al_2O_3	10	3.5	4.5	< 2hrs
17	ZTA	ZrO_2	0	4.5	2.5	7 days
18	ZTA	CeO_2	5	3	3.5	14 days

Table 4.3.3.8.2-2 L18: Test Matrix for Washcoat Adhesion with Ceramic Substrates

The metallic substrate experiment will be performed in a nitrogen-hydrogen atmosphere, while the ceramic substrate study will be conducted in air. The reason for the difference is the nature of the substrate. The reformer washcoat is not protective. Hence, the metallic substrate will undergo oxidation. Deleterious phases may occur at the interface between a metallic substrate and the washcoat due to this oxidation. If this phase is brittle and posses low fracture toughness than thermal cyclic loadings will cause the scale to spall. The oxidation of the metallic substrates may be different for some of the alloys in different atmospheres, an atmosphere containing water, hydrogen and nitrogen was deemed necessary to mimic, as closely as possible, the reformer reformate. However, CO could not be included in the testing due to the poisonous nature of the substance and the large size of this experiment.

It is planned to select promising combinations from these first 2 experiments to do further testing in a smaller study which will include simulated reformate as the oxidant. The metallic substrate materials include ferritic and austenitic stainless steels, nickel-based and Fe-based super alloys. The alloys chosen are MA956, H230, H214, FeCralloy, Incoloy DS, I600, 29-4C, H230/NiCrAlY, H214/NiCrAlY, I600/NiCrAlY, FeCralloy/FeCrAlY, 302SS, 29-4C/FeCrAlY, H230/NiCrAlY, H214/NiCrAlY, I600/NiCrAlY, Crofer 22 APU, 430Ti. Because the metallic substrate test must be performed in a controlled atmosphere furnace the thermal cycles will not be as rapid as will be achieved in the actual reformer. However, the thermal cycle will be performed as

rapidly as can be accomplished with the equipment. Preliminary tests suggest that the thermal cycles will be room temperature to 900 ^{o}C in 1 hour and 900 ^{o}C to room temperature in 3 hours.

The ceramic substrate experiment can be placed in conventional furnace because the substrate will not be oxidized. The major stress on the ceramic substrate study will be thermal cyclic loading due to the rapid startups of the reformer. Since conventional furnaces can be used on this study, very rapid thermal cycles such as those experienced by the reformer can be used. The main stress on the ceramic substrates is the weight bearing capability of the ceramic foam. Ceramic foams come in a variety of pore sizes, porosities and compositions. The greater the surface area of the ceramic foam, the smaller the reformer volume. However, the greater the surface area, the more fragile the ceramic foam will be to thermal loadings and vibrational loadings. The fracture of the ceramic foam struts leads to loss of catalyst and subsequent failure of the reformer. The more porous the ceramic foam, the weaker the struts of the ceramic foam will be. The addition of severe, thermal cyclic, loading to the already stressed struts of the ceramic foam has already proven detrimental to the longevity of these foams. Figure DE-3 shows the strut of a ceramic foam. The ceramic materials choices include: Silicon Carbide, Zirconium Toughened Alumina, Yttrium Stabilized Zirconia (8% Yttrium), Oxygen-Bonded Silicon Carbide, Partially Stabilized Zirconia and Fully Stabilized Zirconia.

STATUS OF WASHCOAT ADHESION EXPERIMENTATION:

All samples have been fabricated, weighed, and an undercoat has been added where needed. The samples are currently being washcoated. They are expected to be finished at the end of August. The samples will then be reweighed and the thermal cycling portion of the experiment will be started

4.3.4 Desulfurization of Gasoline and Natural Gas

Sulfur is a poison for the nickel anode of the stack and the reforming catalyst. According to particular Westinghouse publications, H_2S level must be less than 1 ppmw in order to prevent poisoning of the nickel anodes in their Solid Oxide Fuel Cell.

In the United Stated States and Europe, increasingly stringent regulations are attempting to reduce sulfur levels in gasoline. Recently, the US Environmental Protection Agency has issued regulations that will require the refineries to reduce the sulfur content in gasoline from a current average of 300 ppmw to 30 ppmw by 2006. In Europe, the current sulfur limit in gasoline will be lowered from 150 ppmw to 50 ppmw by 2005 and it is planned to limit sulfur at 10 ppmw by 2010. Major sulfur species present in gasoline are thiophene, methylthiophene, dimethylthiophene, benzothiophene, methylbenzothiophene and dimethylbenzothiophene.

However, the sulfur content in natural gas is dependent on the extraction site. In Europe, sulfur content in natural gas can reach levels as high as 105 ppmv in peaks and the annual average limit is approximately 21 ppmv. In the US, the Code of Federal

Regulation indicates a sulfur limit of 8 ppmv but the actual sulfur levels have been recorded at levels as high as 338 ppmv in certain areas. Major sulfur species present in natural gas are sulfides (hydrogen sulfide, carbonyl sulfide, dimethyl sulfide), disulfides (carbon disulfide, dimethyl sulfide) and mercaptan, some thiophene compounds are also found.

There are several ways to desulfurize. The following desulfurization processes were investigated:

- Hydrodesulfurization (HDS)
- Claus Process
- Partial oxidation
- Adsorption
- Composite membranes
- Polymer membranes.

The most promising process is sulfur adsorption, which has the advantages of low investment, low operating cost, easy maintenance, no further sulfur processing and low temperature and pressure operation. According to calculations, the volume of adsorbent necessary to desulfurize current gasoline with an operating window of 1000 hours is in the range of 200 liters. The desulfurization of natural gas would require 20 and 50 liters of adsorbent for an operating window of 10,000 hours. Additional research to increase the adsorption level of sulfur and reduce the volume of the desulfurizer is still required for this technology. The Energy Institute of Penn State University is currently focusing on these points and their results seem promising.

The literature has stated that some very refractory sulfur species do not react with the nickel in the anode of a Solid Oxide Fuel Cell stack and the some precious metal catalysts. Research is currently being proposed to find the acceptable levels for every sulfur species in gasoline and natural gas. Since refractory sulfur compounds do not react readily, the desulfurizer volume must be large to compensate for the lack of reaction rate. However, if these refractory sulfur species do not react with the nickel anode or the reformer catalyst then the desulfurizer volume can be significantly reduced.

Delphi is planning on developing different adsorption solutions for on-board sulfur removal (gasoline) and for on-site sulfur removal (natural gas). Because of vibrations, foam structures will be favored in the mobile applications. Because of cost considerations, pellets will be favored in stationary applications. Pellets cannot be used in mobile application due to abrasive wear, which breaks down the pellets and leads to deactivation of the adsorption properties of the pellets.

4.3.5 Develop Reformer and System – General

4.3.5.1 Labview

As mentioned previously, the labview system was enhanced to the point where all data was available on a single file. In addition, preliminary real time calculations were enabled. These calculations include Mass Spectrometer corrections for water content when the water knockout system is in place. They also include calculations for reformer efficiency.

In addition, variable passing was greatly simplified with respect to how variables are ultimately logged by Labview by allowing Labview control of the final variable labeling.

The Labview graphing utility was also enhanced to allow the user to view data that is being generated real-time over as long as period as 6-hours. This allows the operator to more accurately evaluate performance during the test, and determine steady state conditions.

4.3.5.2 Lab Test System Development

Two Gas Chromatographs were added to our lab equipment. One is used for reformer development and the other is dedicated to the Catalyst durability stands.

Additionally, a third Mass Spectrometer was received.

This equipment will ultimately reside in a new facility that recently opened. The facility has both Reformer Development Lab (equipped with 3 development stands) and Reformer/Catalyst Durability Lab (currently equipped with 3 stands with plans for as many as 11 total).

4.3.6 Investigate Integration of Reformer and ERU Functions.

This subject covered under “Develop CPO Reformer” Section.

4.3.7 Fabricate Developmental Reformers.

See related discussion under “Develop CPO Reformer Section.

4.4 Development of Balance of Plant Components (Task 4.0)

4.4.1.1 Develop Hydrogen Sensors for High and Low Concentration Measurement

4.4.1.2 High Concentration Hydrogen Sensor

No additional test results at this time; Co-development with reformer team continues.

4.4.1.3 Combustible Gas Sensor

Results pending test at system level.

4.4.2 Develop Air Delivery and Process Air Sub-System

4.4.2.1 Mass Air Flow Sensor Calibration

Figure 4.4.2.1-1 below shows results for mass air flow sensor calibration test. Flow versus sensor voltage is shown at three valve positions for each of the four mass air flow sensors, (S5, S8, S9 & S10).

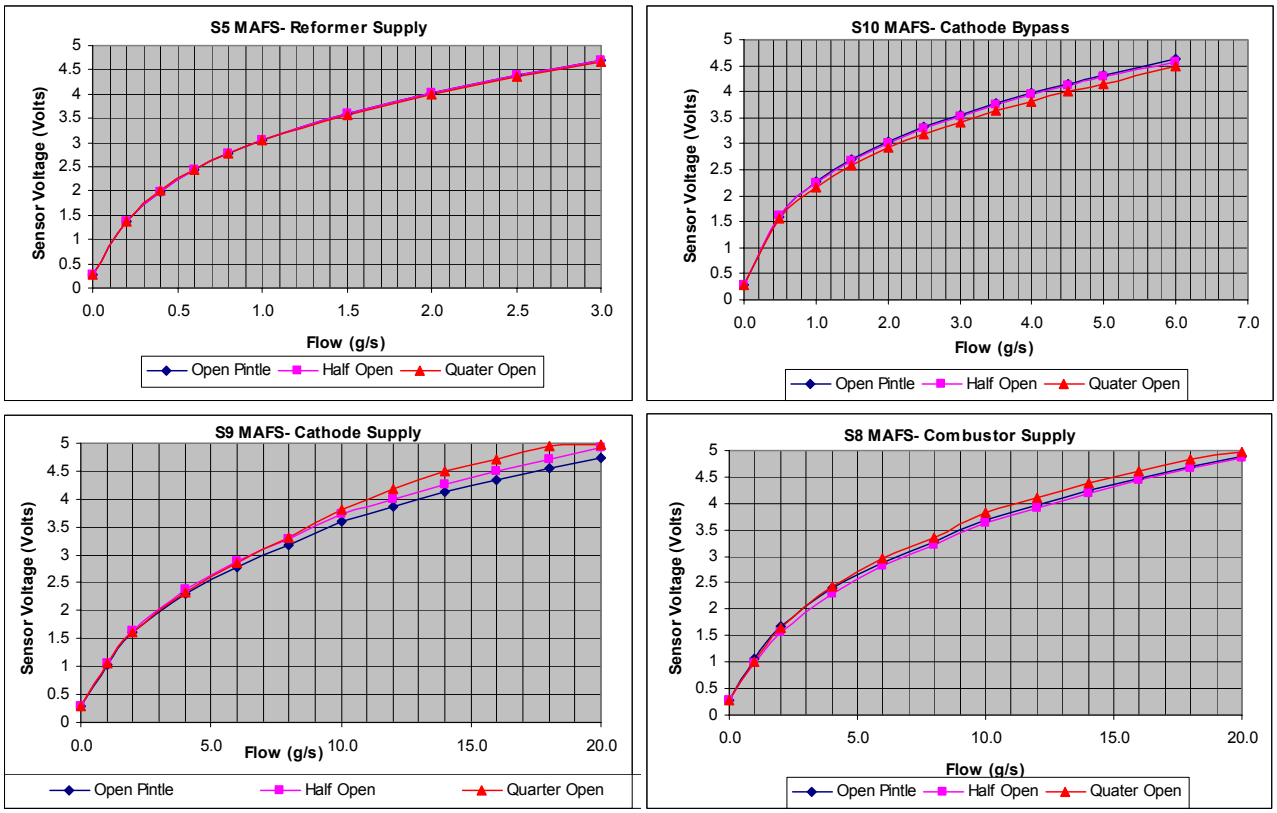

Figure 4.4.2.1-1: Mass Air Flow Sensor Calibration Curves

Calibration of the S5 Mass Air Flow Sensor showed good repeatability of sensor output voltage versus pintle position.

Calibration of the S10 Mass Air Flow Sensor indicated slight deviation from an ideal calibration curve indicating flow instability induced from the pintle. A 4-Volt DC-sensor output voltage, results in a 9.7% increase in sensed flow, depending on pintle position.

Calibration of the S9 and S8 mass airflow sensors indicate an increased sensitivity of sensor output to pintle position. A 4-vdc-sensor output voltage, results in an 18.2% increase in sensed flow depending on pintle position.

Continued development of the process air system is expected to result in mass flow readings that are less sensitive to pintle induced flow disturbances. Part of continued

development activities will include a redesign the system where the air control valves are placed down stream of the Mass Air Flow Sensor. This will result in less flow steering or flow disturbances which result from valve opening and closing, thereby creating flow disturbances which result in signal noise on the flow sensor.

4.4.2.2 Mass Air Flow Sensor Stability Test

Without any flow conditioner and the Mass Air Flow Sensor close coupled to the manifold, output voltage variations were 0.035 volts.

By placing a flow conditioner made of Honey Cell directly behind the pintle, a similar effect to adding 18-inchs of straight pipe between the pintle and the Mass Air Flow Sensor was achieved. The output voltage variations were only 0.01 volts.

Placing the flow conditioner directly in the Mass Air Flow Sensor had a detrimental effect on flow stability resulting in voltage variations of 0.07 volts. Data from the following conditions is shown in Figure 4.4.2.2-1.

UPPER LEFT: Mass Air Flow Sensor removed from the manifold with 18-inch straight pipe resulting in ideal flow stability.

UPPER RIGHT: Effect of placing Mass Air Flow Sensor directly on manifold without any flow conditioner; resulting in unstable voltage output.

LOWER LEFT: Effect on flow stability by placing conditioner directly downstream of pintle.

LOWER RIGHT: Reduced effect on flow stability with flow conditioner located in Mass Air Flow Sensor.

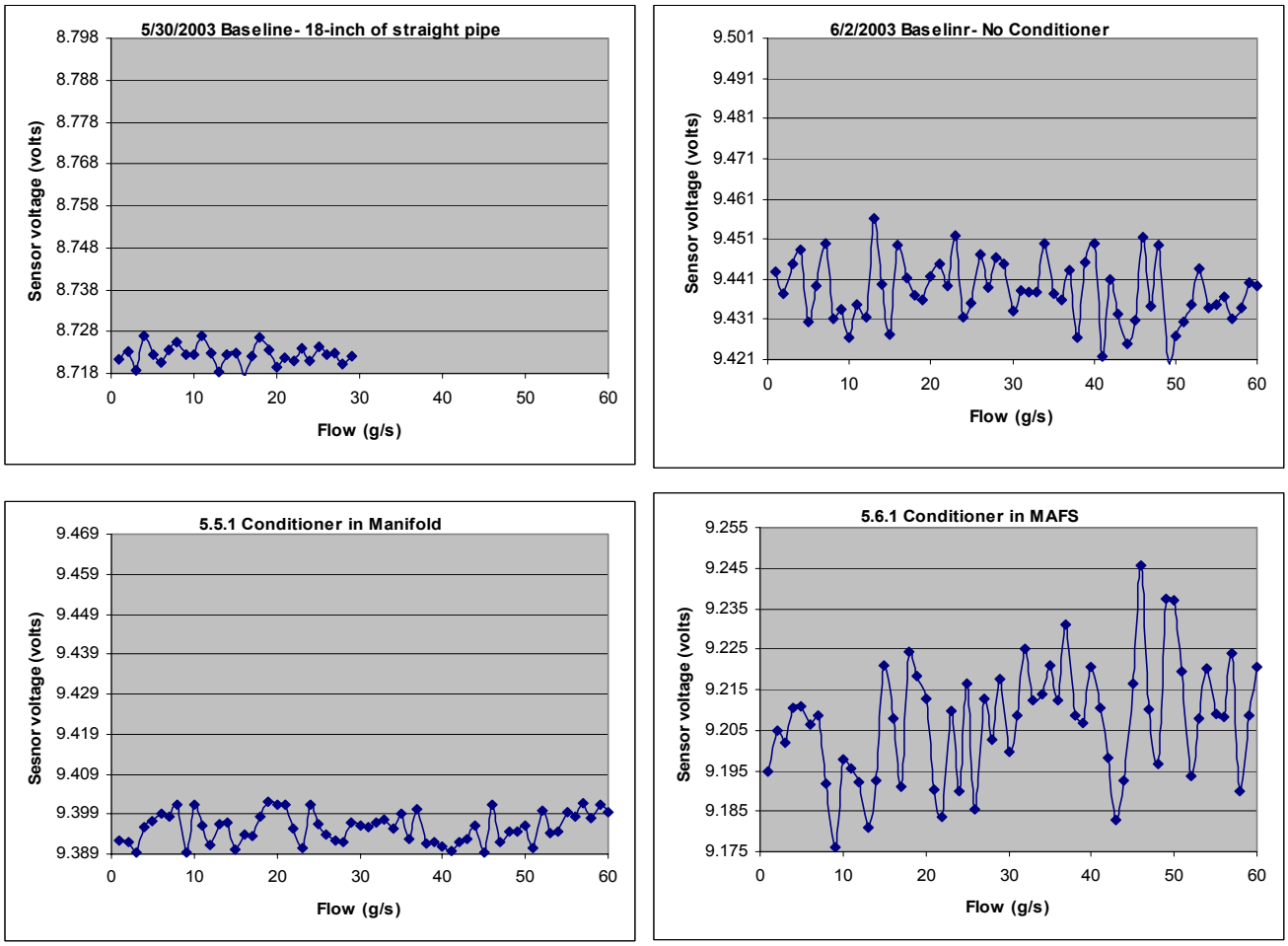

Figure 4.4.2.2-1: Manifold Stability Test

4.4.2.3 Delphi Manifold versus Rietschle Manifold

The GEN-2B manifold designed by Delphi had the approximately the same performance as the manifold supplied by Rietschle. However, there appears to be a slight increase in performance at unloaded end and a slight decrease at the loaded end. This deviation in performance is typical, resulting from a change in the flow paths and slightly increased flow resistance (see Figure 4.4.2.3-1).

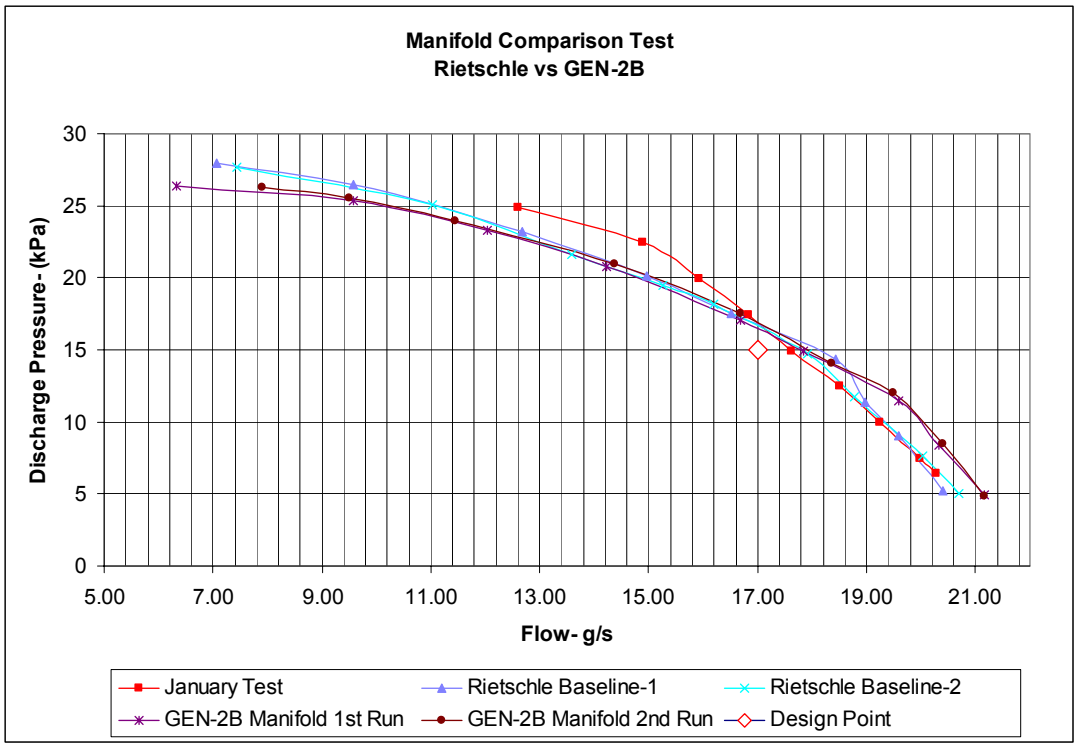

Figure 4.4.2.3-1: Manifold Test Comparison

4.4.2.4 Rietschle Impeller versus Impeller Designed by Delphi

The performance plot of both the Rietschle impeller and the impeller designed by Delphi indicated similar performance. However, there were some differences in geometry that was noticed with a side-by-side comparison of the two impellers. These differences have been addressed and new Delphi engineered impellers will be machined and tested.

Additionally, improvements to the dynamic elements of the impeller have been identified and will be incorporated in future impellers. These dynamic improvements include (see Figure 4.4.2.4-1):

- Swept vane design versus a straight vane
- Splitter vanes incorporated to prevent or minimize flow separation
- Extending the leading edge of the vanes farther into the throat of the impeller

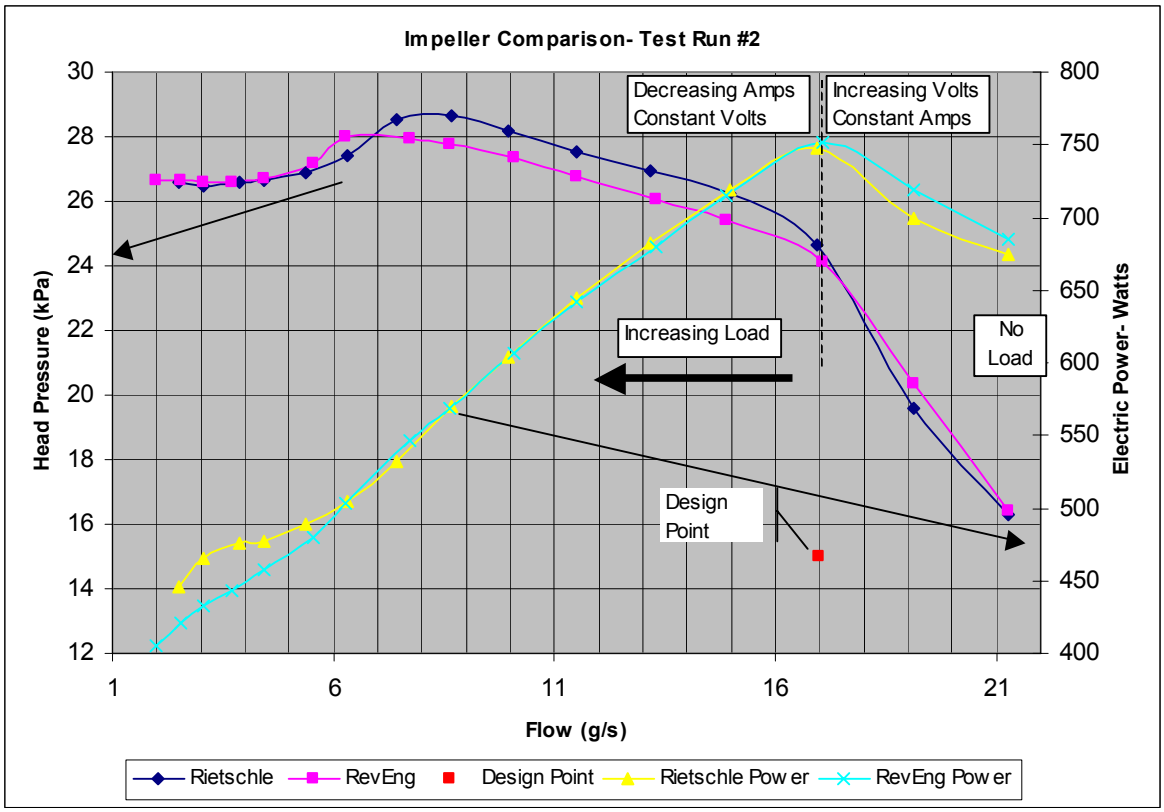

Figure 4.4.2.4-1: Impeller Design

4.4.3 Gasket

Figure 4.4.3-1 shows reformer gasket test data to date. Sealing in area 4 is the most difficult due to non-uniform seal loading. Copper and annealed nickel, at this development stage appears to be better than other gasket material combinations. Figure 4.4.3-2 shows the gasket test data for the Cathode heat exchangers. Figure Figure 4.4.3-3 shows the gasket test data for the Stack. From the graphs it can be concluded that improved processing of the Integrated Component Manifold with focus on surface finish and flatness of mating surfaces has resulted in overall improvements in sealing. The F-mica gasket test results for Stack Gaskets are somewhat promising, and are consistent with system test experience. Currently the F-Mica gaskets, in use, at the system level have with stood 3 thermal cycles with no significant leaks. This has allowed for system testing and development to continue. F-mica gaskets are not the long-term solution; but rather an intermediate one. Gasket development will continue.

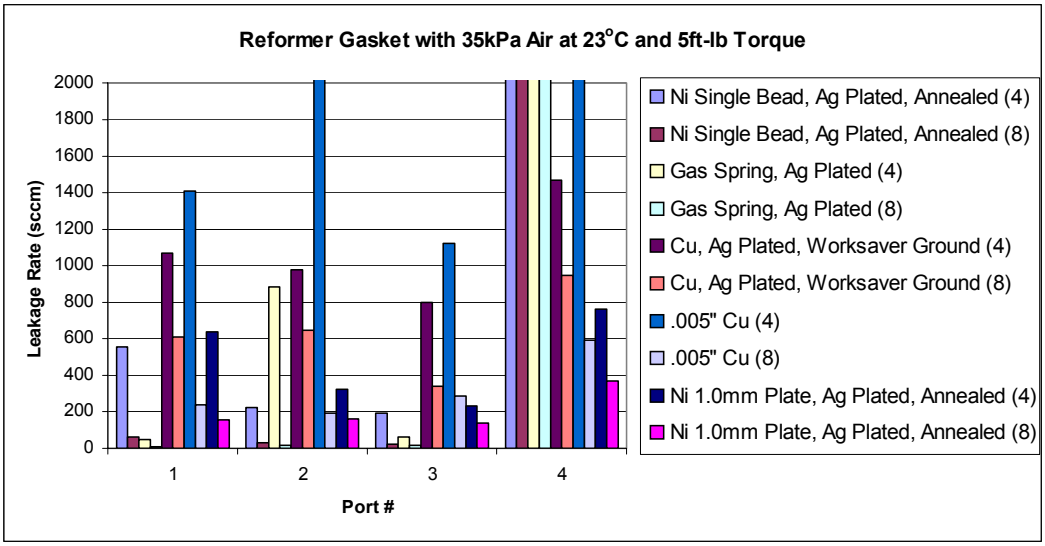

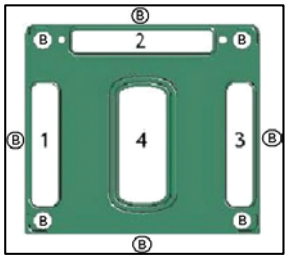

Approximate bolt locations marked with "B".
-(4) denotes use of bolts at the four corners of the gasket only.
-(8) denotes use of original 4 bolts at corners of gasket as well as additional 4 bolts at the centers of the edges of the gasket.

Figure 4.4.3-1: Reformer Gasket Testing

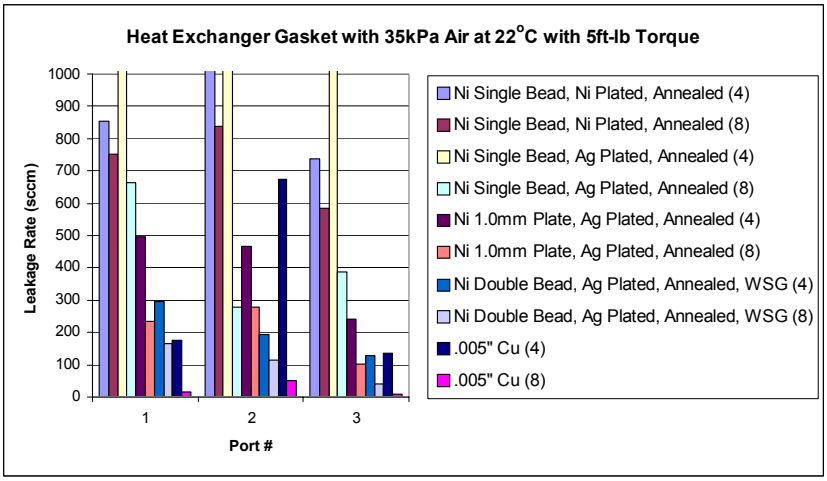

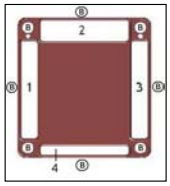

Approximate bolt locations marked with "B".
-(4) denotes use of bolts at the four corners of the gasket only.
-(8) denotes use of original 4 bolts at corners of gasket as well as additional 4 bolts at the centers of the edges of the gasket.
-WSG: Work Saver Ground

Figure 4.4.3-2: Cathode Heat Exchanger Gasket Testing

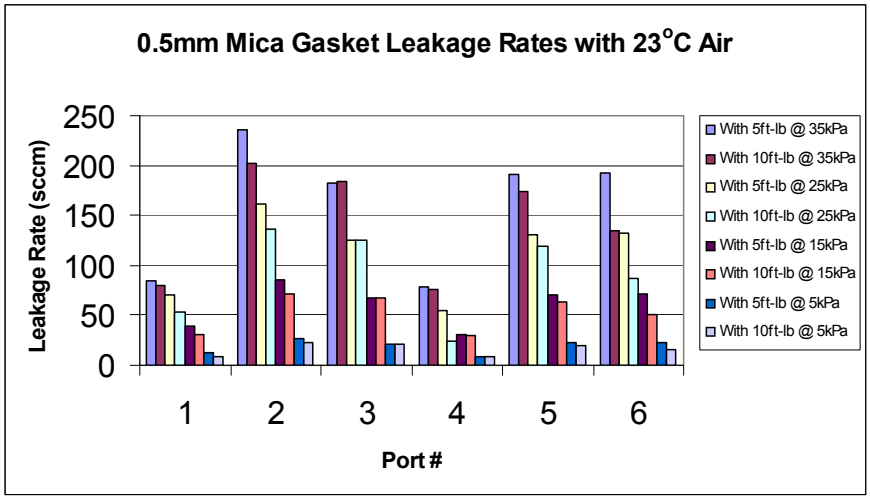

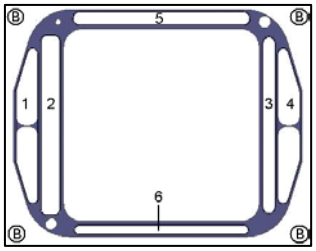

Figure 4.4.3-3: Stack Gasket Testing

4.4.4 Integrated Component Module

Figure 4.4.4-1 below shows the steady state modeling results for the temperature profile of the ICM.

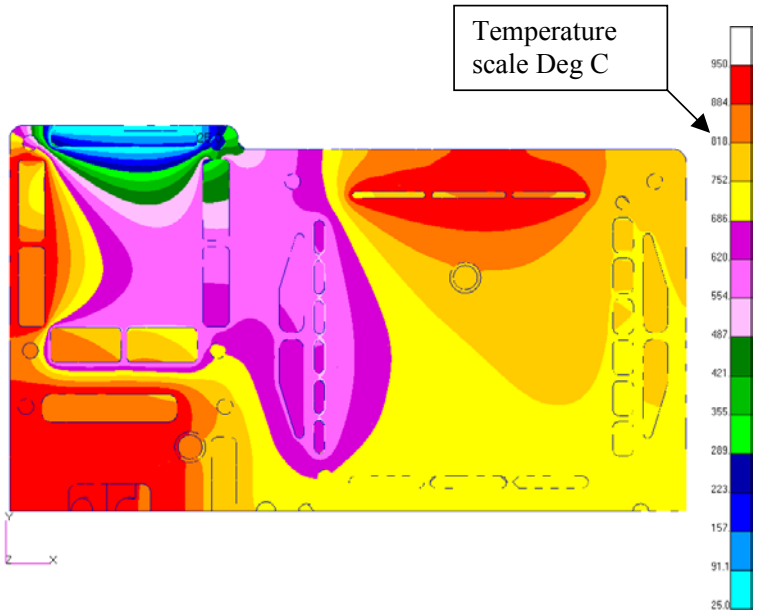

Figure 4.4.4-1: Steady State Temperature Profile

Top surface Z displacements (mm)

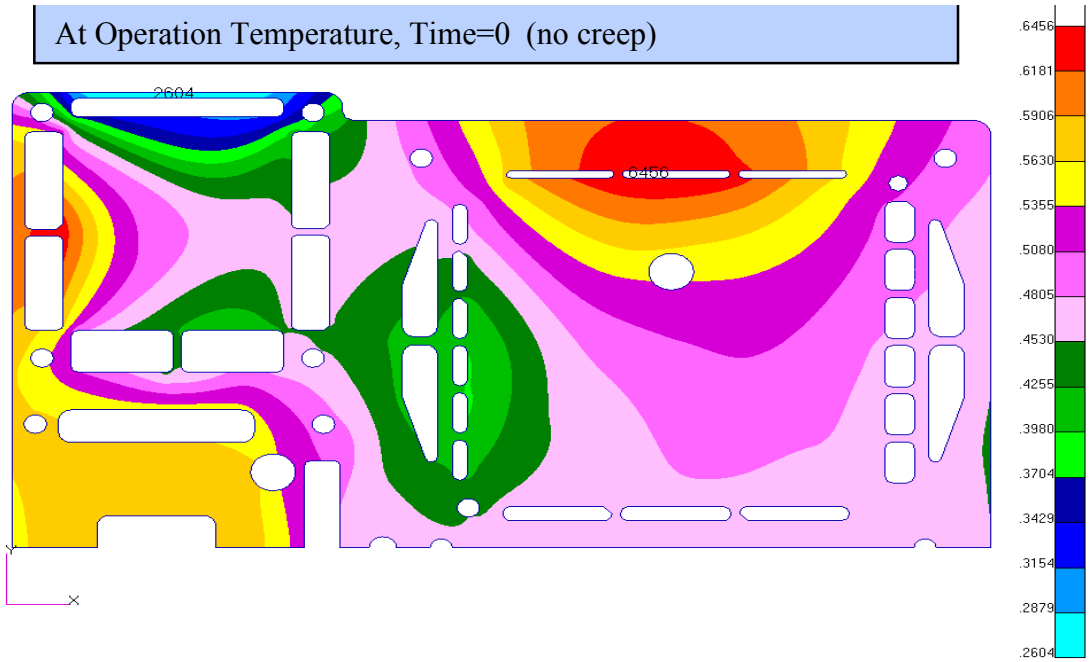

Figure 4.4.4-2: Structural Results

Figure 4.4.4-3 below shows the structural results cooled to 20 ^{0}C.

Top surface Z displacements (mm)

Cooled to 20ºC (no creep)

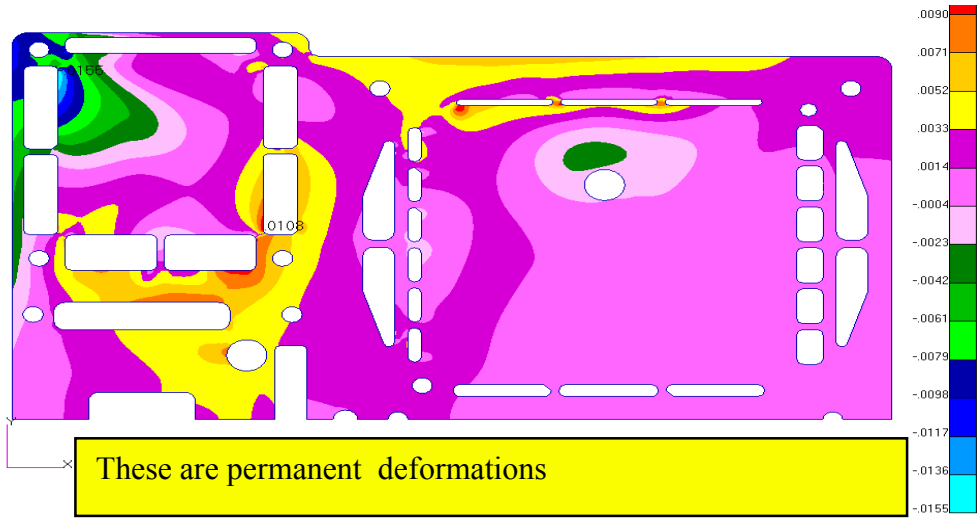

Figure 4.4.4-3: Structural Results Upon Cooling to 20 ^{0}C

Figure 4.4.4-4 shows structural results upon cooling to 20 ^{0}C after 10 hours at operating temperature

Top surface Z displacements (mm) Cooled to 20C after 10hrs at operating temperature

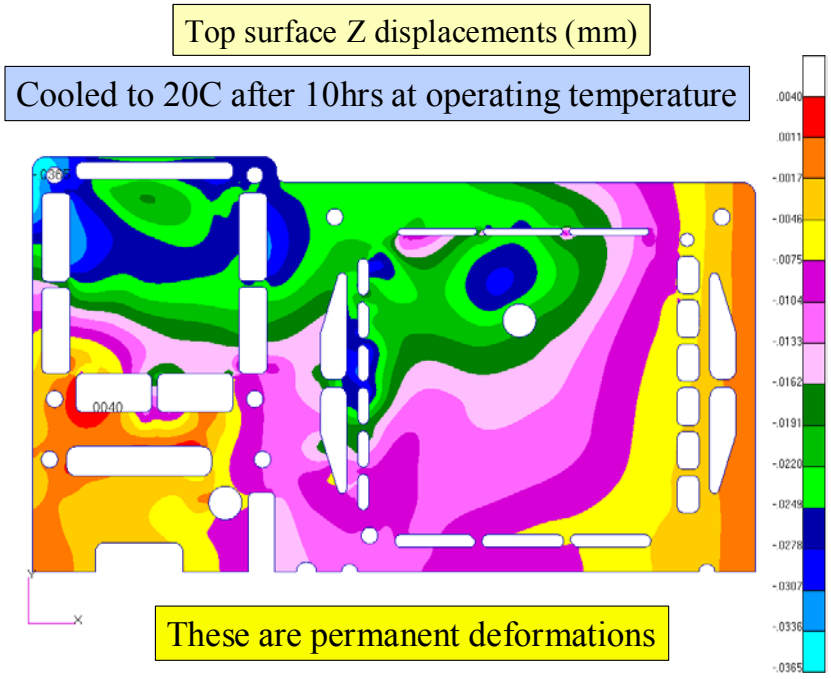

Figure 4.4.4-4: Structural Results

Next, the analytical modeling results were compared to the experimental data taken using the top plate characterization procedure outlined in the experimental approach. Figure 4.4.4-5 shows a side-by-side comparison of the modeling results with experimental results.

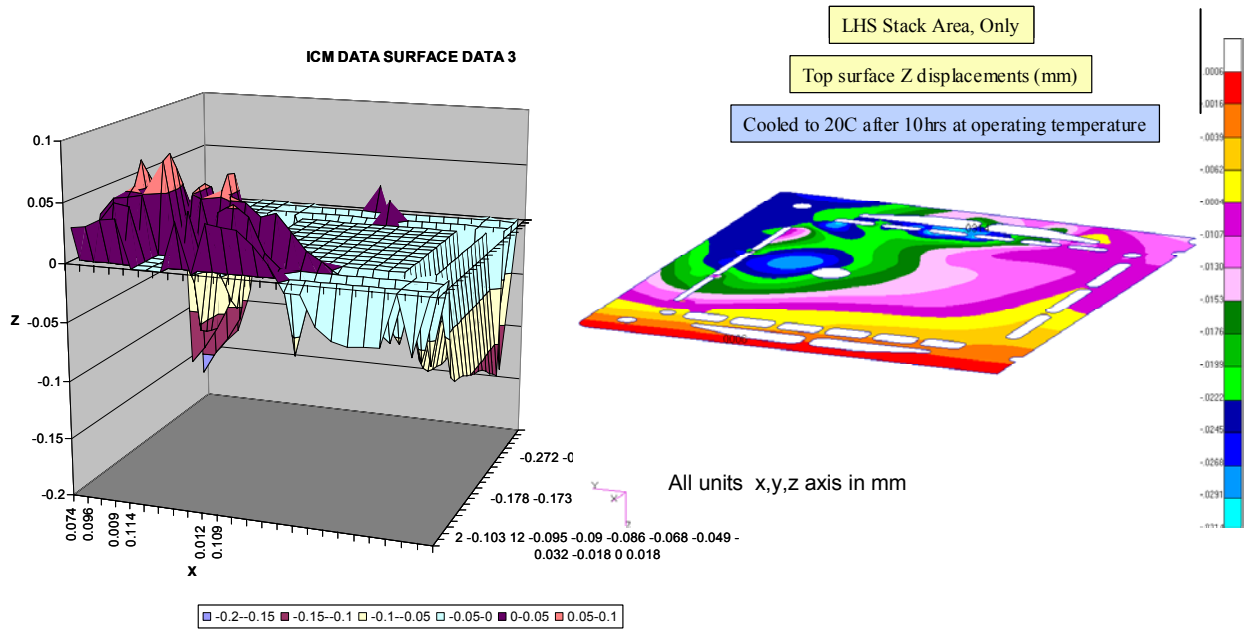

Figure 4.4.4-5: Modeling vs. Experimental Results

Although difficult to see in the above figure, the experimental results showed that the top plate deflection was on the order of + 60 µm and - 150µm, while the modeling predicted deflections on the order of only +0.6 µm and - 31 µm. The following remarks are stated about these results:

- Deformed ICM surface is believed to be the result of creep
- Analysis results seem to show poor correlation with measurement due to
  - Different loads applied (only an assumed ΔT in FEA)
  - Different load history applied (no cycling or re-grinds in FEA)
  - How well is measurement understood? (e.g., gravity sag shown?)
  - Analytical creep model poorly developed, calibrated

In its current state, analytical creep modeling, while apparently not useful for matching complex hardware behavior after it has undergone a very complex loading history, may still be used for qualitative purposes, (e.g. determining the benefit of thickening the top plate).

Another key learning during this timeframe was the discovery that the top plate material was not actually heat treated to achieve the high strength properties of the Haynes 230 material. The material was assumed to be received from the supplier in the heat-treated state. In actuality, the material is received in a wrought state with a solution treatment to get it to an annealed state. A process change has been made such that all

new top plates are now properly heat-treated after machining. In addition, the top plate has been made thicker for added strength, and a thermal barrier coating has been applied to the internal passages of the ICM to help with the thermal stress gradients across the part. New ICM's numbers 6 through 8 have been manufactured with these improvements. Full assessment of these changes will need to be verified going forward. It is also anticipated that additional modeling will be performed to investigate other possible design improvements.

4.4.5 Resistance Temperature Detector /Thermocouples

4.4.5.1 Resistance Temperature Detector Endurance testing

Failure of the Resistance Temperature Detector was defined as a reading that drifted more than 10 °C from the furnace set temperature. Of the six Resistance Temperature Detector's tested:

- One failed almost immediately (Resistance Temperature Detector-3)
- Two exceeded the arbitrary failure criteria (Resistance Temperature Detector's 1 and 2)
- Three Resistance Temperature Detector's (4, 5 and 6) successfully completed the 1000-hour test

This data was forwarded to several suppliers; of those, only one supplier was willing to take on an effort to develop a Resistance Temperature Detector to our dimensional and temperature requirements.

Currently, this developmental Resistance Temperature Detector's from Hi-Stat, a Stoneridge Company, are on test with completion due later next month. This testing was done in an oxidizing atmosphere since oxidation of the Platinum element is the most frequent mode of failure. Future testing will also be done in a reducing environment.

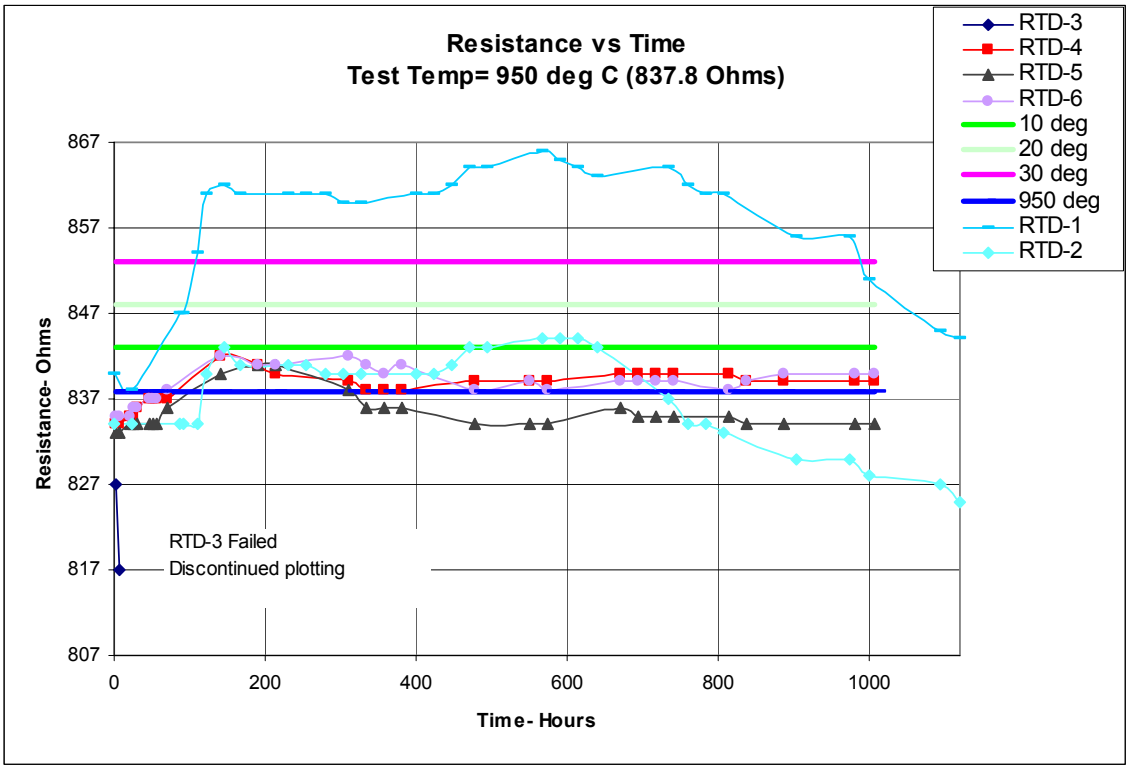

Figure 4.4.5.1-1: Resistance Temperature Detector Endurance Test

4.4.5.2 Thermocouple Testing

Five Thermocouples from Marchi, a Celerity group company, were tested. The test period lasted for over 800 hours and was terminated due to plant shutdown. However, all T/C's successfully completed the test with only a slight increasing drift after 500 hours. The amplified is calibrated such that:

- At 0 °C the output is 0.0-vdc
- At 1000 °C the output is 10-vdc

The data shows that total drift for all T/C's were within a 5 °C band, well within requirements. As with the Resistance Temperature Detector testing, this testing was done in an oxidizing environment, future testing will be done in a reducing environment.

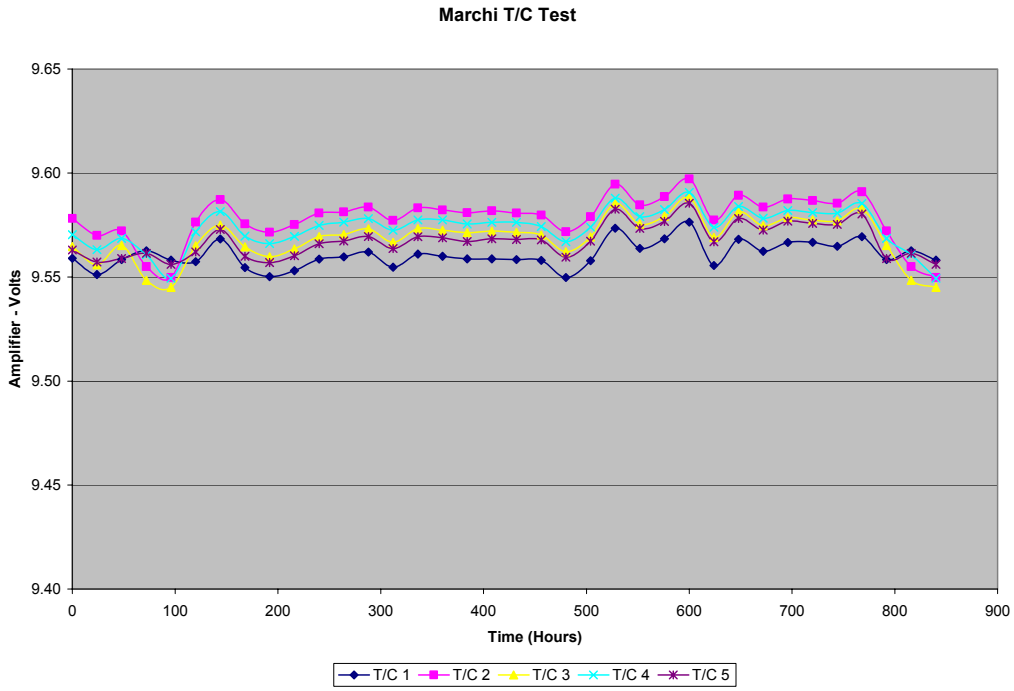

Figure 4.4.5.2-1: Thermocouple Endurance Test

4.4.6 Develop Fuel Metering and Fuel Delivery

Figure 4.4.6-1, and Figure 4.4.6-2 show the injector test characterization results for flow curves, spray patternation and particle sizing, respectively. These results are consistent with the Beta build reported previously, and thus indicated that this injector design has good manufacturing repeatability.

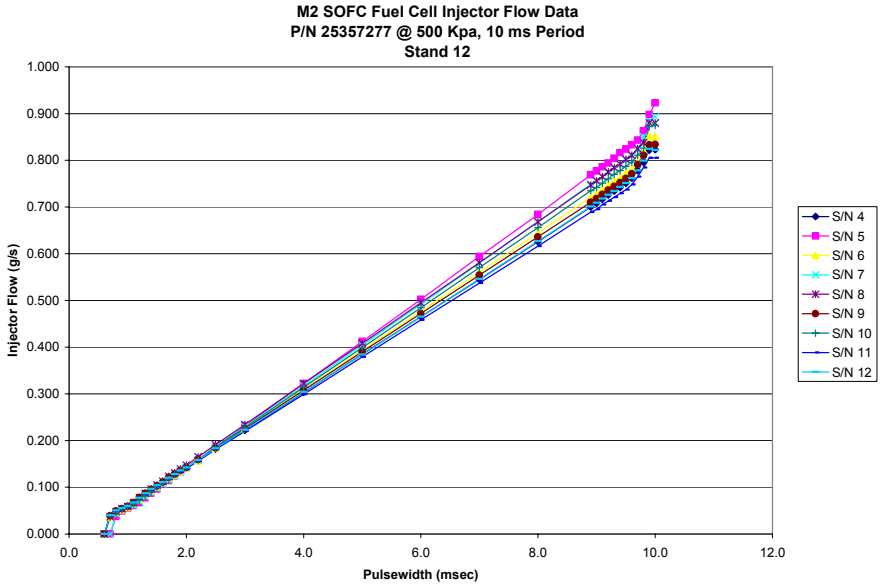

Figure 4.4.6-1: Injector Flow Curve Data

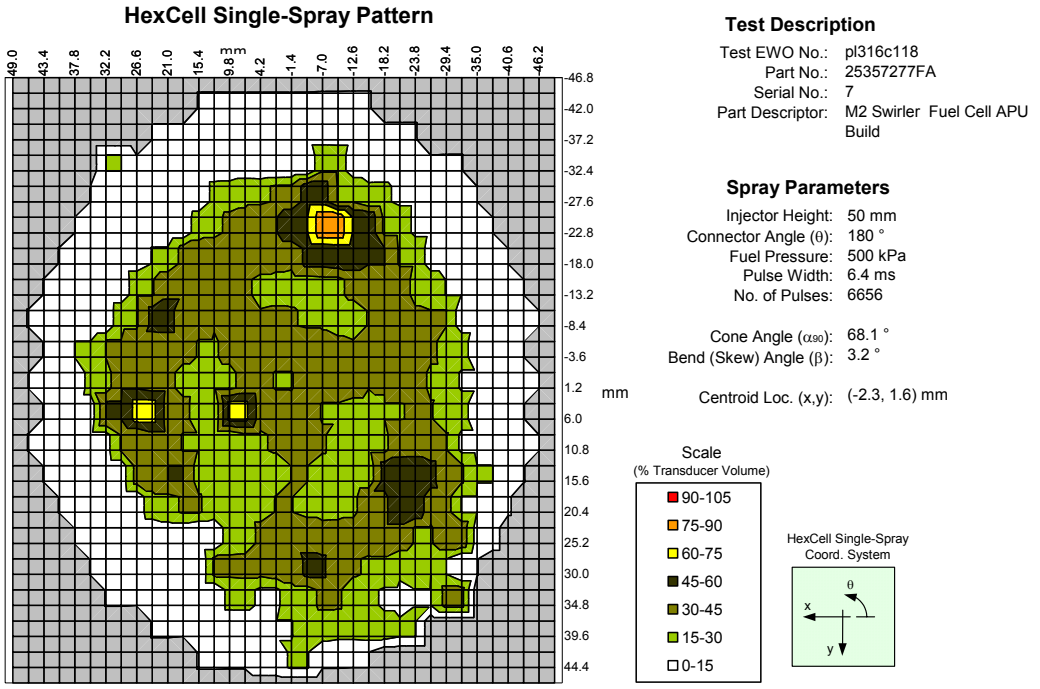

Figure 4.4.6-2: Injector Spray Patternation using Delphi Proprietary Hexcell Patternator

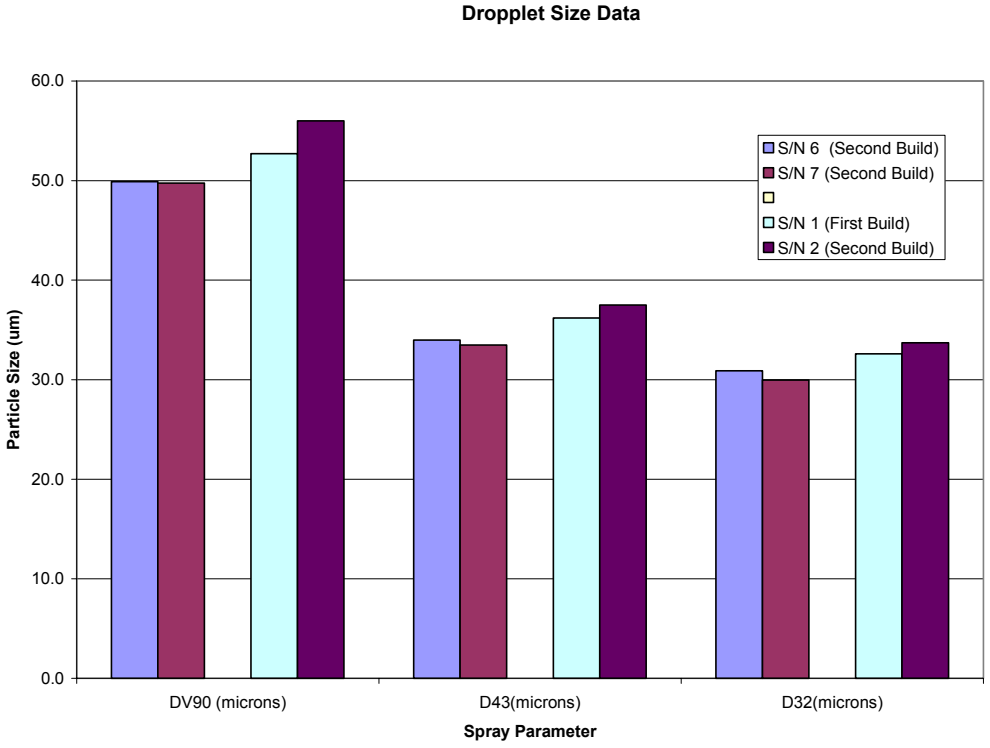

Figure 4.4.6-3: Injector Particle Size Data

4.5 Manufacturing Development (Privately Funded) (Task 5.0)

Results to date have indicated that functioning Solid Oxide Fuel Cell components can be built using the prototype processes available to us. The quantities required are small enough that volume throughput is rarely an issue. The welding processes for the reformer are successful as are the brazing processes. Stack component processes have been improved to where the yields are sufficient, but long-term costs are an issue. Glass dispensing has made much improvement in this area in the quality and throughput of the stack assembly process. The area still needing much work is stack component fabrication. The tape casting process through the flattening and noble metal deposition are areas where improvement is not only necessary but also very attractive. Because there are so many of these pieces used in every system, cost and throughput improvements multiply the effect.

The cost study of the system coupled with Crystal Ball^{tm} analysis software will point to areas to focus for improvement. Because the probability is part of the analysis, varying degrees of success can be examined and decisions can be made from that analysis.

4.6 System Fabrication (Task 6.0)

During this reporting period, the system fabrication activities began with the final assembly for operation of the last Gen 2A systems. A review and assessment of that Gen 2A design followed to provide the system design and integration activities further feedback. Preparation of the Gen 2B based system modules for development and testing concluded the report period.

4.6.1 Generation 2A System Fabrication for Final Testing

Material covered in Section 4.1.

4.6.2 Generation 2A System Fabrication Assessment

An analysis of the system to date was completed. Assessment of assembly and fabrication issues of the modules was completed along with mass and volume measurements. These established some of the design goals of the future generations of system components and modules. This data and budget will be used for several significant Gen 3 design decisions in the second reporting period of 2003.

4.6.3 Hot Zone Module Fabrication and Assembly

The Hot Zone Module assembly approach maintained an increased level of measurement ports for additional data collection during system tests. As the core module of the product, a majority of the testing is done with this hardware. Fabrication and assembly of the insulation systems would be compromised at times for this access. Better fitting and developed insulation solutions would be accomplished in final product assembly efforts. Sample ports, repairs, and modifications would be added during initial brazing and build. After initial brazing, additional work would be done using a manual TIG welding process.

The Hot Zone Module assembly was built with new temperature sensors, a revised tubular reformer, revised stack electrodes, revised gas connection tubes (input side) and additional fasteners used to secure and seal the fuel cell stack module to the integrated component manifold within the base of the Hot Zone Module. The insulation package for the Hot Zone Module was unchanged except for altered access points in the front to allow for Plant Support Module connections and better insulation fitment around these penetrations.

4.6.4 Plant Support Module Fabrication and Assembly

The Plant Support Module assembly approach (including the system space frame) was to assemble and complete fabrication of the bracketry and wiring not completed in the basic solid modeling / CAD used to layout the components. Changes would be necessary for the application interface module and the functions that it would undertake for the product. When complete, this module would receive the Hot Zone Module for close-coupled testing. An additional test cart for the system for airflow delivery and control would be developed and fabricated to allow simple reconfigurations of system flows. This approach would allow more precise measurement and fast implementation of air metering concepts (both hardware and software driven).

The Plant Support Module assembly (including the system space frame) underwent a layout change to utilize a new process air delivery system. The space frame redesign allows for easier assembly and development access to hardware within the product assembly. The system module now has easier air connections and clamping surfaces. The system wiring harness has been improved to higher temperature insulations and a power and ground distribution bus. This module has also had the electronics moved out to a new third module called the application interface module.

4.6.5 Application Interface Module Fabrication and Assembly

The Application Interface Module assembly approach focused on fabricating a compact interface that combined all the inputs and outputs to the system (except for system exhaust). The housing for this would need to low in mass and volume. The air filter housing and the electronics hardware would dominate the interface module fabrication. This approach will also allow concurrent development of this module and ultimately allow the adaptation to new markets without large disruption to the other modules.

The Application Interface Module assembly brings several improvements to the preparation and adaptability of the fuel cell system. Assembly now allows the air filtration filter and sound attenuator, the input/output signals and fluid connections, the electric power conditioner, and the system controller to be pre-built before inclusion to the product. This approach will also allow concurrent development of this module and allow adaptation to new markets without large disruption to the other modules.

4.6.6 Product Enclosure Fabrication and Assembly

The housing for the system would have no change in approach in this period except for the new coordination of the application interface module. The main internal modules

(Hot Zone Module and plant support module) are assembled and installed in a vertically oriented manner. The outer enclosure fabrication would not address additional environmental and safety issues in this period

4.7 System Testing (Task 7.0)

An agreed upon test plan for the SOFC system has been developed as incorporated into this cooperative agreement.

5.0 CONCLUSIONS

5.1 System Design and Integration (Task 1.0)

During the period covered by this technical report, a comprehensive product development plan has been created to guide development efforts. Within the context of this plan, various design level generations have been defined. Mass, cost, volume, and efficiency allocations have been created for each of the design levels. General system and subsystem targets, and a feature roadmap have also been defined to support the product development plan.

Within the current generation of hardware, Gen 2, significant design updates and developments have occurred. Key shortcomings and development issues were identified at the outset of the Gen 2A design level. Many of these issues were discussed in the previous period's technical report. During the course of Gen 2B APU development, many significant control issues for the system, including process air system, reformer, and electronics control, have been resolved. Significant improvements to design integration have also been made to improve the overall function, build and serviceability of the APU. Significant gaps in power, efficiency, cost, life, and cycle durability still exist, but they have been identified and future development efforts will address these gaps as a part of technology development.

As core plant technology developments progress, much effort has been placed on ways to leverage successful developments through reuse. The Application Interface Module (AIM) has been introduced as part of the conceptual design for the system so that mobile applications ranging from Automotive, Class 8 Truck, Military Vehicle, and Aircraft may be served with common Hot Zone Module and Plant Support Module hardware, with customizations possibly only needed in the configurable Application Interface Module.

For larger capacity Stationary Power Systems, flexible reuse of core, Solid Oxide Fuel Cell plant development may result in products that are more robust that serve multiple applications. A conceptual design for a Stationary Power System (SPS) utilizing core Hot Zone Module technology has been presented as part of this technical report.

Design improvements driven by Gen 2 system experience are helping to evolve current and future (Gen 3) system mechanizations. The mechanization detailing the

introduction of Anode Tail Gas Recycle (TGR) had been developed and presented in this technical report.

5.2 Solid Oxide Fuel Cell Stack Development (Task 2.0)

Major progress has been achieved in improving cell power density as well as cathode and anode interconnects. In addition, improved bonding has been demonstrated in the seal rupture tests with improved glass seal application and improvements in the braze. Development is ongoing to develop an insulating layer for the braze application between the repeating units in a stack. Intermediate sized cells have demonstrated power densities of greater than 700 mW/cm^2 at 0.7 Volts with hydrogen in single cell stack tests. Multiple 2x15-cell Integrated Stack Modules have been built and tested. Power densities of greater than 400 mW/cm^2 have been achieved on a stack level with simulated reformate compositions.

5.3 Reformer Developments (Task 3.0)

Reformer - Subsystem Level

Control strategy and implementation made a significant advance in this reporting period. Reformer operation has, within the reformer lab environment, now become relatively un-eventful. These controls and the understanding of reformer behavior that begets them are now undergoing trials in our systems lab where the thermal environment in particular is different than that of the reformer lab. Still thermal integration issues exist with CPox reforming.

Presently Pox reactor bed temperatures are higher than the long-term temperature capability of our washcoats. The washcoats are however durable enough to conduct useful tests. Continued work will be needed to properly size the reactor bed given a reasonable estimate of washcoat durability.

Carbon formation at the system level is not yet well understood but reformer subsystem testing is helping to define limits of operation. This will continue with a focus on preventing carbon accumulation on the stack anode with empirical work to capture the difficult kinetics / temperature interactions.

Despite these issues, the current reformer design has shown itself quite capable for short-term system testing needs. While it is not intended to be a final concept relative to highly endothermic reforming (i.e., via stack tailgas recycle, autothermal or steam reforming) it is providing a valuable platform on which to experiment.

Demonstration of recycle based endothermic reforming is expected in the next reporting period on the H_2 planar design. Improved designs with better analytical foundations will begin to displace H_2 as the endothermic capable design shortly.

Reformer Catalyst - Component Level

We are on track to develop highly durable fuel reforming catalysts, to meet the performance needs of fuel reformer devices. However, extensive durability testing is

required to identify the most appropriate catalyst formulations for each application. An improved rapid aging test is required, to be developed based on knowledge that will be gained through details physical and kinetics characterization of the reforming catalysts.

5.4 Develop Balance of Plant Components (Task 4.0)

5.4.1 Develop Hydrogen Sensors for High and Low Concentration Measurement

Three approaches have been outlined for providing closed loop feedback control of reformer performance. Continued development work is necessary to assess these approaches. Additionally, Delphi will continue with its in-house Hydrogen sensor development as well as pursue activities outside of Delphi. The combustible gas sensor has been proven at the bench level and remains to be verified at the system level.

5.4.2 Develop Air Delivery and Process Air Sub-System

Significant progress has been made relative to advancing overall process air sub-system design. The development of this component is moving towards a design that can be easily integrated into a Solid Oxide Fuel Cell system and readily manufactured. Additional work is still required on mass flow sensor instabilities. Delphi has also initiated an in-house development activity for a high-speed motor. This first application for this custom high-speed motor will be for the process air blower. This will alleviate problems of motor availability as system build quantities increase.

5.4.3 Develop Hot Zone Components

5.4.3.1 Gasket Development

Leaks at gasket seal interfaces have continued to improve. The attention to surface finishes and part fabrication process has been responsible for the improvements, as well as the additional bolt loadings of the components. Delphi will continue its development on unique sealing solutions such that thermal cycles can be achieved without gasket degradation.

5.4.3.2 Resistance Temperature Detector/Thermocouples

To date no Resistance Temperature Detector's have passed the 1000-hour at 950 ^{o}C endurance test. Resistance Temperature Detector development will continue. Type K Thermocouples have been specified as an interim replacement for Resistance Temperature Detector's. These thermocouples have passed the 1000-hour endurance test and have proven to be reliable at the system level.

5.4.3.3 Igniters

Design improvements to the igniters have resulted in improved reliability of this component. Additional test experience at the system level is necessary to understand if design improvements sufficiently addressed all failure modes.

5.4.4 Integrated Component Manifold

Manufacturing process development has resulted in an improved assembly. Full assessment of the design improvements and of the effect of thermal barrier coating remain to be verified at the system level.

5.4.5 Cathode Heat Exchanger

Delphi Thermal's expertise in the area of fabrication and braze process development for the heat exchangers has advanced the design. Further improvements are anticipated pending results of proposed tests.

5.4.6 Develop Fuel Delivery and Fuel Metering

While the fuel injector design appears to be complete at this time and manufacturing ability has been repeated, additional work is necessary for developing component specifications of the remaining fuel system components such as fuel pump, pressure regulators, tanks etc.

5.5 Manufacturing Development (Privately Funded) (Task 5.0)

The current status of the process development is highly slanted to the short-term process development required for prototype production. The facets of the program with multiple approaches are being pursued to determine the most feasible design from a performance and cost perspective. The potential for improvement is also part of the analysis. The areas for long-term process development are indicated by the cost study.

It identifies high cost areas of the system. The major areas of need are: the minimization of noble metals, the minimization of exotic high-temperature alloys, and the improvement in yield and cost of the stack component fabrication. These component parts with multiple firings offer much potential cost reduction. Because they are used in high count multiples, reduction in cost multiplies the savings. At this point in time, these three areas are indicated as the most pressing areas for process development.

5.6 System Fabrication (Task 6.0)

No major changes occurred to the overall system assembly process. The main internal modules (Hot Zone Module and plant support module) will be assembled and installed into an outer enclosure that provides a structurally safe and sealed housing for the product. The new application interface module is now fastened to form one of the outer walls of the product.

5.7 System Testing (Task 7.0)

While basic function and control have been demonstrated at the system level in the laboratory, the state of development for both the Auxiliary Power Unit subsystems and controls does not allow for robust operation of the gasoline Auxiliary Power Unit power

plant, nor power output above break-even levels. More meaningful testing at the system level may be conducted with the next design level of subsystem hardware.

6.0 LIST OF GRAPHICAL MATERIALS

List of Figures **Page**

List of Figures **Page**

List of Figures **Page**

List of Figures **Page**

List of Figures **Page**

List of Figures **Page**

List of Tables **Page**

7.0 REFERENCES

None required.

8.0 BIBLIOGRAPHY

None required.

9.0 LIST OF ACRONYMS AND ABBREVIATIONS

A	
APU	Auxiliary Power Unit
B	
BOP	Balance-of-Plant
C	
C F D	Computational Fluid Dynamics
CHX	Cathode Heat Exchanger
CPO	Catalytic Partial Oxidation
D	
DI	Direct Injection
DOE	Department of Energy
E	
ERU	Energy Recovery Unit
F	
FE	Finite Element
H	
HZM	Hot Zone Module
I	
ICM	Integrated Component Manifold
L	
LHV	Lower Heating Value
N	
NETL	National Energy Technology Laboratory
P	
PSM	Plant Support Module
S	
SECA	Solid State Energy Conversion Alliance
SOFC	Solid Oxide Fuel Cell
ULEV	Ultra-Low Emission Vehicle
W	
WRU	Water Recovery Unit

10.0 APPENDICES

Per Cooperative Agreement DE-FC26-02NT41246 EPAct Information considered restricted, proprietary, and confidential to Delphi are presented in Appendix A to this document per FAR 52.227-14, Rights in Data-General.